Impact de la variabilité intra- et inter-spécifique des réponses à la température et au déficit hydrique dans la diversité des scénarios E x M

Boris Parent

Mémoire d' Habilitation à Diriger des Recherches

Impact de la variabilité intra- et inter-spécifique des réponses à la température et au déficit hydrique dans la diversité des scénarios E x M

Boris Parent

Chargé de Recherche UMR LEPSE

Soutenue le 1er Juillet 2021 devant le jury composé de :

Pr. Alain Ourry, Professeur, Université de Caen Normandie, ***Rapporteur***

Pr. Mathieu JAVAUX, Professeur, Université Catholique de Louvain, Belgique, ***Rapporteur***

Dr. Laurent LAPLAZE, Directeur de Recherche, IRD Montpellier, ***Rapporteur***

Dr. Karine CHENU, Senior Research Fellow, The University of Queensland, Australie, ***Examinatrice***

Dr. Anne-Sophie VOISIN, Chargée de recherche, HDR, INRAE Dijon, ***Examinatrice***

1. PREAMBULE ET REMERCIEMENTS

Bien entendu, ce document a comme but premier, pour vous, membres du jury, d'évaluer la pertinence de mes activités de recherches et de mon projet scientifique. Cependant, c'est tout d'abord à mes proches qui liront ce document, peut être des thésards, post-docs, stagiaires passant par le labo, ou même (soyons fou) la personne qui s'ennuie dans la bibliothèque et qui ouvre ce document pour passer le temps, à qui je voulais d'abord m'adresser.

En effet, c'est aujourd'hui le seul document dans lequel je peux résumer mon travail, mes approches, mes projets, de façon simple et exhaustive. C'est aussi la raison pour laquelle ce document est en français, simplifiant la lecture à ceux peu assidus à la lecture de « *Plant Cell & Environment* ». Mais plus généralement, la réalité de notre métier est souvent obscure, jusque dans nos réseaux proches: *« tu travailles à l'INRA, tu fais des OGMs ?* », l'intérêt de nos recherches est moins qu'évident pour le plus grand nombre : « *J'ai vu dans un reportage qu'un mec, arrive à faire pousser des plantes sans eau, avec des variétés anciennes….* », et le métier de chercheur ne fait plus rêver « *ça gagne combien, au fait, un chercheur ?* ».

Comment leur en vouloir quand aujourd'hui le débat scientifique se distribue du politique aux réseaux sociaux, basé sur l'indignation, la subjectivité, et l'affect. Comment leur en vouloir quand la « vérité » scientifique sort aujourd'hui des tribunaux pénaux (ex : condamnations de Monsanto sans base scientifique), médiatiques (ex : reportage France 2 sur le Glyphosate ou sur Limagrain) et populaires (81 % des français ont peur des OGMs ; sondage IFOP 2019). Comment leur en vouloir si crier plus fort (Séralini, Raoult) a plus d'impact sur les politiques publiques que le travail de centaines de chercheurs. Comment, enfin, dans un domaine plus proche, leur en vouloir de ne pas voir l'intérêt de l'amélioration variétale quand seul Pierre Rabhi, « expert sècheresse » médiatique officiel, peut donner sa vision de l'agriculture deux fois par an sur France inter. Pour vous, le stagiaire, les proches, et l'homme de la bibliothèque, voyez donc cette rédaction comme une tentative d'explication exhaustive de ce qu'est mon travail. J'espère que vous y comprendrez ce qui me passionne et y verrez peut-être même un intérêt pour le bien commun.

-Dans ce manuscrit, vous allez trouver une certaine continuité entre mes approches scientifiques passées, et celle de mon projet. Peut-être trouverez-vous aussi une continuité avec les travaux de François Tardieu. Pourtant, s'affranchir des approches et travaux de son directeur de thèse serait **LA** condition pour être un chercheur à part entière capable de mener ses propres recherches. Comme vous vous en rendrez compte, j'assume pleinement, en le revendiquant, cette filiation scientifique : l'hybridation entre phénomique, analyse écophysiologique de processus et de leur diversité génétique, et modélisation des

cultures, mais surtout l'encrage dans la réalité des contraintes agricoles, afin d'offrir à l'agriculture du futur non pas un hypothétique gène miracle de la résistance à la sécheresse, mais plutôt un ensemble de petits éléments, caractères, allèles, qui en les combinant octroient des avantages dans des environnements ciblés. Bref, un compromis ambitieux mais réaliste, plutôt qu'une incertaine nouvelle révolution verte (toute ressemblance avec la politique serait purement fortuite…).

Merci François, pour la formation que tu m'as fournie, ton sérieux et ton intégrité scientifique. Merci surtout de me laisser ….du moins essayer… prendre la suite.

-Dans ce manuscrit, vous allez trouver résumés des résultats impliquant des dizaines d'expériences, et des millions de données, à des échelles allant du gène au rendement au champ. Bien sûr, cela n'aurait pas été possible sans le travail des multiples personnes impliquées, techniciens, thésards, ingénieurs, chercheurs du LEPSE et de l'ACPFG, mais aussi des partenaires nationaux et internationaux qui m'ont souvent beaucoup appris. Certaines de vos idées se retrouveront surement dans ce manuscrit, voyez-le comme une reconnaissance. Ces travaux n'auraient pas non plus été possibles sans les administratifs, gestionnaires, mais aussi vous, les chefs, les chefs d'unité, chefs de centre, chefs de département, petits et grands chefs, qu'on remercie rarement pour le travail invisible qui fait que la boutique tourne.

Merci donc à vous tous, que je ne nommerai pas de peur de vous oublier…….

…… et bien sûr merci encore Achouak pour m'avoir permis de rédiger la majeure partie de ce manuscrit dans de si bonnes conditions, pourtant confinés avec 2 enfants à la maison.

Bonne lecture

2. TABLE DES MATIERES

1. Preambule et remerciements 1

3. Curriculum Vitae 4

4. Publications Scientifiques 10

5. Projet scientifique 14

Contexte 14

Objectifs et Stratégie Générale 20

Points clés 22

6. Activités de recherche 2005 -2020 32

Focus n°1 : Effet de l'ABA sur la croissance foliaire du maïs 32

Focus n°2 : Déchiffrer les interactions G x E sur le rendement du blé 36

Focus n°3 : Analyse comparative des réponses à la température 41

Focus n° 4 : Variabilité génétique du développement et de la croissance foliaire pour des climats futurs . 46

7. Projet de recherche – Activités à moyen terme 51

Focus n° 5 : Des idéotypes réalistes du contrôle de la transpiration sous changement climatique 51

Focus n°6 : Qui, de l'agronomie ou de la génétique dessine(ra) les contours des cultures de Sorgho et de Maïs en France et en Europe ? 56

8. Références 60

9. ANNEXES 69

3. CURRICULUM VITAE

Boris Parent

Né le 17 Avril 1981 à Les Lilas (93)

Nationalité française, Marié, 2 enfants

Situation Actuelle à l'INRA

-Chargé de Recherche INRA Classe Normale, Echelon 6. Date de Titularisation : 1er Février 2014

-Chef d'équipe, équipe MAGE depuis Septembre 2019

-Responsable scientifique de la plateforme de phénotypage « *PhenoDyn* » depuis 2015

-UMR LEPSE, 2 place Viala, 34060 Montpellier cedex 2

Diplômes et Formations

2005-2008 **Doctorat** de Systèmes intégrés en Biologie, Agronomie, Géosciences, Hydrosciences et Environnement. Spécialité de Biologie Intégrative des Plantes (Montpellier Supagro).

2005 **Master** de Microbiologie et catalyse industrielles (Master recherche, INSA Toulouse). Mention B.

1999-2005 **Ingénieur** de l'Institut National des Sciences Appliquées de Toulouse. Spécialité Génie Microbiologique-Génie Biochimique. Orientation Génie Biomoléculaire.

1999 **Baccalauréat** S, option Mathématiques (Montpellier). Mention AB.

Parcours Professionnel

2013-2021 **Chargé de Recherche à l'INRA, Montpellier.** Ecophysiologie et Modélisation de la variabilité intra- et inter-spécifiques des réponses des céréales au déficit hydrique et aux hautes températures. Laboratoire d'Ecophysiologie des Plantes sous Stress Environnementaux (UMR LEPSE).

2009-2012 **Chercheur contractuel, Post-Doctorat, Adelaide, Australie.** Analyse systématique des réponses à la sécheresse et aux hautes températures. Australian Centre for Plant Functional Genomics (ACPFG), University of Adelaide, Australia.

2005-2008 **Doctorat.** Développement foliaire chez le riz et le maïs: cadre d'analyse, réponse comparées à la température et régulation de la croissance en déficit hydrique. INRA de Montpellier. Laboratoire d'Ecophysiologie des Plantes sous Stress Environnementaux (UMR LEPSE).

Encadrements de Thèses :

Stéphane Leveau (thèse en cours, soumission 2021)

50% encadrement avec Dr Pierre Martre (directeur de thèse, INRA Montpellier)

Modélisation de la variabilité génétique des réponses du tallage aux contraintes hydriques et azotées

La thèse de Stéphane s'inscrit dans une volonté de collaboration avec un partenaire privé, l'ITK (Clapier, France) afin de développer des modèles de réponses des plantes aux contraintes abiotiques. Cette thèse fait le lien avec celle de Maeva Baumont afin de modéliser la variabilité génétique des réponses de toutes les composantes de la croissance foliaire chez le blé (développement / phyllochrone, tallage, et croissance de feuilles individuelles). **Un article soumis.**

Leveau S, Parent B, Zaka S, Martre P. Ploidy, phylogeny, and breeding together structure the diversity of traits linked to plant structure, rate of development, and responses to temperature and evaporative demand in wheat-relative species. *soumis à New Phytologist*.

Maeva Baumont (2015-2018)

50% encadrement avec Dr Pierre Martre (directeur de thèse, INRA Montpellier)

Acclimatation de processus de développement, croissance et photosynthèse à la température

La thèse de Maeva a permis de revisiter les modèles de développement foliaire chez le blé. En particulier, sa thèse a mis en évidence un fort impact de l'histoire trophique de la plante sur le développement foliaire. Ce résultat permettait de modéliser les réponses à la température, à la photopériode, à l'intensité lumineuse et au CO_2 à partir d'une hypothèse unique. Ce modèle a été implémenté dans le modèle de culture Sirius.

1 article publié, 1 en préparation

Baumont, M., Parent, B., Manceau, L., Brown, H., Driever, S., Muller, B., Martre, P. (2019). Experimental and modeling evidence of carbon limitation of leaf appearance rate for spring and winter wheat. Journal of Experimental Botany. 70. 2449-2462

Sebastien Lacube (2014-2017)

50% encadrement avec Dr François Tardieu (directeur de thèse, INRA Montpellier)

Modélisation de la surface foliaire chez le maïs, influence de la variabilité génétique sur la production dans de multiples scenarios climatiques

La thèse de Sébastien Lacube couvre les différents aspects de mon approche scientifique sur un processus particulier, la croissance des feuilles du maïs et sa réponse aux contraintes abiotiques. Sébastien a (i) commencé par une analyse fine des processus écophysiologiques pour développer un modèle de croissance foliaire, (ii) a analysé la variabilité génétique des paramètres et (iii) simulé l'impact de cette diversité dans la diversité des scénarios environnementaux européens. ***3 articles publiés, 1 en préparation***

Lacube S, Manceau L, Welcker C, Millet EJ, Gouesnard B, Palaffre C, Ribaut JM, Hammer G, **Parent B,** Tardieu F. (2020). Simulating the effect of flowering time on maize individual leaf area in contrasting environmental scenarios. *Journal of Experimental Botany* 71(18): 5577-5588.

Lacube, S., Fournier, C., Palaffre, C., Millet, E. J., Tardieu, F., **Parent, B.** (2017). Distinct controls of leaf widening and elongation by light and evaporative demand in maize. *Plant, Cell and Environment, 40* (9), 2017-2028.

Parent, B., Leclere, M., **Lacube, S**., Semenov, M. A., Welcker, C., Martre, P., Tardieu, F. (2018). Maize yields over Europe may increase in spite of climate change, with an appropriate use of the genetic variability of flowering time. *PNAS, 115* (42), 10642-10647.

Julien Bonneau (2009-2013)

25% encadrement avec Pr Peter Langridge (directeur de thèse, Adelaide University)

Genetic analysis of a region associated with heat and drought tolerance on chromosome 3BL of wheat

J'ai encadré Julien Bonneau sur l'analyse écophysiologique de son QTL d'étude. Julien a montré que ce QTL avait de forts effets dans certaines situations mais avec de très fortes interactions QTL x Environnement, avec une implication probable de la réponse de la transpiration sous hautes température. Mais ce n'est qu'après sa thèse que l'analyse de toutes les données phénotypiques ont permis de mieux expliquer où et quand ce QTL a un effet positif sur le rendement. ***2 articles publiés en rapport direct avec mon encadrement***

Bonneau, J., Taylor, J., **Parent, B.,** Bennett, D., Reynolds, M., Feuillet, C., Langridge, P., Mather, D. (2013). Multi-environment analysis and improved mapping of a yield-related QTL on chromosome 3B of wheat. *Theoretical and Applied Genetics, 126* (3), 747 - 761.

Parent, B., Bonneau J, Maphosa, Kovalchuk, Langridge, Fleury (2017). Quantifying wheat sensitivities to environmental constraints to dissect G x E in the field. *Plant Physiology, 174* (3), 1669-1682.

Lance Maphosa (2010-2014)

25% encadrement avec Pr Peter Langridge (directeur de thèse, Adelaide University)

Genetic control of grain quality in wheat grown under drought and heat stress conditions.

J'ai encadré Lance Maphosa principalement sur les aspects expérimentaux de physiologie au champ, sa thèse gardant une empreinte fortement « génétique ». ***3 articles publiés en rapport direct avec mon encadrement***

Maphosa, L., Langridge, P., Taylor, H., **Parent, B.**, Emebiri, LC., Reynolds, MP., Okada, A., Mather, DE. (2014). Genetic control of grain yield and grain physical characteristics in a bread wheat population grown under a range of environmental conditions. *Theoretical and Applied Genetics, 127* (7), 1607-1624.

Parent, B., Shahinnia, F., **Maphosa,** L., Berger, B., Rabie, H., Chalmers, K., Kovalchuk, A., Langridge, P., Fleury, D. (2015). Combining field performance with controlled environment plant imaging to identify the genetic control of growth and transpiration underlying yield response to water-deficit stress in wheat. *Journal of Experimental Botany, 66* (18), 5481-5492.

Parent, B., Bonneau**, Maphosa**, Kovalchuk, Langridge, Fleury (2017). Quantifying wheat sensitivities to environmental constraints to dissect G x E in the field. *Plant Physiology, 174* (3), 1669-1682.

Encadrements de CDD Ingénieurs :

Adèle Meziane (2016-2018)

100% encadrement

Analyse de lignées transgéniques de maïs affectées sur la production et dégradation de l'ABA.

Adèle a conduit l'analyse phénomique de transformants issus du projet Morea. Les résultats préliminaires sont fondateurs pour mon projet de recherche portant sur l'impact de la variabilité génétique du contrôle de la transpiration (voir Focus N°5). *J'ai choisi de ne pas publier ces résultats et d'attendre un nouveau projet afin d'augmenter leurs impacts potentiels.*

Nicolas Sutton (2017, 9 mois)

100% encadrement

Analyse de la croissance et de la transpiration à partir des données de la plateforme *Phenodyn*

Nicolas a développé un script d'analyse à partir des données brutes de la plateforme de phénotypage *Phenodyn* pour laquelle je suis responsable scientifique. Toutes les fonctions ont été repensées à partir de brainstormings très réguliers entre Nicolas, Adel et moi-même. La plateforme permet maintenant l'analyse de la croissance et de la transpiration d'espèces variées.

Implications dans des Contrats de Recherche

Participation à des contrats de recherches

-UE DROPS (FP7-KBBE) 2010-2015. DROght-tolerant yielding PlantS.

Responsable des taches WP1 pour l'ACPFG

-UE Water4Crops (FP7-KBBE) 2012-2016.

Responsable des taches INRA-LEPSE

-**UE ModCarboStress** (ERA-NET) 2015-2018.

Responsabilités sur les aspects modélisation. Co-encadrement thèse Maeva Baumont

-UE MODEXTREME (FP7-KBBE) 2013-2017.

Impliqué sur les aspects modélisation, WP1.

-Programme national Investissements d'avenir PHENOME 2012-2021.

Développements méthodologiques sur la plateforme « PhenoDyn ».

-ANR Investissements d'avenir AMAIZING 2012-2020.

Impliqué principalement au travers de l'encadrement de Sébastien Lacube et sur les aspects de modélisation et simulation à large échelle.

Projets soumis comme partenaire et rejeté

-UE PreADAPT (H2020) (coordinateur Pierre Martre).

Responsable Tache 1.5 (Modélisation)

Projets soumis comme coordinateur et rejetés

-Agropolis Open Science 2017 TINGLE: Contributions of TillerING and individual Leaf Expansion to the variability of plant growth in response to soil water deficit: a comparative approach in four cereal species.

-ANR JCJC 2018: AmBITION. *A*chieva*B*le *I*deotypes of *T*ranspirat*ION* optimizing yield under drought

-ANR JCJC 2019: ACTING. *AChievable ideotypes of Transpiration under changING climates*

-**ERC Consolidator Grant 2020. T-time**. *Transpiration timing of water-efficient plants*

Projets soumis

- Projet inter-unités département AgroEnv. PARSEMA - Plant Adaptation to Recurrent Stresses : combining Ecophysiological and Modeling Approaches.

Porteur de projet pour le LEPSE.

- Projet ANR-PRC 2021 RICOCHETS – Resilience to recurrent heat stresses in plants.

Porteur de projet pour le LEPSE.

Activités d'Enseignement / Formations

-Formateur pour CultiVar : International thematic school "Analysing and modelling phenotypes for challenging environments", une semaine en 2017, 2018 et 2019 à Montpellier (public international niveau doctorat)

-**Module HMBA304 Ecophysiologie des relations plante environnement Master BFP**, Université Montpellier. Prise en charge du cours « Intégration des connaissances dans les modèles de culture » depuis 2013 (4 h / an).

-Modélisation des cultures : Effets intégrés de caractères (éco) physiologiques sur les performances des plantes. Formation à direction de professionnels dans le cadre du projet Amaizing (2017-2018)

Autres centres d'intérêts / Vie associative et sportive

Participation à la création d'une association sportive : « Montpellier Eaux-Vives » (2000)

Trésorier de cette association (2002-2009).

Président de cette association (2013 à ce jour), en 2020, 3 employés, 160 k€.

Sportif de haut niveau, sur liste ministérielle (1999-2002):

Champion de France en canoë biplace slalom en individuel (1999)

Vice champion de France en canoë biplace slalom en individuel (1997, 1998)

Vice champion de France par équipe (2000 , 2001 , 2002)

4. PUBLICATIONS SCIENTIFIQUES

Articles scientifiques

34 articles internationaux / 2256 citations / h-index : 21 *(le 25/11/2020)*

Les articles marquants des étapes clefs de la construction de mon projet de recherche, ou représentatifs de mes activités, sont encadrés et annexés en fin de document

(34) Tardieu F, Granato ISC, Van Oosterom EJ, **Parent B,** Hammer GL. 2020. Are crop and detailed physiological models equally "mechanistic" for predicting the genetic variability of whole plant behaviour? "in silico" Plants (accepted 20th Nov 2020)

(33) Lacube S, Manceau L, Welcker C, Millet EJ, Gouesnard B, Palaffre C, Ribaut JM, Hammer G, **Parent B,** Tardieu F.(2020). Simulating the effect of flowering time on maize individual leaf area in contrasting environmental scenarios. *Journal of Experimental Botany* 71(18): 5577-5588.

(32) Nagahatenna DSK, **Parent B,** Edwards EJ, Langridge P, Whitford R. (2020). Barley Plants Overexpressing Ferrochelatases (HvFC1 and HvFC2) Show Improved Photosynthetic Rates and Have Reduced Photo-Oxidative Damage under Drought Stress than Non-Transgenic Controls. *Agronomy-Basel* 10(9).

(31) Ding L, Milhiet T, Couvreur V, Nelissen H, Meziane A, **Parent B,** Aesaert S, Van Lijsebettens M, Inzé D, Tardieu F, Draye X, Chaumont F. (2020). Modification of the Expression of the Aquaporin ZmPIP2;5 Affects Water Relations and Plant Growth. Plant Physiology, 182: 2154-2165.

(30) Baumont, M., **Parent, B**., Manceau, L., Brown, H., Driever, S., Muller, B., Martre, P. (2019). Experimental and modeling evidence of carbon limitation of leaf appearance rate for spring and winter wheat. Journal of Experimental Botany. 70. 2449-2462.

(29) Parent, B., Millet, E. J., Tardieu, F. (2019). The use of thermal time in plant studies has a sound theoretical basis provided that confounding effects are avoided. *Journal of Experimental Botany, 70* (9), 2359-2370.

(28) Parent, B., Leclere, M., Lacube, S., Semenov, M. A., Welcker, C., Martre, P., Tardieu, F. (2018). Maize yields over Europe may increase in spite of climate change, with an appropriate use of the genetic variability of flowering time. *Proceedings of the National Academy of Sciences of the United States of America, 115* (42), 10642-10647.

(27) Lacube, S., Fournier, C., Palaffre, C., Millet, E. J., Tardieu, F**., Parent, B**. (2017). Distinct controls of leaf widening and elongation by light and evaporative demand in maize. *Plant, Cell and Environment, 40* (9), 2017-2028.

(26) Lohraseb, I., Collins, N. C., **Parent, B.** (2017). Diverging temperature responses of CO2 assimilation and plant development explain the overall effect of temperature on biomass accumulation in wheat leaves and grains. *AoB Plants*. DOI : 10.1093/aobpla/plw092

(25) Parent, B., Bonneau, Maphosa, Kovalchuk, Langridge, Fleury (2017). Quantifying wheat sensitivities to environmental constraints to dissect G x E in the field. *Plant Physiology, 174* (3), 1669-1682.

(24) Tardieu, F., **Parent, B.** (2017). Predictable 'meta-mechanisms' emerge from feedbacks between transpiration and plant growth and cannot be simply deduced from short-term mechanisms. *Plant, Cell and Environment, 40* (6), 846-857.

(23) Kovalchuk, N., Laga, H., Cai, J., Kumar, P., **Parent, B.,** Lu, Z., Miklavcic, S. J., Haefele, S. M. (2017). Phenotyping of plants in competitive but controlled environments: a study of drought response in transgenic wheat. *Functional Plant Biology, 44* (3), 290-301.

(22) Parent, B., Vile, D., Violle, C., Tardieu, F. (2016). Towards parsimonious ecophysiological models that bridge ecology and agronomy. *New Phytologist, 210* (2), 380-382.

(21) Shirdelmoghanloo, H., Lohraseb, I., Rabie, H. S., Brien, C., **Parent, B.,** Collins, N. C. (2016). Heat susceptibility of grain filling in wheat (*Triticum aestivum* L.) linked with rapid chlorophyll loss during a 3-day heat treatment. *Acta Physiologiae Plantarum, 38* (8).

(20) Parent, B., Shahinnia, F., Maphosa, L., Berger, B., Rabie, H., Chalmers, K., Kovalchuk, A., Langridge, P., Fleury, D. (2015). Combining field performance with controlled environment plant imaging to identify the genetic control of growth and transpiration underlying yield response to water-deficit stress in wheat. *Journal of Experimental Botany, 66* (18), 5481-5492.

(19) Tardieu, F., Simonneau, T., **Parent, B.** (2015). Modelling the coordination of the controls of stomatal aperture, transpiration, leaf growth, and abscisic acid: update and extension of the Tardieu–Davies model. *Journal of Experimental Botany, 66* (8), 2227-2237.

(18) Yadav, D., Shavrukov, Y. , Bazanova, N., Chirkova, L., Borisjuk, N., Kovalchuk, N., Ismagul, A**., Parent, B.,** Langridge, P., Hrmova, M., Lopato, S. (2015). Constitutive overexpression of the TaNF-YB4 gene in transgenic wheat significantly improves grain yield. *Journal of Experimental Botany, 66* (21), 6635-6650.

(17) Caldeira, C. F., Bosio, M., **Parent, B.,** Jeanguenin, L., Chaumont, F., Tardieu, F. (2014). A hydraulic model is compatible with rapid changes in leaf elongation under fluctuating evaporative demand and soil water status. *Plant Physiology, 164* (4), 1718-1730.

(16) Kumudini, S., Andrade, F., Boote, K., Brown, G., Dzotsi, K., Edmeades, G., Gocken, T., Goodwin, M., Halter, A., Hammer, G., Hatfield, J., Jones, J., Kemanian, A., Kim, S.-H., Kiniry, J., Lizaso, J., Nendel, C., Nielsen, R., **Parent, B.,** Stockle, C., Tardieu, F., Thomison, P., Timlin, D., Vyn, T., Wallach, D., Yang, H., Tollenaar, M. (Auteur

de correspondance) (2014). Predicting maize phenology: intercomparaison of functions for developmental response to temperature. *Agronomy Journal, 106* (6), 2087-2097.

(15) Parent, B., Tardieu, F. (2014). Can current crop models be used in the phenotyping era for predicting the genetic variability of yield of plants subjected to drought or high temperature? *Journal of Experimental Botany, 65* (21), 6179-6189.

(14) Tardieu, F., **Parent, B.,** Caldeira, C. F., Welcker, C. (2014). Genetic and physiological controls of growth under water deficit. *Plant Physiology, 164* (4), 1628-1635.

(13) Maphosa, L., Langridge, P., Taylor, H., **Parent, B.**, Emebiri, LC., Reynolds, MP., Okada, A., Mather, DE. (2014). Genetic control of grain yield and grain physical characteristics in a bread wheat population grown under a range of environmental conditions. *Theoretical and Applied Genetics, 127* (7), 1607-1624.

(12) Bonneau, J., Taylor, J., Parent, B., Bennett, D., Reynolds, M., Feuillet, C., Langridge, P., Mather, D. (2013). Multi-environment analysis and improved mapping of a yield-related QTL on chromosome 3B of wheat. *Theoretical and Applied Genetics, 126* (3), 747 - 761.

(11) Huang, C. Y. ; Kuchel, H. ; Edwards, J. ; Hall, S. ; **Parent, B.** ; Eckermann, P. ; Herdina ; Hartley, D. M. ; Langridge, P. ; McKay, A. C. (2013). A DNA-based method for studying root responses to drought in field-grown wheat genotypes. *Nature Scientific Reports, 3* (3194).

(10) Parent, B., Tardieu, F. (2012). Temperature responses of developmental processes have not been affected by breeding in different ecological areas for 17 crop species. *New Phytologist, 194* (3), 760-774.

(9) Parent, B., Turc, O., Gibon, Y., Tardieu, F. (2010). Modelling temperature-compensated physiological rates, based on the co-ordination of responses to temperature of developmental processes. *Journal of Experimental Botany, 61* (8), 2057-2069.

(8) Parent, B., Suard, B., Serraj, R., Tardieu, F. (2010). Rice leaf growth and water potential are resilient to evaporative demand and soil water deficit once the effects of root system are neutralized. *Plant, Cell and Environment, 33* (8), 1256-1267.

(7) Tardieu, F., **Parent, B.,** Simonneau, T. (2010). Control of leaf growth by abscisic acid: hydraulic or non-hydraulic processes? *Plant Cell and Environnement, 33 (4),* 636-647

(6) Poiré, R., Wiese-Klinkenberg, A., **Parent, B**., Mielewczik, M., Schurr, U., Tardieu, F., Walter, A. (2010). Diel time-courses of leaf growth in monocot and dicot species: endogenous rhythms and temperature effects. *Journal of Experimental Botany, 61* (6), 1751-1759.

(5) Morran S., Eini O., Pyvovarenko T., **Parent B**., Singh R., Ismagul A., Eliby S., Shirley N., Langridge P., Lopato S. (2010). Improvement of stress tolerance of wheat and barley by modulation of expression of DREB/CBF factors. *Plant Biotechnology Journal* 9 (2): 230-249.

(4) Berger B., **Parent B**., Tester M. (2010). High-throughput shoot imaging to study drought responses. *Journal of Experimental Botany* 61 (13): 3519-3528 .

(3) Parent, B., Conejero, G., Tardieu, F. (2009). Spatial and temporal analysis of non-steady elongation of rice leaves. *Plant, Cell and Environment, 32* (11), 1561-72.

(2) Parent, B., Hachez, C., Redondo, E., Simonneau, T., Chaumont, F., Tardieu, F. (2009). Drought and Abscisic Acid Effects on Aquaporin Content Translate into Changes in Hydraulic Conductivity and Leaf Growth Rate: A Trans-Scale Approach. *Plant Physiology, 149* (4), 2000-2012.

(1) Voisin, A.-S., Reidy, B., **Parent, B.,** Rolland, G., Redondo, E., Gerentes, D., Tardieu, F., Muller, B. (2006). Are ABA, ethylene or their interaction involved in the response of leaf growth to soil water deficit? An analysis using naturally occurring variation or genetic transformation of ABA production in maize. *Plant, Cell and Environment, 29* (9), 1829-1840.

Articles de vulgarisation scientifique

(1) Parent, B., Welcker, C., Tardieu, F. (2019). Des rendements maintenus en adaptant la précocité. *Perspectives agricoles*, **462,** 38-41

Modèles publiés

(2) Manceau L, Lacube SZ, Parent B, Tardieu F. 2020. SiriusQuality-BioMa-MaizeLAI-Component. Zenodo http://doi.org/10.5281/zenodo.3569347

(1) Manceau L, Martre P, Beaumont M, Parent B, Muller B. 2018. SiriusQuality-BioMa-Phenology-Component. (Version v1.0.0). Zenodo http://doi.org/10.5281/zenodo.2478791.

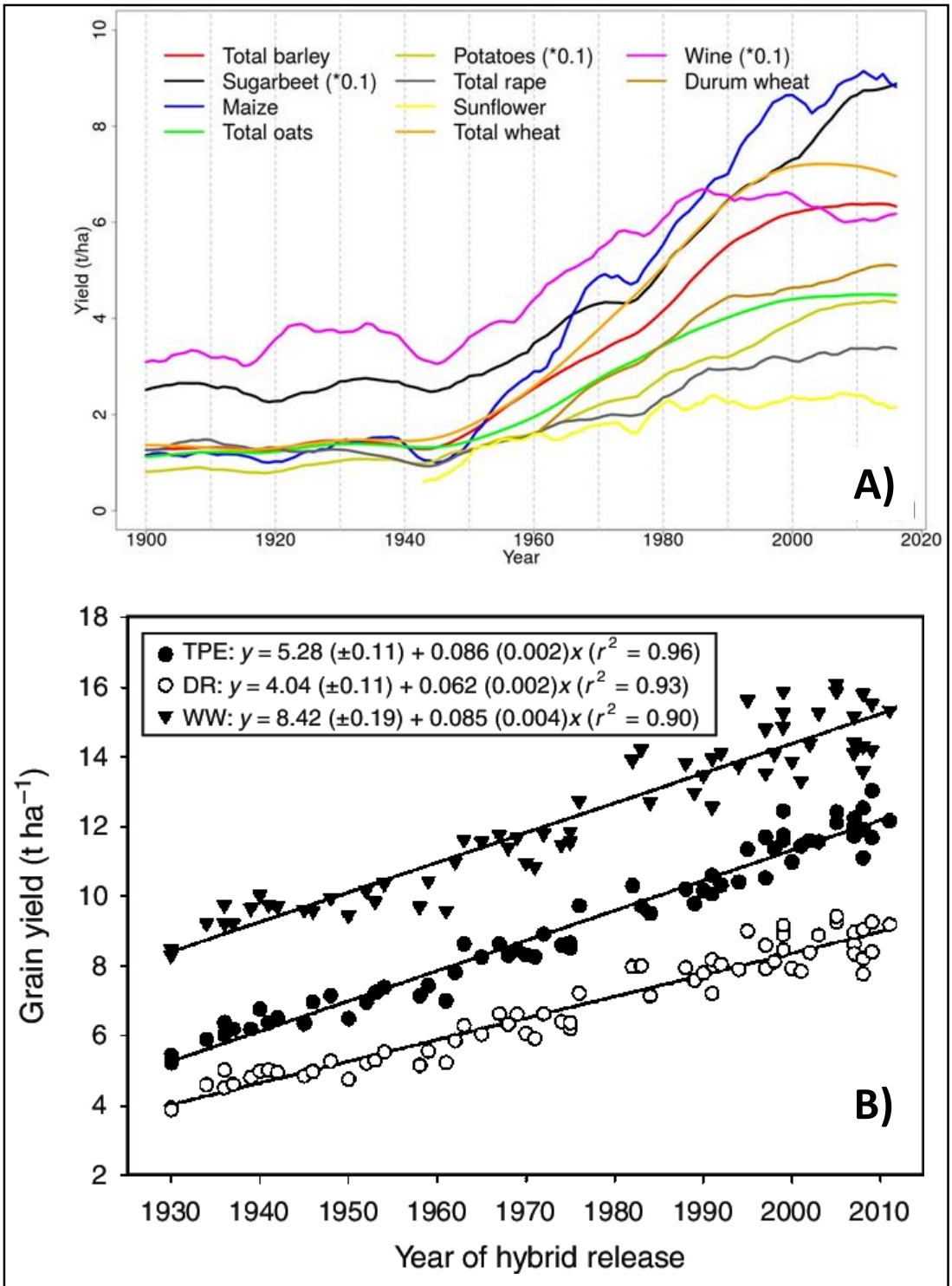

<u>Figure 1</u>: Evolution des rendements en grains.

A) Evolution des rendements en France de 1900 à 2016***. Issus de Schauberger, B., Ben-Ari, T., Makowski, D. et al.. Sci Rep (2018).***

B) Evolution des rendements en grain chez des maïs hybrides mis sur le marché par Pioneer entre 1930 et 2011. TPE. Population cible d'environnements aux US. DR. Expérience ciblées sous sécheresse. WW. Expériences bien irriguées. ***Issus de Cooper et al., Crop & Pasture Science, 2014***.

5. PROJET SCIENTIFIQUE

Contexte

Le changement climatique va accentuer les interactions Génotype x Environnement.

L'agriculture fait face à l'augmentation de la demande de production agricole à l'échelle du globe ainsi qu'au changement climatique, qui augmente la fréquence des épisodes de sècheresse, souvent combinés à de fortes température et une forte demande évaporative (Lobell *et al.*, 2011). La sélection variétale a été jusque-là efficace, avec des progressions observées de l'ordre de +1% de rendement par an chez la plupart des grandes cultures (Fig. 1A, Duvick, 2005 ; Brisson *et al.*, 2010; Cooper *et al.*, 2014), même pour des conditions de sécheresse (Fig1B, Cooper *et al.*, 2014). Cependant, chez la plupart des céréales, on observe une stabilisation des rendements en France et à l'échelle européenne depuis 2010 (Fig.1 A ; Schauberger *et al.*, 2018), ainsi qu'une augmentation des oscillations interannuelles de la production agricole dans différentes régions du globe (Urban *et al.*, 2015), principalement dû à la multiplicité des scénarios de sécheresses (Fischer & Knutti, 2012).

Alors même que ce phénomène s'intensifie, et que l'augmentation de la population mondiale exacerbe les tensions sur l'usage de l'eau, la société et les pouvoirs publics sont en attente d'une évolution rapide de l'agriculture vers une agriculture plus durable (Pe'er *et al.*, 2019), moins gourmande en intrants et plus économe en eau (Alamanos *et al.*, 2019). Dans ce contexte, le maintien des rendements ne sera assuré que par l'optimisation de stratégies d'utilisation de l'eau (Tardieu, 2012; Berger *et al.*, 2016), par l'amélioration variétale (Sinclair, 2017) et des pratiques culturales. **Il est donc urgent de développer rapidement de nouvelles variétés plus économes en eau (Davies & Bennett, 2015) adaptées aux spécificités agronomiques et climatiques locales (Jeuffroy *et al.*, 2014).**

Répondre à ce besoin est pourtant loin d'être élémentaire. En effet, le changement climatique a tendance à augmenter les interactions Génotype x Environnement ('G x E ' : la performance relative d'une variété par rapport aux autres dépend des conditions environnementales). Par exemple, en cas de sécheresse importante, chaque millimètre d'eau économisé pendant la phase végétative permet d'obtenir un état hydrique plus favorable pendant les stades plus tardifs que sont la floraison et le remplissage du grain (Sinclair, 2017). A l'opposé, en cas de sècheresse modérée, une forte réduction d'accumulation de biomasse accompagnant une réduction de la transpiration ne sera pas compensée pendant le cycle, aboutissant à des biomasses finales plus faibles (Tardieu, 2012). **Ainsi, la meilleure variété observée dans un environnement peut être un très mauvais choix dans un scenario de sècheresse différent.**

De même, les locus de caractères quantitatifs ('QTL' : Quantitative Trait Loci, région du génome associée statistiquement avec un caractère quantitatif donné) ont des effets sur le rendement qui dépendent du lieu,

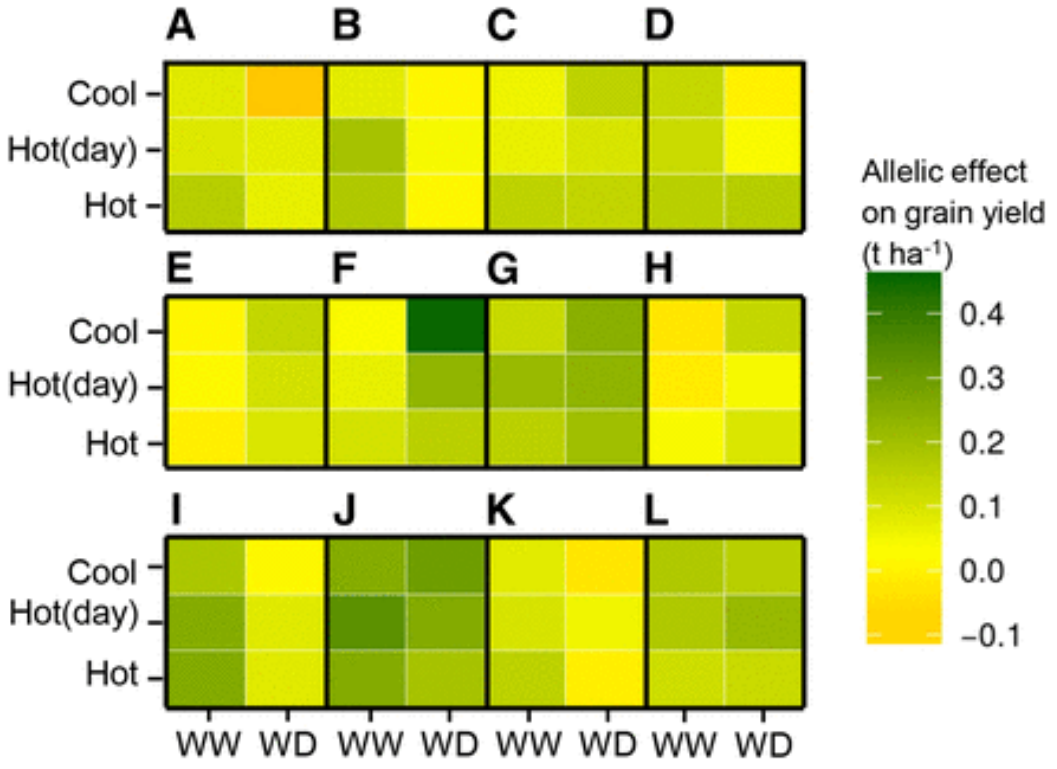

<u>Figure 2</u>. Interactions QTL x E.
Effets alléliques de 12 QTL de rendement en grains dans six scénarios environnementaux représentatifs de 29 essais au total. Vert, l'allèle augmente le rendement en grains; orange, l'allèle diminue le rendement en grains; jaune, l'effet est nul. Les effets alléliques ont été estimés dans chaque essai, puis moyennés par type de scénario environnemental. Notez que pour certains QTLs (ex: A, D, F), l'effet allélique est très dépendant des conditions environnementales (interactions QTL x E). ***Issus de Millet et al. (2016)***.

de l'année, ou des conditions de culture (Maccaferri *et al.*, 2008; Millet *et al.*, 2016; Fig. 2). Par exemple, chez le blé, un allèle spécifique d'un QTL avait un effet positif (jusqu'à +15% de rendement), dans plusieurs essais au Mexique, et un effet négatif dans les scénarios Australiens les plus secs (Bonneau *et al.*, 2013).
Une idée communément acceptée (Fukai & Cooper, 1995; Richards *et al.*, 2002) est que ces interactions G x E augmentent avec le niveau d'intégration et de complexité d'un processus biologique. D'un côté, le rendement en grain résulte de l'intégration tout au long du cycle de multiples processus sous-jacents, qui répondent différemment à l'environnement, qui ont chacun leur propre variabilité génétique, et qui interagissent entre eux directement ou au travers de feedbacks multiples (Tardieu & Parent, 2017). A l'opposé, ces processus sous-jacents seraient moins sujets aux interactions G x E (Fukai & Cooper, 1995; Richards *et al.*, 2002) et la sélection variétale basée sur des traits simples a pu réussir dans certaines situations (Fukai *et al.*, 1999; Richards, 2006). Cependant, plus largement, il est très difficile de préjuger de quelle combinaison de traits physiologiques sera la plus bénéfique dans tel ou tel environnement, tant ces traits interagissent (Drewry *et al.*, 2014). **Dans le contexte de changement climatique et d'exacerbation de ces interactions G x E, il est donc essentiel d'identifier «où et quand » une combinaison donnée de caractéristiques génétiques peut octroyer de meilleurs rendement.**

Des modèles pour prédire les interactions G x E

Une approche purement expérimentale ne peut pas explorer les conséquences sur le rendement de chaque combinaison de caractères dans toute la diversité des scénarios de sécheresse. **Une solution consiste à utiliser un modèle qui prédit les effets de traits génotypiques dans un plus grand nombre de scénarios environnementaux**, pour les conditions climatiques actuelles et futures (Yin *et al.*, 2000; Chapman *et al.*, 2002; Casadebaig *et al.*, 2011; Quilot-Turion *et al.*, 2016). Cette recherche d' « idéotypes » (Donald, 1968) vise à définir la combinaison de traits génétiques pouvant donner le meilleur rendement moyen (Jeuffroy *et al.*, 2014; Perego *et al.*, 2014; Rotter *et al.*, 2015). Un idéotype dépend forcément de l'objectif spécifique qu'il lui est imposé (ex : meilleur rendement, stabilité des rendements, … ; Andrivon *et al.*, 2013) et sera différent selon l'environnement et la conduite de culture (Schmidt & Gaudin, 2017). L'idéotypage basé sur la modélisation (Martre *et al.*, 2015a; Rotter *et al.*, 2015) nécessite donc un modèle avec des paramètres génétiques, capable de simuler l'interaction Génotype x Environnement x Conduite, combiné à des mesures phénotypiques de la variabilité génétique de ses paramètres.

Combiner cette approche avec une approche de génétique quantitative permet de simuler le rendement de plantes virtuelles caractérisées par leur profil allélique aux QTL associés avec les paramètres génétiques du modèle (Yin *et al.*, 2000; Chapman *et al.*, 2002; Tardieu, 2003; Hammer *et al.*, 2006). **Le modèle résultant de**

cette approche peut donc potentiellement indiquer '*où et quand*' une combinaison donnée d'allèles octroie un effet positif ou négatif sur la performance des plantes (Messina *et al.*, 2011).

Cette utilisation de la modélisation est très différente de celle des premiers modèles de cultures (Duncan *et al.*, 1967; de Wit *et al.*, 1970; de Wit *et al.*, 1978), qui ont principalement été construit pour prédire les conséquences de différentes conduites culturales et des conditions climatiques sur le rendement (ex : dates de semis, AcostaGallegos *et al.*, 1996; espacement des rangs, Egli & Bruening, 1992, Whish *et al.*, 2005; irrigation, Chauhan *et al.*, 2013; ou diverses conditions climatiques, Kumar *et al.*, 2009, Kim *et al.*, 2010). Plus récemment (10-15 dernières années), les modèles de cultures ont également été utilisés pour prédire les conséquences du changement climatique sur le rendement (Asseng *et al.*, 2013; Potgieter *et al.*, 2013; Harrison *et al.*, 2014; Parent *et al.*, 2018), ou pour caractériser des environnements (Chenu *et al.*, 2011; Lobell *et al.*, 2015).

Ces modèles de culture ont donc été principalement construits sur la base d'une variété « moyenne », idéalement représentative de l'espèce, pour laquelle les paramètres du modèle ont été majoritairement estimés (calibrés par inversion du modèle) plutôt que mesurés (Wallach *et al.*, 2001; Guo *et al.*, 2006; Makowski *et al.*, 2006). Pour des raisons d'homogénéité du modèle, de parcimonie et de temps de calcul, les modèles de cultures actuels se sont principalement appuyés sur des relations empiriques, et en particulier pour la croissance de la plante et la transpiration en réponse aux conditions environnementales. Par exemple, la grande majorité des modèles ne considérent pas la croissance des feuilles individuelles, et ne tiennent pas explicitement compte de la variabilité génétique des réponses de la croissance aux conditions environnementales (Parent & Tardieu, 2014). **La prédiction de l'impact de la diversité génétique de caractères quantitatifs sur les performances des plantes nécessite donc de repenser ces modèles en profondeur** (Parent & Tardieu, 2014), de telle sorte que les nouveaux paramètres génotypiques soient (1) héritables, (2) indépendants, et (3) puissent être mesurés dans une plate-forme de phénotypage pour des centaines de génotypes.

La Phénomique permet aujourd'hui de mesurer des dizaines de paramètres de modèles dans des panels de diversité de plusieurs centaines de variétés.

Pendant des années, le phénotypage (la caractérisation du phénotype, soit d'un/des caractère(s) observable(s) chez un individus), est resté un obstacle majeur en génétique quantitative (Berger *et al.*, 2010; Furbank & Tester, 2011; Yang *et al.*, 2020), mais aussi pour la modélisation des cultures. Jusqu'à récemment, obtenir des jeux de paramètres génotypique de modèles, soit l'ensemble de caractères génotypiques représentant la variété (le Phénome), pour ne serait-ce que pour quelques dizaines de variétés était plus une gageure, tant

HiT-Me High throughput metabolic phenotyping

-Composition de la Biomasse
-Profiles de métabolites ciblés ou non ciblés
-Métabolisme primaire

PhenoDyn. Phenotypage fin

580 plantes, pas de temps : 3-15 min
Transpiration / Expansion foliaire
Conductances hydrauliques

PhenoArch. High throughput imaging phenotyping

2400 plantes, Pas de temps: 4 h
Transpiration
Architecture aerienne
Croissance plante entiere
RUE, RIE
WUE

Pheno3C and DiaPHEN. High throughput field phenotyping

CO_2 (FACE) et contrôle de l'état hydrique
Thermographie infrarouge
Croissance et architecture
Transpiration

Figure 3: Plateformes pour le phénotypage haut débit de caractères à différentes échelles.

l'effort expérimental pouvait être important pour mesurer ces plusieurs dizaines de valeurs de paramètres (selon le modèle).

Ces 15 dernières années ont été marquées par l'explosion du nombre de plateformes de phénotypage haut-débit (Fiorani & Schurr, 2013), en vue de pouvoir caractériser des phénotypes dynamiques à différentes échelles (Figure 3), de métabolites (HitMe, Bordeaux, HiTMe), jusqu'à la croissance de la plante entière en conditions contrôlées (ex :parties aériennes, PhenoArch, M3P ; ou racines , Dijon, 4PMI), au champ semi-contrôlé (DiaPHEN; Pheno3C) et à l'exploitation agricole (Pieruschka & Schurr, 2019). Cependant, dans un premier temps, cette démonstration technologique ne s'est pas transformée automatiquement en données biologiques d'intérêt (Parent *et al.*, 2015; Yang *et al.*, 2020), tant manquaient des pipelines d'analyses de ces données hétérogènes à différents pas de temps. Aujourd'hui, la « Phénomique » végétale est devenue une science à part entière (Houle *et al.*, 2010; Furbank & Tester, 2011; Yang *et al.*, 2020), développant de nouvelles méthodes de traitement et de modélisation des données (Tardieu *et al.*, 2017), pour tirer parti de l'imagerie à haut débit, des technologies de capteurs, et procurer aux modélisateurs et aux généticiens des ensembles de caractères sur des centaines de variétés.

Au LEPSE, une plateforme de phénotypage avec une résolution temporelle de l'ordre de quelques minutes (PhenoDyn, 560 plantes, M3P, Fig. 3) permet la caractérisation hydraulique de centaines de génotypes; tandis que la plateforme d'imagerie automatisée PhenoArch (2400 plantes, M3P, Fig.3) permet la caractérisation 4D de la transpiration, de la croissance et de l'architecture (Cabrera-Bosquet *et al.*, 2016; Perez *et al.*, 2019). En particulier, il est désormais possible de calculer l'efficience d'interception du rayonnement (RIE, Radiation Interception Efficiency, (Cabrera-Bosquet *et al.*, 2016), l'efficience d'utilisation du rayonnement intercepté (RUE, Radiation Use Efficiency, Cabrera-Bosquet *et al.*, 2016), ainsi que la conductance stomatique de la plante entière à partir du taux de transpiration (Prado *et al.*, 2017). Ces caractères (ex : phyllochrone, vitesse de croissance, RUE, RIE) et leur sensibilité à différentes contraintes environnementales (potentiel hydrique du sol, demande évaporative) sont des paramètres génotypiques clefs des modèles de cultures. **Aujourd'hui, ils peuvent donc être mesurés plutôt qu'estimés pour des centaines de variétés.**

Croissance et transpiration en condition de sécheresse et hautes températures

La vision classique de l'amélioration variétale pour la tolérance à la sécheresse est basée sur le compromis entre disponibilité en eau pendant le cycle végétatif et pendant le remplissage du grain (Sinclair, 2017). Dans ce cadre, les leviers génétiques possibles pour développer de nouvelles variétés adaptées à des épisodes de sécheresse de plus en plus fréquents sont : (i) l'évitement, en jouant sur la précocité des variétés et leur vitesse de développement, afin que la floraison est lieu avant les épisodes de sécheresse sévère (Shavrukov *et al.*,

2017), (ii) la croissance racinaire (Lynch, 2013) et (iii) la modération de la transpiration par le contrôle hydraulique de la transpiration et la croissance foliaire (Basu *et al.*, 2016).

Même si le développement d'outils de phénotypage au champ pourrait inverser cette situation, la caractérisation de ces caractères clefs (dynamique de croissance racinaire et foliaire, contrôle temporel de la transpiration, …) est très difficile à une échelle temporelle fine (minutes à heures), et les généticiens et physiologistes des plantes ont donc eu tendance à travailler principalement sur des traits constitutifs (par exemple, enracinement profond, Lynch, 2013 ; efficience, Curin *et al.*, 2020) dans des conditions artificiellement stables. Pourtant, la plupart du temps, ces caractères constitutifs permettent des gains conséquents uniquement dans une gamme limitée d'environnements types. Par exemple, diminuer fortement la transpiration en ciblant des processus physiologiques constitutifs (ex, le nombre de stomates Chaerle *et al.*, 2005; Bertolino *et al.*, 2019) peut apporter un nouvel éclairage sur leurs contrôles génétiques, mais l'objectif de maintenir les rendements n'est alors remplie que dans des conditions de sécheresse très sévère, qui ne se produisent que rarement dans un contexte agricole. De même, un système racinaire plus profond peut être bénéfique en cas de réserves disponibles en profondeur, mais c'est au contraire un système racinaire superficiel qui sera bénéfique dans le cas de sols peu profonds et en cas d'épisodes réguliers de faibles précipitations (par exemple en Australie du sud, Izanloo *et al.*, 2008), comme semble le montrer une analyse comparative chez des espèces sauvages annuelles (Schenk & Jackson, 2002). Pourtant, la recherche a jusqu'à récemment largement ignoré les processus adaptatifs dynamiques dans des environnements fluctuants, laissant de côté une large gamme de mécanismes temporels d'intérêt pour l'amélioration variétale, et donc les allèles/gènes associés.

Les plantes s'adaptent constamment aux changements rapides de leur microclimat (température, demande évaporative, rayonnement), en particulier par le contrôle de la transpiration (Faralli *et al.*, 2019; Hatfield & Dold, 2019). La transpiration est contrôlée à long terme par la dynamique de la surface foliaire (vitesse d'expansion et senescence) et à court terme par la fermeture des stomates (Sinclair, 2017). Les contrôles de la conductance stomatique et de l'expansion foliaire sont donc des acteurs clés de la variabilité génétique et environnementale de la transpiration (Tardieu & Parent, 2017). Ils dépendent tous deux des potentiels hydriques locaux dans les feuilles, qui eux-mêmes réagissent à la transpiration (Tardieu *et al.*, 2015). De plus, la conductance stomatique et l'expansion foliaire suivent un contrôle chimique impliquant, chez le maïs, l'hormone de stress acide abscissique (ABA, Parent *et al.*, 2009). L'effet de l'ABA sur la fermeture stomatique est bien documenté (Zhang & Davies, 1990; Holbrook *et al.*, 2002; Pantin *et al.*, 2013) mais la contribution de l'ABA à l'expansion foliaire diffère entre les études (voir Focus N°1). Il en résulte de multiples rétroactions à différents pas de temps avec des effets complexes sur le flux de transpiration, ce qui signifie **que les relations entre les processus ne sont pas simples à analyser sans modèles mécanistes** (Tardieu & Parent, 2017).

De plus, le contrôle de la transpiration affecte à la fois les réponses des plantes à la température et au déficit hydrique. Au champ, des épisodes de sécheresse et de stress thermique sont très susceptibles de se produire simultanément (Barnabas *et al.*, 2008), en raison d'un temps ensoleillé, chaud et sec, mais également en raison du contrôle de la transpiration et de ses effets sur la température et l'état hydrique de la plante (Rizhsky *et al.*, 2002):

-Les plantes réagissent à la sécheresse en fermant les stomates, ce qui augmente la température de la feuille.

-L'augmentation de la température de l'air augmente la demande évaporative imposée aux feuilles par l'atmosphère, entraînant une augmentation de la transpiration qui peut à son tour provoquer une déshydratation des tissus, et celle du sol à plus long terme.

En étant fortement lié à la photosynthèse (en raison du passage commun de l'eau et du CO2 à travers les stomates) et en interagissant avec à la fois avec la température et le déficit hydrique, le control temporel de la transpiration (via la croissance foliaire et la conductance stomatique) est donc largement responsable des fortes interactions G x E sous déficit hydrique et fortes températures.

Dissection écophysiologique de caractères

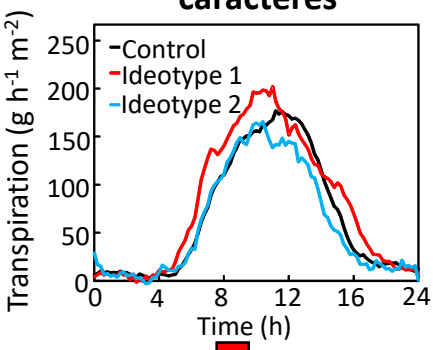

Phénotypage haut débit de la diversité génétique

Co-construction

Modèles écophysiologiques

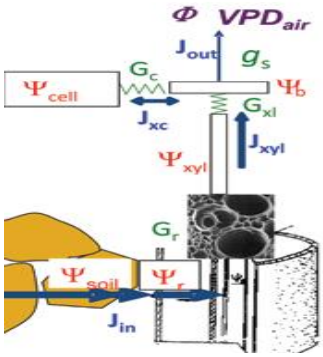

formalismes

paramètres

Modèle de culture incluant la diversité génétique

Espace des possibles dans la combinaison de caractères (espace phénotypique)

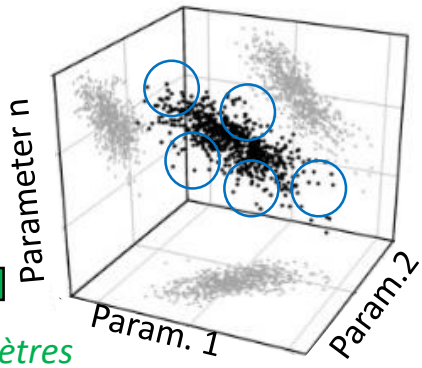

paramètres

Conséquences de la diversité génétique dans des scenarios présents et futurs

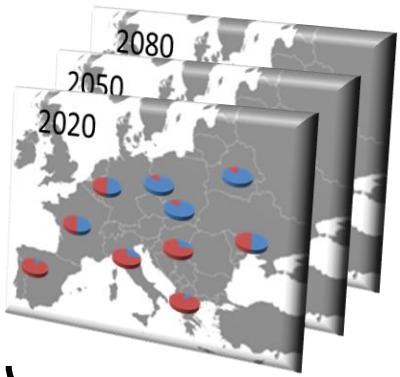

Idéotypes réalistes adaptés à chaque scénarios

Impact: Stratégies d'adaptation et sélection

Figure 4: Stratégie de mon projet de recherche : Diagramme de flux des activités de recherche.

Objectifs et Stratégie Générale

Mon objectif, commun à la fois à ma thèse, mon Postdoc, mes travaux actuels de chargé de recherche à l'UMR LEPSE et mon projet futur, est d'identifier des caractères adaptatifs qui peuvent donner un avantage comparatif (rendement, stabilité et résilience des rendements, bilan environnemental, services écosystémiques…) dans des scénarios climatiques affectés par les changements climatiques, comprenant des périodes de sécheresse et de températures élevées, dans différents systèmes de culture et pratiques culturales.

Dans ce contexte, mon approche fait appel à (i) la dissection écophysiologique de caractères fins, (ii) le phénotypage haut débit pour analyser la diversité génétique de ces caractères, (iii) la modélisation pour prédire l'impact de cette diversité à plus large échelle (Fig.4).

Dissection Ecophysiologique des réponses de processus dynamiques à des contraintes abiotiques

La première étape est d'analyser des caractères d'intérêts pour l'adaptation à des scenarios de sécheresse et de hautes températures, en particulier les réponses de processus dynamiques à ces contraintes abiotiques. Par exemple, les profils temporels (de la minute à toute la durée du cycle, selon le processus) du développement de la plante (initiations des feuilles, phyllochrone, floraison, tallage), des vitesses d'expansion (feuilles, plante entière), et de la transpiration et des échanges gazeux, dans des scénarios environnementaux contrastés de température, de demande évaporative, de déficit hydrique, de rayonnement, et de CO_2. Ces caractères étant parfois difficile à décorréler dans des environnements fluctuants (Tardieu & Parent, 2017), leur analyse nécessite de développer des modèles écophysiologiques pour tester des hypothèses, s'affranchir des effets de variables environnementales, de stades de développement ou plus généralement de différences de vitesses absolues de croissance et de développement.

Analyse haut débit de la variabilité génétique intra- et inter-spécifique

L'analyse de la variabilité génétique de ces processus et de leurs réponses à différentes variables environnementales utilise tous les outils à disposition pour le phénotypage haut débit, en conditions contrôlées et au champ. Cela nécessite souvent d'adapter ces outils, et/ou de développer des pipelines spécifiques d'analyse de ces réponses. L'analyse d'une très grande variabilité génétique chez une espèce, chez des panels de diversité représentatifs de la diversité d'une espèce, ou l'analyse de la diversité à des échelles inter-spécifique nécessite d'autant plus d'adapter les outils, les protocoles et les cadres d'analyse.

Obtenir un vecteur de paramètres de modèle chez des centaines de variétés nécessite de cumuler (i) phénotypage fin de variable dynamiques à l'échelle de l'organe, en utilisant par exemple la plateforme *Phenodyn* (profils temporels d'élongation foliaire et de transpiration, réponses dynamiques aux changements soudains de conditions environnementales, …), (ii) des variables plus intégrées à l'échelle de la plante entière dans la plateforme *PhenoArch* (efficience de transpiration, efficience d'interception du rayonnement, efficience de conversion du rayonnement, conductance stomatique, croissance de la plante entière), (iii) des outils classiques de l'écophysiologie (potentiels foliaires, échanges gazeux, …), (iv) des suivis de mesures manuelles non destructives (tallage, développement foliaire, …) ou (v) destructives (dimensions d'organes individuels, biomasse).

Prédire l'impact de la variabilité génétique à large échelle

Prédire l'impact de cette diversité dans des scénarios présents et futurs nécessite de développer des modèles écophysiologiques dont les paramètres génotypiques peuvent être reliés aux processus étudiés. Ces modèles peuvent être utilisés tels-quels pour prédire l'impact (à court terme) de la variabilité génétique, dans des scenarios qui n'ont pas été testés expérimentalement, et/ou de valider des hypothèses.

Insérer/coupler ce(s) modèle(s) avec un modèle de culture capable de simuler tout le développement de la culture, du semis jusqu'à la récolte, permet de prédire l'impact de la variabilité génétique observée sur des variables intégrées d'intérêt agronomique (rendement, stabilité et résilience des rendements, bilan environnemental, services écosystémiques…), dans de multiples scénarios climatiques présents ou futurs.

Enfin, l'analyse de l'espace phénotypique (l'ensemble des possible dans la combinaison de valeurs de paramètres) et la simulation de génotypes virtuels couvrant cet espace permet de prédire quel sera l'idéotype (meilleur combinaison de caractères/paramètres) adaptés à chaque type d'environnement.

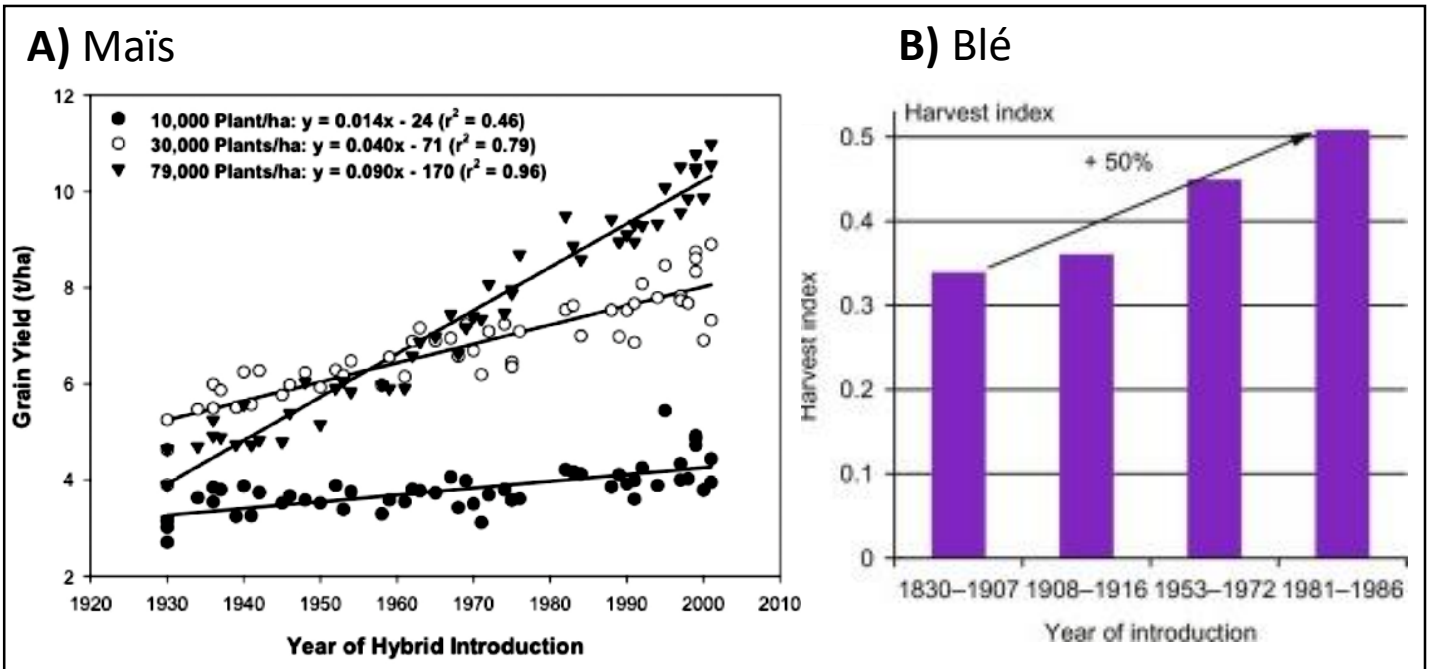

Figure 5. **Progrès génétique chez le maïs et le blé.**
A. Rendement en grain chez des hybrides de maïs mis sur le marché américain de 1930 à 2002 pour trois niveau de densité de semis (Duvick, 2005, Maydica 50: 193-202). **B.** Harvest Index (Index de récolte) pour des variétés de blé mises sur le marché à différentes périodes (Hay, R.K.M., 1995. Ann. Appl. Biol. 126, 197–216).

Points clés

Pourquoi des processus adaptatifs ?

Ce projet s'articule donc autour de processus adaptatifs dynamiques sous conditions fluctuantes. Ces processus ont été longtemps largement oubliés par les sélectionneurs et une grande partie de la recherche académique, au profit de caractères pouvant donner des avantages dans le maximum d'environnements. Cependant, autant mon projet que plus largement celui de MAGE, font le pari que la sélection est bientôt au bout de ces « super-caractères » constitutifs, issus de la révolution verte, qui ont permis d'augmenter les rendements depuis 50 ans, et ce, de manière constitutive (le progrès génétique est similaires dans la plupart des environnements, Fig.2). Par exemple, le progrès génétique chez le blé a été largement porté par l'augmentation de l'index de rendement (HI, Harvest Index, Fig.5B ; (Hay, 1995)), accompagné de statures courtes (Borlaug, 1971). Chez le maïs, le progrès génétique a principalement été le résultat d'une durée de remplissage du grain plus longue (garder des feuilles photosynthétiquement active plus longtemps : stay-green ; et dessèchement plus rapide), un plus court intervalle de floraison Male-Femelle (ASI, Anthesis-Silking Interval) et une tolérance à la forte densité, en augmentant l'efficience d'interception de la lumière dans des couverts fermés (Duvick, 2005; Hammer *et al.*, 2009; Drewry *et al.*, 2014) permise par des architectures adaptées (port érigé, Duvick, 2005). Cependant, pour chacun de ces traits, il existe des limites physiques qui seront (ou sont déjà) bientôt atteintes (ex : Long *et al.*, 2006, l'efficience d'utilisation du rayonnement serait déjà à 70% de son niveau maximal théorique chez les C3 et les C4). Optimiser les durées de phases de développement est forcément limité par la durée du cycle lui-même, l'ASI est d'ores et déjà proche de zéro, les plantes ne pourront pas intercepter plus de rayonnement que celui qu'elles reçoivent, et il faudra toujours un minimum de carbone affecté à la structure de la plante (HI ne peut pas croitre indéfiniment).

Au contraire, ce projet pari sur des processus adaptatifs, qui peuvent constituer un nouveau réservoir de traits et d'allèles pour la sélection si nous sommes capables de prédire dans quelles conditions ils peuvent conduire à améliorer les performances.

Quels modèles pour quels usages ?

Cette approche fait appel à différents types de modèles, que ce soit pour mieux comprendre un processus physiologique (défricher, casser des corrélations, tester des hypothèses), déterminer des variables qui ne sont pas directement mesurables, ou pour prédire l'impact de la variabilité génétique dans des scenarios environnementaux et de conduites contrastés.

Des modèles statistiques, des analyses multivariées :

Ce type de modèles vient la plupart du temps très tôt dans l'analyse. Ils permettent de déchiffrer un jeu de données complexe, d'observer les relations entre variables, d'identifier des variables biologiques clefs et leurs relations avec l'environnement.

Dans un deuxième temps, des analyses multivariées permettent d'analyser les liens et contraintes entre variables biologiques et d'analyser l'espace phénotypique de paramètres dans une diversité génétique donnée (voir dessous).

Des modèles écophysiologiques :

C'est le cœur de l'approche et le cœur de mon savoir-faire. Un modèle écophysiologique essaye de représenter un processus (une/des variable(s) d'état) à partir de facteurs génotypiques et environnementaux, autrement dit simuler l'interaction G x E sur un (des) processus. Une variable d'état découle des interactions entre variables d'états sous-jacentes et l'environnement, et est donc la propriété émergente du modèle. Ils nécessitent des scenarios environnementaux contrastés et des données trans-échelles à pas de temps court, pour formaliser des profils temporels et spatiaux de variables d'état, tester des hypothèses de causalité, et identifier des formalismes valides dans des gammes environnementales larges. Là encore, ces modèles sont développés à différentes échelles d'intégration et utilisés pour différents objectifs.

-Des modèles écophysiologiques sont développés dans un premier temps pour mieux comprendre le phénomène observé, et tester l'hypothèse mécaniste choisie.

-Des modèles écophysiologiques peuvent permettre de s'affranchir de cofacteurs dans l'analyse d'un processus donné (par exemple, s'affranchir de la température pour analyser l'impact de la demande évaporative), ou pour déterminer des variables qui ne sont pas directement mesurables (par exemple, des modèles architecturaux sont nécessaires pour calculer l'interception du rayonnement et donc l'efficience d'interception ou d'utilisation du rayonnement).

-Enfin ces modèles peuvent être développés pour prédire l'impact de conditions environnementales et/ou de la variabilité génétique de caractères sur une variable biologique. Ces modèles sont la plupart du temps construit spécifiquement pour cet usage, ou dérivés (dégradés) de modèles écophysiologiques plus complexes pour qu'ils soient plus limités en nombre de paramètres, prennent en comptes moins de facteurs et soient adaptés à des simulations à plus large échelles.

Ces modèles n'échappent pas sempiternel débat « mécaniste ou statistique ? », qui, bien que dépassé, revient à chaque étape et chaque soumission d'article, et nécessite donc de le théoriser. D'un côté, ces modèles sont mécanistes, au sens qu'ils sont construits pour représenter un processus biologique au plus près de la réalité. Cependant, ces modèles sont développés à une échelle donnée, et les briques de bases sont des formalismes

mathématiques simples, représentant des relations entre variables à leur échelle, temporelle et spatiale, et choisis avec un souci de parcimonie et de simplicité assumé, loin des lois fondamentales de la nature. Un modèle peut donc toujours être vu comme moins mécaniste qu'un modèle à l'échelle temporelle et spatiale inférieure.

Des modèles de culture.

Le modèle de culture est en quelque sorte un 'super' modèle écophysiologique, prenant compte des processus majeurs dans la plante et pouvant simuler le comportement d'un couvert sur un pas de temps long. Intégrer un nouveau module écophysiologique n'est pas forcément facile, tant les modèles ont été construits à l'origine d'une façon très homogène dans un souci de cohérence. Par exemple, remplacer un module de croissance foliaire utilisant le concept « feuille unique » (Big-Leaf, la croissance foliaire est considérée comme la croissance d'une seule grande feuille au lieu de feuilles individuelles) par un module considérant l'expansion en longueur et en largeur de feuilles individuelles, nécessite de prendre en compte d'autres nombres de feuilles, apparaissant dans d'autres modules, et qui étaient déconnectés totalement du module de croissance foliaire (Lacube *et al.*, 2020). De plus, de nouveaux paramètres ou variable d'état peuvent être redondant avec d'autres paramètres, variables, utilisés ailleurs dans le modèle. Modifier / Remplacer des modules pour qu'ils prennent en compte la diversité génétique nécessite donc en réalité de repenser le modèle dans son ensemble.

Cette activité profite du développement du modèle de culture de blé Sirius Quality dans l'équipe, portée par Pierre Martre. Cependant, chez le maïs, nous travaillions avec APSIMmaize, (Hammer *et al.*, 2010) et nous dépendions trop jusque-là de la collaboration (quoique bénéfique) avec l'Université du Queensland (Australie) et du Pr. Graeme Hammer. Pour avoir la main réellement libre sur des développements complexes pour inclure de nouveaux processus et pour inclure la diversité génétique, il a été décidé dans l'équipe MAGE de développer notre propre modèle de maïs, basé sur le modèle Sirius Quality et nos récents développements de APSIMmaize (Lacube *et al.*, 2020).

Co-construire les cadres d'analyse du phénotype et de modélisation

Un modèle écophysiologique ayant pour but de prédire l'impact de la variabilité génétique nécessite que ses paramètres soient indépendants (dans l'autre cas, le modèle est surparamétré) et mesurables. Cela nécessite un dialogue constant entre nos méthodes de phénotypage et le choix des formalismes.

Le phénotypage (mesures, protocoles, scenarios et analyses), par essence, doit s'adapter à la question, et donc ici doit permettre d'obtenir les vecteurs de valeurs de paramètres du modèle (un génotype étant décrit par le vecteur de paramètres génotypiques du modèle). Mais les modèles s'adaptent aussi au phénotypage.

Par exemple, le modèle $APSIM_{maize}$ considère la réponse de la croissance au déficit hydrique par la réponse au ratio Offre / Demande en eau (Hammer *et al.*, 2010). Cette variable n'étant pas directement mesurable, il n'est pas possible d'analyser la réponse à cette variable, et a fortiori sur des centaines de variétés (Parent & Tardieu, 2014). Un modèle écophysiologique prenant en compte les capacités réelles de mesure d'une plateforme de phénotypage (par exemple la réponse de l'expansion d'une feuille individuelle au potentiel hydrique du sol sur la plateforme *PhenoDyn*) permettra au contraire de caractériser la variabilité génétique, et l'analyse de son impact dans différents scénarios.

Les modèles peuvent être modifiés par les résultats même du phénotypage à large échelle. Par exemple, l'interdépendance de 2 paramètres n'est dans certains cas observée qu'après le phénotypage d'une large gamme de variétés dans différents scenarios environnementaux. Dans ce cas-là le modèle peut être revu, les variables explicatives modifiées, dans le but d'obtenir un formalisme avec de nouveaux paramètres mesurables et indépendants.

Le phénotypage (outils, méthodes, scenarios, protocoles, pipelines d'analyses) et le modèle sont donc co-construits afin que chacun soit adapté aux possibilités de l'autre. Autant le fait que le phénotypage réponde aux demande d'un modèle est assez classique, mais le fait que le choix d'un formalisme dépende du fait qu'il soit adapté au phénotypage à grande échelle représente une rupture majeure avec les premiers modèles développés pour étudier l'impact de pratiques agronomiques.

Que nous apprennent les études comparatives ?

Les communautés de scientifiques (généticiens, physiologistes des plantes…) sont largement articulées autour des espèces. Il en est de même chez les modélisateurs ; par exemple, le plus large consortium de modélisateurs, AgMIP (Agricultural Model Intercomparison and Improvement Project, Rosenzweig *et al.*, 2013) s'organise autour des espèces. Les comparaisons inter-specifiques sont principalement limitées à l'écologie (évolution, fitness…) et à la génétique/génomique (synthénie). Pourtant, les analyses comparatives, et, plus largement, les analyses à l'échelle inter-specifique peuvent amener des éclairages cruciaux en écophysiologie et en modélisation.

1) D'une façon classique en analyses comparatives, l'analyse des différences / similarités entre espèces et de la structure de la variabilité génétique peut permettre d'approcher les probables mécanismes explicatifs sous-jacents, ainsi que les facteurs externes structurant la diversité (ex : climat d'origine, pression de sélection, ploïdie, allométrie, ontogénie, …)

2) Pour la compréhension d'un processus donné, l'échelle interspécifique permet d'exploser la diversité génétique et augmenter la puissance pour tester des hypothèses fonctionnelles. Par exemple, cette échelle

peut permettre de casser des corrélations entre variables ou d'observer des corrélations qui n'apparaissaient pas à l'échelle intra-spécifique, et donc de mieux tester l'interdépendance de variables / processus. Un test d'hypothèse à cette échelle et une validité trans-espèces amène une robustesse qui n'aurait pas été possible dans une gamme de diversité génétique limitée.

3) L'analyse d'une large diversité génétique peut permettre d'indiquer ou aller chercher la variabilité génétique (et « faut-il la chercher ? »). Par exemple, nous avons montré qu'il était surement vain de rechercher une variabilité génétique de la réponse de la vitesse de développement à la température chez une espèce, car aucune variabilité génétique n'était observée chez aucune des 18 espèces étudiées (Parent & Tardieu, 2012). Dans le cas d'espèces apparentées, une telle analyse peut au contraire indiquer qu'une source de diversité peut être trouvée dans une espèce voisine, comme cela peut être le cas chez des ancêtres du blé moderne, dont la variabilité génétique pourrait être introduite au moyen de blés synthétiques (Gorafi *et al.*, 2018).

4) Enfin, et peut être l'intérêt le plus important, analyser des espèces différentes en parallèle permet de revisiter une espèce avec un nouveau regard. En étudiant une seule espèce, nos recherches se focalisent vite sur quelques processus qui apparaissent les plus importants. De possibles variables explicatives peuvent être oubliées aux profit d'effets majeurs d'autres variables. Par exemple, le phyllochrone est très stable chez le maïs. Mais observer des effets majeurs du statut carboné (voir Focus n° 4) chez le blé peut amener à réétudier des jeux de données chez le maïs et interpréter différemment les observations.

Définir l'espace Phénotypique : pour des idéotypes réalistes

Aussi indépendants que possible du point de vue mécaniste, des caractères génotypiques (ou paramètres de modèle) peuvent être corrélés entre eux dans des panels de diversité en raison de contraintes communes sur ces caractères (Donovan *et al.*, 2011). Une liste non-exhaustive de ces contraintes (Antonovics & Vantienderen, 1991, pour une approche absurde de la définition de « contraintes ») chez les plantes comprend :

(i) L'évolution et la sélection. Des variétés / espèces ont pu évoluer dans la même direction sur plusieurs caractères car soumises aux même contraintes environnementales ou agronomiques (Mayr & Provine, 1980).

(ii) La génétique. En effet, l'espace génétique est lui-même contraint, car l'architecture génétique est robuste (Koonin & Wolf, 2010). De plus, des gènes peuvent co-évoluer car situés à une très faible distance génétique. Enfin, des caractères différents peuvent être contrôlés par les même facteurs de transcriptions ou autre processus de régulation de transcription peu spécifiques).

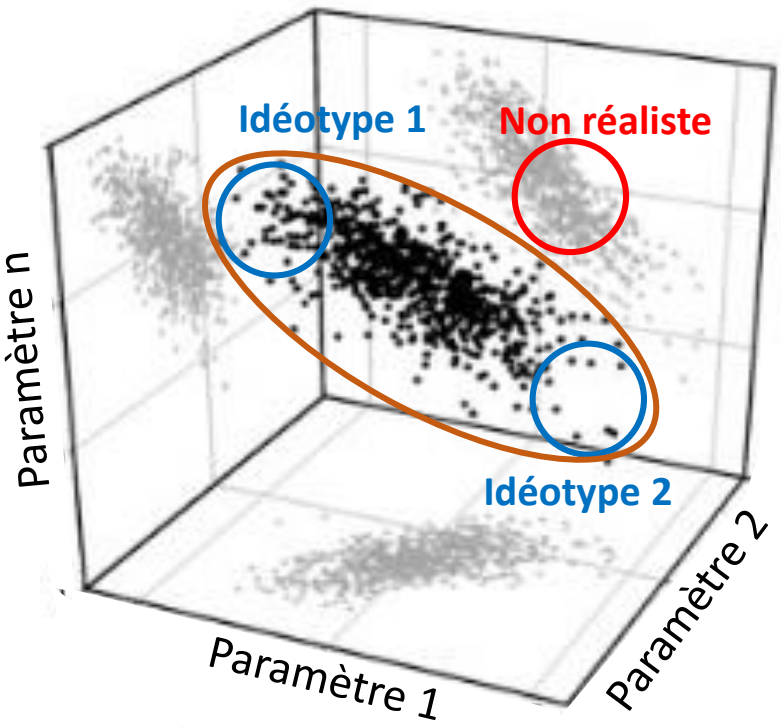

Figure 6. Exemple d'un espace phénotypique sur trois caractères (ou paramètres génotypiques d'un modèle). L'espace théorique des combinaisons de valeurs possibles est un cube (3 dimensions). Mais toutes les combinaisons de valeurs de paramètres ne sont pas possibles. L'ensemble des combinaisons possibles de valeurs de paramètres délimitent l'espace phénotypique (représenté en orange). Des combinaisons de paramètres sont possibles (Idéotypes, en bleu), d'autres ne sont pas présentes dans la diversité naturelle et ne sont surement pas atteignables par la sélection (en rouge).

(iii) La biophysique. Par exemple, toutes les réactions chimiques suivent la loi d'Arrhenius, et les vitesses de processus biologiques plus intégrés suivent aussi cette loi (Dell *et al.*, 2011; Parent & Tardieu, 2012).

(iv) La structure et l'architecture même des plantes. Par exemple, l'eau et le CO_2 diffusent par les mêmes stomates, liant fortement photosynthèse et transpiration, et limitant la chance d'observer une variété avec une très forte photosynthèse et une faible transpiration (du moins chez les C4, et sur un pas de temps court, voir Cas d'étude N°5).

Ainsi, toutes les combinaisons de valeurs de *n* traits ne représentent pas un hyper-cube de *n* dimensions (le cube de la vie, Raup & Michelso, 1965) et ne sont pas disponibles dans la variabilité naturelle. L'ensemble des contraintes et des corrélations génétiques entre les traits définit l'ensemble des possibilités, appelé ***espace phénotypique***, ne représentant qu'une partie de l'hyper-cube (Fig.6). L'espace phénotypique est un concept très utile en écologie, en recherche perpétuelle de lois simple, valides chez un grand nombre d'espèces et de genres. Parmi, les cas concrets les plus connus d'espaces phénotypiques très contraints, on peut citer le compromis foliaire entre allocation et acquisition des ressources (Leaf Economics Spectrum, Wright *et al.*, 2004; Shipley *et al.*, 2006).

Jusqu'à présent, la plupart des études d'idéotypes ont utilisé des espaces phénotypiques non contraints (Casadebaig *et al.*, 2016; Paleari *et al.*, 2017), « surfant » dans l'hypercube des paramètres pour en rechercher la meilleur combinaison (Paleari *et al.*, 2017). Cela peut aboutir à conclure sur l'avantage de telle ou telle combinaison de caractères, mais il est fort possible que cette combinaison ne puisse être rencontrée dans la diversité génétique naturelle et ne puisse être réalisée en sélection. La définition de cet espace phénotypique est donc cruciale si l'objectif est de déterminer des idéotypes réalistes pour le sélectionneur. Le phénotypage haut-débit et l'analyse de dizaines de caractères sur des centaines de variétés (Tardieu *et al.*, 2017) peut permettre de mettre en évidence les compromis potentiels entre les traits, et de déterminer la limite multidimensionnelle des combinaisons de paramètres possibles (Townsend *et al.*, 2017). C'est un point commun à plusieurs cas d'étude que j'ai mené, ou que je vais mener à moyen terme.

Insertion dans le projet d'équipe et du LEPSE

Depuis le 1er Janvier 2020, je suis responsable de l'équipe MAGE au LEPSE. Le projet de l'équipe MAGE (Modélisation et Analyse de l'interaction Génotype x Environnement) a été co-construits avec les scientifiques de l'équipe, si bien que nos projets personnels ont été adaptés afin qu'ils forment les briques de bases de ce projet plus large. C'est bien sur le cas du projet que je présente ici.

Le projet de MAGE repose sur les mêmes bases que mon projet ; il est de modéliser et prédire l'impact de traits et d'allèles dans des scenarios contrastés d'environnement et de conduite de culture (G x E x M). Pour

cela, MAGE, (i) améliore des modèles de culture en ajoutant de nouveaux modules intégrant de nouvelles connaissance écophysiologiques. La gamme de processus étudiée dans MAGE est plus large que celle de mon projet, et comprend l'effet de traits racinaires, des processus reproducteurs, en passant par le rôle du compromis eau/carbone sur la croissance et le développement, dans des conditions contrastées (eau, température, azote, …). (ii) MAGE analyse la diversité génétique sur ces traits, en particulier chez le blé et le Maïs, dans des plateformes haut-débit au champ et en conditions contrôlées. (iii) MAGE analyse le contrôle génétique de ces traits par génétique quantitative et utilise la prédiction génomique pour prédire les valeurs de traits à partir de profils alléliques de variétés réelles mais non testées, ou virtuelles issues de modèles de sélection prédisant les profils alléliques dans des générations de descendance. (iv) Enfin, MAGE prédit les conséquences de ces traits (ou de ces combinaisons d'allèles) dans des scenarios présents et futurs.

Mon projet s'insère donc complètement dans ce cadre global, mais sur des processus précis (caractères adaptatifs de développement, croissance foliaire et transpiration), avec un fort focus sur les comparaisons interspécifiques et l'impact de l'espace phénotypique dans la prédiction d'idéotypes. Mon projet s'appuie sur des relations fortes avec les membres de l'équipe, pour soutenir les activités d'analyses comparatives (Denis Vile), de modélisation (Pierre Martre), et pour intégrer mon projet plus largement dans celui de MAGE, en particulier les liens avec d'autres processus (Olivier Turc, Bertrand Muller), et la génétique (François Tardieu, Claude Welcker).

Plus largement, ce projet tire profit des interactions avec l'équipe de Phénomique du LEPSE (Llorenç Cabrera), et des réflexions et projet transversaux au LEPSE, sur le Phénotypage et la modélisation.

Principales collaborations nécessaires à mon projet de recherche

Mais ce projet de recherche ne peut être mené qu'au travers de collaborations qui dépassent le cadre du LEPSE.

Ce projet va profiter de partenariat déjà bien établis avec (i) l'équipe AGAP-PAM et l'IRD-Diade, en ce qui concerne la physiologie du Sorgho (voir Focus N°6) ; (ii) l'Université Catholique de Louvain (UCL, Belgique) pour le phénotypage racinaire (Xavier Draye) et les aquaporines (François Chaumont ; voir Focus N°5) ; les plateformes DIAPHEN (Montpellier) et Pheno3C (Clermont-Ferrand) pour le phénotypage au champ (Focus N°5 et 6) ; l'UMR BFP (Bordeaux, Yves Gibon) pour l'analyse de l'état carboné et des rapports Source / Puit (Focus N° 5) ; L'UMR GDEC (blé) et GQE (mais) en génétique (Focus N°5 et 6) ; l' ITK (Montpellier) et Université de Rothamsted (UK, Mikhail Semenov) pour la modélisation et les scénarios climatiques (Focus N°5 et 6).

Quels impacts

Ce projet a une portée en science académique mais est aussi tourné vers des applications concrètes pour les sélectionneurs

Impacts scientifiques

-Ce projet contribue à l'amélioration des connaissances académiques en physiologie des plantes et essaye de répondre à plusieurs questions : (i) Quels sont les processus clefs de la réponse des plantes à des contraintes environnementales exacerbées par le changement climatique ? (ii) Quels sont les mécanismes sous-jacents qui contrôlent ces processus et comment sont-ils interconnectés? (iii) Quelle est la diversité génétique de ces mécanismes dans des espèces données ? (iv) Qu'est ce qui structure cette diversité aux échelles intra- et inter-spécifiques.

-Ce projet s'intéresse à des processus dynamiques adaptatifs, relativement peu étudiés et largement ignorés par la sélection, qui cible principalement des caractères constitutifs améliorant le rendement dans un grand nombre de situations. Pourtant, cette stratégie, qui peut donc sembler orthogonale à celle des gros consortiums qui ciblent de nouveaux processus constitutif, comme ceux visant à améliorer la photosynthèse (ex : projets RIPE, C4Rice, CropBooster, total > $150 M) peut proposer de nouvelles pistes et de nouveaux réservoirs de traits d'intérêt et d'allèles pour la génétique et la sélection, à condition que l'on soit capable d'indiquer « où et quand « ces derniers peuvent présenter un avantage comparatif.

- Ce projet produit des modèles à différentes échelles qui permettent d'intégrer des processus et leur diversité génétique à des échelles temporelles et spatiales supérieures. Ces modèles sont ou seront disponibles (open science) pour analyser l'impact de ces caractères sur des variables biologiques ou agronomiques d'intérêt.

Applications

-Les modèles développés le sont au travers de partenariats bilatéraux avec des entreprises privées de modélisation (ex, modèle blé, ITK), ou des sélectionneurs (ex Sirius Maïs, Limagrain) ou dans le cadre de projets impliquant ces mêmes entreprises. Cela augmente fortement la chance de voir ces modèles, ou l'adaptation de ces modèles directement intégrés à des outils d'aide à la décision pour les agriculteurs, ou intégrés à des stratégies de sélection.

-Plus largement, ce projet est clairement orienté vers l'amélioration variétale et peut influer les stratégies d'adaptation et de sélection, en proposant aux sélectionneurs des indications sur (i) des processus d'intérêt pour des scenarios incluant des périodes de fortes contraintes abiotiques, (ii) où chercher la variabilité génétique associée à ces processus, (iii) les scenarios dans lesquels des combinaisons de caractères peuvent améliorer la performance des variétés.

Limites de l'approche

J'ai cependant bien conscience qu'une approche de l'amélioration variétale basée sur des idéotypes peut être éloignée des réalités du monde de la sélection. Des idéotypes sont des prototypes de plantes virtuels qui n'existent pas sur le moment (Andrivon *et al.*, 2013) et dépendent d'un objectif spécifique. Les quatre 'dimensions' de cet objectif (génétique, agronomique, modélisation, et socio-économique ; Andrivon *et al.*, 2013) et les méthodes pour y parvenir peuvent toutes présenter des biais et ralentir l'acceptation du fait d'inclure ces caractères / allèles dans les processus de sélection.

-**Modélisation.** Les idéotypes proposés sont des combinaisons de paramètres de modèles (Model-based ideotyping, Martre *et al.*, 2015a). Bien que toutes les précautions aient été prises pour proposer des modèles reflétant la réalité des processus physiologiques, ces modèles ne sont que la retranscription mathématique de notre vision du fonctionnement de la plante au temps t, et intègrent les biais subjectifs systématiques à tout choix de formalisme. Ainsi des études basées sur des modèles eux-mêmes basés sur des hypothèses biologiques différentes pourront présenter des idéotypes très différents. Par exemple, des modèles centré-carbone (ex : GECROS, Yin & van Laar, 2005 ; Cropsyst, Stockle *et al.*, 2003) risquent de conclure sur l'intérêt de tels ou tels caractères liés aux réponses des processus d'acquisition de biomasse, mais ce ne sera pas le cas pour d'autres types de modèles (plusieurs exemples sont donnés dans Parent et Tardieu, 2014). De plus, l'approche proposée sera toujours limitée par le nombre de caractères et processus étudiés et pris en compte dans les modèles, qui ne représentent qu'une fraction des traits d'intérêt potentiels (Paleari *et al.*, 2017).

-Génétique. Les idéotypes finaux résultant de mon approche sont principalement des combinaisons de caractères et moins souvent des combinaisons d'allèles ou des profils alléliques plus complets. Cependant, les possibilités offertes par la génétique pour atteindre de tels idéotypes sont prises en comptes indirectement par l'analyse des corrélations entre caractères (et donc des contraintes génétiques sur ces caractères) et de l'espace phénotypique. De plus, à l'échelle du projet MAGE et dans le Focus N°5 de mon projet de recherche, les combinaisons d'allèles (idéotypes génétiques) permettant d'obtenir ces combinaisons de caractères (idéotypes fonctionnels) seront proposées. Pourtant, l'approche proposée sera toujours limitée par le nombre de caractères et processus étudiés et pris en compte dans l'analyse de l'espace phénotypique.

-**Agronomique.** Un idéotype élargi au cadre agronomique informe soit sur quelle combinaison de caractères est la plus adaptée à un modèle de conduite donné, soit quelle est le meilleur compromis variété / conduite de culture pour un environnement donné. La conduite de culture est considérée de façon marginale dans mon projet, se limitant à des niveaux d'irrigation, de fertilisation et de dates de semis. Cependant, quoique en se limitant à ces variables-là, mon projet répond à cet objectif d'idéotype agronomique. La conduite de culture n'est pas ajoutée dans un second temps pour s'ajouter aux gains génétique (ex : Duvick *et al.*, 2003), mais est

incluse dès le départ dans le factoriel (traits x environnement x conduite). Chaque combinaison de caractères est testée dans chaque environnement pour plusieurs modes de conduites, et les idéotypes proposés sont donc adaptés à chaque scénario environnemental et de conduite.

-Socio-économique. C'est la dimension qui a été la moins étudiée jusque-là dans mes activités de recherche. Pourtant, un idéotype dans un contexte socio-économique donné ne le sera pas forcément dans un autre (Andrivon *et al.*, 2013). Cette dimension est cruciale pour les sélectionneurs et les instituts techniques. Dans la suite de mon projet, je souhaite inclure cette dimension, du moins à un niveau relatif. Dans le Focus 6, au moins la partie économique sera prise en compte avec comme objectif de comprendre comment les dimensions génétiques, agronomiques ou économiques peuvent rendre compte de l'explosion de la culture du sorgho en France.

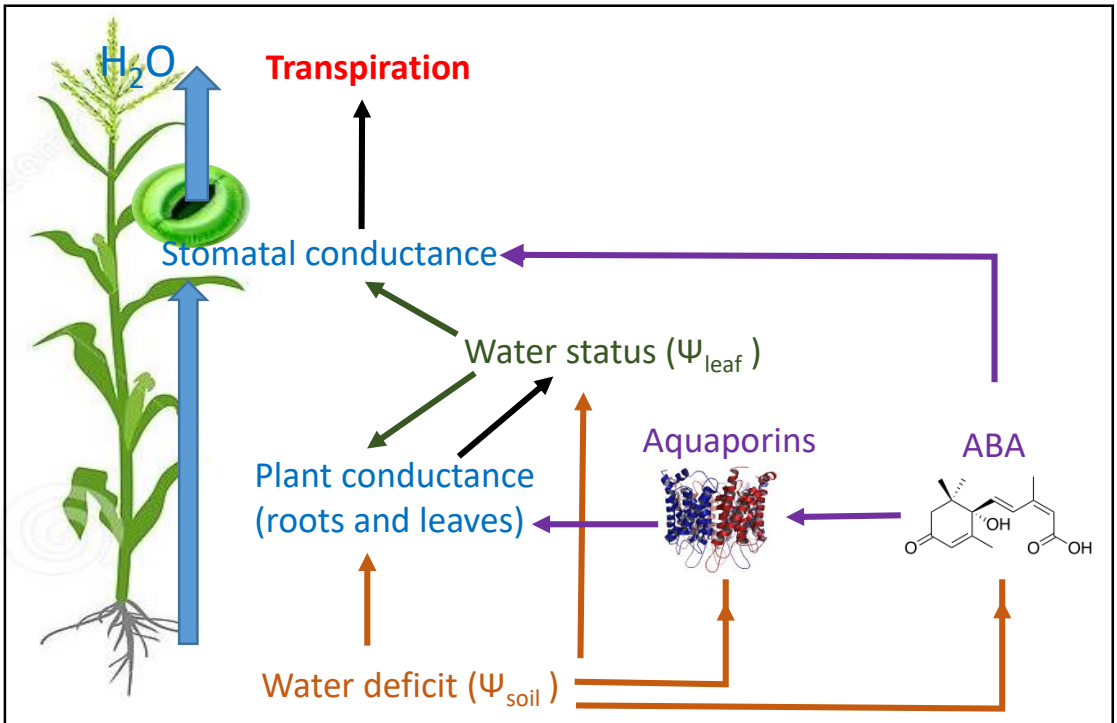

Figure 7. Schéma simplifié des interactions entre ABA et processus hydrauliques. La conductance stomatique dépend du statut hydrique des feuilles (potentiel hydrique Ψleaf) et de l' ABA. L'état hydrique foliaire résulte de la tension hydraulique entre la feuille et le sol et est contrôlé par les conductances hydrauliques des racines et des feuilles. Les conductances hydrauliques dépendent à la fois d'un effet direct des potentiels hydriques locaux, des aquaporines PIP et de l'ABA.

6. ACTIVITES DE RECHERCHE 2005 -2020

Focus n°1 : Effet de l'ABA sur la croissance foliaire du maïs

Ce travail, principalement issu de mes travaux de thèse, mais repris récemment, propose une approche typique d'écophysiologie-modélisation et de biologie intégrative, du gène à la plante entière (Articles 1, 2, 7, 17, 19, 24). Cette thématique est encore cruciale dans mes projets actuels et à moyen terme (voir Focus N°6).

Contexte

La phytohormone acide abscissique (ABA) est depuis longtemps une cible privilégiée pour l'amélioration des plantes dans des environnements sujets à des périodes de déficit hydrique (Wilkinson *et al.*, 2012; Blum, 2015; Mega *et al.*, 2019). En effet, son impact sur la fermeture stomatique faisant consensus dans la communauté scientifique (Zhang & Davies, 1990; Munemasa *et al.*, 2015), il permettrait d'améliorer l'efficience de transpiration, et donc la productivité en conditions de sécheresse (Blum, 2015; Mega *et al.*, 2019). Cependant, l'impact du taux d'ABA ou de la sensibilité des plantes à l'ABA sur le rendement n'est pas clair (Saradadevi *et al.*, 2017). D'un côté, des plantes issues d'ingénierie génétique pour sur-synthétiser l'ABA semblent montrer un avantage en condition de sécheresse (Xiao *et al.*, 2009; Du *et al.*, 2010; Miao *et al.*, 2018), mais de l'autre, la concentration d'ABA a été indirectement négativement sélectionnée de 1930 à aujourd'hui chez le maïs (Sanguineti *et al.*, 2006), et au jour d'aujourd'hui, malgré 30 ans de recherches (depuis Zhang & Davies, 1990), il n'y a pas eu à ma connaissance de success-story impliquant l'ABA dans la sélection variétale.

C'est surement dû au fait que l'ABA n'est pas spécifique à un seul type de stress, qu'il a de multiples sites d'actions (Kuromori *et al.*, 2018), qu'il interagit dynamiquement avec de multiples processus hydrauliques (Pantin *et al.*, 2013; Merilo *et al.*, 2018; Yoshida *et al.*, 2019), et selon le scenarios environnemental (Fig.7). Tous ces processus, dont l'ouverture stomatique, la croissance des feuilles, la conductance hydraulique et la concentration d'acide abscissique dans la sève du xylème ([ABA] xyl) varient rapidement avec l'heure de la journée (Zweifel *et al.*, 2007, Tardieu, ,2017; Caldeira *et al.*, 2014; Steppe *et al.*, 2015). Ils suivent des relations déterministes avec les conditions environnementales et interagissent de manière à ce que toute modification de l'une de ces variables affecte toutes les autres (Buckley *et al.*, 2003; Dodd, 2003; Messinger *et al.*, 2006; Tardieu & Parent, 2017, Fig. 8). Ainsi, les approches basées sur les mesures d'une variable à un moment donné ou sur des corrélations appariées sont sujettes à des confusions d'effets, en particulier pour étudier leur variabilité génétique (Tardieu & Parent, 2017).

Ces relations peuvent être analysées avec des modèles dynamiques dans lesquels les relations de cause à effet entre les variables sont prises en compte à chaque pas de temps (Edwards *et al.*, 1986; Dewar, 2002; Buckley

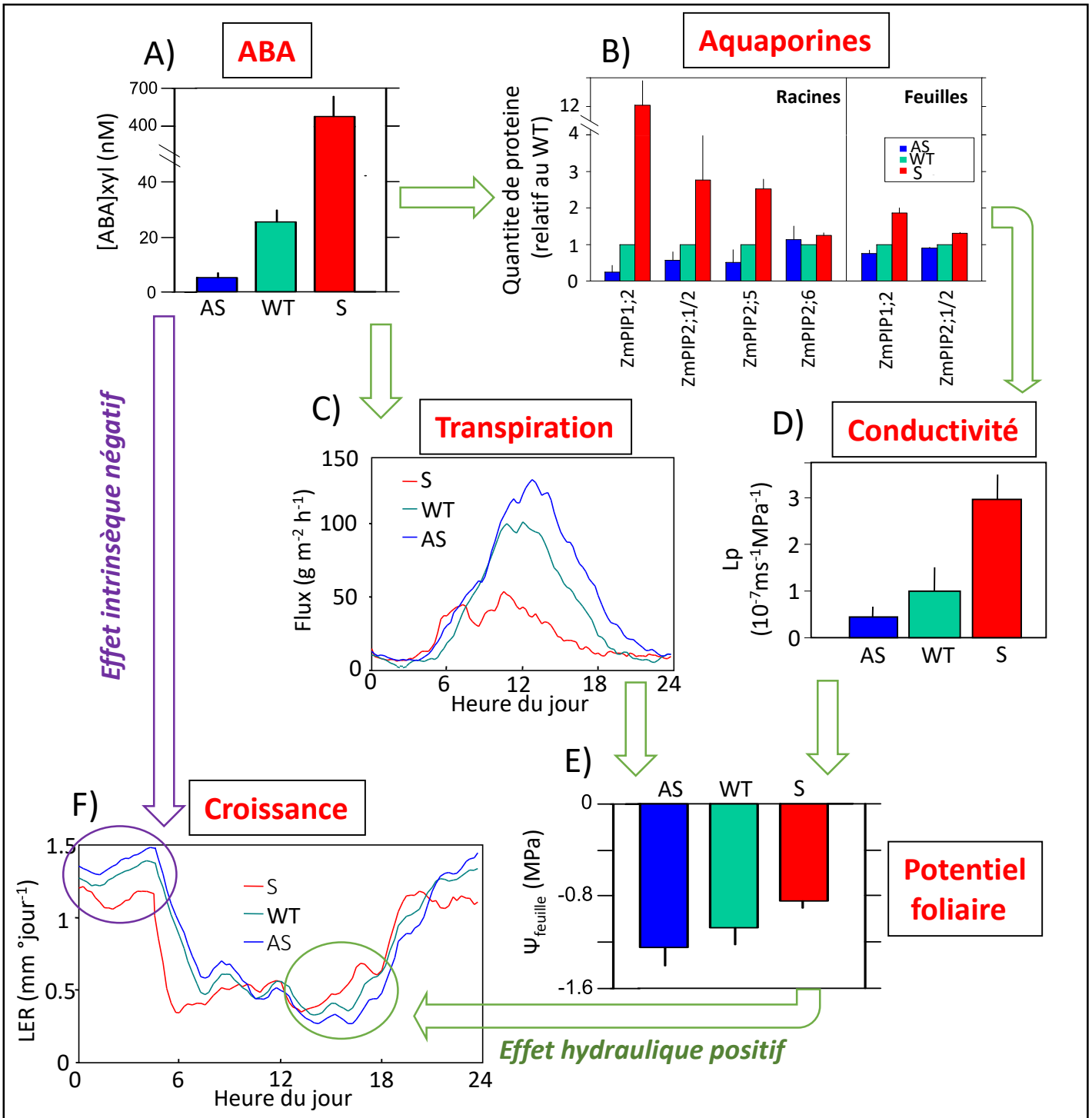

<u>Figure 8</u>. Impact de l'ABA sur croissance foliaire du maïs.

Le phénotype complexe observé sur les croissance (F) peut être expliqué par un effet intrinsèque négatif de l'ABA sur la croissance, observable de nuit, et un effet hydraulique positif , observable de jour, *via* une sur-expression des aquaporines, une augmentation de la conductivité racinaire, une régulation stomatique réduisant la transpiration, et un maintien du potentiel foliaire. **A)** Concentration en ABA dans la sève. **B)** Quantité d'aquaporines dans les racines et dans les feuilles. **C)** Cinétiques du flux de transpiration. **D)** Conductivité hydraulique racinaire. **E)** Potentiel foliaire a midi. **F)** Cinétiques des vitesse d' élongation foliaire pour 2 lignées transgéniques de maïs et leur lignée sauvage relative sous déficit hydrique (-0.4 MPa) et forte demande évaporative. Ces lignées transgéniques ont été affectées sur le gène *NCED/VP14*, avec 1 lignées antisens (AS, bleu), sous-exprimant le gène et une lignée sens (S, rouge) sur-exprimant le gène. ***Issus de Parent et al., 2009, Tardieu et al., 2010 et résultats non publiés.***

et al., 2003; Tuzet *et al.*, 2003; Zweifel *et al.*, 2007). Au commencement de ce projet, un tel model avait déjà été développé pour le maïs (Tardieu & Davies, 1993). Il impliquait un effet négatif de l'ABA sur la croissance foliaire. Pourtant, différents travaux démontraient des effets opposés de l'ABA sur la croissance, soit positifs (Sharp & LeNoble, 2002; Sansberro *et al.*, 2004; Thompson *et al.*, 2007), soit négatifs (Zhang & Davies, 1990; Salah & Tardieu, 1997; Bacon *et al.*, 1998). De même, son effet sur l'expression des aquaporines était très controversé (Kaldenhoff *et al.*, 2008), ainsi que l'était encore plus largement son effet sur la conductivités des tissus (ex : positif : Morillon & Chrispeels, 2001; Thompson *et al.*, 2007; ou négatif :Wan & Zwiazek, 2001; Aroca *et al.*, 2003). Les principales méthodes employées dans ces travaux consistaient en ajout d'ABA exogène dans la solution nutritive, dans la sève ou par spray foliaire, parfois en quantité non-physiologique, aboutissant à des effets transitoires, et très dépendant des concentrations testées (Zhu *et al.*, 2005; Beaudette *et al.*, 2007).

Par l'étude de lignées transgéniques de maïs sur- ou sous-exprimant une enzyme de la voie de biosynthèse de l'ABA (la NCED, *9-cis*-epoxycarotenoid dioxygenase , Tan *et al.*, 1997; Qin & Zeevaart, 1999), l'objectif de mon travail était de décorréler les effets propres de la sécheresse, des effets de l'ABA, qu'ils soient dépendant ou non de processus hydrauliques. Outre de clarifier au niveau fonctionnel le rôle de l'ABA, de l'échelle moléculaires au niveau intégré de la croissance des feuilles, ce travail devait permettre de modéliser les effets de la production d'ABA par la plante dans différent scenarios de déficit hydrique du sol et de demande évaporative sur les transfert d'eau et la croissance de la plante. Le modèle découlant devait permettre de prédire dans quels scenarios environnementaux des paramètres génotypiques hydrauliques liés à l'ABA (production, dégradation, sensibilités) pouvait conduire à des avantages comparatifs sur la croissance foliaire du maïs.

Principaux Résultats

Une approche trans-échelle a pu démêler les effets apparemment contradictoires de l'ABA sur la croissance foliaire.

La caractérisation moléculaire, biochimique et physiologique de ces lignées a tout d'abord pu valider notre approche, c.à.d. ces lignées sur- ou sous-exprimaient la protéine ciblée (NCED), affectant la concentration en ABA dans la sève et dans les feuilles, tout en restant dans des gammes physiologiques (Fig.8A), et l'effet de l'ABA sur le contrôle stomatique était vérifié sur la transpiration (Fig.8C) (Voisin *et al.*, 2006).

La caractérisation hydraulique à différentes échelles de ces lignées (Parent et al., 2009) a permis de démêler le phénotype complexe observé sur la croissance, avec un effet négatif de l'ABA observable la nuit et un effet positif en journée (Tardieu et al., 2010):

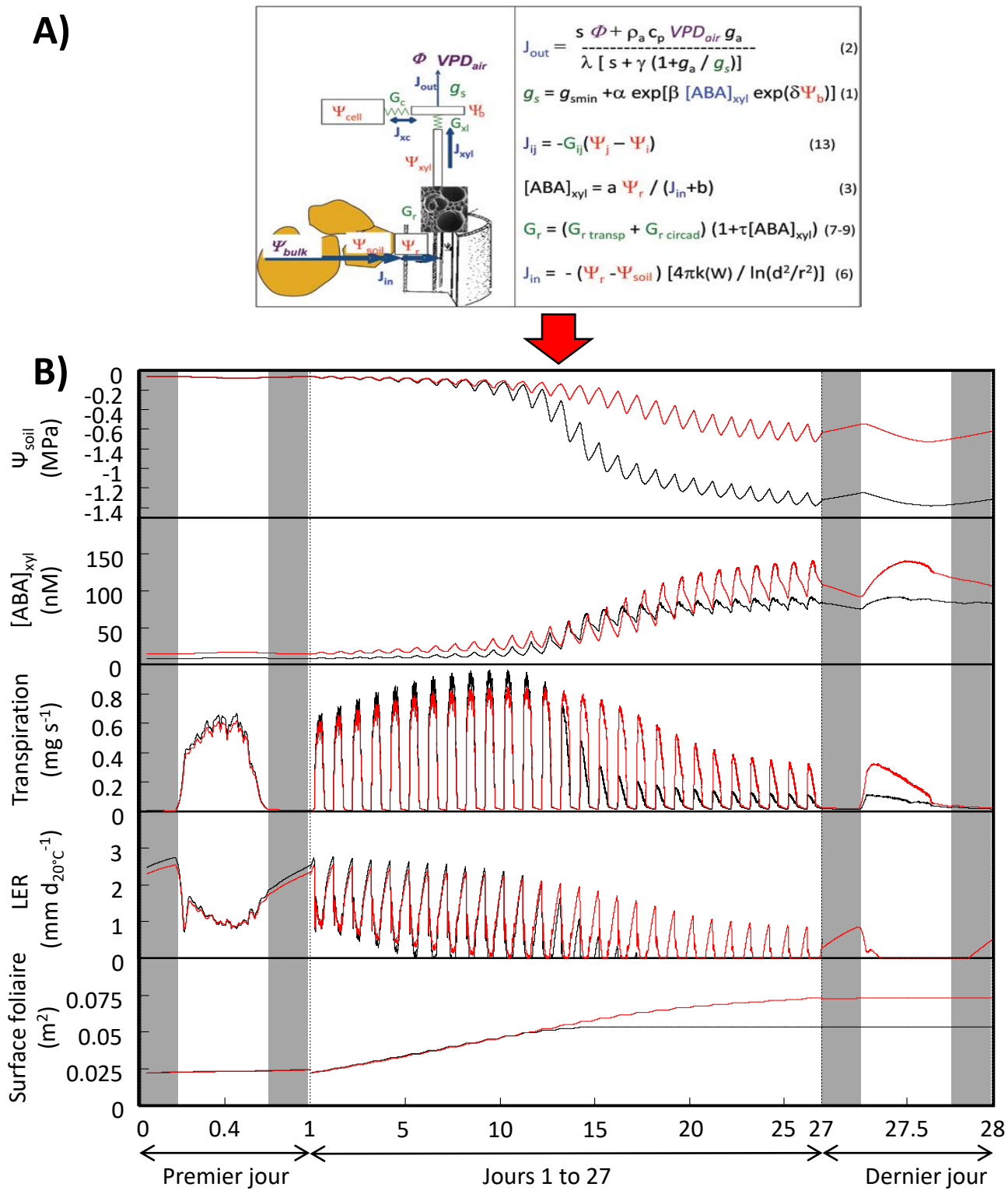

<u>Figure 9</u>. Un modèle de croissance et de transpiration impliquant les effets de l'ABA est capable de reproduire les phénotypes complexes observés chez les lignées transgéniques de maïs.

A) Schéma et principales équations du modèle hydraulique de transfert d'eau. **B)** Sorties du modèle pour 28 jours de croissance chez les lignées transgénique de maïs affectées constitutivement sur la production d'ABA (rouge, surproducteur d'ABA; noir, contrôle). Le modèle reproduit les cinétiques de croissance observées avec les vitesses de croissances opposées entre jour et nuit, et montre qu'une capacité de surproduction d'acide abscisique (ABA) peut entraîner une concentration inférieure d'ABA dans la sève du xylème (jours 13 à 17). ***Issus de Tardieu et al., 2015 et Tardieu et Parent, 2017.***

-De jour, les aquaporines étaient plus fortement exprimées et leur quantité protéique augmentées par l'ABA dans les racines et dans les feuilles (Fig.8B). Il en découlait une plus forte conductivité hydraulique racinaire (Fig.8D) chez les plantes surproduisant l'ABA. Les deux processus hydrauliques concomitants de (i) diminution de la transpiration et (ii) d'augmentation de la conductivité hydraulique racinaire permettaient aux plantes surproduisant l'ABA de mieux maintenir mieux leur statut hydrique pendant la journée (Fig.8E), et d'autant plus que le déficit hydrique était sévère et la demande évaporative forte. En maintenant mieux leur statut hydrique et en se réhydratant plus rapidement (non présenté, Parent et al., 2009), les plantes surproduisant l'ABA maintenaient mieux leur vitesse de croissance en journée (Fig.8F).

-Au contraire, la nuit, en absence de contrainte hydraulique, les plantes surproduisant l'ABA avaient des croissances plus faibles, indiquant un autre effet de l'ABA sur la croissance foliaire, négatif, et non-dépendant de l'hydraulique.

Ces résultats ont pu réconcilier les résultats opposés de la littérature en démontrant que l'ABA avait deux effets opposés sur la croissance, l'un positif et hydraulique, l'autre négatif et non-hydraulique, conduisant à des impacts à long termes différents selon le scénario environnemental (Tardieu et al., 2010).

Un modèle hydraulique permet de prédire l'impact de la variabilité génétique de la biosynthèse d'ABA sur la transpiration et la croissance foliaire.

Ces effets quantitatifs de l'ABA sur les propriétés hydrauliques de la plante et sur sa croissance ont été traduit en équations (Fig.9A) pour mettre à jour le modèle de Tardieu & Davies (1993). Ce modèle comprend maintenant les progrès récents dans la compréhension des contrôles intrinsèques et environnementaux de la conductance hydraulique des tissus en fonction du taux de transpiration, des rythmes circadiens et de l'ABA (Tardieu *et al.*, 2015). Il en résulte un modèle dynamique capable de simuler des variables hydrauliques et de croissance avec des paramètres spécifiques au génotype. Cela permet de proposer des hypothèses de rôles adaptatifs pour les processus hydrauliques, en particulier les oscillations circadiennes de la conductance hydraulique des racines (Caldeira *et al.*, 2014). Ce modèle est capable de reproduire les phénotypes complexes observés chez les lignées transgéniques de maïs (Fig.9B), comme les vitesses de croissances opposées entre jour et nuit, de prédire l'impact de la variabilité génétique de biosynthèse d'ABA sur la transpiration et la croissance foliaire, mais aussi expliquer des observations parfois contradictoires, comme le fait qu'une capacité de surproduction d'acide abscisique (ABA) peut entraîner une concentration inférieure d'ABA dans la sève du xylème" (Fig.9B). ***Couplé avec un modèle de culture, ce modèle pourrait permettre d'indiquer dans quels scénarios il est préférable de synthétiser plus ou moins d'ABA. Il est la base de mon nouveau projet de recherche que j'engagerai à moyen terme (Focus N°5).***

Bilan et Conséquences pour mon projet de recherche

Ce travail a été fondateur pour mon projet de recherche. Il s'est appuyé sur une approche de biologie intégrative, du gène à la plante entière, en tirant parti des outils de l'écophysiologie et de la modélisation pour démêler un phénotype complexe. Ainsi, en proposant une nouvelle vision synthétique de l'effet de l'ABA sur la croissance des plantes, cette étude peut mettre d'accord des résultats discordants de la littérature, lancer de nouvelle pistes de recherche sur l'impact de l'hydraulique, et des nouvelles approches en sélection. En effet, la question n'est donc pas de savoir s'il vaut mieux sélectionner des plantes avec plus ou moins d'ABA car son impact est incertain, mais plutôt de savoir « où et quand » l'ABA peut conduire à des effets positifs sur la productivité. Cette question est la base d'un nouveau projet de recherche détaillé dans le Focus N°5.

Articles issus de ce travail

(24) Tardieu, F., **Parent, B.** (2017). Predictable 'meta-mechanisms' emerge from feedbacks between transpiration and plant growth and cannot be simply deduced from short-term mechanisms. *Plant, Cell and Environment, 40* (6), 846-857.

(19) Tardieu, F., Simonneau, T., **Parent, B.** (2015). Modelling the coordination of the controls of stomatal aperture, transpiration, leaf growth, and abscisic acid: update and extension of the Tardieu–Davies model. *Journal of Experimental Botany, 66* (8), 2227-2237.

(17) Caldeira, C. F., Bosio, M., **Parent, B.,** Jeanguenin, L., Chaumont, F., Tardieu, F. (2014). A hydraulic model is compatible with rapid changes in leaf elongation under fluctuating evaporative demand and soil water status. *Plant Physiology, 164* (4), 1718-1730.

(7) Tardieu, F., **Parent, B.,** Simonneau, T. (2010). Control of leaf growth by abscisic acid: hydraulic or non-hydraulic processes? *Plant Cell and Environnement, 33 (4),* 636-647

(2) Parent, B., Hachez, C., Redondo, E., Simonneau, T., Chaumont, F., Tardieu, F. (2009). Drought and Abscisic Acid Effects on Aquaporin Content Translate into Changes in Hydraulic Conductivity and Leaf Growth Rate: A Trans-Scale Approach. *Plant Physiology, 149* (4), 2000-2012.

(1) Voisin, A.-S., Reidy, B., **Parent, B.,** Rolland, G., Redondo, E., Gerentes, D., Tardieu, F., Muller, B. (2006). Are ABA, ethylene or their interaction involved in the response of leaf growth to soil water deficit? An analysis using naturally occurring variation or genetic transformation of ABA production in maize. *Plant, Cell and Environment, 29* (9), 1829-1840.

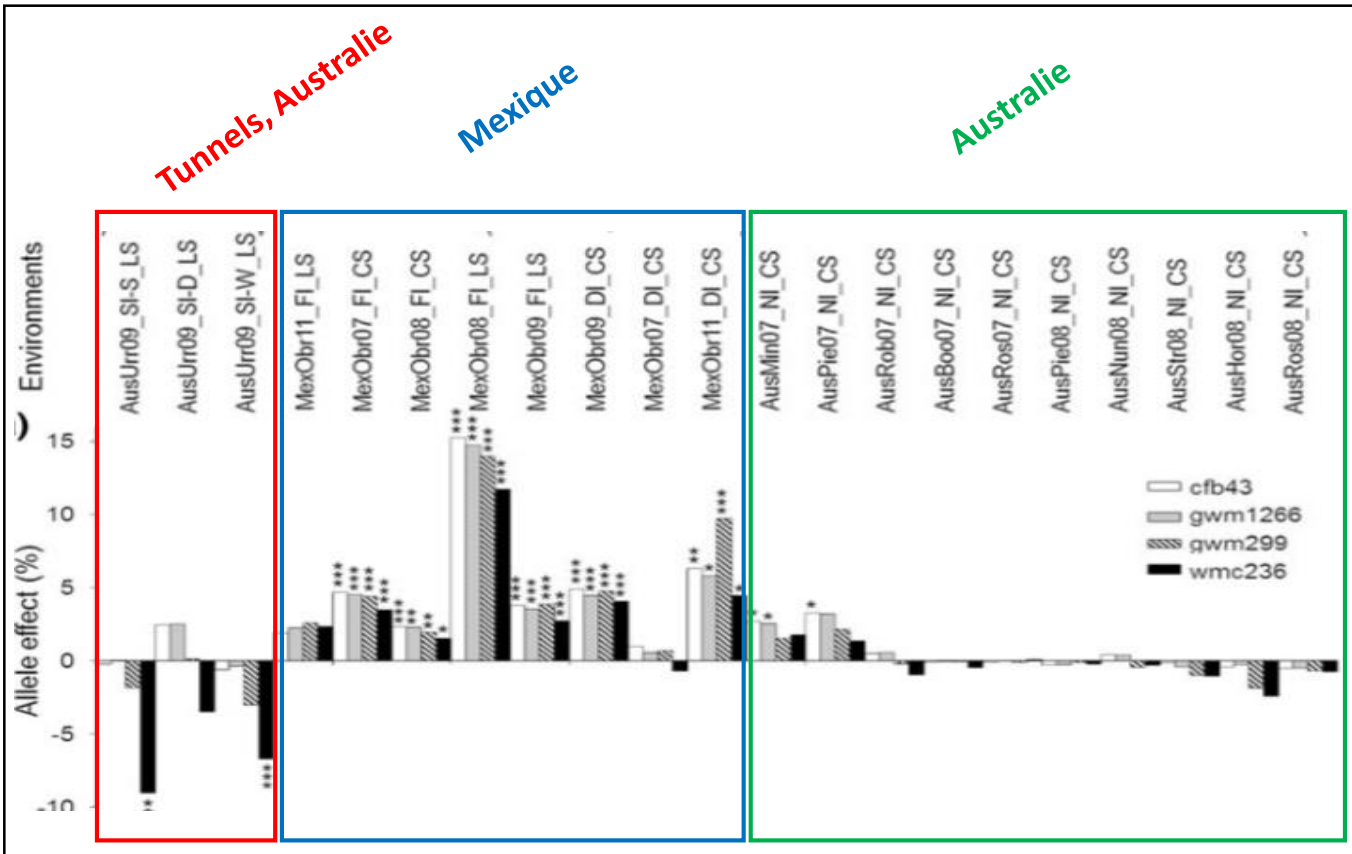

<u>Figure 10</u>: Effets alléliques sur le rendement pour l'allèle de RAC875 à 4 marqueurs d'un QTL de rendement sur le chromosome 3B, dans une population de lignées recombinantes RAC875 / Kukri de blé cultivées dans 21 sites. Les trois premiers sont des essais en tunnel avec de fortes températures et différents niveaux de déficit hydrique réalisées à l'ACPFG, Adelaïde, Australie. Les 8 suivants sont des essais réalisés à Ciudad Obregón, Mexico, et les 10 suivants dans différents sites Australiens. Noter la différence d'effets allélique entre ces sites.

Issus de Bonneau et al., 2013, TAG

Focus n°2 : Déchiffrer les interactions G x E sur le rendement du blé

Cet axe est principalement le fruit de mes travaux de postdoctorat à l'Université d'Adelaïde et participait à des objectifs plus larges de clonage positionnel de QTLs de rendement du blé adaptés aux climats sec et chaud de l'Australie du Sud (Articles. 12, 13, 18, 20, 23, 25).

Contexte

Dans des environnements Sud-Australien associant des périodes, souvent combinées, de déficit hydrique et de hautes températures, le compromis stomatique entre (i) fermeture, pour éviter le dessèchement, et (ii) ouverture, pour éviter l'échauffement des tissus (Rizhsky *et al.*, 2002) est l'une des causes des fortes interactions Génotype x Environnement observées sur le rendement (Parent *et al.*, 2017). Il en découle que les impacts de QTL associés au rendement sont eux aussi très dépendant de l'environnement de culture (Maccaferri *et al.*, 2008; Millet *et al.*, 2016), et en particulier dans des scenarios complexes de déficit hydriques cyclique chroniques et de hautes température observés sous climats méditerranéens ou en Australie du Sud (Izanloo *et al.*, 2008).

Au début de ce projet, des QTLs de rendements avec des effets majeurs dans certains environnements (jusqu'à +15 % de rendement selon l'allèle) étaient à l'étude à l'ACPFG (Australian Center for Plant Fonctional Genomics, Université d'Adelaïde) en vue d'un clonage positionnel (Fleury et al., 2010). Ces QTLs étaient observés en parallèle dans deux populations de lignées recombinantes (Drysdale / Gladius et RAC875 / Kukri, (Fleury *et al.*, 2010). Gladius, Drysdale et RAC875 sont des lignées modernes de blé tendre (*Triticum aestivum*) avec des comportements contrastés sous contrainte (Rebetzke *et al.*, 2002; Condon *et al.*, 2006; Fleury *et al.*, 2010) et constituent donc un matériel intéressant pour l'étude de stratégies d'adaptation aux environnements chauds et secs. Cependant, ces QTLs de rendements étaient en très forte interaction avec l'environnement (Fleury *et al.*, 2010; Bennett *et al.*, 2012a; Bennett *et al.*, 2012b; Fig.10) sans aucune piste quant au mécanisme sous-jacent et/ou les conditions environnementales dans lesquelles ils pouvaient présenter un avantage comparatif. Il en était de même pour des gènes cibles issus de génétique inverse transformés chez le blé.

Mon objectif visait donc à démêler les interactions G x E observées chez des lignées transgéniques ou des lignées parentales de populations de lignées recombinantes, et les interactions QTL x E (2 QTLs en particulier) observées dans les 2 populations issus de ces lignées. Ma stratégie a été de (i) développer des moyens de phénotypage au champ et en conditions contrôlées pour des conditions contrastées de déficit hydrique et de hautes températures, (ii) d'utiliser ces nouveaux moyens pour analyser la dimension temporelle de l'impact des contraintes environnementales sur les processus clefs sous-jacents au rendement, (iii) d'utiliser ce cadre d'analyse pour déterminer les variations génétiques et l'impact de QTLs sur les réponses de variables

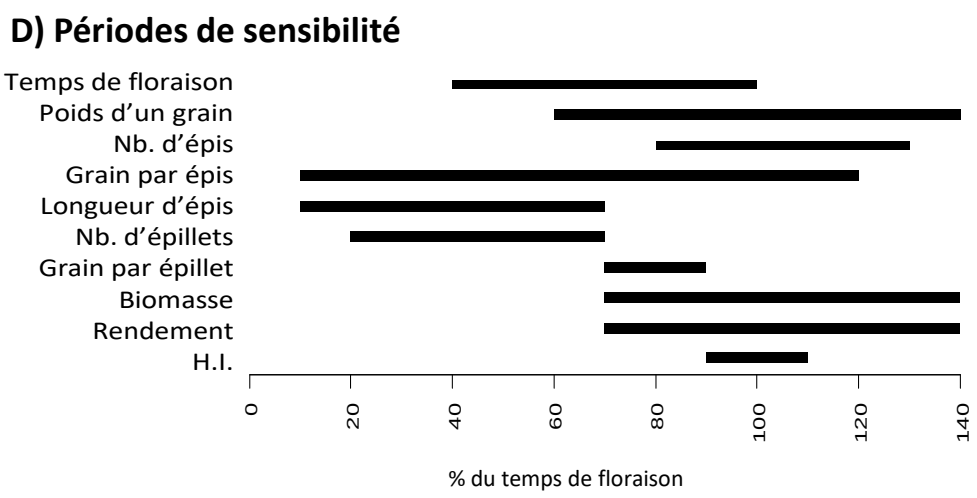

Figure 11. Pipeline d'analyse des interactions G x E sur des variables dynamiques et intégrées pour des populations de lignées transgéniques et des populations de lignées recombinantes.

A, B, C. Les trois plateformes de phénotypage utilisées. J'ai développé le pipeline et les scripts d'analyse pour les réponses de variables dynamiques au déficit hydrique du sol de la plateforme d'imagerie du « Plant Accelerator » (Adélaïde, Australie), et développé 2 plateformes complémentaires pour les variables intégrées, au champ (lignées recombinantes) et en serre S2 (lignées transgéniques). Un fort accent était mis quand aux corrélations entre les réponses de variables dynamiques et intégrées.

D. Période de sensibilité utilisées pour analyser les réponses de variables intégrées aux contraintes environnementales ***Parent et al., 2015, 2017, Kovalchuk et al., 2017.***

dynamiques et intégrées au déficit hydrique du sol et à la température. Cela devait permettre d'indiquer au sélectionneur les conditions environnementales dans lesquelles les gènes (dans le cadre d'approches de génétique inverse) et les allèles ciblés (dans le cadre de génétique quantitative) pouvaient créer un avantage comparatif sur le rendement.

Résultats Principaux

Un cadre d'analyse des réponses au déficit hydrique et aux hautes températures du rendement pour l'analyse des interactions G x E sur le rendement au champ

Les analyses en conditions contrôlées, bien que permettant une analyse fine, ciblée *a priori* sur un stade développement, peuvent masquer des effets majeurs à d'autres stades de développement de la plante dans les conditions réelles de culture au champ. J'ai donc développé un pipeline d'analyse combinant (i) expériences en conditions contrôlées, pour analyser des variables dynamiques sous-jacentes aux composantes du rendement (croissance, transpiration, …), moins sensibles aux interactions G x E mais pouvant expliquer les interactions G x E et QTL x E observées sur le rendement au champ, et (ii) des expériences très proches du champ, dans des environnements semi-contrôlés pour analyser les interactions G x E et QTL x E sur le rendement et ses composantes.

-En conditions contrôlées. La plateforme d'imagerie du Plant Accelerator étant livrée à mon arrivée, j'ai développé des pipelines pour transformer la donnée brute en variables biologiques d'intérêt (expansion foliaire, transpiration, efficience de transpiration, …) et leurs réponses au déficit hydrique (Parent *et al.*, 2015). Ce pipeline m'a permis d'analyser des panels de diversité, des lignées recombinantes de plusieurs populations et des populations transgéniques selon les projets dans lesquels mon groupe était impliqué (Fig. 11A).

-Au champ. A mon arrivée, le laboratoire ne disposait d'aucun outil de phénotypage au champ et de contrôle de l'environnement. J'ai donc développé une nouvelle infrastructure au champ, équipée d'abris anti-pluie, de systèmes d'irrigation et de capteurs environnementaux dans l'air et le sol. Cette plateforme a permis une analyse dans 11 scenarios hydriques et thermiques contrastés (Fig.11B) de lignées parentales et de population de lignées recombinantes (Bonneau *et al.*, 2013; Maphosa *et al.*, 2014).

-Pour les plantes transgéniques, la législation australienne étant très contraignante, j'ai développé une plateforme de dizaines de bacs de 650 L, en serre S2, permettant de reproduire des scénarios proches du champ, et équipé de systèmes d'irrigation et de capteurs environnementaux dans l'air et le sol (Fig. 11C, Kovalchuk *et al.*, 2017).

-L'analyse de réponses de variable intégrées à des variables environnementales dans un environnement fluctuant fait face au problème du choix des métriques pour représenter cet environnement. Il m'est apparu

A) QTL 1B: Effet constitutif sur le tallage et al croissance

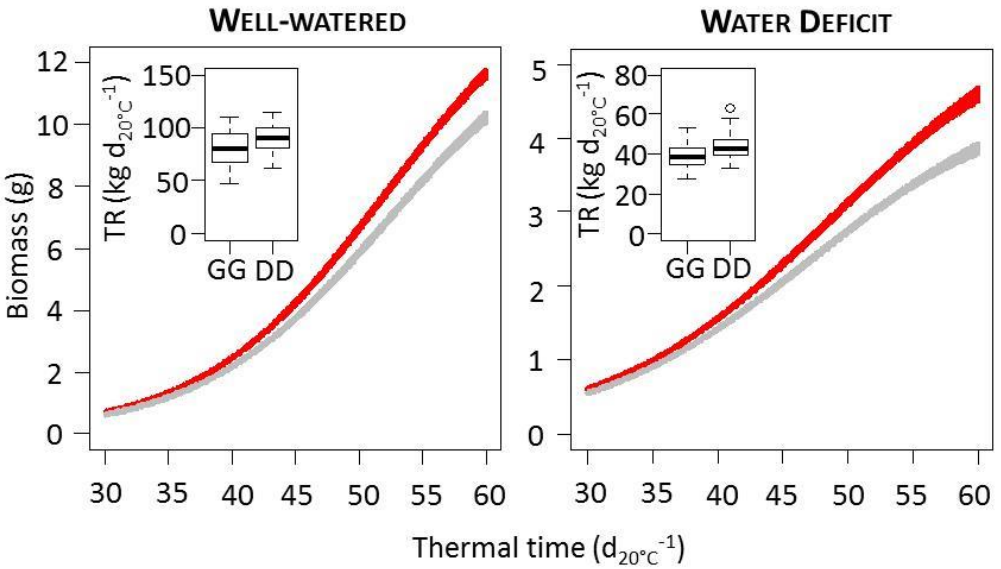

B) QTL 3B: Effet dépendant de la température

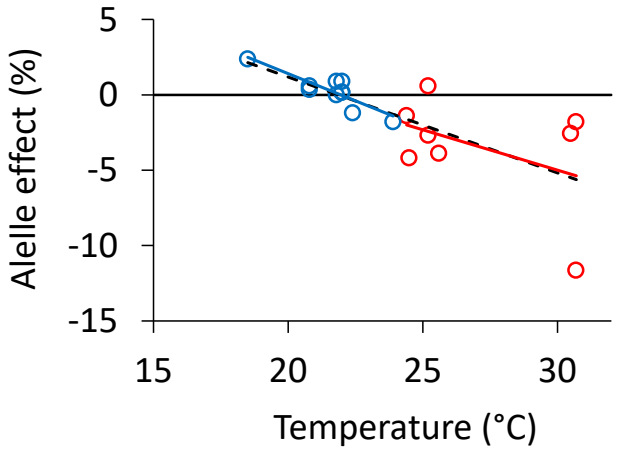

<u>Figure 12</u>. Caractères constitutifs ou adaptatifs de deux QTL de blé.
Ces deux QTL dont les deux principalement travaillés dans le cadre de mon postdoctorat.
A) Effet allélique au marker wsnp_CAP11_c1902_1022590 (QTL 1B, **Parent et al., 2015**) dans une population de lignées recombinantes (Gladius x Drysdale). L'allèle de Drysdale (en rouge) apporte une plus forte croissance de la plante entière et une plus forte transpiration en conditions bien irriguées et de sècheresse (-0.5 MPa) en plateforme, et un tallage plus important au champ. Son effet apparait donc comme constitutif sur la croissance.
B) Effet allélique pour l'allèle Kukri au marker Xwmc236 (QTL 3B, Bonneau et al., 2013; **Parent et al., 2017**) dans la population de lignées recombinantes (RAC875 x Kukri). L'effet allélique sur le rendement dépend de la température autour de la floraison. Rouge, essais au Mexique (voir Fig.10). Bleu: essais Australiens.
Issus de Parent et al., 2015, 2017.

nécessaire de réaliser une étude sans *a priori*, avec une approche purement statistique, des effets des contraintes hydriques et thermiques et de leurs interactions sur les composantes du rendement au champ. Le model final a permis de déterminer les périodes de sensibilité des différentes composantes du rendement, rendant possible une analyse génétique de ces réponses à un environnement rendu quantitatif (Parent *et al.*, 2017, Fig.11D).

Ainsi, j'ai développé des outils et des méthodes pour l'analyse des réponses de variables dynamiques et intégrées au déficit hydrique et à la température, permettant d'approcher les fonctions et les gènes de QTLs de rendements ou ceux issus de génétique inverse, et d'analyser leur interaction avec l'environnement, afin de définir leurs avantages comparatifs dans des scénarios environnementaux contrastés.

Dissections des interactions QTLs x E

Les deux populations basées sur les croisements entre Drysdale et Gladius, et RAC875 et Kukri présentaient des QTL communs de rendement au champ, tels que ceux ciblés ici sur les chromosomes 1B et 3B.

-Dans la population Gladius x Drysdale, l'allèle de Drysdale au QTL 1B (marker wsnp_CAP11_c1902_1022590) était associée à de plus forts rendements en conditions de déficit hydrique limité. Ce QTL recoupait le QTL QKpsl.aww-1B, donnant un effet moindre sur le rendement dans la population RAC875 x Kukri. L'analyse en conditions semi-contrôlées a montré que cet allèle était associé à un tallage plus important. En serre, elle contrôlait la vitesse de croissance et d'autres variables liées à la surface foliaire, et ce, de manière constitutive, peu importe le niveau de déficit hydrique (Fig.12 A, Parent et al., 2015). Le QTL1 B implique donc un tallage plus important et donc la croissance de la plante entière, de manière constitutive. Cet effet peut se traduire par des effets positifs sur les composantes du rendement en condition bien –irrigué ou de déficit hydrique modéré, ou négatif, en condition de déficit hydrique plus sévère (Parent et al., 2015).

-Le QTL sur le chromosome 3B, qYDH.3BL, affectant le rendement et le poids de mille grains dans la population RAC875 x Kukri (Bonneau et al., 2013) a aussi été trouvé dans la population Drysdale / Gladius (Maphosa et al., 2014). Les effets les plus important ont été observés sur des essais au Mexique (Fig.10), RAC875 et Drysdale portant l'allèle positif dans chaque population. L'analyse des effets des variables pendant les périodes de sensibilité a permis de démontrer que la température autour de la floraison était la variable environnementale principale, expliquant les interactions G x E observées sur les lignées parentales, et les interactions QTLs x E observées sur le rendement dans les deux populations de lignées recombinantes, l'allèle de RAC875 étant positive au-dessus de 22°C, quand l'allèle de Kukri l'est en dessous de ce seuil (Fig.12B ; Parent et al., 2017).

Le cadre d'analyse développé plus haut a permis d'améliorer la compréhension de ces QTLs complexes, avec des effets constitutifs sur des variables dynamiques sous-jacentes pouvant expliquer les interactions QTL x E observées sur des variables plus intégrées (rendement, poids d'un grain).

Bilan et Conséquences pour mon projet de recherche

Le contexte de ce postdoctorat était très différent de celui de ma thèse et de mon poste actuel. Bien que lié à l'Université d'Adélaïde, l'ACPFG était une entreprise privée, orientée dans la pré-selection, visant à donner aux sélectionneurs des gènes et des allèles d'intérêt. J'étais le seul physiologiste dans un groupe de près de 100 personnes et n'avais aucun outil de phénotypage à mon arrivée.

J'ai dû faire preuve d'opportunisme, pour développer rapidement des pipelines d'outils, méthodes et analyses pour pouvoir répondre à la demande, à savoir délivrer des traits d'intérêt aux généticiens et biologistes moléculaires de mon groupe. Cette expérience m'a mis à l'épreuve du concret, savoir faire l'impasse sur certains aspects pour faire preuve du maximum d'efficacité. Mis à part le coté frustrant du manque de temps et de projets pour affiner ces mécanismes biologiques, cette expérience a été cruciale pour comprendre les attentes réelles des privés et de la pré-selection en général, contexte qui me manquait cruellement aux vues de ma formation préalable.

Mes projets actuels et futurs tiennent compte de ces attentes, et proposent une approche trans-échelle, des mécanismes biologiques, jusqu'aux impacts de la diversité génétique sur la production à large échelle.

Articles issus de ce travail

(25) Parent, B., Bonneau, Maphosa, Kovalchuk, Langridge, Fleury (2017). Quantifying wheat sensitivities to environmental constraints to dissect G x E in the field. *Plant Physiology, 174* (3), 1669-1682.

(23) Kovalchuk, N., Laga, H., Cai, J., Kumar, P., **Parent, B.,** Lu, Z., Miklavcic, S. J., Haefele, S. M (2017). Phenotyping of plants in competitive but controlled environments: a study of drought response in transgenic wheat. *Functional Plant Biology, 44* (3), 290-301.

(20) Parent, B., Shahinnia, F., Maphosa, L., Berger, B., Rabie, H., Chalmers, K., Kovalchuk, A., Langridge, P., Fleury, D. (2015). Combining field performance with controlled environment plant imaging to identify the genetic control of growth and transpiration underlying yield response to water-deficit stress in wheat. *Journal of Experimental Botany, 66* (18), 5481-5492.

(18) Yadav, D., Shavrukov, Y. , Bazanova, N., Chirkova, L., Borisjuk, N., Kovalchuk, N., Ismagul, A**., Parent, B.,** Langridge, P., Hrmova, M., Lopato, S. (2015). Constitutive overexpression of the TaNF-YB4 gene in transgenic wheat significantly improves grain yield. *Journal of Experimental Botany, 66* (21), 6635-6650.

(13) Maphosa, L., Langridge, P., Taylor, H., **Parent, B.**, Emebiri, LC., Reynolds, MP., Okada, A., Mather, DE. (2014). Genetic control of grain yield and grain physical characteristics in a bread wheat population grown under a range of environmental conditions. *Theoretical and Applied Genetics, 127* (7), 1607-1624.

(12) Bonneau, J., Taylor, J., Parent, B., Bennett, D., Reynolds, M., Feuillet, C., Langridge, P., Mather, D. (2013). Multi-environment analysis and improved mapping of a yield-related QTL on chromosome 3B of wheat. *Theoretical and Applied Genetics, 126* (3), 747 - 761.

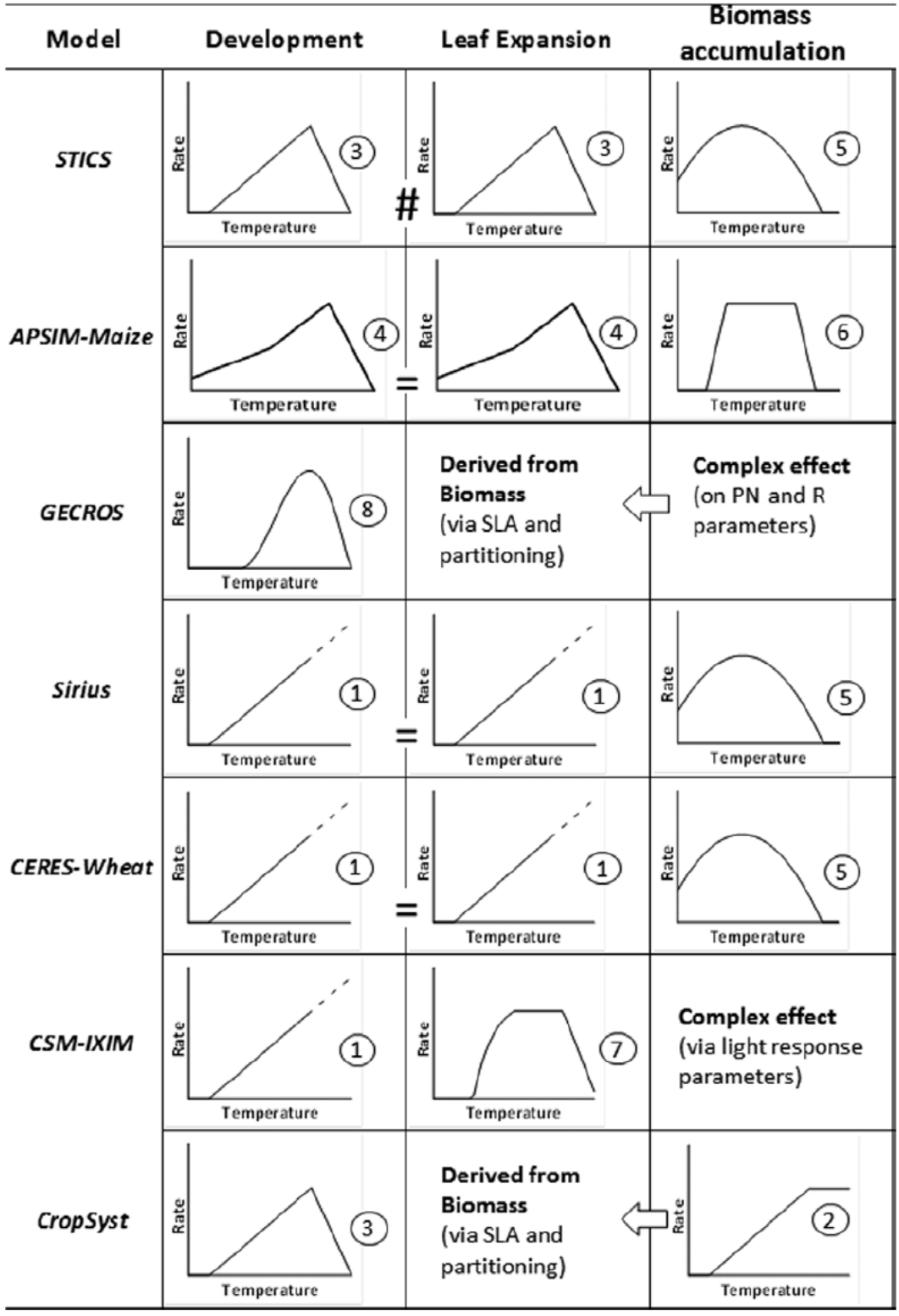

Figure 13. Formalismes de réponse à la température utilisés dans 7 modèles de culture pour la vitesse de développement, la vitesse d'expansion foliaire et l'accumulation de biomasse**.** ***Figure issue de Parent & Tardieu, 2014.***

Focus n°3 : Analyse comparative des réponses à la température

Cet axe, initié pendant ma thèse, a été depuis largement enrichi d'analyses, études et réflexions pendant mon post-doctorat et mon poste actuel

Contexte

Les variations thermiques du microenvironnement de la plante modifient toutes les vitesses chimiques, biochimiques et de processus biologiques intégrés. Les modèles de culture rendent tous compte des effets de la température sur les processus modélisés, mais présentent des formalismes et paramètres différents entre modèles, en particulier pour les processus de développement, de croissance et d'accumulation de biomasse (Fig. 13 ; Parent et Tardieu, 2014 ; Kumudini et al., 2014). Par exemple, certains modèles utilisent des formalismes et paramètres différents entre processus de croissance et développement (Parent et Tardieu, 2014), certains des effets différents entre le jour et la nuit (Kumudini *et al.*, 2014), d'autres entre différentes phases du cycle de la plante (Kumudini *et al.*, 2014). Pourtant, la formalisation des effets de la température est déterminante pour la justesse des prédictions (Wang *et al.*, 2017).

De même, certains modèles considèrent les paramètres de réponse à la température comme paramètres génétiques. Pourtant, le calcul du temps thermique, largement utilisé pour comparer des variétés et prédire des stades clefs du développement de la plante implique une réponse commune des variétés dans chaque espèce. Outre l'intérêt évident en modélisation des cultures, répondre à cette controverse en déterminant la diversité génétique intra- et inter-spécifique des réponses des processus de développement et de croissance à la température, ainsi que les facteurs et contraintes qui la structurent doit permettre à la fois de (i) donner des éléments essentiels quant à l'adaptation thermique de génotypes cultivés, (ii) d'approcher les mécanismes explicatifs sous-jacents à ces réponses, et (iii) déterminer les sources d'amélioration variétale.

Depuis ma thèse et jusqu'à aujourd'hui, j'ai proposé un cadre (Parent *et al.*, 2010; Parent *et al.*, 2016) pour l'analyse et la modélisation de la diversité des réponses entre processus (Parent et al., 2010), génotypes et espèces (Poire *et al.*, 2010; Parent & Tardieu, 2012), et essayé de démêler les différentes hypothèses apparemment contradictoires quant aux réponses de nuit / de jour (Lohraseb *et al.*, 2017) ou d'autres cofacteurs putatifs (Lohraseb *et al.*, 2017; Parent *et al.*, 2019).

Diversité des réponses à la température

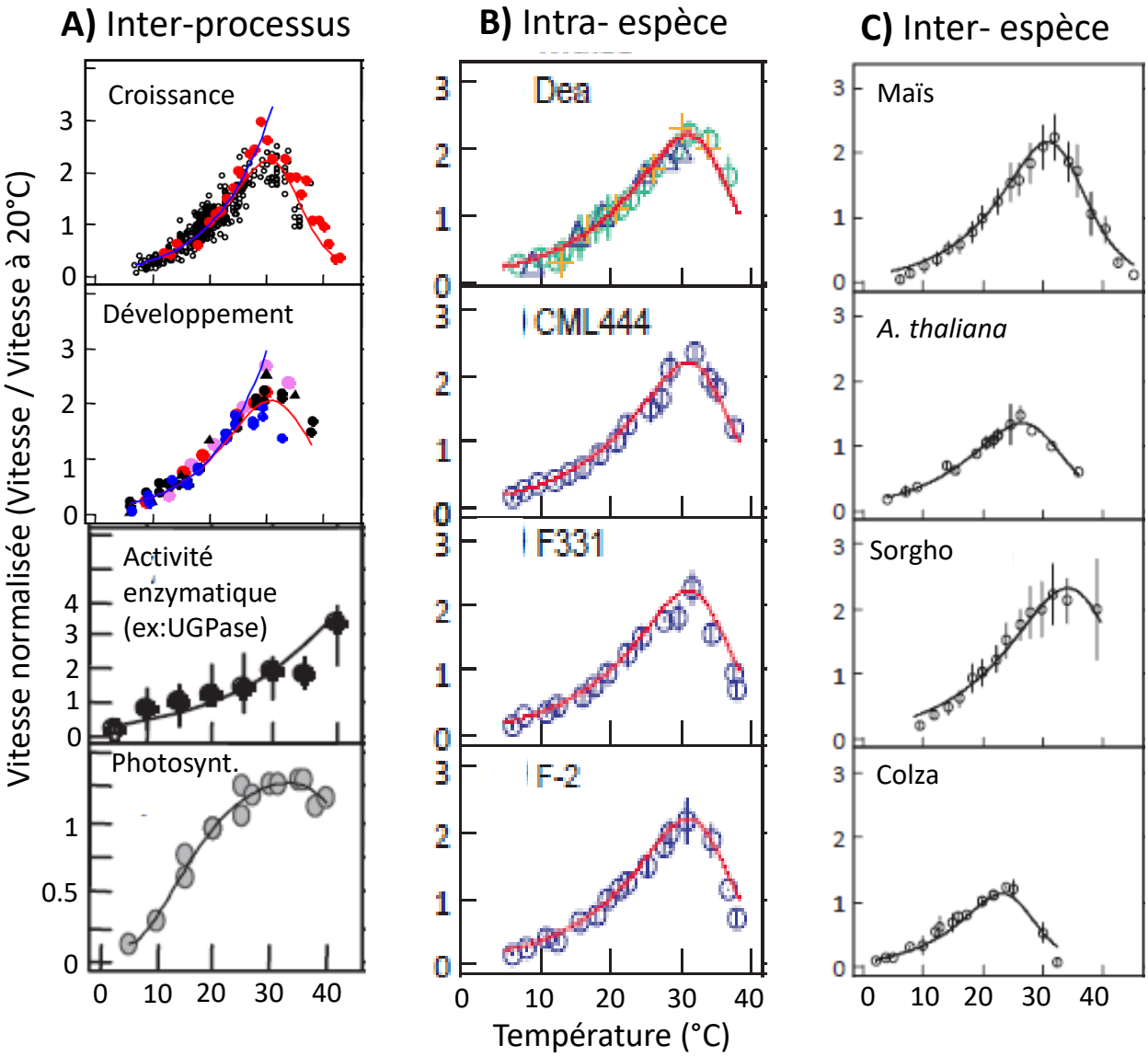

Figure 14. Diversité des réponses à la température entre processus (A), entre variétés dans une espèce (B) et entre espèces (C).

Pour faciliter les comparaison, toutes les vitesses sont normalisées par la vitesse du même processus à 20°C ***(Parent et al., 2010).***

A) Réponses à la température de processus d'expansion des tissus (feuille et plantules), de développement (initiation et apparition des feuilles, division cellulaire, germination), d'enzymes *in vitro* (ici l'UGPase) et de la photosynthèse chez le maïs. Notez que les processus d'expansion et de développement ont la même réponse à la température mais que ce n'est pas le cas des activités enzymatique et de la photosynthèse. ***Issu de Parent et al., 2010.***

B) Réponses à la température de processus de développement et d'expansion des tissus chez 4 génotypes de maïs issus de milieux tempérés ou tropicaux. La courbe rouge est commune aux 4 génotypes. Notez que les réponses sont similaires (ou très proches) dans une même espèce. ***Issu de Parent et Tardieu, 2012.***

C) Réponses à la température de processus de développement et d'expansion des tissus chez 4 espèces. Notez que les réponses sont différentes entre espèces. ***Issu de Parent et Tardieu, 2012.***

Résultats Principaux

Un cadre général à l'analyse comparative des réponses à la température

Une condition nécessaire à la méta-analyse des réponses à la température de processus aussi diverses que la photosynthèse nette, la vitesse de réaction enzymatiques, la vitesse de division cellulaire, ou la vitesse des cycles de développement chez différents génotypes (> 12000 données, 55 processus biologiques dans 130 génotypes appartenant à 18 espèces, issues d'expériences propres ou de la littérature) est de disposer d'un formalisme (i) suffisamment plastique pour représenter ces différentes données, (ii) utilisé dans des disciplines différentes (agronomie, écologie, physiologie végétale) (iii) pouvant être paramétré avec des jeux de données limités et donc parcimonieux en nombre de paramètres, (iv) avec des paramètres indépendants, robustes, permettant des analyses comparatives basées sur les valeurs de paramètres (Parent et al., 2016).

La principale raison pour laquelle nous avons adopté (Parent et al., 2010) une équation de réponse enzymatique avec une base thermodynamique (Johnson *et al.*, 1942) est qu'elle a été largement appliquée aux sciences végétales et animales à différents niveaux d'organisation (voir références dans Parent et al., 2012 et Dell *et al.*, 2011). Ce formalisme a été modifié pour tenir compte d'interdépendances entre paramètres, aboutissant à l'un des modèles les plus parcimonieux disponibles, avec seulement deux paramètres indépendants. Lorsqu'elle est utilisée dans un contexte différent de l'activité d'une enzyme donnée, cette équation peut être interprétée comme le comportement d'une enzyme virtuelle qui résume toutes les réactions biochimiques impliquées dans le processus étudié. C'est donc une représentation de la réalité dont les paramètres ont une signification biologique qui peut traverser les disciplines et aider à identifier des lois générales du fonctionnement des plantes (Marquet *et al.*, 2014).

Unicité des réponses des processus de développement et de croissance dans chaque espèce

Une méta-analyse chez 18 espèces montre une réponse commune des différents processus de développement et d'expansion des tissus dans chaque espèce mais des divergences avec les processus du métabolisme (Parent et al., 2010, 2012). Dans chaque espèce, des processus de développement et de croissance aussi diverses que la germination, l'initiation des feuilles, l'élongation foliaire ou les vitesses de division cellulaire mesurés au champ, en serre ou en chambre de culture avaient une réponse commune à la température (Fig.14A) mais différentes des réponses de vitesses d'activités enzymatiques, de photosynthèse et d'accumulation de biomasse. Ainsi, un modèle unique par espèce pouvait être considéré, valide pour la totalité des processus de développement et de croissance, et pour des variétés cultivées dans des environnements tempérés ou tropicaux, ou provenant de différents cycles de sélection (Parent et al., 2010, 2012).

Structure de la diversité interspécifique des réponses à la température

A) Chez 17 espèces cultivées

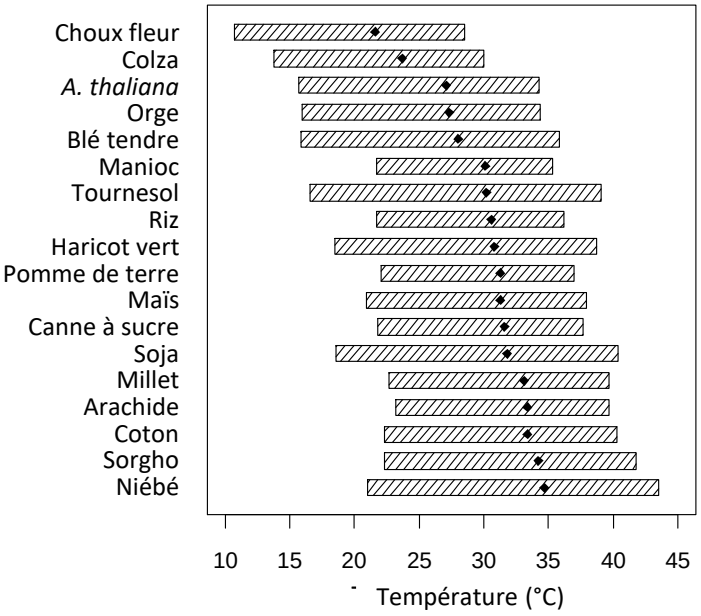

Figure 15. Structure de la diversité interspécifique des réponses à la température.
A) Chez 17 espèces cultivées et *A thaliana*. Ce graphique indique la température pour laquelle la vitesse est maximum, ainsi que plage de température pour laquelle la vitesse de développement est à plus de 50% de sa vitesse maximale. Notez que les 5 espèces avec des température optimale élevées sont toutes adaptées à des climats chauds. ***Issu de Parent et Tardieu, 2012.***
B) Chez 12 espèces et sous-espèces apparentées au blé. La classification hiérarchique des paramètres de réponse à la température et au VPD indique un lien étroit avec la phylogénie des blés. ***Issu de Leveau et al. Soumis)***

B) Chez 12 espèces et sous espèces apparentées au blé

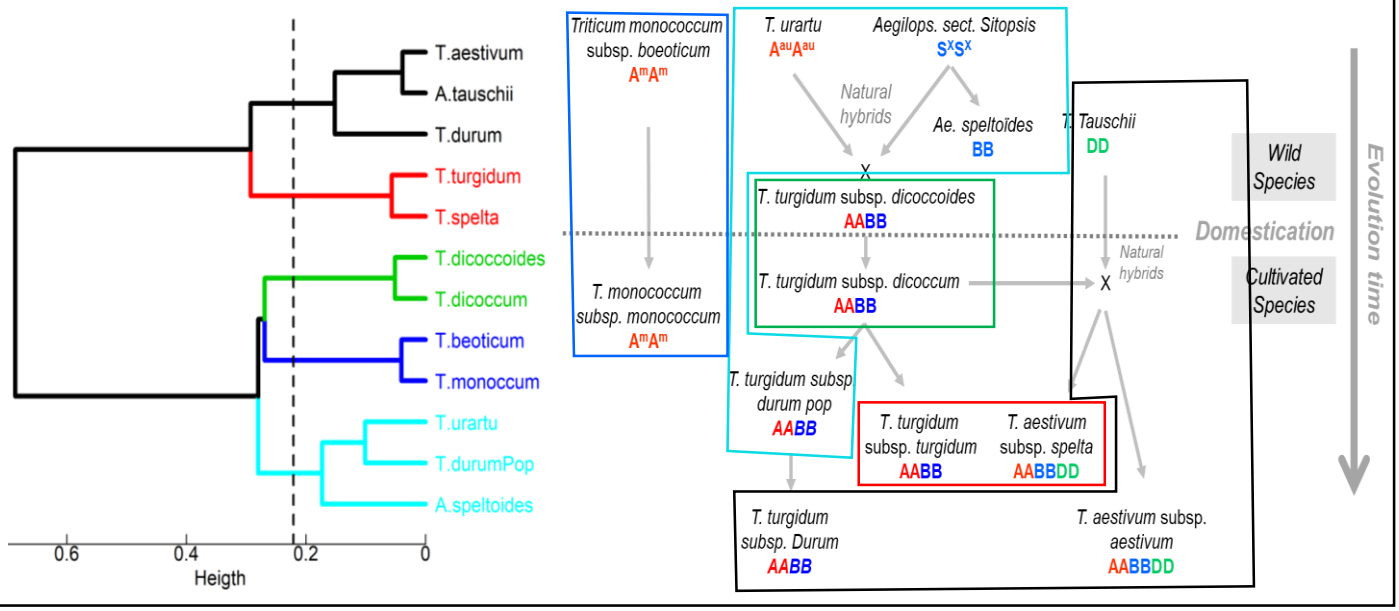

Ces résultats permettaient une nouvelle méthode de calcul de temps thermique valide pour une large gamme de températures, de processus et d'espèces. Cette méthode revient à calculer pour chaque couple de données vitesse / température, quelle serait cette vitesse à la température standard de 20°C, compensant ainsi toute vitesse par l'effet de la température. Le temps, considéré comme du temps de développement, et donc l'inverse d'une vitesse de développement pouvait être compensé de la même façon. Ce nouveau calcul de temps thermique et de vitesses compensées montrait une plus large gamme d'utilisation et une unité plus intuitive ($h_{20°C}$) comparé à la méthode conventionnelle.

Ces résultats ont été fortement remis en cause à leur publication (Michelangeli *et al.*, 2016) ou lors de présentations, en particulier pour les choix de modélisation défendus plus haut (Parent et al., 2016), mais aussi car ils étaient contradictoires avec des résultats semblant démontrer un processus de plasticité du développement dans des scenarios thermiques différents, contraire à l'idée d'une réponse unique. J'y ai répondu en démontrant que ces différences de masse surfacique observées dans les feuilles pouvaient être expliquées par la différence entre réponses à la température des processus de développement et d'accumulation de biomasse (Lograseb et al., 2017). De plus, les différences rapportées dans la littérature d'effets nuit/jours, entre processus ou entre stades de développements pouvaient être expliqués par un mauvais choix de modèle (ex : modèle linéaire dans une gamme non-linéaire), ou du pas de temps considéré pour des processus dynamiques dans des environnements fluctuants (Parent et al., 2019).

Une lente évolution dans des environnements contrastés structure la diversité génétique de cette réponse très conservée

L'analyse comparée des réponses chez les 18 espèces montrait une forte variabilité interspécifique, avec des températures optimales (T_{opt}, température pour laquelle la vitesse de développement est maximale) variant de 22 à 35 °C (Fig.15A ; Parent et al., 2012). Le gradient de T_{opt} montrait un fort lien avec les climats types de culture de ces espèces. Par exemple, les 4 espèces cultivées avec les T_{opt} les plus basses (choux fleur, colza, orge, blé) sont majoritairement cultivées dans des zones tempérées ou en hiver, quand les 5 espèces cultivées avec les T_{opt} les plus hautes sont majoritairement cultivées dans des zones subtropicales (millet, arachide, coton, sorgho, niébé). Cependant, des espèces proches phyllogénétiquement présentaient des réponses très proches (Sorgho- maïs, ou Orge-Blé tendre).

De même, l'analyse de ces réponses chez 12 espèces et sous-espèces apparentées au blé montrait des réponses très proches (T_{opt} variant de moins de 2°C) quoique significatives (Leveau et al., non-publié). Une classification hiérarchique de ces groupes d'espèces ou sous espèces basée sur l'espace phénotypique des paramètres de réponses à la température et au VPD aboutissait à un arbre hiérarchique très proche de l'arbre phyllogénétique (Fig.15B).

Globalement, ces résultats montraient que ces réponses étaient très conservées, à l'intérieur d'une espèce ou entre espèces proche, indiquant un processus surement très complexe, multigénique, et qu'une évolution lente peut faire diverger ces réponses qu'à condition d'espèces très éloignées et des climats d'origine très différents.

Bilan et Conséquences pour mon projet de recherche

Les conclusions de cette étude vont plus loin qu'une simple description et modélisation de ces processus, en apportant des réponses dans différents domaines scientifiques. (i) Pour l'écophysiologiste, la nouvelle conception du temps thermique permet de s'affranchir de l'effet de la température sous conditions fluctuantes et sur une large gamme. (ii) Du point de vue évolutif, ce travail montre des mécanismes très conservés et une évolution lente entre espèces, réfutant un contrôle par une loi thermodynamique universelle. (iii) Pour le modélisateur, ce travail simplifie les modèles de culture en proposant que des espèces peu étudiées puissent avoir les mêmes paramètres que d'autres espèces proches. (iv) Pour le généticien et le sélectionneur, ce travail propose une faible possibilité d'évolution de ces réponses dans les prochaines décennies.

Comme évoqué plus haut, ce travail est de loin celui pour lequel la controverse scientifique a été la plus forte. Conclure en un manque de variabilité génétique sur un caractère donné est de fait un exercice risqué, car un seul contre-exemple peut contredire la théorie. Cependant, cet exercice de simplification des hypothèses est un processus clé pour la modélisation des cultures et la communication entre disciplines.

L'approche de la diversité génétique présentée ici, combinant des choix de modélisation les plus parcimonieux, l'analyse comparative des diversités intra- et inter-spécifiques, les tests d'hypothèses alternatives par modélisation, et l'analyse des facteurs génétique et environnementaux qui structurent l'espace phénotypique, est fondatrice de mes projets de recherche, et grandement reprise pour mes projets futurs (en particulier Cas 6).

Articles issus de ce travail

(34) Tardieu F, Granato ISC, Van Oosterom EJ, **Parent B,** Hammer GL. 2020. Are crop and detailed physiological models equally "mechanistic" for predicting the genetic variability of whole plant behaviour? "in silico" Plants (accepted 20th Nov 2020)

(29) Parent, B., Millet, E. J., Tardieu, F. (2019). The use of thermal time in plant studies has a sound theoretical basis provided that confounding effects are avoided. *Journal of Experimental Botany, 70* (9), 2359-2370. ,

(28) Parent, B., Leclere, M., Lacube, S., Semenov, M. A., Welcker, C., Martre, P., Tardieu, F. (2018). Maize yields over Europe may increase in spite of climate change, with an appropriate use of the genetic variability of flowering time. *Proceedings of the National Academy of Sciences of the United States of America, 115* (42), 10642-10647.

(26) Lohraseb, I., Collins, N. C., **Parent, B.** (2017). Diverging temperature responses of CO2 assimilation and plant development explain the overall effect of temperature on biomass accumulation in wheat leaves and grains. *AoB Plants*. DOI : 10.1093/aobpla/plw092

(22) Parent, B., Vile, D., Violle, C., Tardieu, F. (2016). Towards parsimonious ecophysiological models that bridge ecology and agronomy. *New Phytologist, 210* (2), 380-382.

(16) Kumudini, S., Andrade, F., Boote, K., Brown, G., Dzotsi, K., Edmeades, G., Gocken, T., Goodwin, M., Halter, A., Hammer, G., Hatfield, J., Jones, J., Kemanian, A., Kim, S.-H., Kiniry, J., Lizaso, J., Nendel, C., Nielsen, R., **Parent, B.,** Stockle, C., Tardieu, F., Thomison, P., Timlin, D., Vyn, T., Wallach, D., Yang, H., Tollenaar, M. (2014). Predicting maize phenology: intercomparaison of functions for developmental response to temperature. *Agronomy Journal, 106* (6), 2087-2097.

(10) Parent, B., Tardieu, F. (2012). Temperature responses of developmental processes have not been affected by breeding in different ecological areas for 17 crop species. *New Phytologist, 194* (3), 760-774.

(9) Parent, B., Turc, O., Gibon, Y., Tardieu, F. (2010). Modelling temperature-compensated physiological rates, based on the co-ordination of responses to temperature of developmental processes. *Journal of Experimental Botany, 61* (8), 2057-2069.

(6) Poiré, R., Wiese-Klinkenberg, A., **Parent, B**., Mielewczik, M., Schurr, U., Tardieu, F., Walter, A. (2010). Diel time-courses of leaf growth in monocot and dicot species: endogenous rhythms and temperature effects. *Journal of Experimental Botany, 61* (6), 1751-1759.

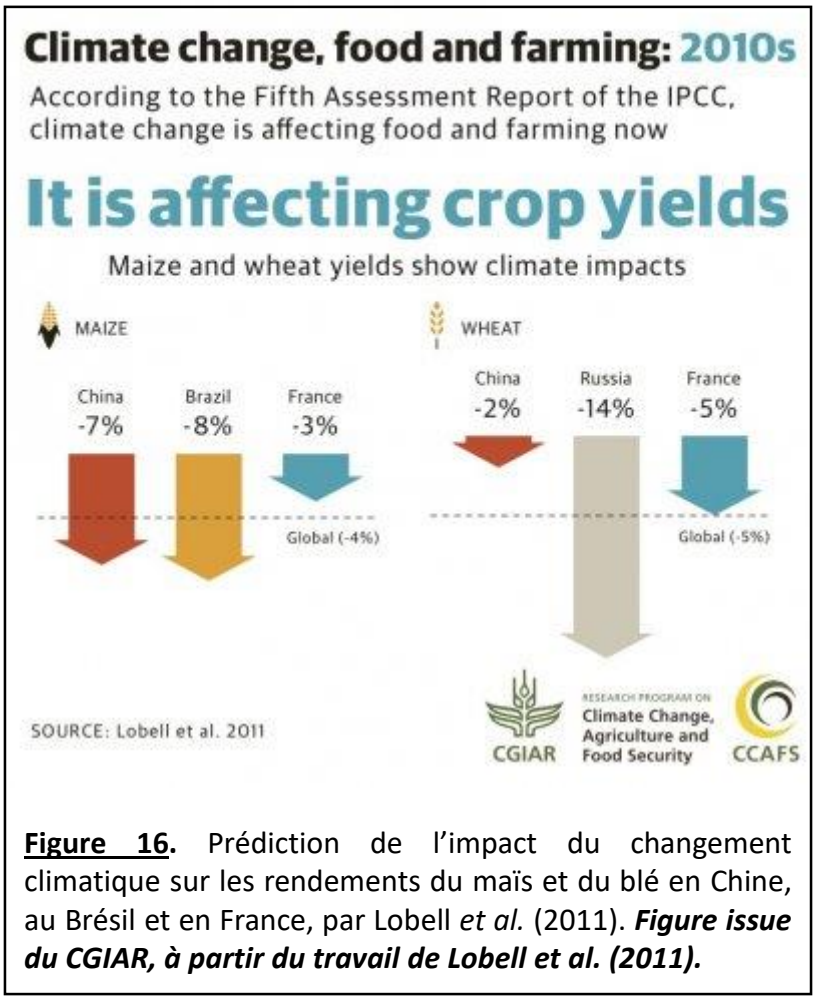

<u>Figure 16</u>. Prédiction de l'impact du changement climatique sur les rendements du maïs et du blé en Chine, au Brésil et en France, par Lobell *et al.* (2011). ***Figure issue du CGIAR, à partir du travail de Lobell et al. (2011).***

Focus n° 4 : Variabilité génétique du développement et de la croissance foliaire pour des climats futurs

Cet axe, initié pendant ma thèse a été largement repris et approfondis depuis ma titularisation comme Chargé de Recherche au LEPSE. Plutôt qu'un aspect chronologique ou thématique, je vous propose une lecture suivant la stratégie proposée en introduction.

Contexte

La plupart des simulations d'impacts des changements climatiques prédisent des réductions de rendements pour la plupart des espèces cultivées (Zhang *et al.*, 2015; Cammarano *et al.*, 2016; Xu *et al.*, 2016; Yang *et al.*, 2017). Cependant, la majorité de ces études ne considère pas d'adaptation des agriculteurs, en particulier le choix de variétés présentes ou futures (ex : Fig. 16, Lobell *et al.*, 2011). Pourtant, par exemple, les semenciers proposent de larges gammes de précocité pour la plupart des céréales annuelles, et les agriculteurs adaptent déjà leur choix de variétés et de dates de semis au réchauffement climatique actuel (Butler & Huybers, 2013; Moore & Lobell, 2014). Une question importante est donc de savoir si les agriculteurs pourront contrer les effets des changements climatiques en utilisant au mieux cette diversité génétique.

Comme déjà discuté en introduction, la variabilité génétique de la durée de cycle et le développement foliaire sont des leviers importants pour l'amélioration variétale en condition de déficit hydrique. Prédire l'impact de cette variabilité sur la production peut donc guider la sélection à concevoir des idéotypes pour des climats présents et futurs. La comparaison de 27 modèles a montré qu'une mauvaise prédiction de surface foliaire est une cause majeure de l'inexactitude des simulations (Martre *et al.*, 2015b). Cependant, la majorité des modèles de culture ont adoptés une approche Big-Leaf (la croissance est prise dans son ensemble, à l'échelle de la plante ou du couvert, et les feuilles individuelles ne sont pas considérées). Ces modèles ne prennent pas en compte toute la richesse des informations phénotypiques qui caractérisent les génotypes individuels et qu'il est maintenant possible de caractériser en plateforme de phénotypage (Parent et Tardieu, 2014), en particulier la variabilité génétique du développement foliaire, de l'expansion foliaire et de leur sensibilité aux contraintes environnementales à l'échelle de la feuille individuelle.

Dans ce cas d'étude, j'ai donc (i) développé des modèles basés sur la phénomique (dont la diversité génétique des paramètres est mesurable en plateforme), pour les différentes composantes du développement foliaire chez plusieurs céréales (vitesse de développement ; profils d'expansion maximum ; et sensibilités à différentes contraintes environnementales) ; (ii) analysé la diversité génétique et les contraintes limitant l'espace phénotypique ; (iii) défini les meilleurs combinaisons de paramètres (idéotypes) pour des climats présents et futurs, (iv) et analysé leur disponibilité (ou la possibilité de les atteindre) dans la diversité actuelle, et leur impact potentiel sur le rendement.

Modéliser la croissance foliaire

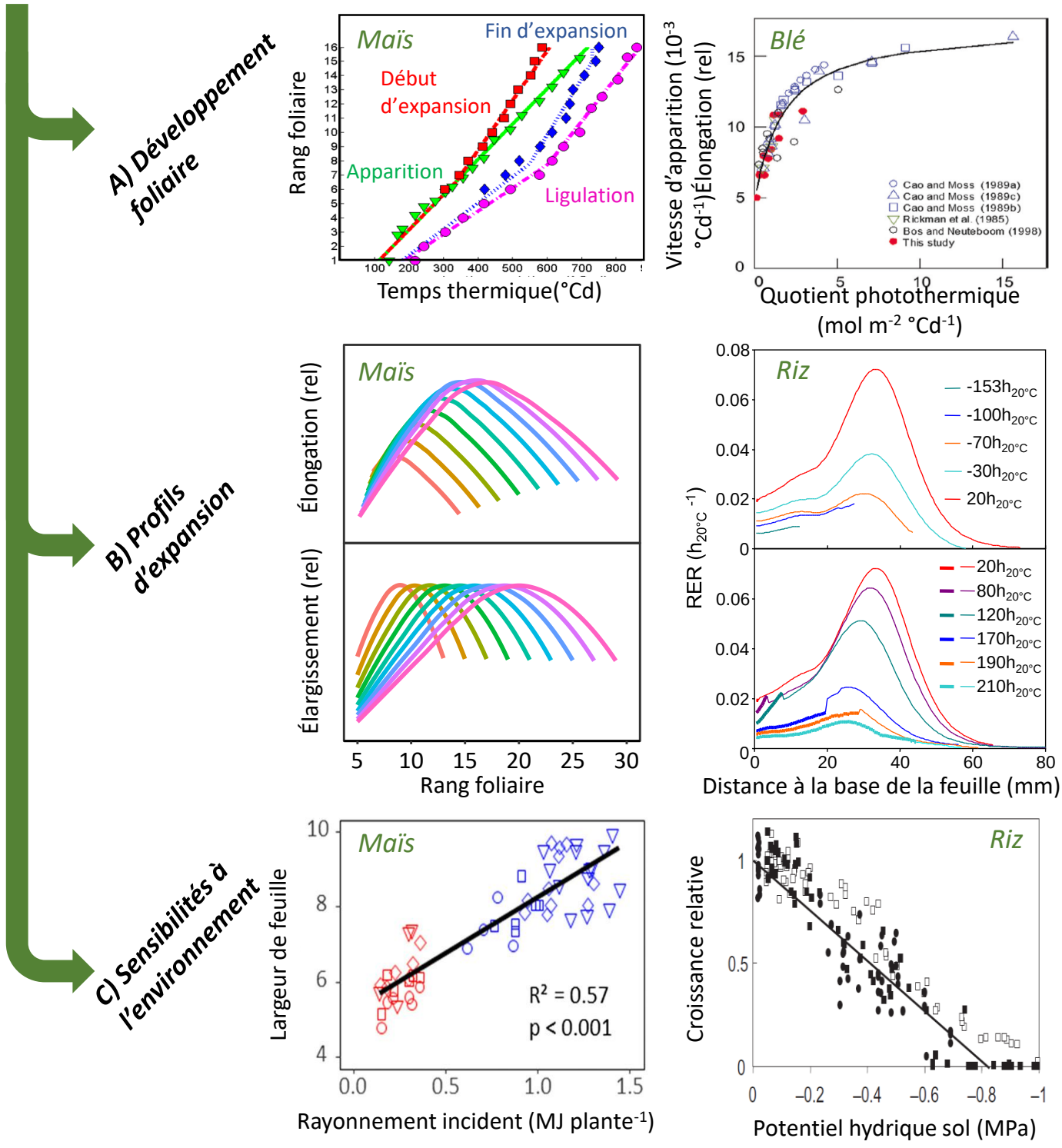

Figure 17. Modélisation de trois composantes de la croissance foliaire chez les céréales.

A) Développement des feuilles individuelles. Modèles de développement en fonction du temps thermique chez le Maïs (Lacube et al., 2020) et de la vitesse d'apparition des feuilles à partir du coefficient photothermique chez le blé (Baumont et al., 2019).

B) Profils d'expansion des feuilles. Profils d'expansion maximum (en longueur et largeur) en fonction du nombre de feuilles finales chez le maïs (Lacube et al., 2020) et profils spatiaux-temporels de vitesse d'expansion relative dans la feuille de riz (Parent et al., 2009).

C) Réponses de l'expansion foliaire. Réponse de l'élargissement des feuilles au rayonnement incident chez le Mais (Lacube et al., 2017) et réponse de l'élongation foliaire du riz au déficit hydrique du sol (Parent et al., 2010).

Résultats Principaux

Des modèles phénomique-compatibles pour le développement de la surface foliaire

Développement des feuilles individuelles

Prédire l'impact de variables environnementales sur la croissance de feuilles individuelles dans un environnement fluctuant nécessite de connaitre précisément la période pendant laquelle une feuille est en croissance et peut donc être affectée par des contraintes extérieures. Chez le maïs, un modèle de développement de feuilles individuelles avait été développé (Chenu *et al.*, 2008) mais n'était valable que pour un nombre de feuilles finales donné et comportait des paramètres difficilement mesurables pour des centaines de génotypes (ex : temps thermique d'initiation des feuilles). Pendant la thèse de Sébastien Lacube, nous avons repris ce modèle, pour qu'il soit valable pour une grande gamme de nombres de feuilles finales, et avec le cahier des charges d'un modèle axé sur la phénomique, à savoir que ces paramètres soient mesurables dans des grands panels de génotypes. Le modèle final (Fig.17A, (Lacube *et al.*, 2020)) simule les périodes d'expansion (longueur et largeur) de chaque feuille, et comporte seulement 5 paramètres génotypiques facilement mesurable (254 hybrides de mais ont été paramétrés).

Chez le blé, les modèles d'apparition des feuilles dans les modèles de culture étaient principalement basés sur des relations empiriques avec le temps thermique et la photopériode, souvent modifiées par la latitude, la date de semis et le numéro de feuille. Pendant la thèse de Maeva Baumont, nous avons montré que le rythme d'apparition des feuilles était lié à l'état trophique de la plante, dont le quotient photo-thermique (rayonnement intercepté/ temps thermique) était un bon proxy (Fig.17A, Baumont *et al.*, 2019). Cet effet résumait à lui seul les différents effets du rayonnement, de la photopériode, de la température, du stade foliaire, et du CO_2. Intégré dans le modèle Sirius, il faisait aussi bien que des modèles intégrant ces multiples effets et leurs nombreux paramètres associés.

Profils temporels et spatiaux de l'expansion et d'élargissement des feuilles.

La vitesse maximale d'expansion dépend du rang foliaire. Sachant qu'il serait couteux de mesurer cette vitesse pour chaque feuille pour chaque génotype, nous avions besoin d'un model capable de simuler ces profils d'élongation et d'élargissement à partir de quelques observations. Le modèle développé dans Lacube et al. (2020) pour le maïs est capable de simuler ces profils à partir de 3 paramètres, le nombre final de feuille, la vitesse maximale d'expansion d'une feuille (la 6^{eme}) et la largeur d'une feuille, et ce pour des génotypes contrastés allant de 12 à 26 feuilles finales (Fig.17B).

Connaitre précisément le profil spatial d'expansion relative d'une feuille au cours du temps permet de de ne pas confondre des effets développementaux et environnementaux dans un environnement fluctuant, et de diriger l'échantillonnage de zones de croissance (division cellulaire, expansion) pour des études -omiques des

Impact de la diversité génétique (sensibilité de la croissance au déficit hydrique et demande évaporative)

Diversité

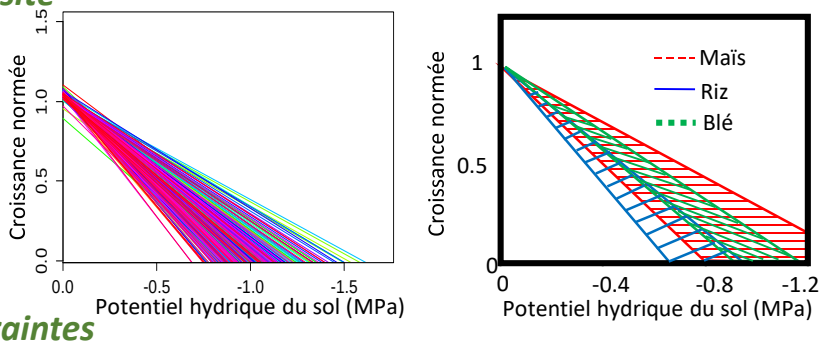

Contraintes

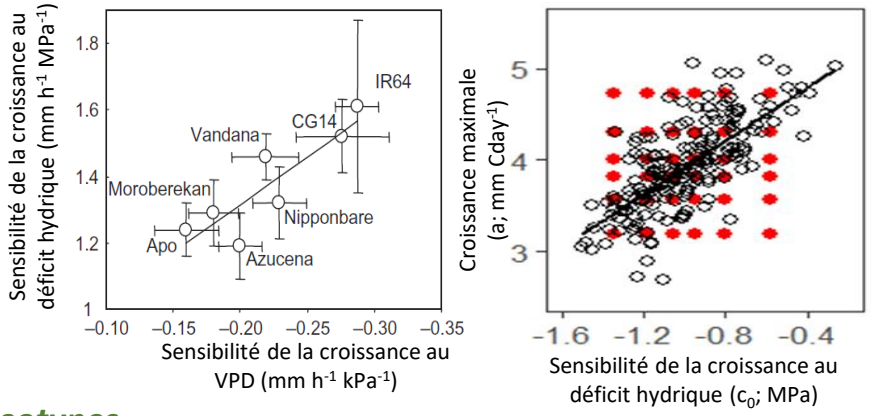

Ideotypes

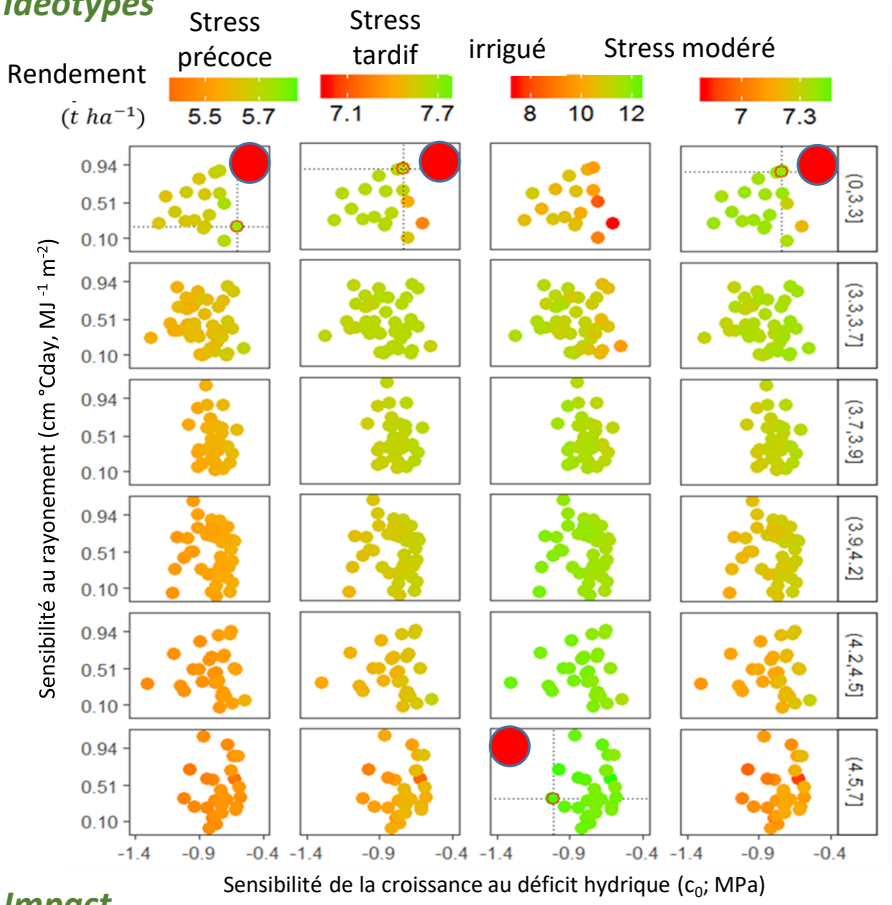

Impact

Rendement

-4 % **-4 %** **-3 %** **-5 %**

Figure 18. Impact de la diversité génétique des réponses de la croissance à l'environnement.

-Diversité génétique intra et inter-spécifique. Variabilité des réponses de l'expansion foliaire au déficit hydrique du sol chez 254 hybrides de maïs et gamme de variabilité observée chez le maïs, le riz et le blé tendre. Données issues de maïs: Lacube et al. (2017); Riz: Parent et al. (2010); Blé: Parent et al. (2015).

-Corrélations entre paramètres (contraintes limitant l'espace phénotypique). Entre les sensibilités de l'expansion foliaire au déficit hydrique du sol et au VPD chez le riz (Parent et al. 2010, observée aussi chez le maïs); et entre expansion maximale intrinsèque et sensibilités au déficit hydrique du sol et au VPD chez le maïs (Non publié).

-Idéotypes théoriques et réalistes de 3 paramètres dans 4 scenarios environnementaux. Les 4 scénarios sont représentatifs des scénarios européens (59 sites sur 30 ans, Harrisson et al. 2014). Les Idéotype théoriques (ronds rouges) sont les meilleures combinaisons de valeurs de paramètres (limités par la gamme observée pour chaque paramètre), mais sans tenir compte des corrélations observées entre paramètres (hypercube non-contraint des valeurs de paramètres). Les Idéotypes réalistes (points) ont les mêmes combinaisons de paramètres qu'observé chez 254 hybrides (mais sont différents sur les autres paramètres du modèle). (Lacube et al. Non publié).

-Impact sur le rendement dans chaque scénario. Différence de rendement moyen entre l'Idéotype théorique et l'Idéotype réaliste. (Lacube et al. Non publié).

déterminants moléculaires associés à la croissance. Avant ma thèse, une telle étude n'existait pas encore pour le riz. C'était surement dû au fait que les deux méthodes classiques, les trous d'épingles (Schnyder & Nelson, 1989; Bernstein *et al.*, 1993; Beemster *et al.*, 1996) et la méthode anatomique (Gandar & Rasmussen, 1991) se heurtaient au fait que l'expansion d'une feuille de riz n'était jamais en état permanent. J'ai donc développé une nouvelle méthode adaptée à ces profils non-stables, basée sur des mesures anatomiques et la résolution de l'équation de continuité en condition non-permanente (Fig. 17B ; Parent et al., 2010).

Effets environnementaux.

Ces cadres d'analyses développés plus haut (développement foliaire, profils d'expansion, effet de la température) m'ont permis d'analyser les réponses de l'expansion foliaire à des contraintes abiotiques (déficit hydrique, demande évaporative, rayonnement) dans toutes les espèces que j'ai travaillées (riz, blé, maïs, millet, sorgho). La majeure partie des réponses analysées étaient formalisées à partir de modèles simples (linéaires, bi-linéaires), comportant donc peu de paramètres, robustes, sur la base desquels la variabilité génétique était analysée (ex : Fig. 17C ; riz : Parent et al., 2010 ; blé : Parent et al., 2015, Leveau et al., 2020, article soumis ; maïs : Lacube et al., 2017 ; Millet et sorgho : non publié).

Quelle variabilité génétique disponible pour les climats présents et futurs et quel impact ?

La variabilité génétique intra-spécifique de la croissance foliaire et de ses réponses au déficit hydrique et à la demande évaporative était importante dans chaque espèce (Fig. 18). Plus étonnant, ces gammes de variabilité intra-spécifiques se recoupaient largement au niveau inter –spécifique. Ainsi, par exemple, des génotypes de blé ou de maïs étaient plus sensibles que les génotypes de riz les moins sensibles (Parent et al., 2010). La principale origine de la sensibilité à la sécheresse du riz n'est donc surement pas sa sensibilité au potentiel hydrique du sol mais plutôt son mauvais système racinaire, dont l'effet disparait dans cette étude en pot. Mais globalement, ces résultats montraient une large variabilité génétique disponible pour la sélection, dans chaque espèce.

L'analyse de l'espace phénotypique de ces réponses montrait cependant que des contraintes (physiologiques, génétiques ?) limitait cet espace et que toutes les combinaisons de valeurs de paramètres n'étaient pas possibles (Fig.18). Ainsi, les sensibilités au déficit hydrique et au VPD étaient corrélées chez le riz (Parent et al., 2010) ou le maïs (Lacube *et al.*, 2017; Lacube *et al.*, 2020) et il en était de même entre la croissance maximale et la sensibilité à ces deux contraintes (article en préparation). Il en découlait que les meilleurs idéotypes théoriques de maïs pour les valeurs de ces paramètres (en considérant l'hypercube de ces paramètres et sans considérer ces contraintes), identifiés dans 4 types de scénarios hydriques majoritaires en Europe (Harrison *et al.*, 2014), n'étaient pas disponible dans la diversité génétique actuelle (Fig.18, article en préparation). La différence de rendement entre les meilleurs idéotypes disponibles dans l'espace

Impact de la diversité génétique (développement, précocité)

Diversité

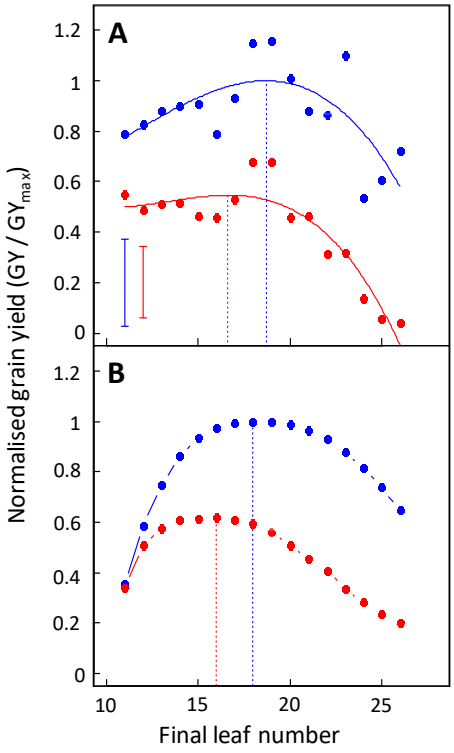

Idéotypes

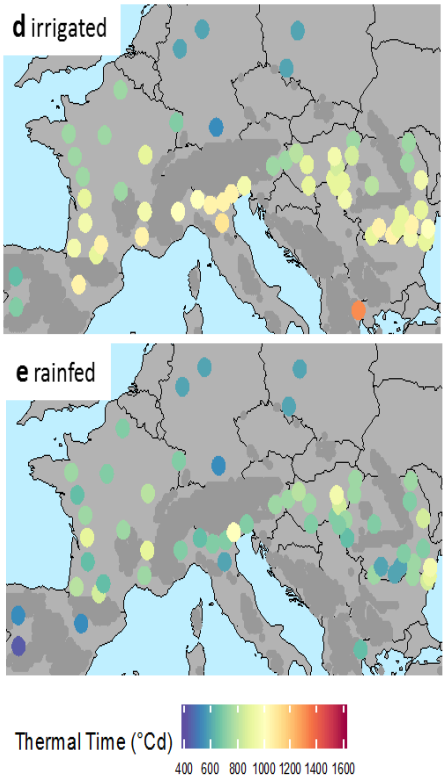

Impact

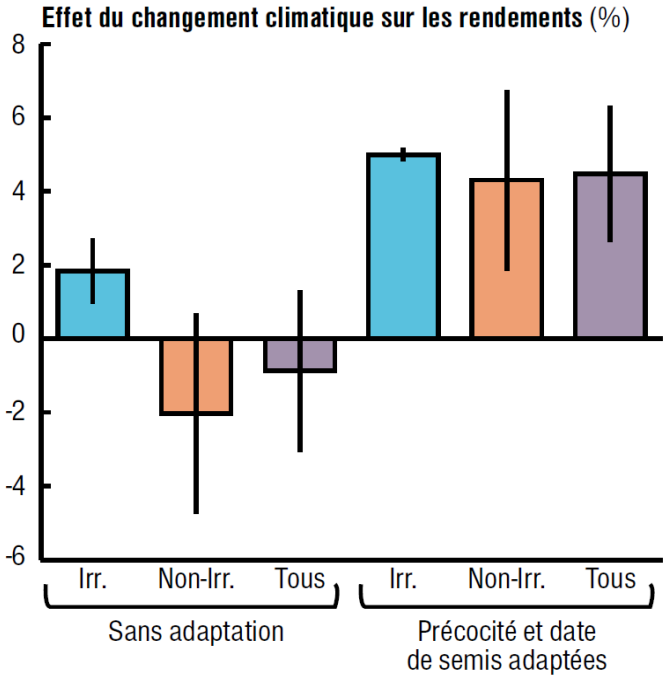

Figure 19. Impact de la diversité génétique de la précocité sur les rendements présents et futurs

-Variabilité de précocité dans un panel de lignées de maïs maximisant la diversité génétique. Effet du nombre de feuilles finales (corrélé à la durée du cycle végétatif) sur le rendement dans un site expérimental (Sainte-Pexine) pour 2 conditions de déficit hydrique (A). Une précocité optimale est déterminée expérimentalement. B) Précocité optimale déterminée avec un nouveau modèle de culture.

-**Idéotypes de précocité** (temps thermique à floraison) pour 59 sites en Europe, en condition irrigué ou non-irrigué.

-Impact sur le rendement du choix de nouveaux Idéotypes de précocité en 2050 (adaptation de l'agriculteur) comparé au fait de garder l'idéotype actuel dans le futur. Résultat issus de simulation avec deux scenarios d'émission de CO2 (RCP 4.5 et 8.5) et 6 modèles climatiques.

Issu de Parent et al., 2018

phénotypique et ces idéotypes théoriques étaient de 4 à 7 % en moyenne. Globalement, ces résultats indiquent au sélectionneur les meilleures combinaisons possibles de valeurs de caractères liés à la croissance foliaire dans chaque type de scénarios, mais sachant que la meilleure combinaison théorique n'est pas disponible, et ne le sera peut-être jamais, due à des contraintes fortes, qu'elles soient génétiques, biophysiques ou physiologiques (article en préparation).

Ces résultats contrastent avec une analyse similaire concernant la vitesse de développement et la durée du cycle chez le maïs (Parent et al., 2018). En effet, la vitesse d'apparition des feuilles était très peu liée à la durée du cycle et le seul nombre de feuilles finales rendait largement compte de la très large variabilité génétique de durée de cycle observée chez le maïs. Dans cet espace phénotypique réduit ainsi à une dimension, des idéotypes pouvaient être déterminés expérimentalement dans chaque scénario environnemental ou à plus large échelle avec le modèle précédemment développé (Lacube *et al.*, 2020) pour des milliers de scénarios (sites x année x date de semis x irrigation) en Europe (Parent *et al.*, 2018, Fig.19). La comparaison de ces données (meilleurs idéotypes identifiés) avec les bases de données européenne pour les dates de semis et la date de floraison a montré que les agriculteurs utilisaient déjà les durées de cycle optimales, adaptées à leurs conditions locales. Alors que les simulations utilisant les génotypes actuels pour prédire le future prédisaient une chute du rendement à l'échelle européenne en 2050 (Fig.19), considérer que les agriculteurs continueront d'adapter au mieux leur date de semis et le choix de précocité de leur variété aboutissait à des prédictions de rendement augmentées de +4 à +8 % en 2050, dépendant du scénarios d'émission de CO2 envisagé. De plus, ces précocités optimales pour toutes les localités sont déjà disponibles dans la diversité génétique actuelle.

Bilan et Conséquences pour mon projet de recherche

L'étude écophysiologique et la modélisation de la variabilité génétique des réponses au déficit hydrique est surement le fil rouge de ma carrière scientifique. J'ai fait l'exercice ici d'expliciter toute la stratégie générale de mon projet au travers de ce cas concret, tout en m'affranchissant de l'aspect chronologique et donc des questions associées qui m'animaient aux différentes époques pendant lesquelles ces études ont étés menées. Bien sûr, ma réflexion n'a pas été aussi linéaire, se nourrissant de questions spécifiques relatives aux espèces étudiées et aux projets financés. Cependant, c'est bien l'ensemble de ces études qui m'ont permis de dessiner le schéma d'ensemble de la stratégie proposée. Chaque étude a nourri l'autre. C'est bien la diversité des réponses chez le maïs qui m'a permis de prendre du recul sur celle observée chez le riz ou le blé. C'est bien l'observation d'un effet trophique majeur sur le développement du blé qui me pousse à ré-analyser des données chez le maïs. Le travail de Sébastien Lacube a été le premier dans lequel l'espace phénotypique a été bien caractérisé et pour lequel je me suis rendu compte de son importance pour la conception d'idéotypes.

Globalement, c'est donc cette approche, ici reconstruite au travers de différentes études apparemment décorrelées que je me propose de poursuivre dans les deux cas d'étude futurs présentés ci-après.

Articles issus de ce travail

(33) Lacube S, Manceau L, Welcker C, Millet EJ, Gouesnard B, Palaffre C, Ribaut JM, Hammer G, **Parent B,** Tardieu F.(2020). Simulating the effect of flowering time on maize individual leaf area in contrasting environmental scenarios. *Journal of Experimental Botany* 71(18): 5577-5588.

(30) Baumont, M., **Parent, B**., Manceau, L., Brown, H., Driever, S., Muller, B., Martre, P. (2019). Experimental and modeling evidence of carbon limitation of leaf appearance rate for spring and winter wheat. Journal of Experimental Botany. 70. 2449-2462. 10.1093/jxb/erz012.

(27) Lacube, S., Fournier, C., Palaffre, C., Millet, E. J., Tardieu, F**., Parent, B**. (2017). Distinct controls of leaf widening and elongation by light and evaporative demand in maize. *Plant, Cell and Environment, 40* (9), 2017-2028. DOI : 10.1111/pce.13005

(14) Tardieu, F., **Parent, B.,** Caldeira, C. F., Welcker, C. (2014). Genetic and physiological controls of growth under water deficit. *Plant Physiology, 164* (4), 1628-1635. DOI : 10.1104/pp.113.233353

(8) Parent, B., Suard, B., Serraj, R., Tardieu, F. (2010). Rice leaf growth and water potential are resilient to evaporative demand and soil water deficit once the effects of root system are neutralized. *Plant, Cell and Environment, 33* (8), 1256-1267. DOI : 10.1111/j.1365-3040.2010.02145.x

(3) Parent, B., Conejero, G., Tardieu, F. (2009). Spatial and temporal analysis of non-steady elongation of rice leaves. *Plant, Cell and Environment, 32* (11), 1561-72. DOI : 10.1111/j.1365-3040.2009.02020.x

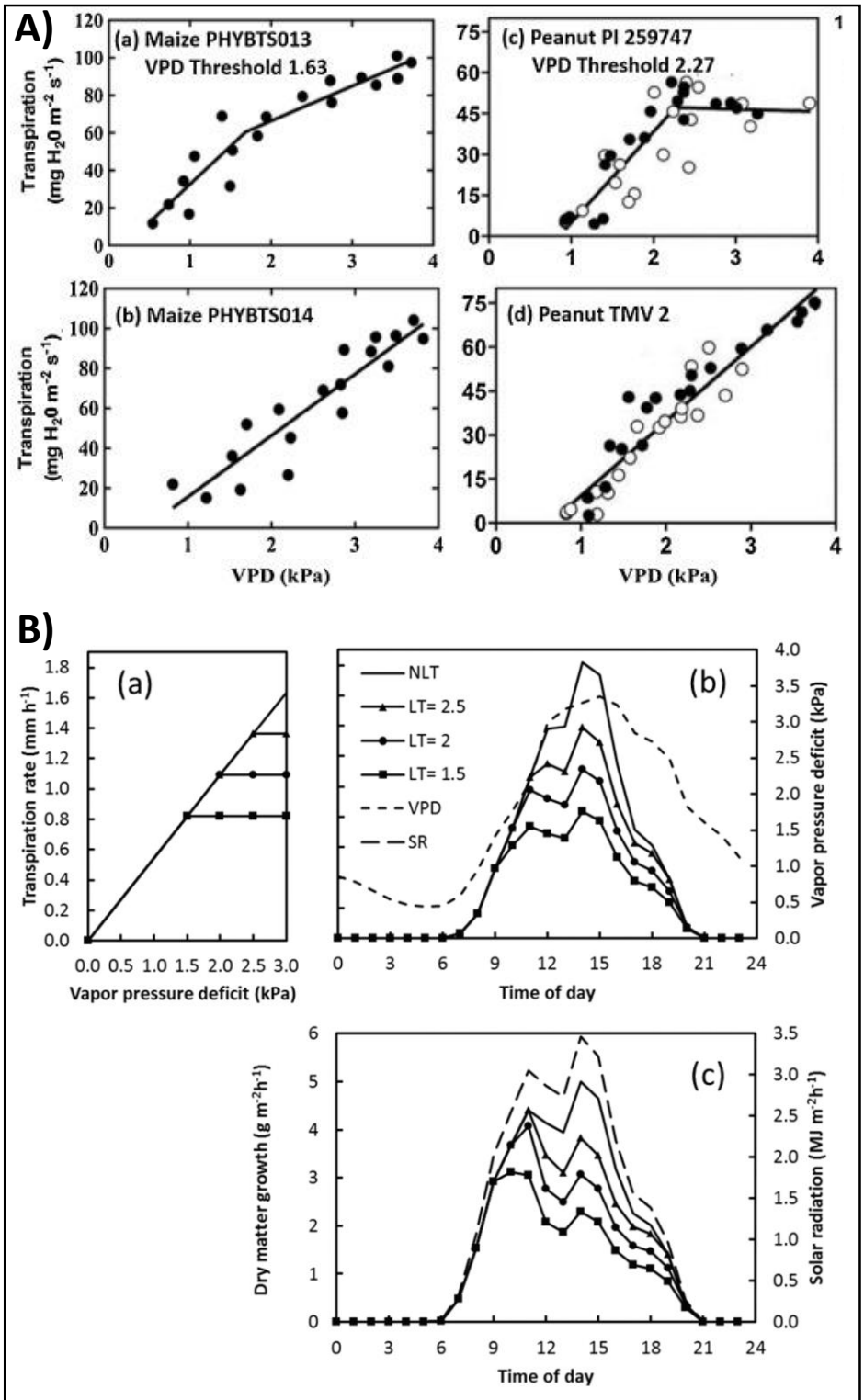

<u>Figure 20</u>. Variabilité génétique de la réponse de la transpiration à la demande évaporative.

A) Chez le maïs et l'arachide. Issu de Sinclair et al., 2017.

B) Variabilité théorique d'idéotypes de maïs AquaMax et impact sur la transpiration journalière. Issu de Messina et al., 2015.

7. PROJET DE RECHERCHE – ACTIVITES A MOYEN TERME

Focus n° 5 : Des idéotypes réalistes du contrôle de la transpiration sous changement climatique

Ce projet synthétise à lui seul l'approche générale présentée en introduction, et capitalise sur les outils, méthodes et réflexions développées dans les quatre premiers cas d'étude. Bien que proposé à plusieurs appels d'offres (ANR, ERC), il n'a pour le moment pas été financé.

Contexte

Classiquement, le développement de plantes économes en eau est envisagé en fonction du compromis stomatique entre l'avantage de fermer les stomates pour économiser l'eau pour les stades tardifs du cycle (floraison et remplissage du grain) et les effets négatifs qui en résultent sur la photosynthèse cumulée. Optimiser ce compromis reviendrai à augmenter l'efficacité d'utilisation de l'eau (WUE) définie comme le ratio entre production de biomasse et eau transpirée. Sous déficit hydrique, un idéotype produirait donc davantage de biomasse pour la même quantité d'eau transpirée. Cependant, la sélection directe sur WUE entraîne souvent une réduction de transpiration mais accompagnée également d'une réduction de biomasse (Blum, 2009). De même la transformation de lignées de maïs pour qu'elles soient affectées de manière constitutive sur la production d'ABA (voir Focus 1, Parent et al., 2009) a abouti à des phénotypes trop extrêmes (ex : plantes surproductrice d'ABA trop petites) pour qu'ils soient intéressants dans des scénarios agricoles habituels de sécheresse modérée (non publié). ***Ce projet va explorer une autre stratégie, en manipulant ``où et quand '' la plante doit transpirer plutôt que 'de combien'' la modifier.***

Les plantes s'adaptent constamment aux changements rapides de température, de rayonnement et d'eau disponible dans le sol. En particulier, les trois principaux composants de la plante qui contrôlent le flux d'eau (conductance racinaire, foliaire et stomatique) réagissent en synergie à ces signaux externes (par exemple la lumière) ou indirectement via des signaux internes (acide abscissique, ABA), les potentiels hydriques et le flux d'eau (Parent *et al.*, 2009; Tardieu *et al.*, 2010; Tardieu *et al.*, 2015). Il en résulte des changements rapides du taux de transpiration et de la photosynthèse au cours de la journée. Ces dernières années, des sélectionneurs privés ont placés le contrôle de la transpiration comme cible privilégiés pour l'amélioration variétales dans des zones à fortes contraintes hydriques. Chez le maïs, le contrôle de la transpiration est la base pour le développement d'hybrides de maïs commerciaux adaptés aux environnements secs (par exemple, Pionneer Aquamax® et Monsanto DroughtGard®). Le caractère principal visé est le fait de réduire la transpiration à

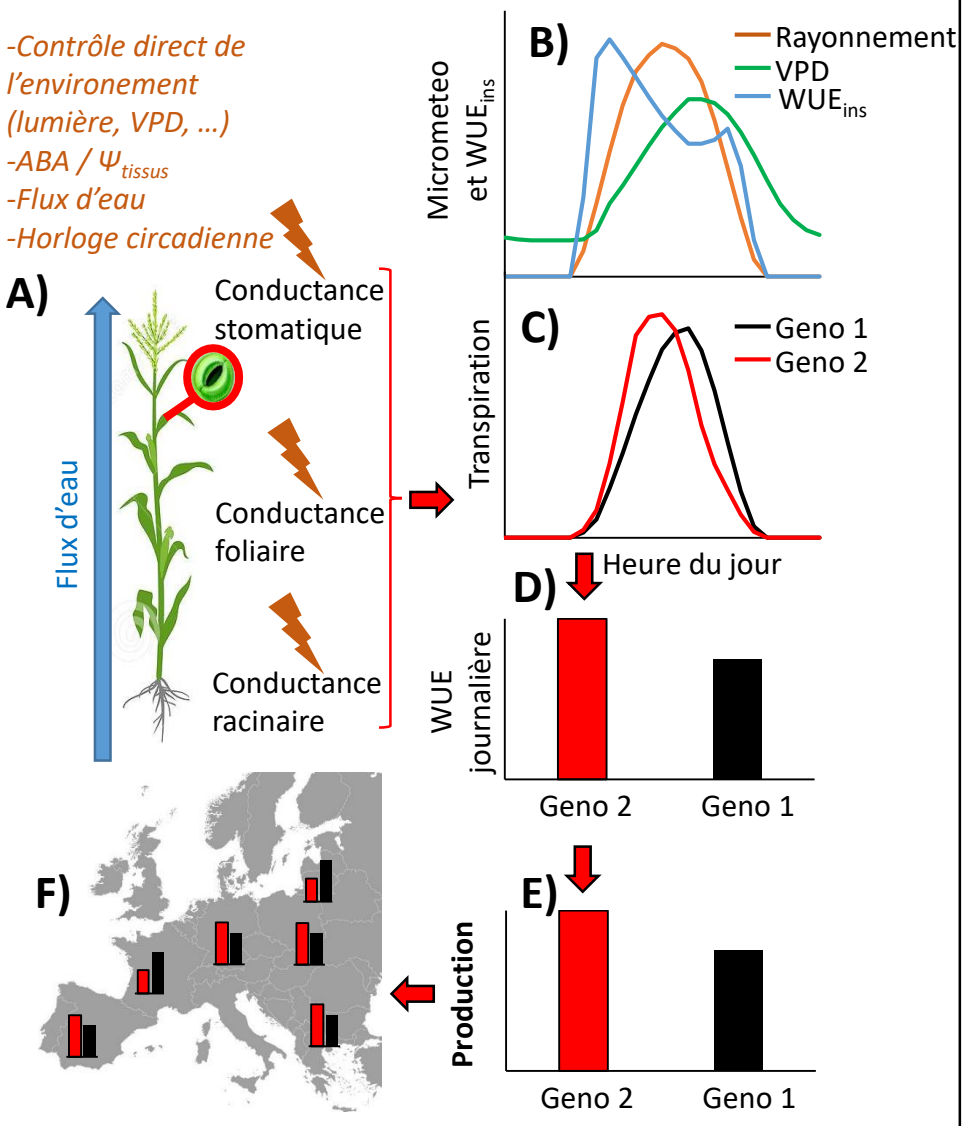

Figure 21. Stratégie pour concevoir des idéotypes efficients en eau. A) Exploiter la diversité des contrôles temporels de la transpiration pour **(C)** manipuler les cinétiques journalières de la transpiration et de la photosynthèse. Concevoir des plantes qui transpirent plus pendant le matin (**C**, courbe rouge) quand la demande évaporative est faible et l'efficience de transpiration instantanée (WUE_{ins}) est maximale **(B)**, et moins pendant l'après midi devrait aboutir à une meilleur efficience à l'échelle de la journée **(D)** et du cycle de culture, améliorant les rendements **(E)** dans la plupart des scenarios d'étés chauds et secs **(F)**.

partir d'un seuil de VPD. En effet, chez la plupart des espèces cultivées, il existe une large variabilité génétique ; pour ce caractère (Sinclair, 2017; Fig.20A). Les hybrides Pionneer Aquamax® visent à réduire très tôt la transpiration quand le VPD augmente (Messina *et al.*, 2015; Fig.20B). Il en découle une meilleur efficience d'utilisation de l'eau et des rendements augmentés de l'ordre de 5% en conditions de sécheresse (Cooper *et al.*, 2014).

Une autre solution serait de jouer sur la régulation circadienne de la transpiration. Par exemple, pendant une journée d'été ensoleillée typique, la photosynthèse augmente rapidement le matin tandis que la transpiration augmente plus lentement en raison d'une température et d'une demande évaporative modérées. Inversement, la transpiration est à son maximum dans l'après-midi, lorsque la température et la demande évaporative sont également à leur maximum, tandis que la photosynthèse diminue avec la lumière incidente. La WUE fluctue donc naturellement en étant plus forte le matin (Figure 21B). Par conséquent, la manipulation de la synchronisation diurne de la transpiration et de la photosynthèse peut induire de fortes augmentations de WUE. **Ce projet veut tester les optimisations possibles du contrôle temporel de la transpiration dans des scénarios environnementaux spécifiques, un déterminisme peu (pas ?) étudié de l'efficience de transpiration, avec des impacts potentiellement importants sur la performance des plantes.**

Parce que les plantes cultivées ont été sélectionnées sous différents climats, plusieurs optimisations de la transpiration dépendant du contexte ont probablement émergé, engendrant une probable variabilité génétique du profil temporel de la transpiration. **Ce projet doit exploiter la diversité des contrôles de transpiration disponibles dans les ressources génétiques naturelles et contribuera à la compréhension des contrôles dynamiques qui sous-tendent le couplage temporel entre transpiration et photosynthèse.**

Prédire les effets génotypiques de ces processus qui contrôlent les dynamiques temporelles de transpiration et photosynthèse sur la production au champ dans des scénarios multiples ne peut être déterminé qu'à l'aide de modèles de culture. Cependant, aujourd'hui, il n'y a pas de modèle disponible capable de simuler les performances des plantes tout en tenant compte de la diversité des contrôles de transpiration**. Ce projet doit permettre de construire un modèle qui permettra d'explorer les effets des processus dynamiques contrôlant la dynamique de transpiration sur les performances des plantes dans les environnements actuels et futurs.**

Axe 1: Preuve du concept avec des transformants

1) Phénotype hydraulique et caractérisation

Upscalling

2) Impact sur la biomasse et la WUE

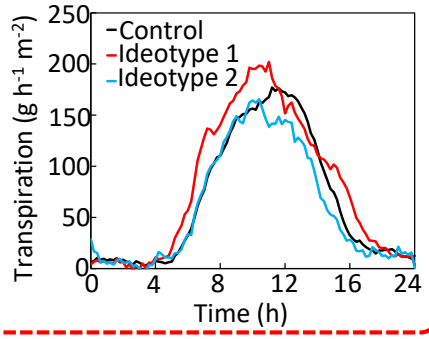

protocoles

Axe 2: Diversité génétique des contrôles dynamiques de la transpiration

1) Diversité génétique des profils temporels

Downscaling

2) Processus sous-jacents

Downscaling

3) Architecture génétique / Prédiction génomique

formalismes

-valeurs de paramètres
-prédiction génomique

Axe 3: Idéotypes dans des scénarios présents et futurs

1) Modèle de culture avec contrôles dynamiques de la transpiration

Upscaling

2) Prédiction à large échelle / Impact de la variabilité génétique

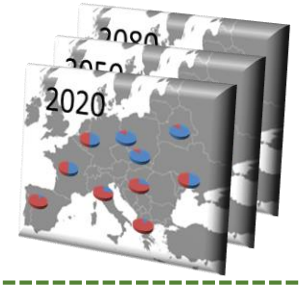

Figure 22. Activités envisagées pour le projet et diagramme des interactions et flux d'informations entre les axes de travail et activités.

Objectif et Stratégie

L'objectif principal est donc de mieux comprendre les variations spatiales et temporelles de l'efficience de transpiration, en étudiant les connexions dynamiques entre les différents processus qui contrôlent la transpiration et en exploitant la variabilité disponible dans les ressources génétiques naturelles. Cela afin d'optimiser le couplage temporel entre la transpiration et la photosynthèse sous les climats européens présents et futurs. Cet objectif se déclines en trois axes (Fig.22):

Axe 1: Démontrer que désynchroniser la transpiration et la photosynthèse peut avoir un impact important sur l'efficience de transpiration et les performances des plantes. Par l'analyse phénomique de plantes transgéniques affectées de manière circadienne sur la production et la dégradation de l'ABA.

Axe 2: Démêler les différents régulateurs de la cinétique journalière de la transpiration, en identifiant les mécanismes centraux et leurs connexions, de l'échelle de la plante entière aux gènes. Cela, en utilisant des panels de diversité de maïs, et en développant des modèles de prédiction génomique pour le caractère dynamique des processus sous-jacents à la transpiration et à l'acquisition de carbone.

Axe 3: Explorer les effets de différentes combinaisons de caractères liés au contrôle de la transpiration (et des allèles sous-jacents) sur les performances des plantes dans divers scénarios européens actuels et futurs, et identifier dans chaque scénario les meilleures combinaisons de traits et d'allèles (idéotypes), sur la base d'un nouveau modèle alimenté par la prédiction génomique de ces caractères.

Programme de recherche

Axe 1 : Preuve de concept avec des plantes transgéniques.

L'axe 1 doit évaluer dans quelle mesure le contrôle temporel fin de la transpiration peut avoir un impact sur l'efficience de transpiration et les performances des plantes. La seule approche possible était fonctionnelle plutôt que statistique, et basée sur la modification artificielle de la transpiration sans effets collatéraux causés par d'autres caractères qui pourraient être corrélés génétiquement dans des panels de génotypes. Parce que l'ABA agit sur la plupart des conductances hydrauliques (voir Focus N°1), il était la cible la plus appropriée pour concevoir des idéotypes de contrôle de la transpiration.

Résultats préliminaires

Récemment, dans le cadre d'un partenariat avec Biogemma / Limagrain, nous avons conçu et analysé des lignées de maïs transgéniques affectées sur la composante circadienne de la biosynthèse et de la dégradation de l'ABA (Fig.23). En bref, ces constructions impliquent des gènes de biosynthèse et de dégradation d'ABA et

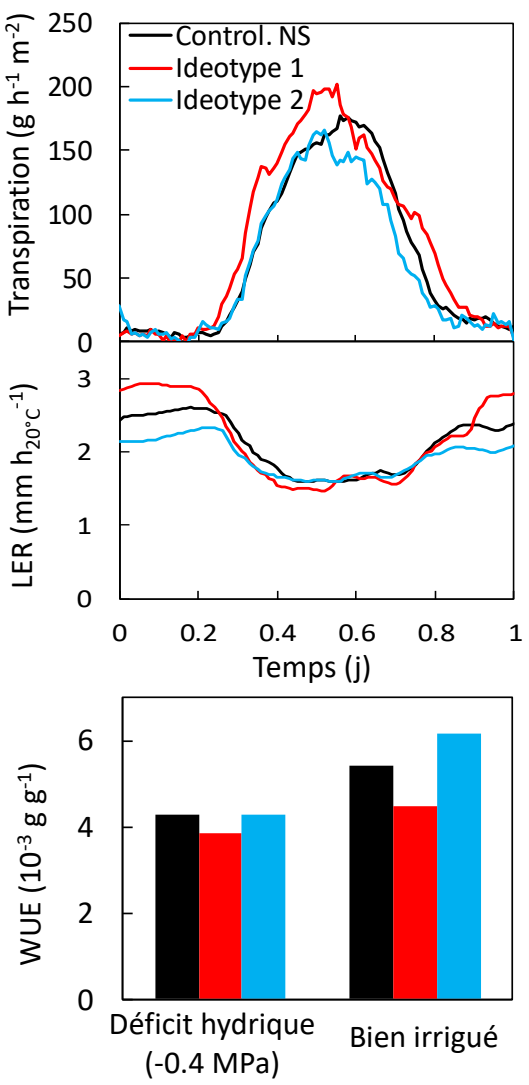

Figure 23. Cinétiques de transpiration et de croissance foliaire (LER), pour des lignées de maïs transformées, représentant 2 idéotypes contrastés: idéotype 1 (maximise la transpiration et la croissance foliaire) et idéotype 2 (efficient en eau), comparés aux plantes contrôles (transformants nuls, NS). Non-publié.

des promoteurs circadiens. Les concentrations d'ABA dans la sève du xylème se situaient dans la plage physiologique de la diversité génétique du maïs, évitant ainsi des effets pléiotropiques massifs. Les plantes correspondant à l'idéotype 1 montraient une diminution de la production d'ABA et une dégradation accrue le matin, et un comportement opposé l'après-midi et la nuit (Fig.23). Celles de l'idéotype 2 augmentaient la production d'ABA au cours de l'après-midi.

Les lignées transgéniques limitant les concentrations d'ABA le matin (idéotype 1) présentaient un taux de transpiration plus élevé le matin et une expansion des feuilles augmentée la nuit. Avec comme résultat des plantes plus grandes (à tous niveaux), mais avec une efficacité d'utilisation de l'eau inférieure à celle des transformant nuls (résultats non publiés, Fig.23). Un comportement opposé a été observé chez les plantes de l'idéotype 2, avec une transpiration inférieure pendant la journée, un taux de croissance inférieur et une efficacité l'utilisation de l'eau améliorée.

Dans cet axe, nous analyserons plus finement ces lignées ainsi que des hybrides descendants de ces lignées, afin de déterminer les différents processus impliqués à différentes échelles et leur impact sur les dynamiques de WUE. Ce sera réalisé en caractérisant (i) la dynamique de l'expression des gènes (gènes transformés / endogènes et autres gènes clés impliqués dans l'hydraulique et le métabolisme primaire; (ii) la dynamique des processus hydrauliques, de la plante entière à l'échelle moléculaire (transpiration, conductances hydrauliques, aquaporines, ABA); et (iii) leurs conséquences sur la dynamique des relations source-puits de carbone (photosynthèse, flux de carbone et composition de la biomasse). Cela doit améliorer la compréhension des connexions dynamiques entre les contrôles de transpiration à différentes échelles et permettre de les formaliser dans le modèle hydraulique.

Nous déterminerons ensuite dans quelle mesure et dans quel type de scénario cette approche peut améliorer significativement la WUE et les performances des plantes (démonstration de l'approche), en analysant les comportements de ces plantes transgéniques à l'échelle plante entière (croissance et architecture des plantes, utilisation de l'eau, production de biomasse, WUE dans des scénarios contrastés de demande évaporative, de déficit hydrique et de CO2.

Axe 2: Diversité naturelle des contrôles de transpiration dynamique

Dans cet axe, nous chercherons à exploiter la diversité génétique des contrôles dynamiques de la transpiration: (i) des processus à l'échelle de la plante entière, (ii) aux mécanismes sous-jacents et (iii) aux gènes.

Nous commencerons par caractériser la structure de la variabilité génétique des cinétiques journalières de la transpiration et de la photosynthèse : (i) en caractérisant l'espace phénotypiques des caractères temporels de la transpiration et de la photosynthèse dans un panel de diversité comprenant les principaux groupes génétiques du maïs (tropical et tempéré, ~ 350 génotypes), et une série historique de maïs commercialisés de 1950 à aujourd'hui (~ 100 génotypes); (ii) en déterminant ce qui structure cette diversité vis-à-vis des grands groupes génétiques et des générations de sélection; et (iii) en indiquant ainsi comment ces caractères ont été sélectionnés dans le matériel génétique élite, et leurs implications possibles dans l'adaptation des plantes à leurs climats d'origine. Nous sélectionnerons des idéotypes aux comportements et/ou origines géographiques contrastés pour une caractérisation plus approfondie et pour des simulations (Axe 3).

Nous chercherons ensuite à déterminer l'implication de processus sous-jacents et leurs relations dans ces idéotypes : dynamiques des contrôles de transpiration (conductances, ABA, aquaporines PIP) et relations source-puits de carbone (flux de carbone, composition de la biomasse).

Enfin, nous déterminerons l'architecture génétique de ces processus dynamiques (gènes, allèles et réseaux de co-expression associés aux profils dynamiques de transpiration et à la WUE) par génétique d'association (GWAS) et par l'analyse du transcriptome dynamique de l'ensemble du panel de diversité (séquençage d'ARNm et 3'ARNm). Ces informations seront ensuite utilisées pour **développer des modèles de prédiction génomique qui permettront de prédire les dynamiques temporelles de transpiration** à partir de profils alléliques virtuels.

Axe 3: Idéotypes de contrôle de la transpiration adaptés aux scénarios.

Dans cet axe, nous développerons le premier modèle de culture prenant en compte la diversité des contrôles dynamiques de la transpiration (processus et gènes) afin d'explorer leurs effets sur la WUE et les performances des plantes, et d'identifier des idéotypes adaptés à chaque scénario climatique spécifique.

Nous allons développer un nouveau modèle écophysiologique de contrôle de la transpiration qui inclut les relations dynamiques nouvellement identifiées dans les axes 1 et 2. Ce modèle sera intégré dans un modèle de culture (Sirius Maize, en cours de développement au LEPSE) qui aboutira au premier modèle de culture capable de prédire les performances des plantes dans des simulations à grande échelle tout en tenant compte les contrôles temporels de la transpiration. Ce modèle sera ensuite évalué et étalonné sur des plates-formes de phénotypage au champ (Pheno3C, Diaphen). Il permettra (i) de prédire les conséquences de la diversité des contrôles de la transpiration sur la production dans les climats européens actuels et futurs; (ii) déterminer les meilleures combinaisons de caractères disponible dans l'espace phénotypique (idéotypes fonctionnels); et (iii) utiliser la prédiction génomique pour identifier le meilleur profil allélique qui permettrait la construction de tels idéotypes dans chaque scénario (idéotype génétique).

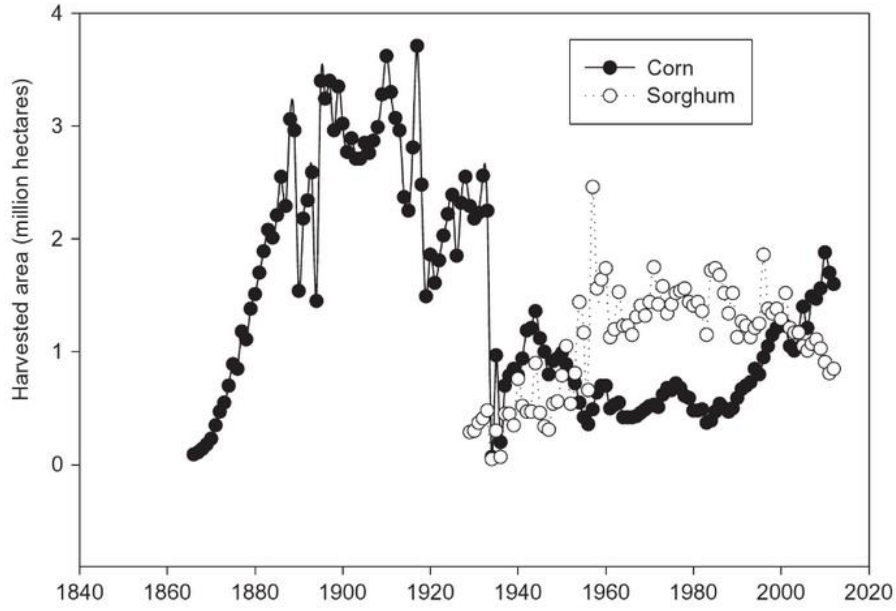

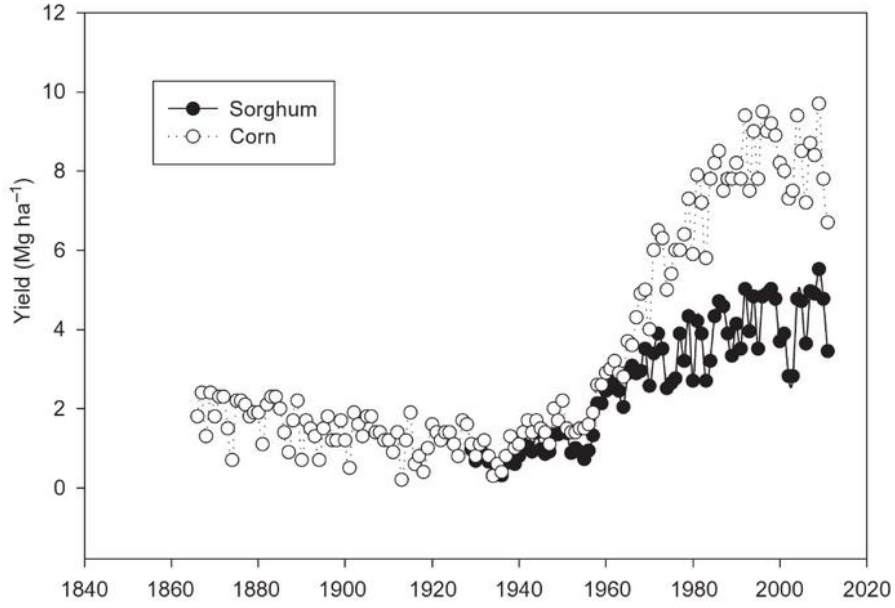

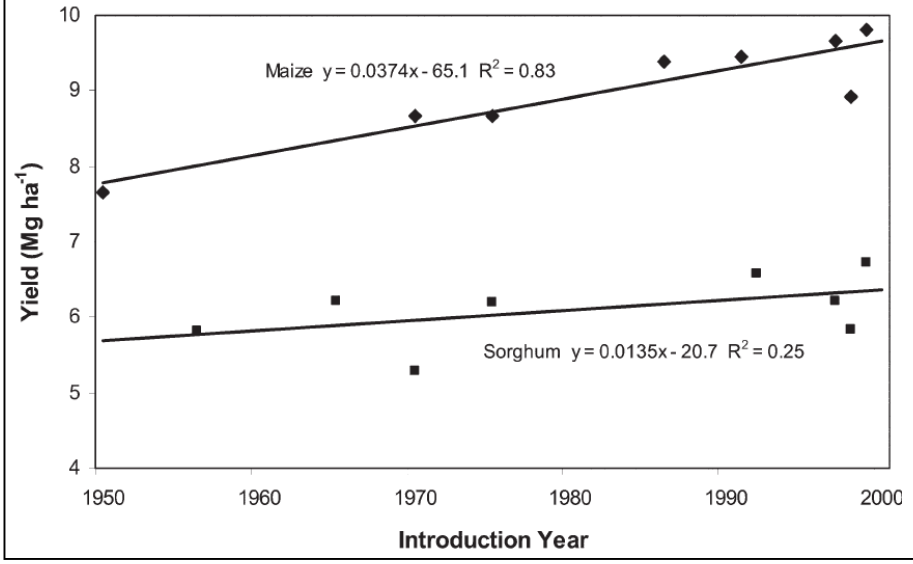

<u>Figure 24</u>: Historiques des surfaces cultivées, rendement et gain génétique pour le maïs et le sorgho aux Etats Unis.

A) Historique des surfaces cultivées au Kansas de 1866 à 2011 pour le sorgho et le maïs. ***Issu de Assefa et al., 2014.***

B) Historique des rendements au Kansas de 1866 à 2011 pour le sorgho et le maïs. ***Issu de Assefa et al., 2014.***

C) Gain génétique chez le sorgho et le maïs au Texas. ***Issu de Masson et al., 2008***

Focus n°6 : Qui, de l'agronomie ou de la génétique dessine(ra) les contours des cultures de Sorgho et de Maïs en France et en Europe ?

Ce projet est un projet à plus long terme et n'en est encore qu'à ses balbutiements. Il n'a pas encore été soumis dans son ensemble à aucun appel d'offre. Cependant, il se construit, et certaines de ces activités ont déjà été inclues dans des projets soumis (ex : PreAdapt, Concept-note à Agropolis fondation, Projet inter-unité PARSEMA).

Contexte

Le sorgho est la 5e céréale la plus cultivée dans le monde avec plus de 40 millions d'hectares (maïs : 179 millions) mais qui reste relativement peu cultivée en Europe, qui est fortement importatrice. Le sorgho (*Sorghum bicolor*) et les progéniteurs du maïs (*Zea mays*) ont divergé il y a relativement peu (11.9 millions d'années ; Swigonová *et al.*, 2004) et sont finalement encore très proches sur beaucoup d'aspects. Ce sont toutes les deux des espèces en C4, utilisées comme cultures d'été dans des conditions agronomiques similaires, qui peuvent prendre la même place dans la rotation et qui ont des débouchés proches (grain pour alimentation animale, fourrager, biomasse, …).

Le résultat est que ce sont deux cultures alternatives dont la concurrence est visible lorsqu'on regarde l'historique des surfaces cultivées par région (ex. Figure 24A). Les surfaces cultivées en sorgho en France enregistrent une progression de 54 % sur quatre ans (La France Agricole 29/01/2020) et totalisent 85 400 ha en 2019 (vs 1500 000 ha pour le maïs, Eurostat). L'Hexagone progresse donc à contre-courant de la production mondiale, qui recule de 2 millions d'hectares par rapport à 2018 (La France Agricole 29/01/2020). Au contraire, le maïs passe de 1800 000 à 1500 000 ha en 10 ans (Eurostat). ***L'idée centrale de ce projet est donc de comprendre ce qui dirige, et dirigera à moyen terme, le compromis entre cultures de sorgho et de maïs en Europe.***

Bien que proches, les cultures du maïs et du sorgho divergeraient du point de vue agronomique et de leurs potentiels génétiques. Le sorgho serait moins gourmand en intrants que le maïs, et 'très résistant' à la sécheresse et aux hautes températures :

- Alors que 100 à 150 kg d'azote et 60 kg de phosphore et potassium suffisent pour atteindre le meilleur rendement en sorgho, une large partie est restituée au sol après la récolte : 40 % de l'azote, 80-85 % du potassium et 20-30 % du phosphore (source Arvalis).

-Le sorgho a une réputation de céréale très résistante à la sécheresse (Krieg & Lascano, 1990). Cette résistance est principalement attribuée à son système racinaire profond (Wright & Smith, 1983; Singh & Singh, 1995), et le maintien de la conductance stomatique et de la photosynthèse à des potentiels hydrique très

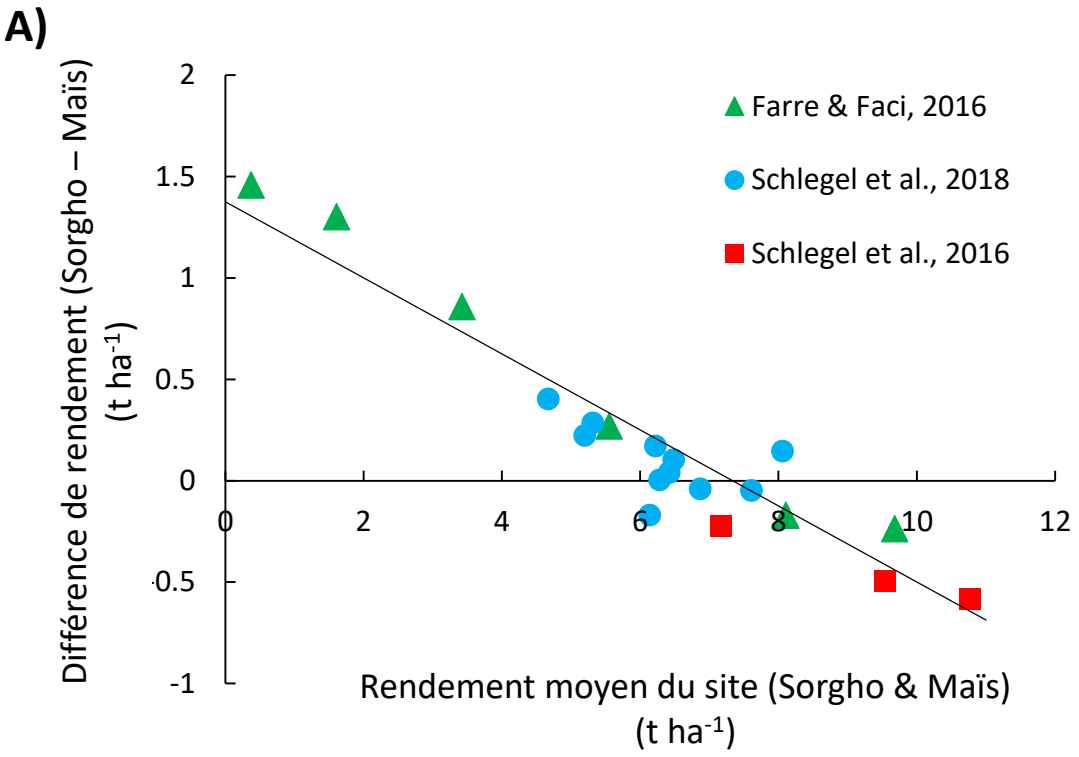

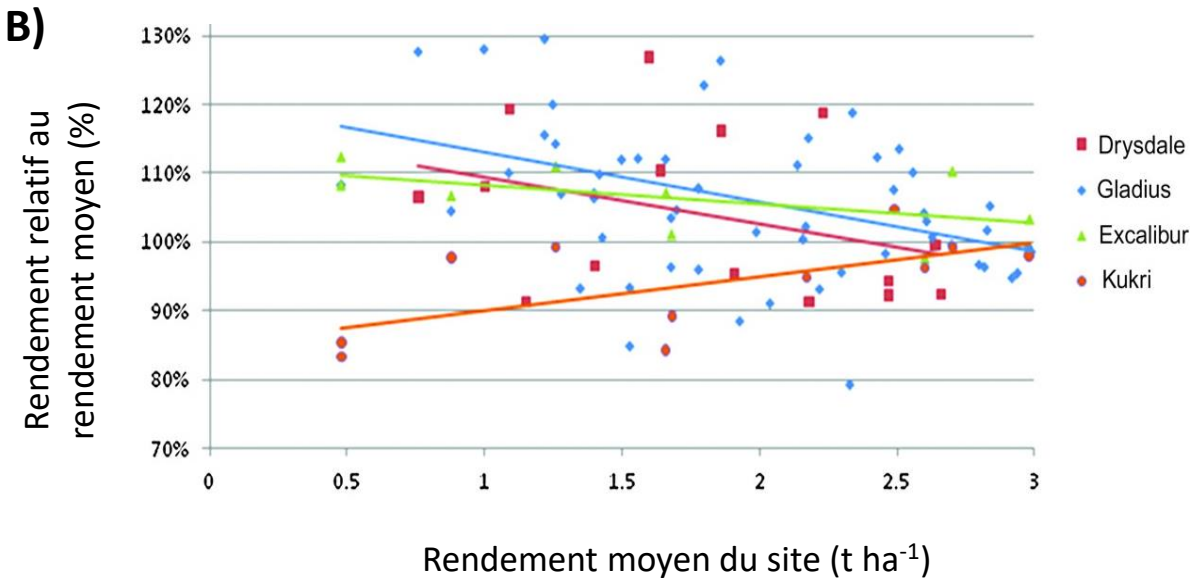

Figure 24:
A) Rendement du sorgho vis-à-vis de celui du maïs en fonction du rendement moyen du site.*. **Données issue de la littérature.***
B) Rendement de 4 variétés de blés dans différent sites en Australie en fonction du rendement moyen du site. ***Figure issue de Fleury et al., 2010.***

défavorables (Wright & Smith, 1983; Singh & Singh, 1995). En général, sa réputation est d'être plus tolérant à la « sècheresse » que le maïs (Muchow, 1989; Singh & Singh, 1995).

Bien que la littérature ne soit pas très riche en essais comparatif, lorsqu'ils existent (Australie, (Muchow, 1989); Inde, (Singh & Singh, 1995) ; Espagne, (Farré & Faci, 2006); US, Kansas et Nebraska, (Staggenborg *et al.*, 2008)), ils indiquent un avantage pour le maïs sous bonnes conditions hydrique, et l'inverse pour le sorgho (Staggenborg *et al.*, 2008; Schittenhelm & Schroetter, 2014; Fig.24A). Cependant, ces essais comparatifs sont la plupart du temps menés sur peu de génotypes, représentant idéalement LE Maïs vs. LE Sorgho.

C'est assez étonnant, mais ces différentes publications indiquent toutes un croisement des courbes (la production du sorgho passant au-dessus de celle du maïs) aux alentours de 6-7 t ha^{-1} (Fig.24A). On aurait affaire à deux espèces au comportement constitutif très différents ? Pourtant, ce type d'interaction G x E peut être observé même à l'échelle d'une seule espèce, dans la diversité génétique intra-spécifique, comme chez le blé présenté en Figure 24B. De plus, la sélection variétale doit probablement jouer un rôle prépondérant dans ce type de comparaisons. Les variétés de maïs actuelles ont été développées pour maximiser les rendements en condition optimales (Fig. 23C). Cela est moins vrai chez le sorgho, plus traditionnellement cultivé en pluvial, et pour lesquelles la pression de sélection a été moins forte.

L'hypothèse centrale de ce projet est donc qu'il n'y aurait pas une courbe définissant l'avantage relatif du sorgho sur le maïs mais autant de courbes que le permet la diversité génétique dans chaque espèce.

Les corolaires sont nombreux, et pour n'en citer qu'un :- *Est ce qu'un génotype de maïs très robuste ne peut pas avoir les même caractéristiques qu'un sorgho dans des zones ou le rendement est inférieur à 60 quintaux ?*

En d'autres termes, -*Est ce que l'analyse des espaces phénotypique des réponses du sorgho et du maïs dans des panels de diversité montre des espaces communs, ou au contraire réellement divergeant ?*

Cette hypothèse, axée principalement sur la génétique n'expliquera pas seule l'adoption ou non d'une culture par un agriculteur et, à plus grande échelle, l'évolution de sa distribution géographique, qui répondent à la fois à des contraintes génétiques, agronomiques, socio-économique et climatiques.

Au travers de partenariats forts, ce projet considèrera donc les contraintes agronomiques et socio-économiques, comme les conséquences à l'échelle de l'exploitation des changements dans la rotation, les politiques publiques sur les usages d'intrants, l'évolution du cours des céréales….

Axe 1. Construction d'un modèle commun adapté à la diversité génétique du sorgho et du maïs

1) Analyse de caractères clefs

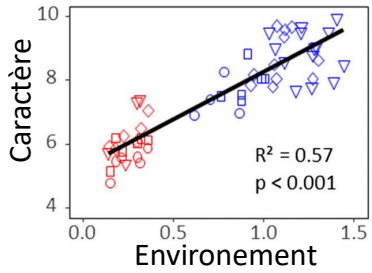

Protocoles / Scénarios

formalismes

2) Modèle de culture commun

(basé sur Sirius)

paramètres

Axe 2. Espace phénotypiques du sorgho et du maïs dans des gammes de diversité élargies

1) Phénotypage de la diversité

caractères

2) Espaces phénotypiques

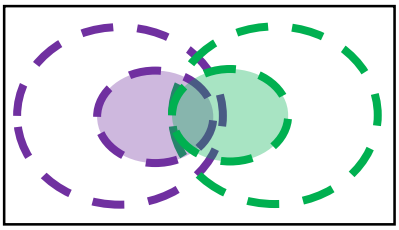

1) Simulations à large échelle

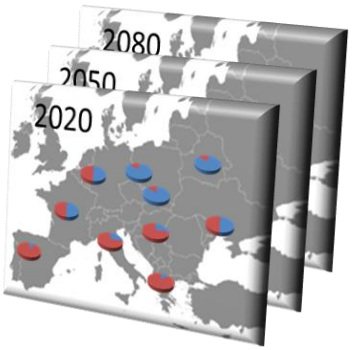

rendements

2) Analyse économique

€

Axe 3. Impacts de la diversité génétique dans des scenarios présents et futurs

Impacts sur le rendement: Stratégies d'adaptation et sélection

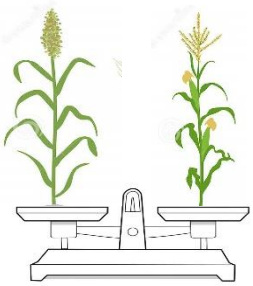

Impact économique: Choix culturaux, répartitions géographiques présentes et futures

Figure 25 Stratégie et Activités du projet Focus N°6

Objectif et Stratégie

L'objectif principal de ce projet est de prédire où (géographique), quand (présent, futur) et comment (dans quel contexte agro-socio-économique), un génotype constitué d'une combinaison de caractères génétiques accessible par la sélection peut présenter un avantage vis-à-vis de la diversité intra-et inter-espèces du sorgho et du maïs.

Pour répondre à cet objectif, **une stratégie utilisant le phénotypage et la modélisation** pour prédire les intéractions G x E s'impose, sachant qu'en plus de la difficulté habituelle des tailles de dispositifs expérimentaux dans l'analyse des intéractions GxE à larges échelles environnementales et génétiques, les essais comparatifs au champs sont limités par les gammes de précocités, assez différentes, du maïs et du sorgho (dans une zone géographique donnée, les sorgho cultivés sont en général plus précoces).

Ce projet sera donc découpé en trois axes (Fig.25) :

Axe 1. Un modèle commun adapté à la diversité génétique du sorgho et du maïs

L'Axe 1 va développer un modèle de culture générique pour le sorgho et le maïs et comportant les paramètres génétiques clefs de réponses aux hautes température et au déficit hydrique

Aujourd'hui, on ne dispose pas d'un tel modèle sorgho-maïs permettant de prédire les intéractions GxE à l'échelle intra- et inter-espèces. De plus, il n'existe que peu d'analyses communes en conditions contrôlées, des réponses à des contraintes abiotiques chez le sorgho et le maïs. Ce projet se focalisera donc en premier lieu sur l'analyse écophysiologique des réponses de processus clefs (ex : croissance, développement, transpiration, photosynthèse) au déficit hydrique et aux hautes température pour des génotypes contrastés de maïs et de sorgho. Un accent particulier sera mis sur l'analyse des effets de seuils, ainsi que sur l'impact de stress récurrents et combinés. Des modèles de réponse génériques pour les 2 espèces devraient être développés afin de pouvoir phénotyper de large panels avec le même cadre d'analyse.

Le modèle de culture Sirius-maïs actuellement développé au LEPSE sera modifié pour d'inclure ces nouveaux formalismes afin d'être valable pour le sorgho et le maïs. Il sera évalué avec des essais au champ comportant du maïs et du sorgho.

Axe 2. Quels espaces communs dans la diversité phénotypique du sorgho et du maïs ?

Par l'analyse des espaces phénotypiques, l'Axe 2 cherchera à comprendre si la génétique bride réellement les potentiels respectifs du maïs et du sorgho dans des conditions optimales ou limitantes, ou si la sélection a créé ou amplifié la divergence des caractères entre les 2 espèces.

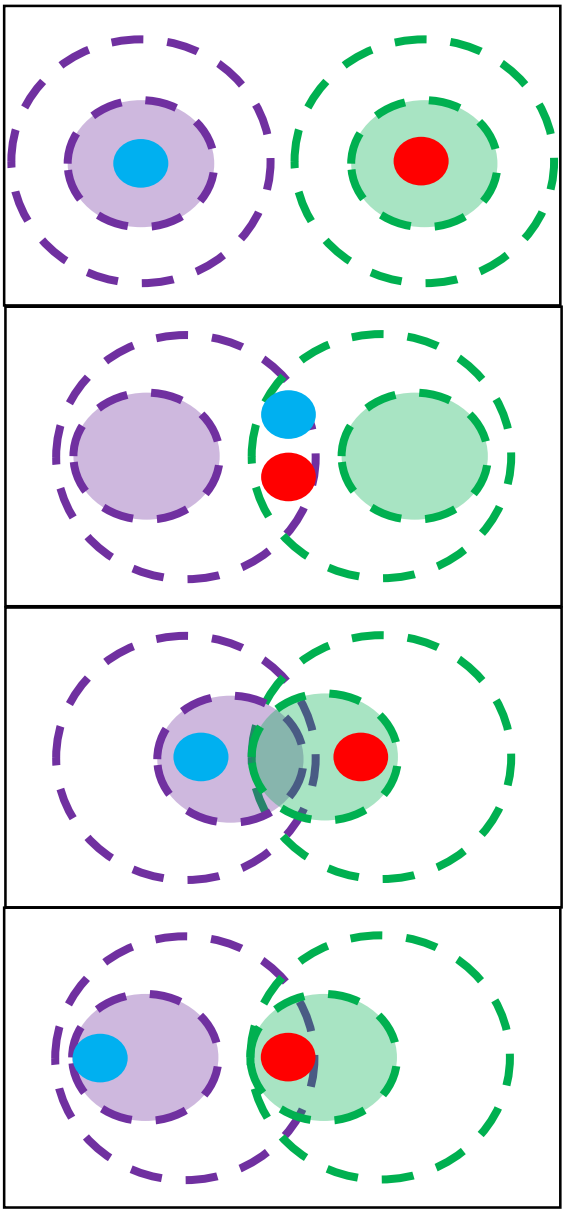

Cas 1: Les espaces phénotypiques du sorgho et du maïs sont distincts et ne se recouvrent pas. Le maïs sera toujours meilleur en conditions favorables et le sorgho en conditions limitantes

Cas 2: Les espaces phénotypiques du sorgho et du maïs se recouvrent. La meilleur combinaison de traits est disponible dans chacune des espèces mais pas dans le pool élite cultivé actuel.

Cas 3: Les espaces phénotypiques du sorgho et du maïs se recouvrent, même pour les pool élites. Cependant, le meilleur sorgho reste le meilleur en conditions limitantes, et le meilleur maïs reste le meilleur en conditions optimales

Cas 4: Une espèce (ici le maïs) à la diversité génétique pour atteindre les optimums dans les 2 conditions. Mais aujourd'hui, la diversité génétique du maïs pour des conditions limitantes n'est pas exploitée.

Espace phenotypique dans une large diversité génétique chez le maïs et le sorgho

Espace phenotypique des maïs et sorgho cultivés

Meilleur combinaison de caractères dans 2 scénarios hydriques contrastés (ex bien irrigué et sec)

Figure 26: Espaces phénotypiques dans la diversité génétique du maïs et du sorgho et dans leurs pools élites, et meilleurs combinaisons de caractères en conditions optimale et limitantes.
4 possibilités (non-exaustif) sont présentées

Cet axe profitera des protocoles, cadres d'analyse et modèles développé dans l'axe 1 pour déterminer les paramètres des modèles de réponses dans des panels de diversité et des génotypes de différentes générations de sélection. La comparaison des espaces phénotypiques constitués par ces caractères dans les pools élites et pour une diversité élargie (landraces, différentes origines et groupes génétiques) doit permettre d'indiquer l'impact de la sélection dans la divergence (ou convergence) de caractères clés entre le sorgho et le maïs, ainsi que le caractère constitutif (ou au contraire artificiellement bridé par la sélection) des différences de caractères, et donc de potentiel génétique dans des environnements contrastés. Plusieurs cas possibles sont présentés dans la Figure 26.

Axe 3 : Impacts de la diversité génétique dans des scenarios présents et futurs

Cet axe sera initié dans un second temps. Il cherchera à prédire les conséquences de l'utilisation de gammes génétiques élargies sur le rendement, et considèrera des hypothèses socio-économiques pour prédire l'évolution possible des surfaces dans des scénarios européens affectés par le changement climatique.

Dans un premier temps, des génotypes virtuels représentant idéalement les espaces phénotypiques respectifs du sorgho et du maïs seront simulés dans des scénarios climatiques et agronomiques européens présents et futurs. Cela devrait indiquer où, quand et comment chaque combinaison de caractères de sorgho ou de maïs peut présenter un avantage comparatif, et définir ainsi les meilleurs idéotypes de maïs et de sorgho accessibles par la sélection.

Dans un deuxième temps, ces simulations seront combinées à une analyse économique afin de prédire les conséquences économiques de tels choix, et d'ainsi de proposer des hypothèses quant à l'évolution possible des surfaces cultivées de maïs et de sorgho en Europe.

8. REFERENCES

4PMI. https://www6.dijon.inrae.fr/plateforme4pmi_eng/Technical-description/High-Throughput-phenotyping.

AcostaGallegos JA, VargasVazquez P, White JW. 1996. Effect of sowing date on the growth and seed yield of common bean (Phaseolus vulgaris L) in highland environments. *Field Crops Research* **49**(1): 1-10.

Alamanos A, Latinopoulos D, Papaioannou G, Mylopoulos N. 2019. Integrated Hydro-Economic Modeling for Sustainable Water Resources Management in Data-Scarce Areas: The Case of Lake Karla Watershed in Greece. *Water Resources Management* **33**(8): 2775-2790.

Andrivon D, Giorgetti C, Baranger A, Calonnec A, Cartolaro P, Faivre R, Guyader S, Lauri PE, Lescourret F, Parisi L, et al. 2013. Defining and designing plant architectural ideotypes to control epidemics? *European Journal of Plant Pathology* **135**(3): 611-617.

Antonovics J, Vantienderen PH. 1991. Ontoecogenophyloconstraints - The chaos of constraint terminology. *Trends in Ecology & Evolution* **6**(5): 166-168.

Aroca R, Vernieri P, Irigoyen JJ, Sanchez-Diaz M, Tognoni F, Pardossi A. 2003. Involvement of abscisic acid in leaf and root of maize (Zea mays L.) in avoiding chilling-induced water stress. *Plant Science* **165**(3): 671-679.

Asseng S, Ewert F, Rosenzweig C, Jones JW, Hatfield JL, Ruane AC, Boote KJ, Thorburn PJ, Rotter RP, Cammarano D, et al. 2013. Uncertainty in simulating wheat yields under climate change. *Nature Climate Change* **3**(9): 827-832.

Bacon MA, Wilkinson S, Davies WJ. 1998. pH-regulated leaf cell expansion in droughted plants is abscisic acid dependent. *Plant Physiology* **118**(4): 1507-1515.

Barnabas B, Jaeger K, Feher A. 2008. The effect of drought and heat stress on reproductive processes in cereals. *Plant Cell and Environment* **31**(1): 11-38.

Basu S, Ramegowda V, Kumar A, Pereira A. 2016. Plant adaptation to drought stress. *F1000Research* **5**.

Baumont M, Parent B, Manceau L, Brown HE, Driever SM, Muller B, Martre P. 2019. Experimental and modeling evidence of carbon limitation of leaf appearance rate for spring and winter wheat. *J Exp Bot* **70**(9): 2449-2462.

Beaudette PC, Chlup M, Yee J, Emery RJN. 2007. Relationships of root conductivity and aquaporin gene expression in Pisum sativum: diurnal patterns and the response to HgCl2 and ABA. *J Exp Bot* **58**(6): 1291-1300.

Beemster GTS, Masle J, Williamson RE, Farquhar GD. 1996. Effects of soil resistance to root penetration on leaf expansion in wheat (Triticum aestivum L): Kinematic analysis of leaf elongation. *J Exp Bot* **47**(304): 1663-1678.

Bennett D, Izanloo A, Reynolds M, Kuchel H, Langridge P, Schnurbusch T. 2012a. Genetic dissection of grain yield and physical grain quality in bread wheat (Triticum aestivum L.) under water-limited environments. *Theoretical and Applied Genetics* **125**(2): 255-271.

Bennett D, Reynolds M, Mullan D, Izanloo A, Kuchel H, Langridge P, Schnurbusch T. 2012b. Detection of two major grain yield QTL in bread wheat (Triticum aestivum L.) under heat, drought and high yield potential environments. *Theoretical and Applied Genetics* **125**(7): 1473-1485.

Berger B, Parent B, Tester M. 2010. High-throughput shoot imaging to study drought responses. *J Exp Bot* **61**(13): 3519-3528.

Berger J, Palta J, Vadez V. 2016. Review: An integrated framework for crop adaptation to dry environments: Responses to transient and terminal drought. *Plant Science* **253**: 58-67.

Bernstein N, Silk WK, Lauchli A. 1993. Growth and development of sorghum leaves under conditions of NaCl stress - spatial and temporal aspects of leaf growth-inhibition. *Planta* **191**(4): 433-439.

Bertolino LT, Caine RS, Gray JE. 2019. Impact of Stomatal Density and Morphology on Water-Use Efficiency in a Changing World. *Frontiers in Plant Science* **10**.

Blum A. 2015. Towards a conceptual ABA ideotype in plant breeding for water limited environments. *Functional Plant Biology* **42**(6): 502-513.

Bonneau J, Taylor J, Parent B, Bennett D, Reynolds M, Feuillet C, Langridge P, Mather D. 2013. Multi-environment analysis and improved mapping of a yield-related QTL on chromosome 3B of wheat. *Theoretical and Applied Genetics* **126**(3): 747-761.

Borlaug NE. 1971. The Green Revolution : For Bread and Peace. . *Special Nobel Lecture. Bulletin of Atomic Scientists.*

Brisson N, Gate P, Gouache D, Charmet G, Oury F-X, Huard F. 2010. Why are wheat yields stagnating in Europe? A comprehensive data analysis for France. *Field Crops Research* **119**(1): 201-212.

Buckley TN, Mott KA, Farquhar GD. 2003. A hydromechanical and biochemical model of stomatal conductance. *Plant Cell and Environment* **26**(10): 1767-1785.

Butler EE, Huybers P. 2013. Adaptation of US maize to temperature variations. *Nature Climate Change* **3**(1): 68-72.

Cabrera-Bosquet L, Fournier C, Brichet N, Welcker C, Suard B, Tardieu F. 2016. High-throughput estimation of incident light, light interception and radiation-use efficiency of thousands of plants in a phenotyping platform. *New Phytologist* **212**(1): 269-281.

Caldeira CF, Jeanguenin L, Chaumont F, Tardieu F. 2014. Circadian rhythms of hydraulic conductance and growth are enhanced by drought and improve plant performance. *Nature Communications* **5**.

Cammarano D, Zierden D, Stefanova L, Asseng S, O'Brien JJ, Jones JW. 2016. Using historical climate observations to understand future climate change crop yield impacts in the Southeastern US. *Climatic Change* **134**(1-2): 311-326.

Casadebaig P, Guilioni L, Lecoeur J, Christophe A, Champolivier L, Debaeke P. 2011. SUNFLO, a model to simulate genotype-specific performance of the sunflower crop in contrasting environments. *Agricultural and Forest Meteorology* **151**(2): 163-178.

Casadebaig P, Zheng B, Chapman S, Huth N, Faivre R, Chenu K. 2016. Assessment of the Potential Impacts of Wheat Plant Traits across Environments by Combining Crop Modeling and Global Sensitivity Analysis. *Plos One* **11**(1).

Chaerle L, Saibo N, Van Der Straeten D. 2005. Tuning the pores: towards engineering plants for improved water use efficiency. *Trends in Biotechnology* **23**(6): 308-315.

Chapman SC, Cooper M, Hammer GL. 2002. Using crop simulation to generate genotype by environment interaction effects for sorghum in water-limited environments. *Australian Journal of Agricultural Research* **53**(4): 379-389.

Chauhan YS, Wright GC, Holzworth D, Rachaputi RCN, Payero JO. 2013. AQUAMAN: a web-based decision support system for irrigation scheduling in peanuts. *Irrigation Science* **31**(3): 271-283.

Chenu K, Chapman SC, Hammer GL, McLean G, Salah HBH, Tardieu F. 2008. Short-term responses of leaf growth rate to water deficit scale up to whole-plant and crop levels: an integrated modelling approach in maize. *Plant Cell and Environment* **31**(3): 378-391.

Chenu K, Cooper M, Hammer GL, Mathews KL, Dreccer MF, Chapman SC. 2011. Environment characterization as an aid to wheat improvement: interpreting genotype-environment interactions by modelling water-deficit patterns in North-Eastern Australia. *J Exp Bot* **62**(6): 1743-1755.

Condon AG, Farquhar GD, Rebetzke GJ, Richards RA. 2006. *The application of carbon isotope discrimination in cereal improvement for water-limited environments*.

Cooper M, Gho C, Leafgren R, Tang T, Messina C. 2014. Breeding drought-tolerant maize hybrids for the US corn-belt: discovery to product. *J Exp Bot* **65**(21): 6191-6204.

Curin F, Severini AD, Gonzalez FG, Otegui ME. 2020. Water and radiation use efficiencies in maize: Breeding effects on single-cross Argentine hybrids released between 1980 and 2012. *Field Crops Research* **246**.

Davies WJ, Bennett MJ. 2015. Achieving more crop per drop. *Nature Plants* **1**(8).

de Wit CT, Brouwer R, Penning de Vries FWT 1970. The simulation of photosynthetic systems. In: Setlik I ed. *Prediction and Measurements of Photosynthetic Productivity.*: Proc. IBP/PP Technical Meeting, Trebon, Pudoc, Wageningen, 47-50.

de Wit CT, Goudriaan J, VanLaar HH, Penning de Vries FWT, Rabbinge R, VanKeulen H, Louwerse W, Sibma L, DeJonge C 1978. Simulation of assimilation, respiration and translocation of crops. *Simulation monographs.*

Dell AI, Pawar S, Savage VM. 2011. Systematic variation in the temperature dependence of physiological and ecological traits. *Proceedings of the National Academy of Sciences of the United States of America* **108**(26): 10591-10596.

Dewar RC. 2002. The Ball-Berry-Leuning and Tardieu-Davies stomatal models: synthesis and extension within a spatially aggregated picture of guard cell function. *Plant Cell and Environment* **25**(11): 1383-1398.

DiaPHEN https://www.phenome-emphasis.fr/phenome_eng/Installations/Montpellier-Field.

Dodd IC. 2003. Hormonal interactions and stomatal responses. *Journal of Plant Growth Regulation* **22**(1): 32-46.

Donald CM. 1968. Breeding of crop ideotypes. *Euphytica* **17**(3): 385-&.

Donovan LA, Maherali H, Caruso CM, Huber H, de Kroon H. 2011. The evolution of the worldwide leaf economics spectrum. *Trends in Ecology & Evolution* **26**(2): 88-95.

Drewry DT, Kumar P, Long SP. 2014. Simultaneous improvement in productivity, water use, and albedo through crop structural modification. *Global Change Biology* **20**(6): 1955-1967.

Du H, Wang NL, Cui F, Li XH, Xiao JH, Xiong LZ. 2010. Characterization of the beta-Carotene Hydroxylase Gene DSM2 Conferring Drought and Oxidative Stress Resistance by Increasing Xanthophylls and Abscisic Acid Synthesis in Rice. *Plant Physiology* **154**(3): 1304-1318.

Duncan WG, R.S. L, W.A. W, R. H. 1967. A model for simulating photosynthesis in plant communities. *Hilgardia* **38**(4): 181-205.

Duvick DN. 2005. Genetic progress in yield of united states maize (Zea mays L.). *Maydica* **50**(3-4): 193-202.

Duvick DN, Smith JSC, M. Cooper M 2003. Long-Term Selection in a Commercial Hybrid Maize Breeding Program. *Plant Breeding Reviews*, 109-151.

Edwards WRN, Jarvis PG, Landsberg JJ, Talbot H. 1986. A dynamic model for studying flow of water in single trees. *Tree Physiology* **1**(3): 309-324.

Egli DB, Bruening W. 1992. Planting date and soybean yield. Evaluation of environmental effects with a crop simulation model. Soygro. *Agricultural and Forest Meteorology* **62**(1-2): 19-29.

Faralli M, Cockram J, Ober E, Wall S, Galle A, Van Rie J, Raines C, Lawson T. 2019. Genotypic, Developmental and Environmental Effects on the Rapidity of gs in Wheat: Impacts on Carbon Gain and Water-Use Efficiency. *Frontiers in Plant Science* **10**(492).

Farré I, Faci JM. 2006. Comparative response of maize (Zea mays L.) and sorghum (Sorghum bicolor L. Moench) to deficit irrigation in a Mediterranean environment. *Agricultural Water Management* **83**(1): 135-143.

Fiorani F, Schurr U 2013. Future Scenarios for Plant Phenotyping. In: Merchant SS ed. *Annual Review of Plant Biology, Vol 64*, 267-291.

Fischer EM, Knutti R. 2012. Robust projections of combined humidity and temperature extremes. *Nature Climate Change* **3**: 126.

Fleury D, Jefferies S, Kuchel H, Langridge P. 2010. Genetic and genomic tools to improve drought tolerance in wheat. *J Exp Bot* **61**(12): 3211-3222.

Fukai S, Cooper M. 1995. Development of drought-resistant cultivars using physio-morphological traits in rice. *Field Crops Research* **40**(2): 67-86.

Fukai S, Pantuwan G, Jongdee B, Cooper M. 1999. Screening for drought resistance in rainfed lowland rice. *Field Crops Research* **64**(1-2): 61-74.

Furbank RT, Tester M. 2011. Phenomics - technologies to relieve the phenotyping bottleneck. *Trends in Plant Science* **16**(12): 635-644.

Gandar PW, Rasmussen H. 1991. Growth-pattern and movement of epidermal-cells within leaves of Asphodelus-tenuifolius *Annals of Botany* **68**(4): 307-315.

Gorafi YSA, Kim J-S, Elbashir AAE, Tsujimoto H. 2018. A population of wheat multiple synthetic derivatives: an effective platform to explore, harness and utilize genetic diversity of Aegilops tauschii for wheat improvement. *Theoretical and Applied Genetics* **131**(8): 1615-1626.

Guo Y, Ma Y, Zhan Z, Li B, Dingkuhn M, Luquet D, De Reffye P. 2006. Parameter optimization and field validation of the functional-structural model GREENLAB for maize. *Annals of Botany* **97**(2): 217-230.

Hammer G, Cooper M, Tardieu F, Welch S, Walsh B, van Eeuwijk F, Chapman S, Podlich D. 2006. Models for navigating biological complexity in breeding improved crop plants. *Trends in Plant Science* **11**(12): 587-593.

Hammer GL, Dong ZS, McLean G, Doherty A, Messina C, Schusler J, Zinselmeier C, Paszkiewicz S, Cooper M. 2009. Can Changes in Canopy and/or Root System Architecture Explain Historical Maize Yield Trends in the US Corn Belt? *Crop Science* **49**(1): 299-312.

Hammer GL, van Oosterom E, McLean G, Chapman SC, Broad I, Harland P, Muchow RC. 2010. Adapting APSIM to model the physiology and genetics of complex adaptive traits in field crops. *J Exp Bot* **61**(8): 2185-2202.

Harrison MT, Tardieu F, Dong Z, Messina CD, Hammer GL. 2014. Characterizing drought stress and trait influence on maize yield under current and future conditions. *Global Change Biology* **20**(3): 867-878.

Hatfield JL, Dold C. 2019. Water-Use Efficiency: Advances and Challenges in a Changing Climate. *Frontiers in Plant Science* **10**.

Hay RKM. 1995. Harvest index - A review of its use in plant-breeding and crop physiology. *Annals of Applied Biology* **126**(1): 197-216.

HiTMe https://www.phenome-emphasis.fr/phenome_eng/Installations/Bordeaux-Omic.

Holbrook NM, Shashidhar VR, James RA, Munns R. 2002. Stomatal control in tomato with ABA-deficient roots: response of grafted plants to soil drying. *J Exp Bot* **53**(373): 1503-1514.

Houle D, Govindaraju DR, Omholt S. 2010. Phenomics: the next challenge. *Nature Reviews Genetics* **11**(12): 855-866.

Izanloo A, Condon AG, Langridge P, Tester M, Schnurbusch T. 2008. Different mechanisms of adaptation to cyclic water stress in two South Australian bread wheat cultivars. *J Exp Bot* **59**(12): 3327-3346.

Jeuffroy M-H, Casadebaig P, Debaeke P, Loyce C, Meynard J-M. 2014. Agronomic model uses to predict cultivar performance in various environments and cropping systems. A review. *Agronomy for Sustainable Development* **34**(1): 121-137.

Johnson FH, Eyring H, Williams RW. 1942. The nature of enzyme inhibitions in bacterial luminescence: Sulfanilamide, urethane, temperature and pressure. *Journal of Cellular and Comparative Physiology* **20**(3): 247-268.

Kaldenhoff R, Ribas-Carbo M, Flexas J, Lovisolo C, Heckwolf M, Uehlein N. 2008. Aquaporins and plant water balance. *Plant Cell and Environment* **31**(5): 658-666.

Kim HK, van Oosterom E, Dingkuhn M, Luquet D, Hammer G. 2010. Regulation of tillering in sorghum: environmental effects. *Annals of Botany* **106**(1): 57-67.

Koonin EV, Wolf YI. 2010. Constraints and plasticity in genome and molecular-phenome evolution. *Nature Reviews Genetics* **11**(7): 487-498.

Kovalchuk N, Laga H, Cai JC, Kumar P, Parent B, Lu Z, Miklavcic SJ, Haefele SM. 2017. Phenotyping of plants in competitive but controlled environments: a study of drought response in transgenic wheat. *Functional Plant Biology* **44**(3): 290-301.

Krieg DR, Lascano RJ. 1990. Sorghum. *Agronomy*(No. 30): 719-739.

Kumar SR, Hammer GL, Broad I, Harland P, McLean G. 2009. Modelling environmental effects on phenology and canopy development of diverse sorghum genotypes. *Field Crops Research* **111**(1-2): 157-165.

Kumudini S, Andrade FH, Boote KJ, Brown GA, Dzotsi KA, Edmeades GO, Gocken T, Goodwin M, Halter AL, Hammer GL, et al. 2014. Predicting Maize Phenology: Intercomparison of Functions for Developmental Response to Temperature. *Agronomy Journal* **106**(6): 2087-2097.

Kuromori T, Seo M, Shinozaki K. 2018. ABA Transport and Plant Water Stress Responses. *Trends in Plant Science* **23**(6): 513-522.

Lacube S. 2017. *A phenomic-based dynamic model of growth and yield to simulate hundreds of maize hybrids in the diversity of European environments.* Montpellier SupAgro, http://tel.archives-ouvertes.fr Montpellier, France.

Lacube S, Fournier C, Palaffre C, Millet EJ, Tardieu F, Parent B. 2017. Distinct controls of leaf widening and elongation by light and evaporative demand in maize. *Plant Cell and Environment* **40**(9): 2017-2028.

Lacube S, Manceau L, Welcker C, Millet EJ, Gouesnard B, Palaffre C, Ribaut JM, Hammer G, Parent B, Tardieu F. 2020. Simulating the effect of flowering time on maize individual leaf area in contrasting environmental scenarios. *J Exp Bot* **71**(18): 5577-5588.

Lobell DB, Hammer GL, Chenu K, Zheng B, McLean G, Chapman SC. 2015. The shifting influence of drought and heat stress for crops in northeast Australia. *Global Change Biology* **21**(11): 4115-4127.

Lobell DB, Schlenker W, Costa-Roberts J. 2011. Climate Trends and Global Crop Production Since 1980. *Science* **333**(6042): 616-620.

Lohraseb I, Collins NC, Parent B. 2017. Diverging temperature responses of CO2 assimilation and plant development explain the overall effect of temperature on biomass accumulation in wheat leaves and grains. *Aob Plants* **9**.

Long SP, Zhu X-G, Naidu SL, Ort DR. 2006. Can improvement in photosynthesis increase crop yields? *Plant, Cell & Environment* **29**(3): 315-330.

Lynch JP. 2013. Steep, cheap and deep: an ideotype to optimize water and N acquisition by maize root systems. *Annals of Botany* **112**(2): 347-357.

M3P https://www6.montpellier.inra.fr/lepse/M3P.

Maccaferri M, Sanguineti MC, Corneti S, Ortega JLA, Ben Salem M, Bort J, DeAmbrogio E, Fernando Garcia del Moral L, Demontis A, El-Ahmed A, et al. 2008. Quantitative trait loci for grain yield and adaptation of durum wheat (Triticum durum Desf.) across a wide range of water availability. *Genetics* **178**(1): 489-511.

MAGE https://www6.montpellier.inrae.fr/lepse/Equipes/MAGE.

Makowski D, Hillier J, Wallach D, Andrieu B, Jeuffroy M-H 2006. Parameter estimation for crop models. In: Wallach D, Makowski, D., and Jones, J. ed. *Working with Dynamic Crop Models*: Elsevier, 55–100.

Maphosa L, Langridge P, Taylor H, Parent B, Emebiri LC, Kuchel H, Reynolds MP, Chalmers KJ, Okada A, Edwards J, et al. 2014. Genetic control of grain yield and grain physical characteristics in a bread wheat population grown under a range of environmental conditions. *Theoretical and Applied Genetics* **127**(7): 1607-1624.

Marquet PA, Allen AP, Brown JH, Dunne JA, Enquist BJ, Gillooly JF, Gowaty PA, Green JL, Harte J, Hubbell SP, et al. 2014. On Theory in Ecology. *Bioscience* **64**(8): 701-710.

Martre P, Quilot-Turion B, Luquet D, Memmah M-MO-S, Chenu K, Debaeke P. 2015a. *Model-assisted phenotyping and ideotype design*.

Martre P, Wallach D, Asseng S, Ewert F, Jones JW, Rötter RP, Boote KJ, Ruane AC, Thorburn PJ, Cammarano D, et al. 2015b. Multimodel ensembles of wheat growth: many models are better than one. *Global Change Biology* **21**(2): 911-925.

Mayr E, Provine WB. 1980. *The evolutionary synthesis: perspectives on the unification of biology.* . Cambridge , MA . : Harvard Univ. Press.

Mega R, Abe F, Kim J-S, Tsuboi Y, Tanaka K, Kobayashi H, Sakata Y, Hanada K, Tsujimoto H, Kikuchi J, et al. 2019. Tuning water-use efficiency and drought tolerance in wheat using abscisic acid receptors. *Nature Plants* **5**(2): 153-+.

Merilo E, Yarmolinsky D, Jalakas P, Parik H, Tulva I, Rasulov B, Kilk K, Kollist H. 2018. Stomatal VPD Response: There Is More to the Story Than ABA. *Plant Physiology* **176**(1): 851-864.

Messina CD, Podlich D, Dong Z, Samples M, Cooper M. 2011. Yield-trait performance landscapes: from theory to application in breeding maize for drought tolerance. *J Exp Bot* **62**(3): 855-868.

Messina CD, Sinclair TR, Hammer GL, Curan D, Thompson J, Oler Z, Gho C, Cooper M. 2015. Limited-Transpiration Trait May Increase Maize Drought Tolerance in the US Corn Belt. *Agronomy Journal* **107**(6): 1978-1986.

Messinger SM, Buckley TN, Mott KA. 2006. Evidence for involvement of photosynthetic processes in the stomatal response to CO2. *Plant Physiology* **140**(2): 771-778.

Miao C, Xiao L, Huaa K, Zou C, Zhao Y, Bressan RA, Zhu J-K. 2018. Mutations in a subfamily of abscisic acid receptor genes promote rice growth and productivity. *Proceedings of the National Academy of Sciences of the United States of America* **115**(23): 6058-6063.

Michelangeli JAC, Sinclair TR, Bliznyuk N. 2016. Using an Arrhenius-type function to describe temperature response of plant developmental processes: inference and cautions. *New Phytologist* **210**(2): 377-379.

Millet EJ, Welcker C, Kruijer W, Negro S, Coupel-Ledru A, Nicolas SD, Laborde J, Bauland C, Praud S, Ranc N, et al. 2016. Genome-Wide Analysis of Yield in Europe: Allelic Effects Vary with Drought and Heat Scenarios. *Plant Physiol* **172**(2): 749-764.

Moore FC, Lobell DB. 2014. Adaptation potential of European agriculture in response to climate change. *Nature Climate Change* **4**(7): 610-614.

Morillon R, Chrispeels MJ. 2001. The role of ABA and the transpiration stream in the regulation of the osmotic water permeability of leaf cells. *Proceedings of the National Academy of Sciences of the United States of America* **98**(24): 14138-14143.

Muchow RC. 1989. Comparative productivity of maize, sorghum and pearl-millet in a semi-arid tropical environment .2. Effect of water deficits. *Field Crops Research* **20**(3): 207-219.

Munemasa S, Hauser F, Park J, Waadt R, Brandt B, Schroeder JI. 2015. Mechanisms of abscisic acid-mediated control of stomata! aperture. *Current Opinion in Plant Biology* **28**: 154-162.

Paleari L, Movedi E, Cappelli G, Wilson LT, Confalonieri R. 2017. Surfing parameter hyperspaces under climate change scenarios to design future rice ideotypes. *Global Change Biology* **23**(11): 4651-4662.

Pantin F, Monnet F, Jannaud D, Costa JM, Renaud J, Muller B, Simonneau T, Genty B. 2013. The dual effect of abscisic acid on stomata. *New Phytologist* **197**(1): 65-72.

Parent B, Bonneau J, Maphosa L, Kovalchuk A, Langridge P, Fleury D. 2017. Quantifying Wheat Sensitivities to Environmental Constraints to Dissect Genotype x Environment Interactions in the Field. *Plant Physiology* **174**(3): 1669-1682.

Parent B, Hachez C, Redondo E, Simonneau T, Chaumont F, Tardieu F. 2009. Drought and Abscisic Acid Effects on Aquaporin Content Translate into Changes in Hydraulic Conductivity and Leaf Growth Rate: A Trans-Scale Approach. *Plant Physiology* **149**(4): 2000-2012.

Parent B, Lacube S, Semenov M, Welcker C, Martre P, Tardieu F. 2018. Maize yields over Europe may increase in spite of climate change, with an appropriate use of the genetic variability of flowering time. *PNAS* **115**(42): 10642-10647.

Parent B, Millet EJ, Tardieu F. 2019. The use of thermal time in plant studies has a sound theoretical basis provided that confounding effects are avoided. *J Exp Bot* **70**(9): 2359-2370.

Parent B, Shahinnia F, Maphosa L, Berger B, Rabie H, Chalmers K, Kovalchuk A, Langridge P, Fleury D. 2015. Combining field performance with controlled environment plant imaging to identify the genetic control of growth and transpiration underlying yield response to water-deficit stress in wheat. *J Exp Bot* **66**(18): 5481-5492.

Parent B, Tardieu F. 2012. Temperature responses of developmental processes have not been affected by breeding in different ecological areas for 17 crop species. *New Phytologist* **194**(3): 760-774.

Parent B, Tardieu F. 2014. Can current crop models be used in the phenotyping era for predicting the genetic variability of yield of plants subjected to drought or high temperature? *J Exp Bot* **65**(21): 6179-6189.

Parent B, Turc O, Gibon Y, Stitt M, Tardieu F. 2010. Modelling temperature-compensated physiological rates, based on the co-ordination of responses to temperature of developmental processes. *J Exp Bot* **61**(8): 2057-2069.

Parent B, Vile D, Violle C, Tardieu F. 2016. Towards parsimonious ecophysiological models that bridge ecology and agronomy. *New Phytologist* **210**(2): 380-382.

Pe'er G, Zinngrebe Y, Moreira F, Sirami C, Schindler S, Muller R, Bontzorlos V, Clough D, Bezak P, Bonn A, et al. 2019. A greener path for the EU Common Agricultural Policy. *Science* **365**(6452): 449-+.

Perego A, Sanna M, Giussani A, Chiodini ME, Fumagalli M, Pilu SR, Bindi M, Moriondo M, Acutis M. 2014. Designing a high-yielding maize ideotype for a changing climate in Lombardy plain (northern Italy). *Science of the Total Environment* **499**: 497-509.

Perez RPA, Fournier C, Cabrera-Bosquet L, Artzet S, Pradal C, Brichet N, Chen TW, Chapuis R, Welcker C, Tardieu F. 2019. Changes in the vertical distribution of leaf area enhanced light interception efficiency in maize over generations of selection. *Plant Cell and Environment* **42**(7): 2105-2119.

Pheno3C https://www.phenome-emphasis.fr/phenome_eng/Installations/Clermont-Ferrand-Semi-controlled.

Pieruschka R, Schurr U. 2019. Plant Phenotyping: Past, Present, and Future. *Plant Phenomics* **2019**: 6.

Poire R, Wiese-Klinkenberg A, Parent B, Mielewczik M, Schurr U, Tardieu F, Walter A. 2010. Diel time-courses of leaf growth in monocot and dicot species: endogenous rhythms and temperature effects. *J Exp Bot* **61**(6): 1751-1759.

Potgieter A, Meinke H, Doherty A, Sadras VO, Hammer G, Crimp S, Rodriguez D. 2013. Spatial impact of projected changes in rainfall and temperature on wheat yields in Australia. *Climatic Change* **117**(1-2): 163-179.

Prado SA, Cabrera-Bosquet L, Grau A, Coupel-Ledru A, Millet EJ, Welcker C, Tardieu F. 2017. Phenomics allows identification of genomic regions affecting maize stomatal conductance with conditional effects of water deficit and evaporative demand. *Plant, Cell & Environment*: n/a-n/a.

Qin XQ, Zeevaart JAD. 1999. The 9-cis-epoxycarotenoid cleavage reaction is the key regulatory step of abscisic acid biosynthesis in water-stressed bean. *Proceedings of the National Academy of Sciences of the United States of America* **96**(26): 15354-15361.

Quilot-Turion B, Genard M, Valsesia P, Memmah M-M. 2016. Optimization of Allelic Combinations Controlling Parameters of a Peach Quality Model. *Frontiers in Plant Science* **7**.

Raup DM, Michelso.A. 1965. Theoretical morphology of coiled shell. *Science* **147**(3663): 1294-&.

Rebetzke GJ, Condon AG, Richards RA, Farquhar GD. 2002. Selection for reduced carbon isotope discrimination increases aerial biomass and grain yield of rainfed bread wheat. *Crop Science* **42**(3): 739-745.

Richards RA. 2006. Physiological traits used in the breeding of new cultivars for water-scarce environments. *Agricultural Water Management* **80**(1-3): 197-211.

Richards RA, Rebetzke GJ, Condon AG, van Herwaarden AF. 2002. Breeding opportunities for increasing the efficiency of water use and crop yield in temperate cereals. *Crop Science* **42**(1): 111-121.

Rizhsky L, Liang HJ, Mittler R. 2002. The combined effect of drought stress and heat shock on gene expression in tobacco. *Plant Physiology* **130**(3): 1143-1151.

Rosenzweig C, Jones JW, Hatfield JL, Ruane AC, Boote KJ, Thorburne P, Antle JM, Nelson GC, Porter C, Janssen S, et al. 2013. The Agricultural Model Intercomparison and Improvement Project (AgMIP): Protocols and pilot studies. *Agricultural and Forest Meteorology* **170**: 166-182.

Rotter RP, Tao F, Hohn JG, Palosuo T. 2015. Use of crop simulation modelling to aid ideotype design of future cereal cultivars. *J Exp Bot* **66**(12): 3463-3476.

Salah HBH, Tardieu F. 1997. Control of leaf expansion rate of droughted maize plants under fluctuating evaporative demand - A superposition of hydraulic and chemical messages? *Plant Physiology* **114**(3): 893-900.

Sanguineti MC, Duvick DN, Smith S, Landi P, Tuberosa R. 2006. Effects of long-term selection on seedling traits and ABA accumulation in commercial maize hybrids. *Maydica* **51**(2): 329-338.

Sansberro PA, Mroginski LA, Bottini RE. 2004. Foliar sprays with ABA promote growth of Ilex paraguariensis by alleviating diurnal water stress. *Plant Growth Regulation* **42**(2): 105-111.

Saradadevi R, Palta JA, Siddique KHM. 2017. ABA-Mediated Stomatal Response in Regulating Water Use during the Development of Terminal Drought in Wheat. *Frontiers in Plant Science* **8**.

Schauberger B, Ben-Ari T, Makowski D, Kato T, Kato H, Ciais P. 2018. Yield trends, variability and stagnation analysis of major crops in France over more than a century. *Scientific Reports* **8**(1): 16865.

Schenk HJ, Jackson RB. 2002. Rooting depths, lateral root spreads and below-ground/above-ground allometries of plants in water-limited ecosystems. *Journal of Ecology* **90**(3): 480-494.

Schittenhelm S, Schroetter S. 2014. Comparison of Drought Tolerance of Maize, Sweet Sorghum and Sorghum-Sudangrass Hybrids. *Journal of Agronomy and Crop Science* **200**(1): 46-53.

Schmidt JE, Gaudin ACM. 2017. Toward an Integrated Root Ideotype for Irrigated Systems. *Trends in Plant Science* **22**(5): 433-443.

Schnyder H, Nelson CJ. 1989. Growth-rates and assimilate partitioning in the elongation zone of tall fescue leaf blades at high and low irradiance. *Plant Physiology* **90**(3): 1201-1206.

Sharp RE, LeNoble ME. 2002. ABA, ethylene and the control of shoot and root growth under water stress. *J Exp Bot* **53**(366): 33-37.

Shavrukov Y, Kurishbayev A, Jatayev S, Shvidchenko V, Zotova L, Koekemoer F, de Groot S, Soole K, Langridge P. 2017. Early Flowering as a Drought Escape Mechanism in Plants: How Can It Aid Wheat Production? *Frontiers in Plant Science* **8**: 1950-1950.

Shipley B, Lechowicz MJ, Wright I, Reich PB. 2006. Fundamental trade-offs generating the worldwide leaf economics spectrum. *Ecology* **87**(3): 535-541.

Sinclair TR. 2017. *Water-Conservation Traits to Increase Crop Yields in Water-deficit Environments: Case Studies*.

Singh BR, Singh DP. 1995. Agronomic and physiological-responses of sorghum, maize and pearl-millet to irrigation. *Field Crops Research* **42**(2-3): 57-67.

Staggenborg SA, Dhuyvetter KC, Gordon WB. 2008. Grain Sorghum and Corn Comparisons: Yield, Economic, and Environmental Responses. *Agronomy Journal* **100**(6): 1600-1604.

Steppe K, Sterck F, Deslauriers A. 2015. Diel growth dynamics in tree stems: linking anatomy and ecophysiology. *Trends in Plant Science* **20**(6): 335-343.

Stockle CO, Donatelli M, Nelson R. 2003. CropSyst, a cropping systems simulation model. *European Journal of Agronomy* **18**(3-4): 289-307.

Swigonová Z, Lai J, Ma J, Ramakrishna W, Llaca V, Bennetzen JL, Messing J. 2004. Close split of sorghum and maize genome progenitors. *Genome research* **14**(10A): 1916-1923.

Tan BC, Schwartz SH, Zeevaart JAD, McCarty DR. 1997. Genetic control of abscisic acid biosynthesis in maize. *Proceedings of the National Academy of Sciences of the United States of America* **94**(22): 12235-12240.

Tardieu F. 2003. Virtual plants: modelling as a tool for the genomics of tolerance to water deficit. *Trends in Plant Science* **8**(1): 9-14.

Tardieu F. 2012. Any trait or trait-related allele can confer drought tolerance: just design the right drought scenario. *J Exp Bot* **63**(1): 25-31.

Tardieu F, Cabrera-Bosquet L, Pridmore T, Bennett M. 2017. Plant Phenomics, From Sensors to Knowledge. *Current Biology* **27**(15): R770-R783.

Tardieu F, Davies WJ. 1993. Integration of hydraulic and chemical signaling in the control of stomatal conductance and water status of droughted plants. *Plant Cell and Environment* **16**(4): 341-349.

Tardieu F, Parent B. 2017. Predictable 'meta-mechanisms' emerge from feedbacks between transpiration and plant growth and cannot be simply deduced from short-term mechanisms. *Plant Cell and Environment* **40**(6): 846-857.

Tardieu F, Parent B, Simonneau T. 2010. Control of leaf growth by abscisic acid: hydraulic or non-hydraulic processes? *Plant Cell and Environment* **33**(4): 636-647.

Tardieu F, Simonneau T, Parent B. 2015. Modelling the coordination of the controls of stomatal aperture, transpiration, leaf growth, and abscisic acid: update and extension of the Tardieu-Davies model. *J Exp Bot* **66**(8): 2227-2237.

Thompson AJ, Andrews J, Mulholland BJ, McKee JMT, Hilton HW, Horridge JS, Farquhar GD, Smeeton RC, Smillie IRA, Black CR, et al. 2007. Overproduction of abscisic acid in tomato increases transpiration efficiency and root hydraulic conductivity and influences leaf expansion. *Plant Physiology* **143**(4): 1905-1917.

Townsend TJ, Roy J, Wilson P, Tucker GA, Sparkes DL. 2017. Food and bioenergy: Exploring ideotype traits of a dual-purpose wheat cultivar. *Field Crops Research* **201**: 210-221.

Tuzet A, Perrier A, Leuning R. 2003. A coupled model of stomatal conductance, photosynthesis and transpiration. *Plant Cell and Environment* **26**(7): 1097-1116.

Urban DW, Sheffield J, Lobell DB. 2015. The impacts of future climate and carbon dioxide changes on the average and variability of US maize yields under two emission scenarios. *Environmental Research Letters* **10**(4).

Voisin AS, Reidy B, Parent B, Rolland G, Redondo E, Gerentes D, Tardieu F, Muller B. 2006. Are ABA, ethylene or their interaction involved in the response of leaf growth to soil water deficit? An analysis using naturally occurring variation or genetic transformation of ABA production in maize. *Plant Cell and Environment* **29**(9): 1829-1840.

Wallach D, Goffinet B, Bergez JE, Debaeke P, Leenhardt D, Aubertot JN. 2001. Parameter estimation for crop models: A new approach and application to a corn model. *Agronomy Journal* **93**(4): 757-766.

Wan XC, Zwiazek JJ. 2001. Root water flow and leaf stomatal conductance in aspen (Populus tremuloides) seedlings treated with abscisic acid. *Planta* **213**(5): 741-747.

Wang EL, Martre P, Zhao ZG, Ewert F, Maiorano A, Rotter RP, Kimball BA, Ottman MJ, Wall GW, White JW, et al. 2017. The uncertainty of crop yield projections is reduced by improved temperature response functions (vol 3, pg 17102, 2017). *Nature Plants* **3**(10): 833-833.

Whish J, Butler G, Castor M, Cawthray S, Broad I, Carberry P, Hammer G, McLean G, Routley R, Yeates S. 2005. Modelling the effects of row configuration on sorghum yield reliability in north-eastern Australia. *Australian Journal of Agricultural Research* **56**(1): 11-23.

Wilkinson S, Kudoyarova GR, Veselov DS, Arkhipova TN, Davies WJ. 2012. Plant hormone interactions: innovative targets for crop breeding and management. *J Exp Bot* **63**(9): 3499-3509.

Wright GC, Smith RCG. 1983. Differences between 2 grain-sorghum genotypes in adaptation to drought stress .2. Root water-uptake and water-use. *Australian Journal of Agricultural Research* **34**(6): 627-636.

Wright IJ, Reich PB, Westoby M, Ackerly DD, Baruch Z, Bongers F, Cavender-Bares J, Chapin T, Cornelissen JHC, Diemer M, et al. 2004. The worldwide leaf economics spectrum. *Nature* **428**(6985): 821-827.

Xiao B-Z, Chen X, Xiang C-B, Tang N, Zhang Q-F, Xiong L-Z. 2009. Evaluation of seven function-known candidate genes for their effects on improving drought resistance of transgenic rice under field conditions. *Molecular Plant* **2**(1): 73-83.

Xu H, Twine TE, Girvetz E. 2016. Climate Change and Maize Yield in Iowa. *Plos One* **11**(5).

Yang CY, Fraga H, Van Ieperen W, Santos JA. 2017. Assessment of irrigated maize yield response to climate change scenarios in Portugal. *Agricultural Water Management* **184**: 178-190.

Yang WN, Feng H, Zhang XH, Zhang J, Doonan JH, Batchelor WD, Xiong LZ, Yan JB. 2020. Crop Phenomics and High-Throughput Phenotyping: Past Decades, Current Challenges, and Future Perspectives. *Molecular Plant* **13**(2): 187-214.

Yin XY, Chasalow SD, Dourleijn CJ, Stam P, Kropff MJ. 2000. Coupling estimated effects of QTLs for physiological traits to a crop growth model: predicting yield variation among recombinant inbred lines in barley. *Heredity* **85**(6): 539-549.

Yin XY, van Laar HH. 2005. *Crop Systems Dynamics. An ecophysiological simulation model of genotype-by-environment interactions.* Wageningen, The Netherlands: Wageningen Academic Publishers.

Yoshida T, Christmann A, Yamaguchi-Shinozaki K, Grill E, Fernie AR. 2019. Revisiting the Basal Role of ABA - Roles Outside of Stress. *Trends in Plant Science* **24**(7): 625-635.

Zhang JH, Davies WJ. 1990. Does ABA in the xylem control the rate of leaf growth in soil-dried maize and sunflower plants. *J Exp Bot* **41**(230): 1125-1132.

Zhang Y, Zhao YX, Chen SN, Guo JP, Wang EL. 2015. Prediction of Maize Yield Response to Climate Change with Climate and Crop Model Uncertainties. *Journal of Applied Meteorology and Climatology* **54**(4): 785-794.

Zhu CF, Schraut D, Hartung W, Schaffner AR. 2005. Differential responses of maize MIP genes to salt stress and ABA. *J Exp Bot* **56**(421): 2971-2981.

Zweifel R, Steppe K, Sterck FJ. 2007. Stomatal regulation by microclimate and tree water relations: interpreting ecophysiological field data with a hydraulic plant model. *J Exp Bot* **58**(8): 2113-2131.

9. ANNEXES

Publications choisies

Annexe 1. Baumont, M., **Parent, B**., Manceau, L., Brown, H., Driever, S., Muller, B., Martre, P. (2019). Experimental and modeling evidence of carbon limitation of leaf appearance rate for spring and winter wheat. Journal of Experimental Botany. 70. 2449-2462.

Cette publication issue de la thèse de Maeva Baumont est un bon exemple du type de modèles que j'essaye de développer en général. Comment remettre de la biologie dans des modèles permet de simplifier des modèles empiriques, diminuer leur nombre de paramètres, pour qu'ils soient robustes, informatifs et mesurables.

Annexe 2. Parent, B., Leclere, M., Lacube, S., Semenov, M. A., Welcker, C., Martre, P., Tardieu, F. (2018). Maize yields over Europe may increase in spite of climate change, with an appropriate use of the genetic variability of flowering time. *PNAS, 115* (42), 10642-10647.

Cette publication est un exemple d'hybridation entre modélisation écophysiologique, phénotypage au champ et simulations à large échelle pour analyser l'impact de la variabilité génétique dans des scénarios contrastés.

Annexe 3. Parent, B., Tardieu, F. (2014). Can current crop models be used in the phenotyping era for predicting the genetic variability of yield of plants subjected to drought or high temperature?. *Journal of Experimental Botany, 65* (21), 6179-6189.

Cette publication est la première, juste après ma titularisation, dans laquelle je théorise et développe ma stratégie scientifique.

Annexe 4. Parent, B., Tardieu, F. (2012). Temperature responses of developmental processes have not been affected by breeding in different ecological areas for 17 crop species. *New Phytologist, 194* (3), 760-774.

Cette méta-analyse démontre l'intérêt des analyses comparatives pour la biologie des plantes cultivées et la modélisation.

Annexe 5. Parent, B., Hachez, C., Redondo, E., Simonneau, T., Chaumont, F., Tardieu, F. (2009). Drought and Abscisic Acid Effects on Aquaporin Content Translate into Changes in Hydraulic Conductivity and Leaf Growth Rate: A Trans-Scale Approach. *Plant Physiology, 149* (4), 2000-2012.

Cette publication est issue de mon travail de thèse. C'est une étape fondatrice de ma démarche scientifique alliant écophysiologie fine et modélisation.

Journal of Experimental Botany, Vol. 70, No. 9 pp. 2449–2462, 2019
doi:10.1093/jxb/erz012 Advance Access Publication 20 February 2019
This paper is available online free of all access charges (see https://academic.oup.com/jxb/pages/openaccess for further details)

RESEARCH PAPER

Experimental and modeling evidence of carbon limitation of leaf appearance rate for spring and winter wheat

Maeva Baumont[1], Boris Parent[1,*], Loïc Manceau[1], Hamish E. Brown[2], Steven M. Driever[3,†], Bertrand Muller[1] and Pierre Martre[1,*]

[1] LEPSE, Université Montpellier, INRA, Montpellier SupAgro, 34060 Montpellier, France
[2] The New Zealand Institute for Plant & Food Research Limited, Private Bag 4704, Christchurch, New Zealand
[3] Centre for Crop Systems Analysis, Department of Plant Sciences, Wageningen University, PO Box 430, 6700 AK Wageningen, The Netherlands

[†] Present address: Institute for Genomic Biology, University of Illinois, Urbana-Champaign, USA
* Correspondence: boris.parent@inra.fr or pierre.martre@inra.fr

Received 26 August 2018; Editorial decision 7 January 2019; Accepted 29 January 2019

Editor: Christine Raines, University of Essex, UK

Abstract

Accurate predictions of the timing of physiological stages and the development rate are crucial for predicting crop performance under field conditions. Plant development is controlled by the leaf appearance rate (LAR) and our understanding of how LAR responds to environmental factors is still limited. Here, we tested the hypothesis that carbon availability may account for the effects of irradiance, photoperiod, atmospheric CO_2 concentration, and ontogeny on LAR. We conducted three experiments in growth chambers to quantify and disentangle these effects for both winter and spring wheat cultivars. Variations of LAR observed between environmental scenarios were well explained by the supply/demand ratio for carbon, quantified using the photothermal quotient. We therefore developed an ecophysiological model based on the photothermal quotient that accounts for the effects of temperature, irradiance, photoperiod, and ontogeny on LAR. Comparisons of observed leaf stages and LAR with simulations from our model, from a linear thermal-time model, and from a segmented linear thermal-time model corrected for sowing date showed that our model can simulate the observed changes in LAR in the field with the lowest error. Our findings demonstrate that a hypothesis-driven approach that incorporates more physiology in specific processes of crop models can increase their predictive power under variable environments.

Keywords: Carbon, crop model, daylength, leaf appearance rate, photoperiod, photothermal quotient, phyllochron, *SiriusQuality*, temperature, wheat.

Introduction

The rate at which plants develop strongly affects canopy and root structure, radiation interception, and, through the cumulative effects of these factors, biomass production, partitioning, and yield. It is therefore essential to understand how this rate is determined and how it can be modeled in order to accurately predict crop responses to their environment in the field. A widely used metric to quantify plant development rate is the phyllochron, i.e. the time-interval between successive organs at the same stage (Wilhelm and McMaster, 1995), or its reciprocal, the leaf appearance rate (LAR). Both are often

expressed in (or per) thermal-time unit (i.e. in cumulative temperature above a base temperature, classically expressed in degree-days, °Cd). The phyllochron has been used for decades in the plant science community and many growth simulation models use it to model both vegetative and reproductive development (Rickman and Klepper, 1995; Fournier *et al.*, 2005; Evers *et al.*, 2006).

The success of the phyllochron as a straightforward concept relies on the linear relationship between LAR and temperature, and therefore its constancy when expressed in thermal time. However, in many situations, irregular or non-linear relationships between leaf appearance and temperature limit its value to predict development. In several grasses, including wheat, LAR increases with photoperiod (Baker *et al.*, 1980; Cao and Moss, 1989*a*; Masle *et al.*, 1989; Slafer *et al.*, 1994), irradiance (Rickman *et al.*, 1985; Volk and Bugbee, 1991; Bos and Neuteboom, 1998; Birch *et al.*, 1998), and atmospheric CO_2 concentration (Boone *et al.*, 1990; McMaster *et al.*, 1999), whilst it decreases with plant density (Abichou *et al.*, 2018), red/far-red ratio and blue light (Gautier and Varlet-Grancher, 1996), and nitrogen or water deficit (Longnecker and Robson, 1994).

LAR is also often reported to change with ontogeny. Indeed, the relationship between the number of visible leaves and thermal time appears as either bilinear or non-linear, both under fluctuating field conditions (Baker *et al.*, 1986; Hay and Delécolle, 1989) and under constant controlled conditions (Cao and Moss, 1991; Slafer and Rawson, 1997; Miralles and Richards, 2000). Changes in LAR with ontogeny could be related to an increase in the time taken by successive leaves to extend above the whorl of previous leaves (Miglietta, 1991; Skinner and Nelson, 1995; Streck *et al.*, 2003). However, LAR for wheat increases and decreases with leaf rank for late and early sowing, respectively, independently of sheath length (Hay and Delécolle, 1989; Abichou *et al.*, 2018). An alternative hypothesis is that the phyllochron changes with specific developmental stages. In wheat, ontogenic changes in LAR coincide with the initiation of the flag-leaf primordium (Abichou *et al.*, 2018) or first-ridge formation (Boone *et al.*, 1990). However, in other cases, ontogenic changes in LAR occur around the time of appearance of a given leaf, independently of final leaf number and of the state of the apex (Slafer and Rawson, 1997), which suggests that ontogenic changes in LAR are not associated with any particular growth stage. Finally, it has been suggested that, at least in some conditions, apparent ontogenic changes in LAR might be due to the use of an incorrect base temperature (Hay and Delécolle, 1989).

Several models accounting for the effects of temperature and photoperiod on LAR have been proposed and compared with each other (Miglietta, 1991; Kirby, 1995; Bindi *et al.*, 1995; McMaster and Wilhelm, 1995). However, with the exception of Miglietta (1991), these models do not consider changes in LAR with ontogeny. Surprisingly, none of these LAR models have been incorporated into crop growth models, where LAR is modeled predominantly as a linear response to temperature, without any effects of photoperiod or plant age (Muchow and Carberry, 1990; Amir and Sinclair, 1991; Lizaso *et al.*, 2011). Only a few crop growth models consider photoperiod or plant age effects on LAR. For instance, the wheat model Sirius uses three different constant LAR values depending on leaf rank (Jamieson *et al.*, 1995, 1998), and the photoperiod effect is modeled using an empirical relationship between sowing date and LAR (He *et al.*, 2012). A similar approach is used in the APSIM-NWheat model, where the phyllochron is empirically corrected at a fixed date after sowing (Bassu *et al.*, 2009). A recently updated version of APSIM wheat (Brown *et al.*, 2018) models phyllochron as a function of leaf rank and a photoperiod adjustment factor.

In this study, we tested the hypothesis that carbon availability could account for the effects of temperature, irradiance, photoperiod, air CO_2 concentration, and ontogeny on LAR. This hypothesis fits well with most of the effects noted above, such as the positive effect on LAR of the photoperiod or of elevated CO_2, as well as the negative effect of elevated temperature, which decreases the amount of fixed carbon per unit thermal time. Changes in LAR with ontogeny could be related to the strong alterations of source–sink relationships that take place during development (Dingkuhn *et al.*, 2005). Moreover, carbon status, in particular in the lower range, is often reported as driving shoot development (Masle, 2000; Stitt and Zeeman, 2012). Finally, carbon status is often reported to alter LAR in woody species (e.g. Davidson *et al.*, 2016).

We conducted three experiments in growth chambers in order to quantify and disentangle the effects of temperature, light intensity, photoperiod, air CO_2 concentration, and ontogeny for both winter and spring wheat cultivars. The photothermal quotient (PTQ, mol m^{-2} $°Cd^{-1}$), defined as the ratio between daily photosynthetically active radiation (PAR, mol m^{-2} d^{-1}) and mean daily thermal time, was used to quantify the (potential) supply of carbon per unit of development time. Because our experimental results showed good agreement with our hypothesis, we developed a simple ecophysiological model that accounts for temperature, light, and photoperiod effects, as well as the effects of ontogeny on LAR. This model was integrated in the wheat model *SiriusQuality* (Martre *et al.*, 2006; He *et al.*, 2012; Wang *et al.*, 2017). Comparisons of leaf stages simulated with our model or with either a simple linear model or the current LAR model of *SiriusQulity* against field data with a very large range of daily mean temperatures and photoperiods showed that our proposed model accurately simulated the observed changes in LAR with sowing date (photoperiod), temperature, and ontogeny.

Materials and methods

Plant material and growth conditions

Three independent experiments were carried out on wheat (*Triticum aestivum*) under controlled environment conditions using winter and spring cultivars (Table 1, Supplementary Table S1 at *JXB* online). The first experiment studied the response of leaf appearance rate (LAR) to different combinations of temperature, irradiance, and photoperiod; the second studied the response of LAR to elevated CO_2 at two temperatures; and the third studied the genetic variability of the response of LAR to the photothermal quotient (PTQ, mol m^{-2} $°Cd^{-1}$).

In all experiments, seeds were imbibed for 24 h at 4 °C on wet filter paper in Petri dishes, then placed at room temperature (22 °C) for 24 h, and transferred back to 4 °C until the radicles were 5 mm long. In Experiments 1 and 3, uniform-sized seedlings were then transplanted

Table 1. *Cultivars and environmental conditions for the three experiments carried out in this study*

Experiment/ Cultivar[a]	Treatment name	Set point day/night air temperature (°C)	Set point PAR (µmol m^{-2} s^{-1})	Photoperiod (h)	Air CO_2 concentration (ppm)	Mean daily PAR (mol m^{-2} d^{-1})	Mean daily thermal time (°Cd)	Photothermal quotient (mol m^{-2} °Cd^{-1})	Mean day/night leaf–air VPD (kPa)	LAR_i ($\times 10^{-3}$ leaves °Cd^{-1})
Experiment 1. Photothermal effect										
Paragon, ***Renan***,	HT.SD.320	28/24	320	8	400	9.4	24.5	0.38	1.7 /1.1	6.61±0.37
Récital	HT.LD.170	28/24	170	16	400	9.6	26.2	0.37	1.6 /1.0	6.63±0.47
	HT.LD.280	28/24	280	16	400	16.5	26.2	0.63	1.5/0.9	7.94±0.22
	LT.LD.280	18/14	280	16	400	15.9	10.3	1.54	0.8/0.6	10.84±0.52
	HT.MD.450[b]	28/24	450	14	400	22.5	26.4	0.85	1.7 /1.1	7.75±0.83
	LT.MD.320[b]	18/14	320	14	400	15.7	10.5	1.50	1.12/0.8	9.17±0.71
	280→170[c]	28/24	280→170	16	400	16.5→9.6	26.2→26.2	0.63→ 0.37	1.5/0.9→1.6 /1.0	7.80±0.52
	170→280[c]	28/24	170→280	16	400	9.6→16.5	26.2→26.2	0.37→0.63	1.6 /1.0→1.5/0.9	6.49±0.43
Experiment 2. CO_2×temperature effect										
Paragon	HT.aCO_2	28/24	600	14	400	32.3	27.2	1.19	1.1 /1.0	10.80±0.56
	HT.eCO_2	28/24	600	14	800	27.8	27.2	1.02	1.1 /1.0	11.90±0.64
	LT.aCO_2	18/14	600	14	400	31.5	10.6	2.97	1.0 /0.9	11.20±1.19
	LT.eCO_2	18/14	600	14	800	30.0	10.6	2.83	1.1/1.1	15.80±0.83
Experiment 3. Genetic variability										
Apache-sp, *Arche*,	HT.SD	28/24	190	8	400	4.9	25.5	0.20	1.48/0.84	5.00±0.39
Baviacora M92,	HT.LD	28/24	190	16	400	11.1	26.7	0.42	1.52/0.91	6.62±0.54
Cadenza, Chinese	LT.SD	18/14	190	8	400	5.7	8.9	0.64	1.57/0.92	6.58±0.42
Spring, *Courtot*,	LT.LD	18/14	190	16	400	10.6	10.1	1.05	1.43/0.87	8.40±0.59
Drysdale, Feeling,										
Gladius, *Paragon*,										
Récital-sp, Seri M82,										
Specifik, Yecora										
Rojo, Yitpi										

Details of the 17 cultivars used are given in Supplementary Table S1. Initial leaf appearance rates (LAR_i) are given for the spring wheat cv. Paragon, which was grown in all experiments and treatments. LAR_i data are mean (±1SD) for n=4–6 independent replicates. VPD, vapour-pressure deficit.

[a] Italics, photoperiod sensitive cultivars; bold, winter wheat cultivars.[b] Treatments were only applied to the spring wheat cv Paragon.[c] Treatments were only applied to the winter wheat cv. Récital.

into 1.7-L plastic pots (one plant per pot) filled with a 30:70 (v:v) mixture of soil and organic compost. Pots were placed in controlled environment growth chambers with different conditions but with a day/night air vapor-pressure deficit of 1.5/1.0 kPa set as common to all experiments and treatments. Each growth chamber was associated with one treatment, representing a combination of temperature, light intensity, and photoperiod, as detailed in Table 1. In Experiment 1, treatments 280→170 and 170→280 consisted of a swap between growth conditions when plants had 3.5 visible leaves. Six independent replicates were used in each treatment and the genotypes were randomized in the growth chambers. Plants were watered daily and no nutrients were applied as the potting substrate provided enough to the plants for the duration of the experiments.

In Experiment 2, uniform-sized seedlings were transplanted to 3-l plastic pots (one plant per pot) filled with soil. Fifteen plants of each cultivar per growth temperature were placed in a five-block design in two walk-in growth chambers. In both chambers, the air vapor-pressure deficit was maintained constant at 1.0 kPa. Plants were watered daily and additional nutrients were supplied by watering with 300–500 ml of Hoagland solution (Hoagland, 1950) three times per week, from 3 weeks after transplanting.

In all experiments, leaf (T_{leaf}) and apex (T_{apex}) temperatures (°C) were measured with thermocouples secured on the lower surface of leaf blades or inserted vertically between leaf sheaths down to the base of the leaves, respectively.

Determination of leaf appearance rate

Main stem leaf stages were determined every2–3 d from the ligulation of the second leaf to the appearance of the flag-leaf ligule for the spring cultivars or to the ligulation of leaf 10 for the winter cultivars. The Haun stage (Haun, 1973) was calculated as the ratio of the length of the youngest visible (expanding) leaf blade to the length of the blade of the youngest ligulated (mature) leaf. The initial LAR (LAR_i) was calculated as the slope of the relationship between the Haun stage and thermal time calculated using the apex temperature for Haun stage ≤5 to avoid confounding effects due to the increase in final leaf length after leaf 5 (Martre and Dambreville, 2018). To assess the changes in LAR over plant development, a spline function was fitted to Haun stage versus thermal time and LAR was calculated by taking the first derivative of the fitted spline equations.

The daily thermal time (ΔT_t, °Cd) was calculated as:

$$\Delta T_t = \sum_{i=1}^{n} \frac{1}{144} \sum_{i=1}^{n=144} T_{opt} \times f(T) \quad (1)$$

with

$$f(T) = max\left(0, \frac{2(T_{apex} - T_{min})^{\alpha}(T_{opt} - T_{min})^{\alpha} - (T_{apex} - T_{min})^{2\alpha}}{(T_{opt} - T_{min})^{2\alpha}}\right);$$
$$\alpha = \frac{\ln 2}{\ln\left(\frac{T_{max} - T_{min}}{T_{opt} - T_{min}}\right)} \quad (2)$$

Where $f(T)$ (dimensionless) is the non-linear temperature response of leaf initiation and growth (Wang *et al.*, 2017), T_{apex} is the 10-min mean apex temperature, and T_{min}, T_{opt}, and T_{max} are the minimum, optimum, and maximum temperatures, respectively. Values of 0, 27.5, and 40 °C were used for T_{min} T_{min}, T_{opt}, and T_{max}, respectively (Parent and Tardieu, 2012; Wang *et al.*, 2017). The photothermal quotient (mol m^{-2} $°Cd^{-1}$) was calculated as the ratio of daily PAR to ΔT_t (Nix, 1976).

Gas-exchange measurements

In Experiment 1, net carbon assimilation (A_{net}, µmol CO_2 m^{-2} s^{-1}) was measured for cv. Paragon on leaf 3 the day after its ligulation using a CIRAS-2 portable photosynthesis system (PP Systems, Amesbury, MA, USA) equipped with a 25×7-mm bead plate. Measurements were carried out under ambient temperature (leaf temperature set equal to ambient air temperature), light intensity (provided by red-white LEDs), and air CO_2 concentration (400 ppm). The cuvette relative humidity was set to maintain the ambient air vapor-pressure deficit. Daily carbon assimilation (A_{day}, mol CO_2 m^{-2} $°Cd^{-1}$) was calculated by integrating A_{net} over the diurnal period.

In Experiment 2, assimilation at saturating light intensity (PAR=1600 µmol m^{-2} s^{-1}; A_{sat}) was measured instead of A_{net} on leaf 4 with a LI-6400XT portable photosynthesis system (LI-COR, Lincoln NE, USA) fitted with a 6400–40 Leaf Chamber Fluorometer. Light was provided by a red-blue LED light source (10% blue light), leaf temperature was maintained near growth temperature (18 or 24 ±1 °C), the CO_2 concentration of the air was maintained near growth CO_2 (400 or 800 ppm), and the air–leaf vapor-pressure deficit was maintained below 1.5 kPa.

Soluble carbohydrates and starch assays

In Experiment 1, whole shoots of the cultivars Paragon, Renan, and Récital were sampled in treatments HT.SD.320, HT.LD.170, HT.LD.280, and LT.LD.280(see Table 1) at Haun stage 3.5 at the end of the light and of dark periods for measurements of soluble sugars (glucose, fructose, and sucrose) and starch (soluble sugars and starch hereafter collectively referred to as carbohydrates). Six plants of each cultivar were sampled per treatment. Plants were immediately frozen in liquid nitrogen and stored at –80 °C prior to analysis. Plants were ground in liquid nitrogen using a mixer mill (MM 200, Retsch). Soluble sugars and starch were extracted and quantified by enzymatic assays following the procedure described by Hummel *et al.* (2010). Night consumption of carbohydrate (CC_{night}, mg g^{-1} $°Cd^{-1}$) was calculated as the difference in carbohydrate concentration between the measurements at the end of the day and the end of the night divided by the thermal time cumulated during the night.

Modeling leaf appearance rate

Our newly developed LAR model (see Results) was implemented in the wheat phenology model described by He *et al.* (2012). This new phenology model was developed as an independent executable component in the BioMA software framework (http://www.biomamodelling.org). The BioMA component was integrated in the wheat model *SiriusQuality* (Martre *et al.*, 2006; Martre and Dambreville, 2018). The source code and the documentation of the BioMA component of the LAR model (Manceau and Martre, 2018) and the source code binaries of *SiriusQuality* and associated BioMA components (https://github.com/SiriusQuality/Release) are available under the MIT (X11) free and open-source software license.

Our model of LAR (hereafter referred to as model M3) was compared with two other models. The first one (referred to as model M1) is a simple model where LAR expressed in thermal time unit is constant. The second one (referred to as model M2) is the LAR model used in the wheat model Sirius (Jamieson *et al.*, 2008) and described in detail by He *et al.* (2012). In model M2, leaf production follows a segmented linear model in thermal time. The first three leaves appear more rapidly than the next five, and LAR slows for the subsequent leaves independently of the total number of leaves produced. As a surrogate for the apex–air temperature correction for winter sowing (day of the year 1–90 for the Northern hemisphere), the phyllochron decreases linearly with the sowing date until reaching a minimum in mid-July for the Northern hemisphere (Jamieson *et al.*, 2008; He *et al.*, 2012). In the three LAR models, thermal time was calculated using Eqn 1 with the apex temperature assumed to be similar to soil temperature near its surface until Haun stage 4 and thereafter similar to the canopy temperature (Jamieson *et al.*, 1995). Soil and canopy temperatures were calculated from air temperature and the energy balances of soil surface and canopy, respectively (Jamieson *et al.*, 1995; Martre, 2013).

Field experiments for model evaluation

Predictions from the three LAR models were compared against two field experiments with several sowing dates. The first one was the Hot Serial

Cereal (HSC) experiment conducted in Maricopa (33°4'N, 111°58'W, 358 m elevation), AZ, USA, where the spring wheat cultivar Yecora Rojo was sown about every 6 weeks for 2 years (Wall *et al.*, 2011; White *et al.*, 2012). The data of the HSC experiment were obtained from Kimball *et al.* (2018). This experiment provides a very large range of temperature (average temperature between crop emergence and appearance of the flag-leaf = 9.6–22.3 °C) and photoperiod (10.1–13.9 h), with mean daily PTQ ranging from 1.2–3.8 mol m^{-2} $°Cd^{-1}$. Only one year (height sowings) was used here as the results were very similar for the two years. The two summer sowings were not used as the crops died before they reached the flag-leaf ligule stage.

The second experiment (hereafter referred to as NZ2020) was conducted over three consecutive winter growing seasons (2013–2014 to 2015–2016) in Canterbury, New Zealand, near Leeston (43°45'S, 172°15'E, 18 m elevation). Each year, the winter wheat cultivar Wakanui was sown at a density of 150 seeds m^{-2} at three (2013) or four dates (2014 and 2015) between late-February and late-April. Fertilizer, irrigation, insecticide, herbicide, and growth regulators were applied based on local practices. Four plots (replicates) were considered per treatment. Air temperature and relative humidity were recorded in a ventilated screen at 1.6 m height with a Campbell Scientific CS500 temperature and relative humidity probe. Solar radiation was measured in the field in 2013 and 2014 and correlated very closely with solar radiation measured at an automated weather station located at 65 km from the experimental site, so daily solar radiation data from the latter station were used for subsequent years. Following emergence, five plants were marked per plot and the number of ligules that appeared were recorded at 7–14 d intervals until flag-leaf ligule appearance. Plants produced 13–18 main-stem leaves and had a protracted tillering phase, so markers were moved up the stem to a recorded position following each measurement to keep an accurate record of the number of leaves that appeared.

Estimation of LAR model parameters

LAR for models M1 and M2, and LAR_{min} for model M3 were estimated using the January 2009 sowing for the HSC experiment (Supplementary Fig. S1) and the second sowing date in 2014 and 2015 for the NZ200 experiment (Supplementary Fig. S2). In model M3, LAR_{min} and PTQ_{hf} were estimated using Eqn 3 (below) and the data we obtained from our experiments (see Results). α was estimated using the January 2009 sowing of the HSC experiment and the same value was used for both field experiments (Supplementary Table S2). The values of all parameters for the three models are given in Supplementary Table S2. Parameter values were estimated by minimizing the relative root-mean-squared relative error (RMSRE; see Supplementary Methods) for Haun stage >1.0 using a covariance matrix adaptation–evolutionary strategy (Hansen and Ostermeier, 2001) implemented in the *SiriusQuality* software.

Data analysis and statistics

All data analyses and graphs were performed using the R statistical software version 3.4.1 (www.r-project.org). Differences in LAR_i between treatments and genotypes were determined using ANOVA. Genetic differences in the intercept and slope of the linear relationship between LAR_i and PTQ were analysed by reduced major-axis regression with the R package *smatr3* (Warton *et al.*, 2012). All statistical differences were judged at $P < 0.05$.

Depending on the range of PTQ, data for LAR_i versus PTQ were fitted using either a linear equation or a three-parameter asymptotic equation given as:

$$LAR_i = LAR_{min} + \frac{(LAR_{max} - LAR_{min}) \times PTQ}{PTQ_{hf} + PTQ} \quad (3)$$

where, LAR_{min} (leaves $°Cd^{-1}$) is the minimum LAR when PTQ equals zero, LAR_{max} (leaves $°Cd^{-1}$) is the maximum LAR when PTQ tends to infinite, and PTQ_{hf} (mol PAR m^{-2} $°Cd^{-1}$) is the PTQ at which LAR is half LAR_{max} + LAR_{min}.

Several statistics were calculated to assess the quality of the LAR models in the wheat model *SiriusQuality* (Supplementary Methods). Measured and simulated Haun stages were compared using the mean-squared error (MSE) and the root-mean-squared relative error (RMSRE). To get a better understanding of the model errors, the MSE was separated in non-unity slope (NU), squared bias (SB), and lack of correlation (LC; (Gauch *et al.*, 2003). To assess the model skill, we calculated the Nash–Sutcliffe modeling efficiency (EF; (Nash and Sutcliffe, 1970). To avoid confounding effects of leaf development and growth and auto-correlation in the data, MSE was calculated using the observed Haun stage value closest to 5 in all treatments. RMSRE was calculated to compare the models at different leaf stages, using all observed Haun stages >1.0.

Results

Leaf appearance rate depends on temperature, irradiance, photoperiod, and leaf stage

The dynamics of leaf appearance was first analysed for three contrasting cultivars (Fig. 1), Paragon (a photoperiod-insensitive spring wheat), Récital (a photoperiod-insensitive winter wheat), and Renan (a photoperiod-sensitive winter wheat), grown in four treatments with stable environmental conditions differing in temperature, photoperiod, and light intensity (Experiment 1; Table 1) in such a way that we could compare treatments differing in temperature only (LT.LD.280 versus HT.LD.280), irradiance only (HT.LD.280 versus HT.LD.170), or both irradiance and photoperiod but with a similar daily irradiance (HT.SD.170 versus HT.LD.170).

The initial leaf appearance rate (LAR_i, calculated for leaves 1–5) differed significantly between treatments for the three cultivars (Fig. 1, Supplementary Table S3), although they had a similar response of LAR_i to the treatments (i.e. there were no significant treatment × cultivar interactions). The highest values of LAR_i were observed for the treatments with longer photoperiods and higher irradiance (LT.LD.280, HT.LD.280). For plants grown at high temperature, decreasing either the photoperiod (HT.SD.320) or the irradiance (HT.LD.280) decreased LAR_i (Fig. 1). Remarkably, changing both photoperiod and light intensity for a similar daily radiation and PTQ resulted in similar values of LAR (HT.SD.320 versus HT.LD.170).

In treatment LT.LD.280 (which showed the highest LAR_i), LAR decreased with plant age for the three cultivars (insets in Fig. 1), including the winter cultivars (Fig. 1B, C), which stayed in the vegetative stage during the whole experiment. Therefore, the decrease of LAR with plant age in this treatment was related neither to floral transition nor to the development and formation of the spike. In the other treatments, LAR was either stable (for Paragon), increased (for Récital), or decreased (for Renan) with plant age. Overall, the LAR of all cultivar/treatment combinations converged towards the same value as the plants aged.

Changes in leaf appearance rate with environmental conditions is a dynamic process

We analysed the dynamic changes in LAR with changes in irradiance. Plants from the two high-temperature plus long-photoperiod treatments were swapped between irradiance conditions at 270 °Cd after ligulation of leaf 1 (treatments

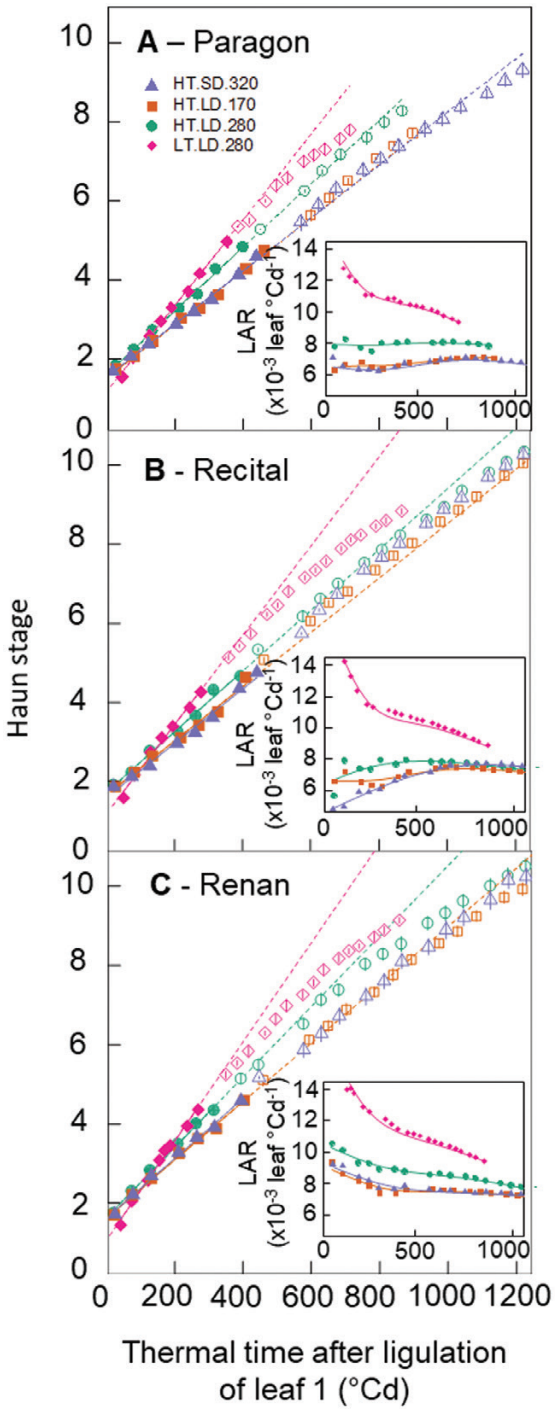

Fig. 1. Relationships between Haun stage and thermal time after ligulation of leaf 1 for three wheat cultivars grown in controlled conditions with different temperatures, irradiances, and photoperiods. The photoperiod-insensitive spring wheat cultivar Paragon (A), the photoperiod-insensitive winter wheat cultivar Récital (B), and the photoperiod-sensitive winter wheat cultivar Renan (B) where grown in growth chambers with day/night conditions of air temperature 28/24 °C (high temperature, HT) or 18/14 °C (low temperature, LT), photoperiod 8 h (short days, SD) or 16 h (long days, LD), and PAR 170 µmol m^{-2} s^{-1} (170), 280 µmol m^{-2} s^{-1} (280), or 320 µmol m^{-2} s^{-1} 320). Treatments are detailed in Table 1. Lines are linear regressions calculated for Haun stage 1.5–5 (closed symbols; data for Huan stage >5 are shown as open symbols). The insets show the leaf appearance rate (LAR) versus thermal time after ligulation of leaf 1 and the lines are non-parametric spline curves fitted to the data. Thermal time was calculated using the apex temperature and Eqn 1. Data are means (±1SD) for *n*=6 independent replicates.

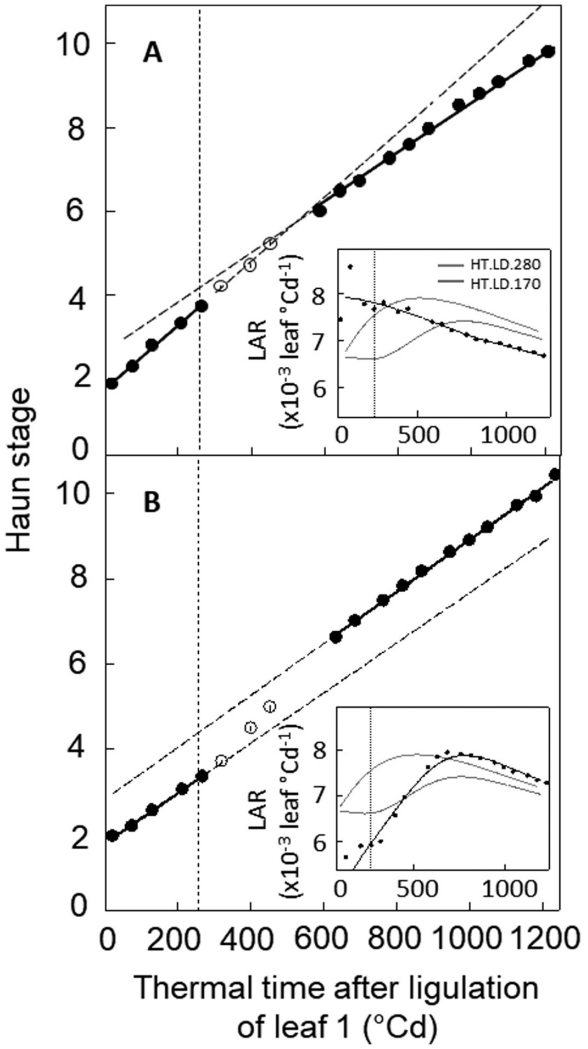

Fig. 2. Relationships between Haun stage and thermal time after ligulation of leaf 1 for the photoperiod-insensitive winter wheat cultivar Récital grown in controlled conditions with different irradiance. The plants were grown from planting to 270 °Cd after ligulation of leaf 1 at 28/24 °C day/night air temperature and with a 16-h photoperiod and either (A) 280 µmol m^{-2} s^{-1} or (B) 170 µmol m^{-2} s^{-1} PAR (see Table 1). At 270 °Cd after ligulation of leaf 1, plants were transferred from low to high PAR (170→280) (A) or from high to low PAR (280→170) (B). Solid symbols are the data used to fit linear regressions before and after the change in irradiance. The insets show leaf appearance rate (LAR) versus thermal time after ligulation of leaf 1. Lines are non-parametric spline curves fitted to the data. Curves for treatments HT.LD.280 (green) and HT.LD.170 (pink) are from Fig. 1 and are shown for comparison. Thermal time was calculated using the apex temperature and Eqn 1. Data are means (±1SD) for *n*=6 independent replicates.

280→170 and 280→170). The environmental conditions before and after the irradiance swap were similar to treatments HT.LD.170 and HT.LD.280 in Fig. 1, in order to compare LARs at similar thermal time and to avoid confounding effects of plant age. Moreover, the winter wheat cultivar Récital was used to avoid confounding effects due to floral transition or spike development because it stayed in the vegetative stage during the whole experiment. The LAR of plants transferred from 280 µmol m^{-2} s^{-1} to 170 µmol m^{-2} s^{-1} PAR started to decrease about 250 °Cd (i.e. ~1.3 phyllochrons) after transfer to low irradiance, and the mean LAR after the transfer was

23% lower than before (Fig. 2A). The opposite behavior was observed when plants were transferred from 170 µmol m^{-2} s^{-1} to 280 µmol m^{-2} s^{-1} PAR, but LAR responded more rapidly to the change in irradiance (Fig. 2B). LAR increased within less than 140 °Cd (i.e. ~0.8 phyllochrons) after the transfer and the mean LAR was 12% higher than before.

Leaf appearance rate is correlated with photothermal quotient, net daily photosynthesis, and carbohydrate turnover during the night

LAR was modified by temperature (even when expressed per unit thermal time), photoperiod, and instantaneous irradiance. To test whether these effects could be accounted for by the mean radiation per thermal-time unit, we calculated the photothermal quotient (PTQ) for all treatments in the three experiments, under ambient air CO_2 concentration. The variation of LAR_i for cv. Paragon in Experiment 1 was well explained by a unique linear relationship linking LAR_i to PTQ independently of the cause of variation of PTQ (r^2=0.965, P=0.018; Fig. 3A). A similar correlation was found between LAR_i and either daily net photosynthesis (r=0.982, P=0.0179; Fig. 3B) or carbohydrate consumption during the night (r=0.985, P=0.0147; Fig. 3C), supporting the hypothesis that LAR is at least partly limited by carbon availability in the plant.

The highest PTQ value tested in our experiments was 1.5 mol m^{-2} °Cd^{-1}, while the range of PTQ sensed by plants in field conditions reached up to 4 mol m^{-2} °Cd^{-1} in our database of wheat field trials. The relationship between LAR and PTQ was therefore further tested on a larger range of PTQ values using data from the literature where the response of LAR to either temperature (Cao and Moss, 1989*b*, 1989*c*; Bos and Neuteboom, 1998), photoperiod (Cao and Moss, 1989*a*, 1989*c*), or irradiance (Rickman *et al.*, 1985; Bos and Neuteboom, 1998) was studied for plants grown in growth chambers or greenhouses (Supplementary Table S4). These data provide a very large range of variation of PTQ (up to 15 mol m^{-2} °Cd^{-1}) and when our data and those from the literature were considered together the relationship between LAR and PTQ was described well by Eqn 3 (Fig. 4, Supplementary Table S5).

Elevated CO_2 increases leaf appearance rate at high temperatures

In order to strengthen our hypothesis of carbon limitation for LAR, we tested the effect of elevated air CO_2 concentration on LAR_i (Experiment 2, Table 1). Plants of cv Paragon were grown under two temperature regimes (18/14 °C and 28/24 °C, day/night) and two atmospheric CO_2 concentrations (400 ppm and 800 ppm). At 18/14 °C, photosynthesis under saturating light was not significantly different (P=0.064) between the two CO_2 treatments (Fig. 5A), while at 28/24 °C it was 33.7% higher under elevated CO_2 compared with ambient CO_2 (P=7.3×10^{-4}). Similarly, LAR_i was not significantly different between the CO_2 treatments at 18/14 °C (P=0.019) but was 29.6% lower at 400 ppm than 800 ppm CO_2 at 28/24 °C (P=1.54×10^{-3}; Fig. 5B).

Genetic variability of the response of leaf appearance rate to photothermal quotient

We assessed the genetic variability of the response of LAR_i to PTQ for 15 spring wheat cultivars grown under two temperature regimes (18/14 °C and 28/24 °C, day/night) and two photoperiod treatments (8 h or 16 h) in factorial combination (Experiment 3, Table 1). The effect of PTQ on LAR_i was highly significant, while the effect of cultivar and the interaction between PTQ and cultivar were not significant (Fig. 6; Supplementary Table S6). The response of LAR_i to PTQ was analysed by linear regression (Supplementary Table S7). The slope of the LAR_i–PTQ relationship was not significantly different among cultivars (P=0.77) and was on average 7.83 leaves m^2 mol^{-1} PAR (95% confidence interval [CI] 6.90–8.90).

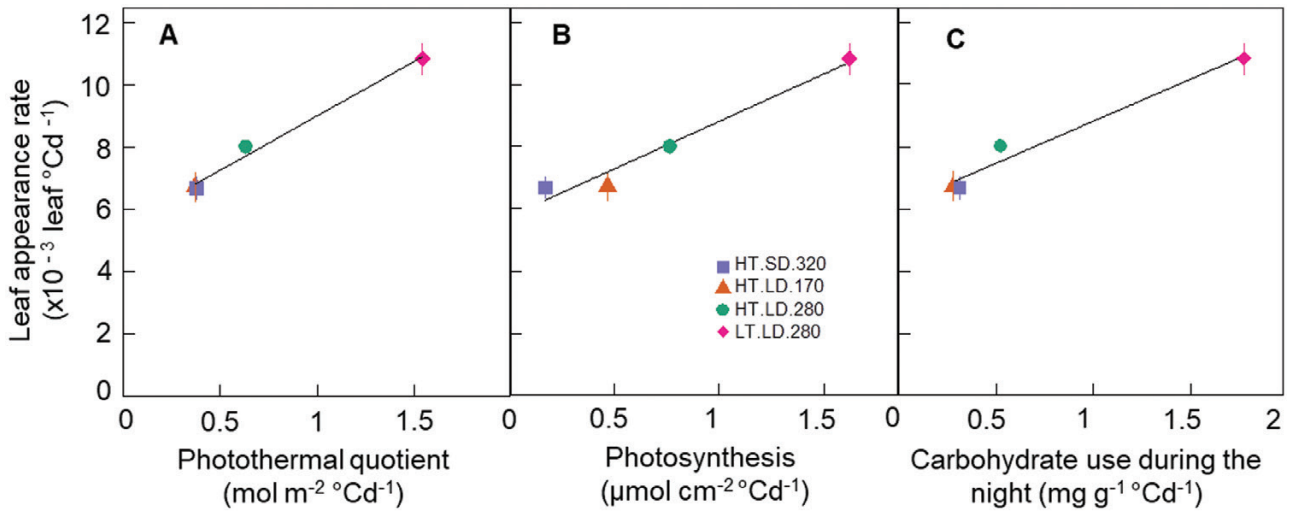

Fig. 3. Relationships between initial leaf appearance rate (calculated for Haun stage ≤5) and photothermal quotient (A), net photosynthesis (B), and carbohydrate use during the night (C) for the photoperiod-insensitive spring wheat cv. Paragon grown in controlled conditions with different combinations of temperature, irradiance, and photoperiod (see Table 1). Thermal time was calculated using the apex temperature and Eqn 1. Treatments are as in Fig. 1. Data are means (±1SD) for n=6 independent replicates.

However, the intercept of the relationship was significantly different among cultivars ($P = 0.02$) and ranged from 2.74×10^{-3} leaves °Cd^{-1} (CI 0.02–5.47) for cv. Feeling to 4.69×10^{-3} leaves °Cd^{-1} (CI 1.98–7.40) for cv. Cadenza.

A model of carbon limitation of leaf appearance rate

We showed that differences in LAR_i due to temperature, light intensity, and photoperiod can be explained by a unique curvilinear relationship between LAR and PTQ (Fig. 4). PTQ reflects the balance between the incident irradiance available for growth and the potential growth of sinks driven by temperature. The demand for carbon for respiration scales with plant size and can be approximated by the green area index [GAI, m (leaf) m^{-2} (ground)]. The demand for carbohydrates for leaf growth increases between leaf 3 and terminal spikelet because of the regular formation and development of axillary tillers and associated roots (Kirby *et al.*, 1985; Abichou *et al.*, 2018). After terminal spikelet, growing leaves also compete for carbohydrates with fast-growing internodes and spikes. These changes in the source–sink balance during the plant growth cycle are at least partially compensated for by the increase in leaf area index. The decrease in LAR with ontogeny observed in our experiments (Fig. 1), as well as in many other studies (see Introduction), may reflect the decrease of the source–sink ratio with ontogeny.

We propose a simple model of LAR that summarizes the results above, in which (1) LAR depends on the supply-to-demand ratio for soluble carbohydrate, estimated by the ratio of intercepted light to thermal time; (2) the demand for soluble carbohydrate is proportional to plant size and this proportionality can be approximated by the green area index; (3) soluble carbohydrates in the plant provide a buffering capacity to fluctuating environments in the field; and (4) leaves are able to maintain a minimum rate of development. The model is given as:

$$LAR = \frac{LAR_{min} + \left(\frac{[LAR_{max} - LAR_{min}] \times [\overline{I_{int}}(d)/\overline{T_t}(d)]}{PTQ_{hf} + [\overline{I_{int}}(d)/\overline{T_t}(d)]} \right)}{S_{C/GAI} \times GAI_{eff}(d)} \quad (4)$$

where, $\overline{I_{int}}(d)$[MJ PAR m^{-2} (ground)] is the cumulative PAR intercepted by the canopy during the period d, $\overline{T_t}(d)$ (°Cd) is the thermal time accumulated during the period d, $\overline{GAI}_{eff}(d)$ [m (leaf) m^{-2} (ground)] is the mean green area fraction over

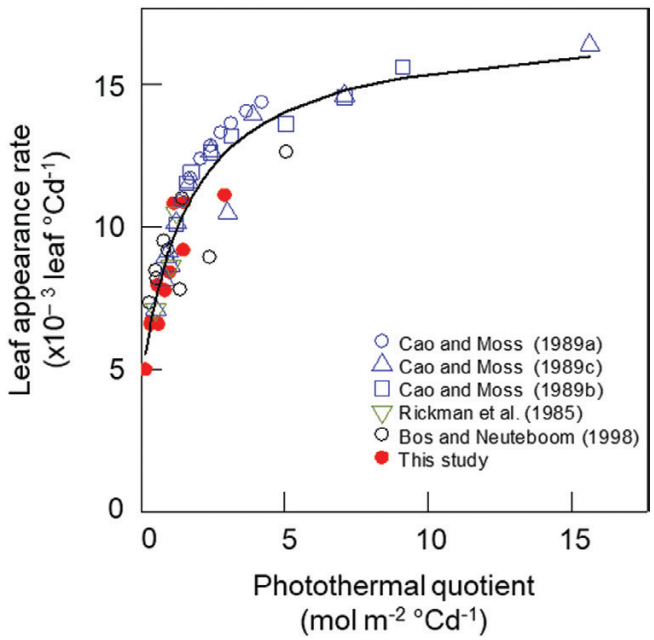

Fig. 4. Relationships between leaf appearance rate and photothermal quotient for several wheat cultivars grown in controlled conditions with different combinations of temperature, irradiance, and photoperiod. Closed symbols are all treatments from Experiments 1–3 at ambient air CO_2 concentration (Table 1). Open symbols are data from the literature (Supplementary Table S4). The curve is Eqn 3 fitted to all data points LAR= 0.004996[±0.000731]+{(0.002364[±0.0007]–0.04996[±0.000731])×PTQ}/ (1.9807[±0.5803]+PTQ).

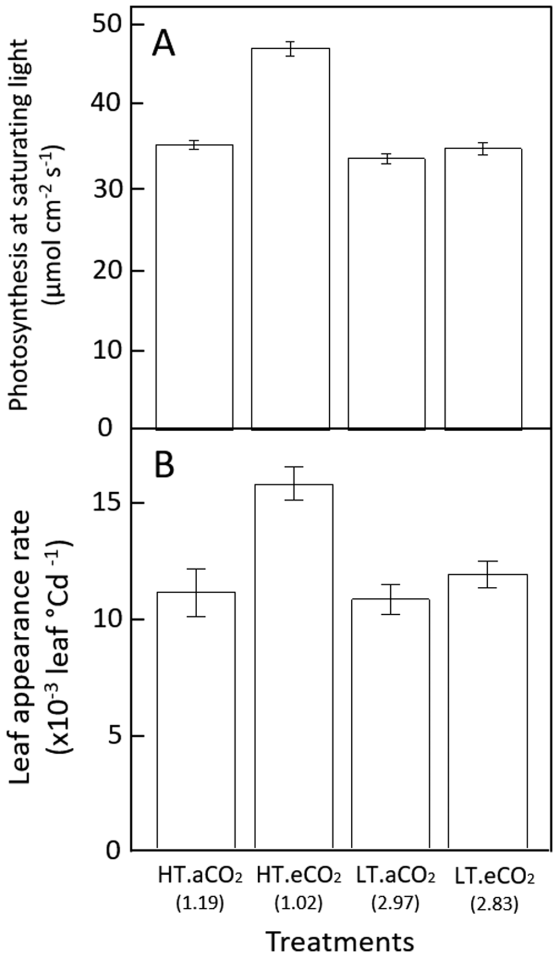

Fig. 5. (A) Photosynthesis at saturating light and (B) initial leaf appearance rate (calculated for Haun stage ≤5) for the photoperiod-insensitive spring wheat cultivar Paragon grown in controlled environments with day/night conditions of air temperature of 18/14 °C (low temperature, LT) or 28/24 °C (high temperature, HT) and air CO_2 concentration of 400 ppm (ambient, aCO_2) or 800 ppm (elevated, eCO_2). The value of the photothermal quotient (mol m^{-2} °Cd^{-1}) is indicated below the treatment names. Details of the cultivars are given in Supplementary Table S1. Data are means (±1SD) for n=5 (A) or n=3 (B) independent replicates.

the period d, d (°Cd) is the thermal time over which intercepted irradiance and thermal time are integrated, and $S_{C/GAI}$ [m^2 (ground) m^{-2} (leaf)] is an empirical parameter that scales carbon demand to GAI. In Eqn 4, LAR tends to infinite when GAI tends to 0. Therefore, a minimum value of $\overline{GAI}_{eff}$ was considered as the potential GAI when Haun stage = 3.5, just after the first tiller appears on the main stem. $\overline{GAI}_{eff}$ is given as:

$$\overline{GAI}_{eff}(d) = \begin{cases} LN_{eff} \times A^{pot}_{L_{juv}} \times PD, & LN < LN_{eff} \\ \overline{GAI}_{max}(d), & LN \geq LN_{ef,f} \end{cases} \quad (5)$$

where A^{pot}_{juv} (cm^2) is the potential surface area of juvenile leaves, as defined in the *SiriusQuality* leaf growth model (Martre and Dambreville, 2018), PD (plants m^{-2}) is the plant density, LN (leaves main $stem^{-1}$) is the number of emerged leaves on the main stem, LN_{eff} (leaves) is the number of main stem leaves above which the demand for respiration increases relative to sink formation, and $\overline{GAI}_{max}(d)$ is the maximum green area index fraction averaged over the period d, starting from emergence. The maximum value of $\overline{GAI}(d)$ is taken so that $\overline{GAI}_{eff}$ does not decrease if the rate of senescence of the oldest leaves is higher than the expansion of the growing leaves.

In Eqn 4, environmental variables are averaged over several days to account for the buffering effect of stored soluble carbohydrates. The parameter d was set equal to 70 °Cd (Rickman *et al.*, 1985; Lattanzi *et al.*, 2005). The fraction of light intercepted by the crop during the period d is calculated from its exponential relationship with GAI (Monsi and Saeki, 2005).

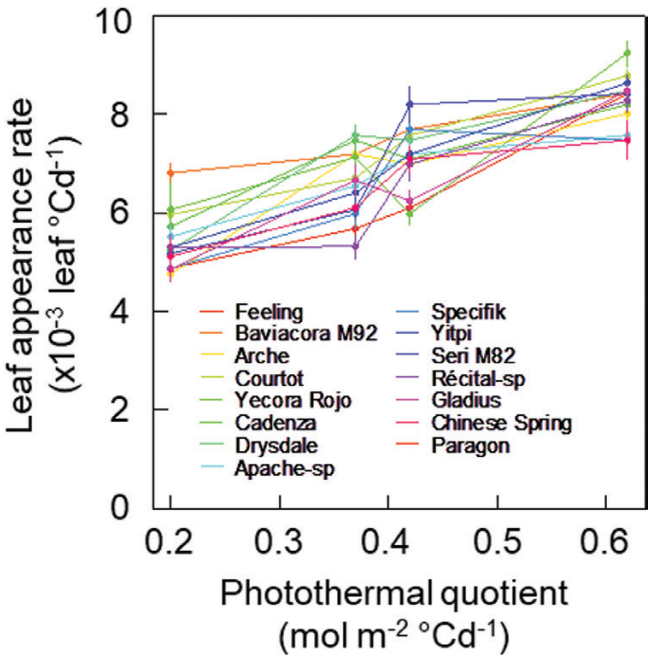

Fig. 6. Relationships between initial leaf appearance rate (calculated for Haun stage ≤5) and photothermal quotient for 15 spring wheat cultivars grown in controlled conditions with different combinations of temperature and photoperiod (Table 1, Experiment 3). Details of the cultivars are given in Supplementary Table S1. Data are means (±1SD) for n=4 independent replicates.

Prediction of leaf stage and leaf appearance rate for different sowing dates in the field

The three LAR models (M1, M2, and M3) were evaluated against two field experiments conducted in contrasting environments (HSC and NZ2020). In both experiments, LAR_i varied significantly with sowing dates. In the HSC experiment, LAR_i was constant and maximum for winter and spring sowings (between January and March, averaging 11.86×10^{-3} leaves $°Cd^{-1}$) and decreased by 27% for the late-autumn sowing. In the NZ2020 experiment, crops were sown between late-summer and mid-autumn and LAR_i was constant and maximum for the first three sowings (averaging 10.45×10^{-3} leaves $°Cd^{-1}$) but decreased on average by 25% for the latest sowing. The final number of leaves on the main stem was very different for the two experiments: 7.0–9.3 leaves main $stem^{-1}$ for HSC and 17.7–12.8 leaves main $stem^{-1}$ for NZ2020.

In the HSC experiment, the error (MSE) of M3 for thermal time to Haun stage 5 was only 82% and 67% of that of M1 and M2, respectively (Fig. 7A). Lack of correlation (LC)

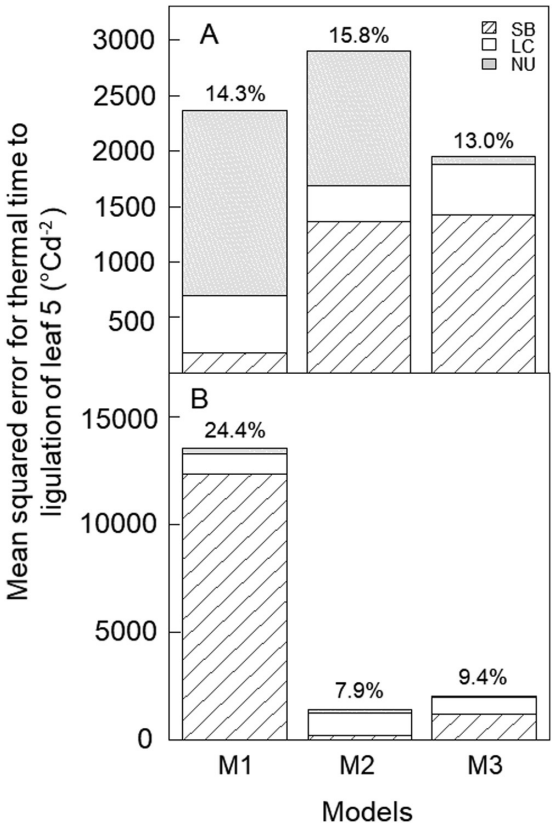

Fig. 7. Mean-squared error (MSE) for thermal time to ligulation of leaf 5 (Haun stage 5) estimated using three alternative models of leaf appearance rate for (A) the photoperiod-insensitive spring wheat cultivar Yecora Rojo sown every ~6 weeks between March 2007 and January 2009 in the field at Maricopa, USA (HSC experiment), and (B) for the winter wheat cultivar Wakanui sown in the field in late-February, March, and April for three consecutive years at Leeston, New Zeland (NZ2020 experiment). MSE was decomposed in squared bias (SB), lack of correlation (LC), and non-unity slope (NU). MSE was calculated for the observed Haun stage closest to 5 to avoid confounding effects between leaf development and growth and autocorrelation in the data. Model M1, constant LAR; model M2, Sirius LAR model; model M3, LAR model developed in this study (see Methods).

contributed to 73% of the total error of M3, while the error of M1 was dominated by non-unity slope (NU) and that of M2 by squared bias (SB) and NU. In the NZ2020 experiment, the error for thermal time to Haun stage 5 was 85% lower for M3 than for M1 but was 41% higher for M3 than for M2 (Fig. 7). Squared bias and LC contributed nearly two-thirds and one-third of the total error of M3, respectively. Therefore, M3 had a much lower error than M1 for both data sets and outperformed M2 in Arizona, but in New Zealand both models had comparable and small errors (RMSRE<9.5%).

In the HSC experiment, M3, which is based on biological hypotheses, provided a good simulation of the dynamics of leaf appearance and the observed changes of LAR with sowing date and plant ontogeny (Fig. 8). Compared with M1 and M2, the relative error (RMSRE) for Haun stage was reduced by 17% and 22%, respectively (Supplementary Table S8). M3 also simulated the dynamics of leaf appearance in the NZ2020 experiment reasonably well (Fig. 9) but the relative error for Haun stage was 10% higher for M3 than for M2 (Supplementary Table S8). Combining the two experiments, the overall RMSRE for Haun stage was 46% and 13% lower for M3 than for M1 and M2, respectively.

Discussion

In this study, we investigated the effects of temperature, photoperiod, irradiance, CO_2 concentration, and cultivars on wheat LAR. We showed that initial LAR (LAR_i) changed significantly with all the factors studied excluding genotype (Figs 1, 5). We also showed that the response of LAR_i to environmental factors could be accounted for by the photothermal quotient (PTQ)(Fig. 4). LAR_i was also correlated with net photosynthesis and carbohydrate use at night (Fig. 3). Our results thus supported our hypothesis that LAR in wheat is carbon-limited. Based on our results, we developed and evaluated under field conditions a new model of LAR (Eqn 4) that accounts for both environmental and ontogenic changes in LAR (Figs 8, 9). The simulation results supported the modelling hypothesis that changes of LAR with ontogeny are due to changes in the carbon supply–demand ratio.

Leaf appearance rate in wheat is carbon-driven

Relationships between temperature, irradiance, photoperiod, and LAR have been observed in a range of plant species, including cereals such as maize (Birch *et al.*, 1998), rice (Yin and Kropff, 1996), wheat and barley (Cao and Moss, 1989*c*; Volk and Bugbee, 1991; Bos and Neuteboom, 1998), and dicots such as quinoa (Bertero, 2001), lucerne (alfalfa, Brown *et al.*, 2005; Teixeira *et al.*, 2011), and lettuce (Kitaya *et al.*, 1998). However, no physiological explanation for the observed variations of LAR in relation to environmental factors has yet been proposed. Here, we found a unique relationship between LAR and PTQ for a large range of environmental conditions (Fig. 4). The fact that the photoperiod effect could be accounted for by a unique source–sink relationship for both photoperiod-insensitive and -sensitive spring and winter wheat cultivars was not expected. The treatments in our experiments allowed us to disentangle the effect of photoperiod *per se* and irradiance, and the results strongly suggested that the effect of photoperiod on LAR was mainly due to the increase of daily irradiance with longer photoperiods. An additional effect of photoperiod *per se* is not incompatible with our results, but this effect would be smaller compared to the effect of irradiance and would bring

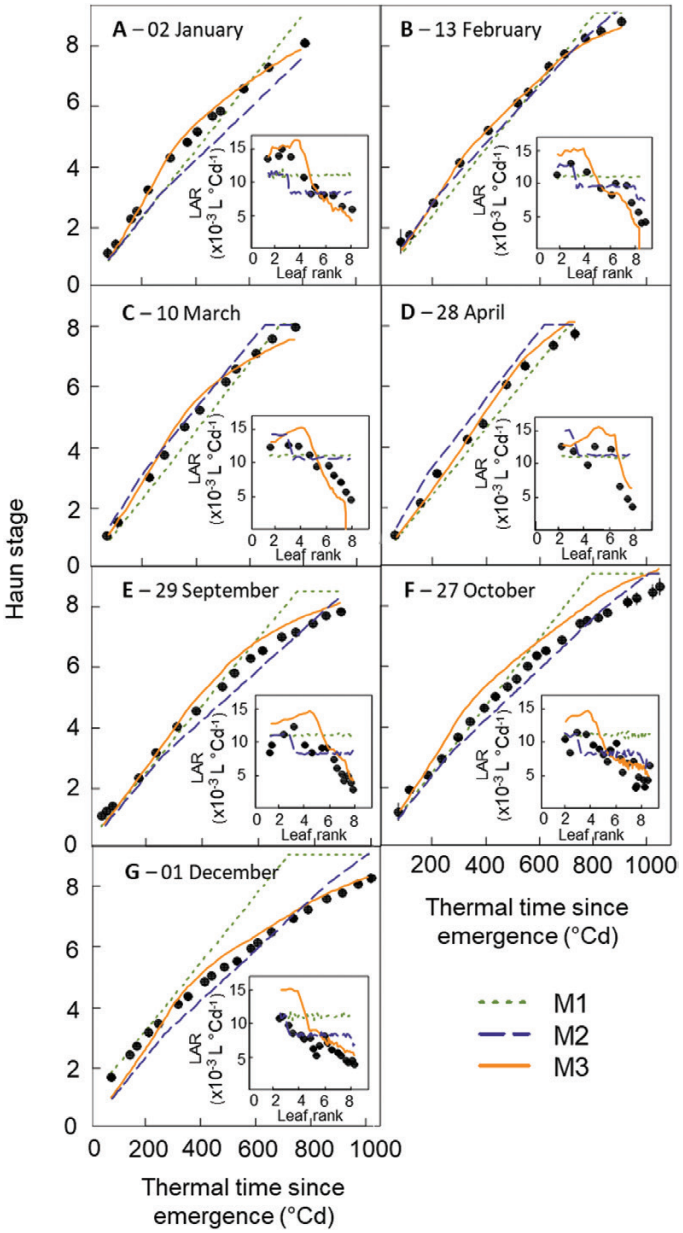

Fig. 8. Relationships between observed (circles) and simulated (lines) Haun stage and thermal time after emergence for the spring wheat cultivar Yecora Rojo grown in field at Maricopa, Arizona, US (HSC experiment). Crops were sown every ~6 weeks between early January and early December 2008, as indicated in the figure. Lines are simulations obtained with the wheat model *SiriusQuality* and using either a constant phyllochron (model M1, dotted green lines), a segmented linear model in thermal time corrected for the sowing date (model M2, dashed blue lines), or Eqn 4 (model M3, solid orange lines). The insets show observed (circles) and simulated (lines) leaf appearance rate (LAR) versus leaf rank. Thermal time was calculated using the apex temperature and Eqn 1 for the observed data and canopy temperature for the simulated data (see Methods). Data are means ±1SD) for *n*=3 independent replicates.

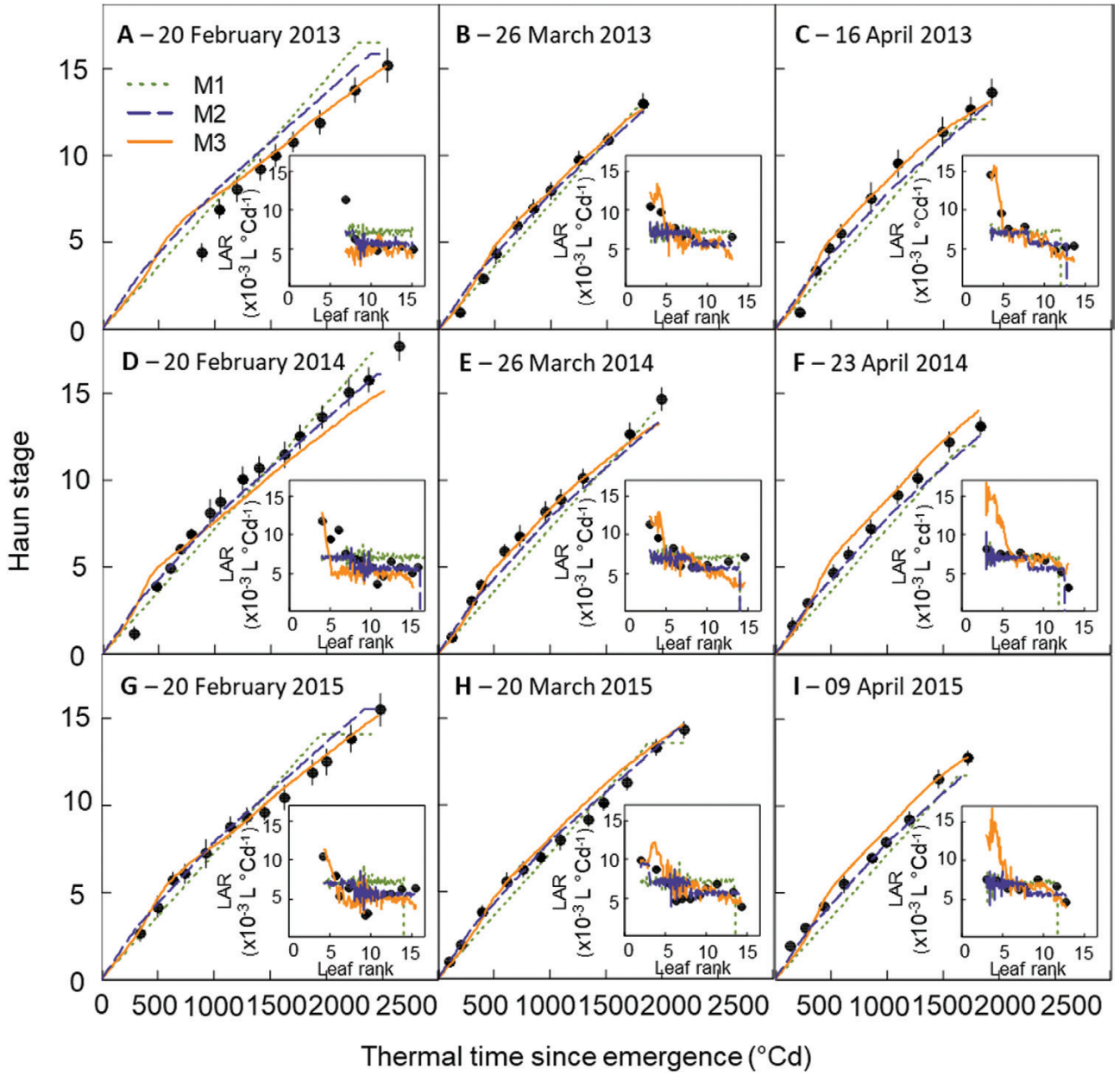

Fig. 9. Relationships between observed (circles) and simulated (lines) Haun stage and thermal time after emergence for the spring wheat cultivar Wakanui grown in field at Leeston, New Zeland (NZ2020 experiment). Crops were sown from 2013 to 2015 in late-February, March, and April. Lines are simulations obtained with the wheat model *SiriusQuality* and using either a constant phyllochron (model M1, dotted green lines), a segmented linear model in thermal time corrected for the sowing date (model M2, dashed blue lines), or Eqn 4 (model M3, solid orange lines). The insets show observed (circles) and simulated (lines) leaf appearance rate (LAR) versus leaf rank. Thermal time was calculated using the canopy temperature and Eqn 1 for the observed data and canopy temperature for the simulated data (see Methods). Data are means (±1SD) for n=4 independent replicates.

its own physiological determinisms and genetic variability. The correlation between LAR and net daily photosynthesis and carbon use during the night (Fig. 3), as well as the increase of LAR at elevated CO_2 (Fig. 5), also supported the hypothesis that LAR in wheat is carbon-limited. In good agreement with our results, (McMaster *et al.* (1999) found that wheat plants grown under elevated CO_2 (725 ppm) had values of LAR that were 10–15% higher than under ambient CO_2 (360 ppm), and leaf photosynthesis and carbohydrate concentration were positively correlated with LAR.

Leaf appearance rate results from three processes: (1) cell division in the apical meristem of the expanding leaf primordium; (2) cell division of the intercalary meristem of the expanding leaf primordium; and (3) expansion of cells derived from the meristem in the leaf lamina and sheath. Christ and Körner (1995) showed that step-changes in CO_2 concentration, and thus in carbon supply, have no effect on leaf elongation rate. This was most likely due to the fact that, in contrast to our current study, the leaves measured were initiated several plastochrons before the air CO_2 concentration was increased. The effect of CO_2 on wheat leaf growth acts mainly through an increased number of dividing cells at the base of expanding leaves, which is determined in the apical meristem before leaf appearance (Masle, 2000). The lack of correlation between soluble carbohydrate concentration

in the elongation zone and leaf expansion rate after their emergence suggests that after leaves have emerged above the whorl of subtending leaves, their elongation rate is not limited by carbon availability (Kemp and Blacklow, 1980). This also agrees with studies showing that the control of leaf growth switches from a metabolic limitation to hydraulic and mechanical control during the course of leaf ontogeny (Pantin *et al.*, 2011).

Changes of LAR with plant age reflect changes in the source–sink relationship

LAR decreases with plant age both in controlled conditions and in the field for wheat (Calderini *et al.*, 1996; Slafer and Rawson, 1997; Streck *et al.*, 2003; Ochagavía *et al.*, 2017) and also for other grass species such as sugarcane (Inman-Bamber, 1994) and tall fescue (Skinner and Nelson, 1995). But to date it has only been included in crop growth models through an empirical effect of leaf rank on LAR (Jamieson *et al.*, 1995) or through an effect of the distance from the meristem to the whorl (Streck *et al.*, 2003). In our results, the decrease of LAR with plant age depended on environmental conditions (Figs 1, 2), which was incompatible with a unique relationship linking LAR and Haun Stage (Streck *et al.*, 2003).

As LAR depends on plant carbon availability, it is tempting to hypothesize that the decrease of LAR with plant age is associated with changes in plant source–sink balance and with a lower availability of carbon. As the wheat plant develops, the formation and development of new tillers increases the demand for carbon, and after the terminal spikelet stage expanding leaves also compete for carbon with the growing internodes and spikes. In tall fescue, LAR decreases rapidly after the appearance of leaf 7, and this can be suppressed if new tillers are trimmed (Skinner and Nelson, 1995). In that study, the decrease in LAR with leaf number was due both to an increase of the duration of the leaf elongation through the whorl of subtending leaves and to a decrease of the interval between the initiation of successive leaves, and both may be due to the slowing down of leaf elongation rate (Skinner and Nelson, 1995). Slafer and Rawson (1997) reported that LAR after leaf 6 is more sensitive to photoperiod than that of leaves appearing before. This is in good agreement with a carbon-limitation of LAR, and the results of (Skinner and Nelson, 1995) in tall fescue.

Consideration of the carbon-limitation of leaf appearance improves the prediction of leaf stages in the field

Many crop growth models calculate leaf appearance assuming a constant LAR and do not consider the effects of photoperiod, light intensity, or plant age. Where there have been attempts to model the response of LAR to photoperiod, these have been empirical models (Jamieson *et al.*, 2008; Abichou *et al.*, 2018; Brown *et al.*, 2018) and they are probably limited in the range of environmental conditions in which they can be used. Moreover, these models have a large number of parameters. Here, we present an ecophysiological model (Eqn 4) that can easily be integrated into crop growth models and has 40% fewer parameters than the Sirius LAR model. Our model was able to simulate the changes in LAR with both sowing date and plant age in two contrasting environments.

Several crop growth models do not use leaf stages and leaf number to simulate heading or anthesis date, but instead use a more empirical approach based on the thermal-time requirement between phenological phases and modifications of thermal time by vernalization and photoperiod (e.g. Ritchie, 1991; Stöckle *et al.*, 2003; Brisson *et al.*, 2009). One of the reasons such phenology models are used in crop growth models is that the error in leaf-stage prediction with the leaf-number approach may lead to large errors in the prediction of anthesis date. Although these two types of approaches may provide very similar results (Jamieson *et al.*, 2007), models based on leaf number allow for separation of the effect of temperature on development and vernalization (Allard *et al.*, 2012) and better represent biological processes, and thus can more directly be related to physiological processes or even genes, for instance those controlling flowering time (Brown *et al.*, 2013; Sanna *et al.*, 2014). A phenology model based on leaf number also allows the linking of phenology with leaf growth (Lawless *et al.*, 2005; Martre and Dambreville, 2018). The improvement of leaf-stage modeling provided by our model is thus an important step to improve models based on leaf number and to introduce more physiological insights into crop growth models.

Supplementary data

Supplementary data are available at *JXB* online.

Methods. Details of statistics used for model evaluation.

Table S1. Details of the cultivars used in this study.

Table S2. Non-varietal and varietal parameters of the Sirius phenology sub-model.

Table S3. ANOVA for the responses of LAR_i to PTQ and cultivar shown in Fig. 1.

Table S4. Environmental conditions and LAR_i taken from the literature and shown in Fig. 4.

Table S5. ANOVA for the responses of LAR_i to temperature, CO_2, and cultivar shown in Fig. 5.

Table S6. ANOVA for the responses of LAR_i to PTQ and cultivar shown in Fig. 6.

Table S7. Summary statistics of the linear regression analysis of LAR_i versus PTQ for 15 spring wheat cultivars.

Table S8. Model errors and skills for leaf stage.

Fig. S1. Relationship between observed and simulated Haun stage and thermal time since emergence for the HSC experiment.

Fig. S2. Relationship between observed and simulated Haun stage and thermal time since emergence for the NZ2020 experiment

Fig. S3. Net photosynthesis and carbohydrate concentration responses for the wheat cv Paragon grown under different conditions of temperature, irradiance, and photoperiod.

Acknowledgements

We thank Mr Stephane Berthézène for his technical help and Drs Jacques Le Gouis (INRA, GDEC, Clermont-Ferrand, France) and Matthew

Reynolds (CIMMYT, Mexico, D.F., Mexico) for providing seeds of several cultivars, and Ms Séverine Rougeol for developing the Apache and Récital spring isogenic lines. This work was funded by the French National Research Agency (ANR) through the ERANET + project MODCARBOSTRESS within the Joint Programming Initiative on Agriculture, Food Security and Climate Change (FACCE-JPI; grant agreement no. 618105).

References

Abichou M, Fournier C, Dornbusch T, Chambon C, de Solan B, Gouache D, Andrieu B. 2018. Parameterising wheat leaf and tiller dynamics for faithful reconstruction of wheat plants by structural plant models. Field Crops Research **218,** 213–230.

Allard V, Veisz O, Kõszegi B, Rousset M, Le Gouis J, Martre P. 2012. The quantitative response of wheat vernalization to environmental variables indicates that vernalization is not a response to cold temperature. Journal of Experimental Botany **63,** 847–857.

Amir J, Sinclair TR. 1991. A model of the temperature and solar-radiation effects on spring wheat growth and yield. Field Crops Research **28,** 47–58.

Baker CK, Gallagher JN, Monteith JL. 1980. Daylength change and leaf appearance in winter wheat. Plant, Cell & Environment **3,** 285–287.

Baker JT, Pinter PJ, Reginato RJ, Kanemasu ET. 1986. Effects of temperature on leaf appearance in spring and winter wheat cultivars. Agronomy Journal **78,** 605–613.

Bassu S, Asseng S, Motzo R, Giunta F. 2009. Optimising sowing date of durum wheat in a variable Mediterranean environment. Field Crops Research **111,** 109–118.

Bertero HD. 2001. Effects of photoperiod, temperature and radiation on the rate of leaf appearance in quinoa (*Chenopodium quinoa* Willd.) under field conditions. Annals of Botany **87,** 495–502.

Bindi M, Porter JR, Miglietta F. 1995. Comparison of models to simulate leaf appearance in wheat. European Journal of Agronomy **4,** 15–25.

Birch CJ, Vos J, Kiniry J, Bos HJ, Elings A. 1998. Phyllochron responds to acclimation to temperature and irradiance in maize. Field Crops Research **59,** 187–200.

Boone MYL, Rickman RW, Whisler FD. 1990. Leaf appearance rates of two winter wheat cultivars under high carbon dioxide conditions. Agronomy Journal **82,** 718–724.

Bos HJ, Neuteboom JH. 1998. Morphological analysis of leaf and tiller number dynamics of wheat (*Triticum aestivum* L.): responses to temperature and light intensity. Annals of Botany **81,** 131–139.

Brisson N, Launay M, Mary B, Beaudoin N (eds). 2009. Conceptual basis, formalisations and parameterization of the STICS crop model. Paris: Éditions Quae.

Brown H, Huth N, Holzworth D. 2018. Crop model improvement in APSIM: using wheat as a case study. European Journal of Agronomy **100,** 141–150.

Brown HE, Jamieson PD, Brooking IR, Moot DJ, Huth NI. 2013. Integration of molecular and physiological models to explain time of anthesis in wheat. Annals of Botany **112,** 1683–1703.

Brown HE, Moot DJ, Teixeira EI. 2005. The components of lucerne (*Medicago sativa*) leaf area index respond to temperature and photoperiod in a temperate environment. European Journal of Agronomy **23,** 348–358.

Calderini DF, Miralles DJ, Sadras VO. 1996. Appearance and growth of individual leaves as affected by semidwarfism in isogenic lines of wheat. Annals of Botany **77,** 583–589.

Cao W, Moss DN. 1989a. Daylength effect on leaf emergence and phyllochron in wheat and barley. Crop Science **29,** 1021–1025.

Cao W, Moss DN. 1989b. Temperature and daylength interaction on phyllochron in wheat and barley. Crop Science **29,** 1046–1048.

Cao W, Moss DN. 1989c. Temperature effect on leaf emergence and phyllochron in wheat and barley. Crop Science **29,** 1018–1021.

Cao W, Moss DN. 1991. Phyllochron change in winter wheat with planting date and environmental changes. Agronomy Journal **83,** 396–401.

Christ RA, Körner C. 1995. Responses of shoot and root gas exchange, leaf blade expansion and biomass production to pulses of elevated CO_2 in hydroponic wheat. Journal of Experimental Botany **46,** 1661–1667.

Davidson AM, Da Silva D, Saa S, Mann P, DeJong TM. 2016. The influence of elevated CO_2 on the photosynthesis, carbohydrate status, and plastochron of young peach (*Prunus persica*) trees. Horticulture, Environment, and Biotechnology **57,** 364–370.

Dingkuhn M, Luquet D, Quilot B, de Reffye P. 2005. Environmental and genetic control of morphogenesis in crops: towards models simulating phenotypic plasticity. Australian Journal of Agricultural Research **56,** 1289–1302.

Evers JB, Vos J, Andrieu B, Struik PC. 2006. Cessation of tillering in spring wheat in relation to light interception and red:far-red ratio. Annals of Botany **97,** 649–658.

Fournier C, Durand JL, Ljutovac S, Schäufele R, Gastal F, Andrieu B. 2005. A functional–structural model of elongation of the grass leaf and its relationships with the phyllochron. New Phytologist **166,** 881–894.

Gauch HG, Gene Hwang JT, Fick GW. 2003. Model evaluation by comparison of model-based predictions and measured values. Agronomy Journal **95,** 1442–1446.

Gautier H, Varlet-Grancher C. 1996. Regulation of leaf growth of grass by blue light. Physiologia Plantarum **98,** 424–430.

Hansen N, Ostermeier A. 2001. Completely derandomized self-adaptation in evolution strategies. Evolutionary Computation **9,** 159–195.

Haun JR. 1973. Visual quantification of wheat development. Agronomy Journal **65,** 116–119.

Hay RKM, Delécolle R. 1989. The setting of rates of development of wheat plants at crop emergence: influence of the environment on rates of leaf appearance. Annals of Applied Biology **115,** 333–341.

He J, Le Gouis J, Stratonovitch P, *et al*. 2012. Simulation of environmental and genotypic variations of final leaf number and anthesis date for wheat. European Journal of Agronomy **42,** 22–33.

Hoagland DR. 1950. The water-culture method for growing plants without soil. Berkeley, CA: College of Agriculture, University of California.

Hummel I, Pantin F, Sulpice R, *et al*. 2010. Arabidopsis plants acclimate to water deficit at low cost through changes of carbon usage: an integrated perspective using growth, metabolite, enzyme, and gene expression analysis. Plant Physiology **154,** 357–372.

Inman-Bamber NG. 1994. Temperature and seasonal effects on canopy development and light interception of sugarcane. Field Crops Research **36,** 41–51.

Jamieson PD, Brooking IR, Porter JR, Wilson DR. 1995. Prediction of leaf appearance in wheat: a question of temperature. Field Crops Research **41,** 35–44.

Jamieson PD, Brooking IR, Semenov MA, McMaster GS, White JW, Porter JR. 2007. Reconciling alternative models of phenological development in winter wheat. Field Crops Research **103,** 36–41.

Jamieson P, Brooking I, Zyskowski R, Munro C. 2008. The vexatious problem of the variation of the phyllochron in wheat. Field Crops Research **108,** 163–168.

Jamieson PD, Semenov MA, Brooking IR, Francis GS. 1998. Sirius: a mechanistic model of wheat response to environmental variation. European Journal of Agronomy **8,** 161–179.

Kemp DR, Blacklow WM. 1980. Diurnal extension rates of wheat leaves in relation to temperatures and carbohydrate concentrations of the extension zone. Journal of Experimental Botany **31,** 821–828.

Kimball BA, White JW, Wall GW, Ottman MJ, Martre P. 2018. Wheat response to a wide range of temperatures, as determined from the Hot Serial Cereal (HSC) Experiment. Open Data Journal for Agricultural Research **4,** 16–21.

Kirby EJM. 1995. Factors affecting rate of leaf emergence in barley and wheat. Crop Science **35,** 11–19.

Kirby EJM, Appleyard M, Fellowes G. 1985. Leaf emergence and tillering in barley and wheat. Agronomie **5,** 193–200.

Kitaya Y, Niu G, Kozai T, Ohashi M. 1998. Photosynthetic photon flux, photoperiod, and CO_2 concentration affect growth and morphology of lettuce plug transplants. HortScience **33,** 988–991.

Lattanzi FA, Schnyder H, Thornton B. 2005. The sources of carbon and nitrogen supplying leaf growth. Assessment of the role of stores with compartmental models. Plant Physiology **137,** 383–395.

Lawless C, Semenov MA, Jamieson PD. 2005. A wheat canopy model linking leaf area and phenology. European Journal of Agronomy **22,** 19–32.

Lizaso JI, Boote KJ, Jones JW, Porter CH, Echarte L, Westgate ME, Sonohat G. 2011. CSM-IXIM: a new maize simulation model for DSSAT version 4.5. Agronomy Journal **103,** 766–779.

Longnecker N, Robson A. 1994. Leaf emergence of spring wheat receiving varying nitrogen supply at different stages of development. Annals of Botany **74,** 1–7.

Manceau L, Martre P. 2018. SiriusQuality-BioMa-Phenology-Component (Version v1.0.0). Zenodo http://doi.org/10.5281/zenodo.2478791.

Martre P. 2013. Temperature responses in the wheat simulation model SiriusQuality. In: Alderman PD, Quilligan E, Asseng S, Ewert F, Reynolds MP, eds. Proceedings of the workshop on modeling wheat response to high temperature. El Batan, Texcoco, Mexico: CIMMYT, 114–119.

Martre P, Dambreville A. 2018. A model of leaf coordination to scale-up leaf expansion from the organ to the canopy. Plant Physiology **176,** 704–716.

Martre P, Jamieson PD, Semenov MA, Zyskowski RF, Porter JR, Triboi E. 2006. Modelling protein content and composition in relation to crop nitrogen dynamics for wheat. European Journal of Agronomy **25,** 138–154.

Masle J. 2000. The effects of elevated CO_2 concentrations on cell division rates, growth patterns, and blade anatomy in young wheat plants are modulated by factors related to leaf position, vernalization, and genotype. Plant Physiology **122,** 1399–1415.

Masle J, Doussinault G, Sun B. 1989. Response of wheat genotypes to temperature and photoperiod in natural conditions. Crop Science **29,** 712–721.

McMaster GS, LeCain DR, Morgan JA, Aiguo L, Hendrix DL. 1999. Elevated CO_2 increases wheat CER, leaf and tiller development, and shoot and root growth. Journal of Agronomy and Crop Science **183,** 119–128.

McMaster GS, Wilhelm WW. 1995. Accuracy of equations predicting the phyllochron of wheat. Crop Science **35,** 30–36.

Miglietta F. 1991. Simulation of wheat ontogenesis. Climate Research **1,** 145–150.

Miralles DJ, Richards RA. 2000. Responses of leaf and tiller emergence and primordium initiation in wheat and barley to interchanged photoperiod. Annals of Botany **85,** 655–663.

Monsi M, Saeki T. 2005. On the factor light in plant communities and its importance for matter production. Annals of Botany **95,** 549–567.

Muchow RC, Carberry PS. 1990. Phenology and leaf-area development in a tropical grain sorghum. Field Crops Research **23,** 221–237.

Nash JE, Sutcliffe JV. 1970. River flow forecasting through conceptual models, part I—A discussion of principles. Journal of Hydrology **10,** 282–290.

Nix HA. 1976. Climate and crop productivity in Australia. Proceedings of the symposium on climate & rice. Los Baños, the Philippines: International Rice Research Institute, 495–507.

Ochagavía H, Prieto P, Savin R, Griffiths S, Slafer GA. 2017. Duration of developmental phases, and dynamics of leaf appearance and tillering, as affected by source and doses of photoperiod insensitivity alleles in wheat under field conditions. Field Crops Research **214,** 45–55.

Pantin F, Simonneau T, Rolland G, Dauzat M, Muller B. 2011. Control of leaf expansion: a developmental switch from metabolics to hydraulics. Plant Physiology **156,** 803–815.

Parent B, Tardieu F. 2012. Temperature responses of developmental processes have not been affected by breeding in different ecological areas for 17 crop species. New Phytologist **194,** 760–774.

Rickman RW, Klepper BL. 1995. The phyllochron: where do we go in the future? Crop Science **35,** 44–49.

Rickman RW, Klepper B, Peterson CM. 1985. Wheat seedling growth and developmental response to incident photosynthetically active radiation. Agronomy Journal **77,** 283–287.

Ritchie JT. 1991. Wheat phasic development. In: Ritchie JT, Hanks RJ, eds. Plant and soil systems. Agronomy Monograph no. 31. Madison, WI: American Society of Agronomy, Crop Science Society of Amercia, Soil Science Society of America, 31–54.

Sanna G, Giunta F, Motzo R, Mastrangelo AM, De Vita P. 2014. Genetic variation for the duration of pre-anthesis development in durum wheat and its interaction with vernalization treatment and photoperiod. Journal of Experimental Botany **65,** 3177–3188.

Skinner RH, Nelson CJ. 1995. Elongation of the grass leaf and its relationship to the phyllochron. Crop Science **35,** 4–10.

Slafer GA, Connor DJ, Halloran GM. 1994. Rate of leaf appearance and final number of leaves in wheat: effects of duration and rate of change of photoperiod. Annals of Botany **74,** 427–436.

Slafer GA, Rawson HM. 1997. Phyllochron in wheat as affected by photoperiod under two temperature regimes. Functional Plant Biology **24,** 151–158.

Stitt M, Zeeman SC. 2012. Starch turnover: pathways, regulation and role in growth. Current Opinion in Plant Biology **15,** 282–292.

Stöckle CO, Donatelli M, Nelson R. 2003. CropSyst, a cropping systems simulation model. European Journal of Agronomy **18,** 289–307.

Streck NA, Weiss A, Xue Q, Baenziger PS. 2003. Incorporating a chronology response into the prediction of leaf appearance rate in winter wheat. Annals of Botany **92,** 181–190.

Teixeira EI, Brown HE, Meenken ED, Moot DJ. 2011. Growth and phenological development patterns differ between seedling and regrowth lucerne crops (*Medicago sativa* L.). European Journal of Agronomy **35,** 47–55.

Volk T, Bugbee B. 1991. Modeling light and temperature effects on leaf emergence in wheat and barley. Crop Science **31,** 1218–1224.

Wall GW, Kimball BA, White JW, Ottman MJ. 2011. Gas exchange and water relations of spring wheat under full-season infrared warming. Global Change Biology **17,** 2113–2133.

Wang E, Martre P, Zhao Z, *et al*. 2017. The uncertainty of crop yield projections is reduced by improved temperature response functions. Nature Plants **3,** 17102.

Warton DI, Duursma RA, Falster DS, Taskinen S. 2012. smatr 3– an R package for estimation and inference about allometric lines. Methods in Ecology and Evolution **3,** 257–259.

White JW, Kimball BA, Wall GW, Ottman MJ. 2012. Cardinal temperatures for wheat leaf appearance as assessed from varied sowing dates and infrared warming. Field Crops Research **137,** 213–220.

Wilhelm WW, McMaster GS. 1995. Importance of the phyllochron in studying development and growth in grasses. Crop Science **35,** 1–3.

Yin X, Kropff MJ. 1996. The effect of temperature on leaf appearance in rice. Annals of Botany **77,** 215–221.

Maize yields over Europe may increase in spite of climate change, with an appropriate use of the genetic variability of flowering time

Boris Parent[a], Margot Leclere[a,1], Sébastien Lacube[a], Mikhail A. Semenov[b], Claude Welcker[a], Pierre Martre[a], and François Tardieu[a,2]

[a]Laboratoire d'Ecophysiologie des Plantes sous Stress Environnementaux (LEPSE), Université de Montpellier, Institut National de la Recherche Agronomique (INRA), F-34000 Montpellier, France; and [b]Plant Sciences Department, Rothamsted Research, Harpenden, AL5 2JQ Herts, United Kingdom

Edited by Edward S. Buckler, USDA-ARS/Cornell University, Ithaca, NY, and approved August 24, 2018 (received for review December 3, 2017)

Projections based on invariant genotypes and agronomic practices indicate that climate change will largely decrease crop yields. The comparatively few studies considering farmers' adaptation result in a diversity of impacts depending on their assumptions. We combined experiments and process-based modeling for analyzing the consequences of climate change on European maize yields if farmers made the best use of the current genetic variability of cycle duration, based on practices they currently use. We first showed that the genetic variability of maize flowering time is sufficient for identifying a cycle duration that maximizes yield in a range of European climatic conditions. This was observed in six field experiments with a panel of 121 accessions and extended to 59 European sites over 36 years with a crop model. The assumption that farmers use optimal cycle duration and sowing date was supported by comparison with historical data. Simulations were then carried out for 2050 with 3 million combinations of crop cycle durations, climate scenarios, management practices, and modeling hypotheses. Simulated grain production over Europe in 2050 was stable (−1 to +1%) compared with the 1975–2010 baseline period under the hypotheses of unchanged cycle duration, whereas it was increased (+4–7%) when crop cycle duration and sowing dates were optimized in each local environment. The combined effects of climate change and farmer adaptation reduced the yield gradient between south and north of Europe and increased European maize production if farmers continued to make the best use of the genetic variability of crop cycle duration.

climate change | yield | flowering time | management practices | modeling

Most projections relying on process-based (1–5) or statistical models (6) predict that climate change will reduce yields of most crop species. Indeed, crops will experience more heat events, dry weather, and an increase in evaporative demand which may all decrease crop production (6–8). However, some species still show yield progress in farmer's fields despite observed climate changes (9). This discrepancy may be due to the fact that many impact studies assume unchanged farmer's genotypes and practices, whereas farmers continuously adapt crop cycle duration and sowing dates to local environmental conditions (10–12). The comparatively few studies of climate change impact that consider adaptation of management practices (13) predict a decrease in yield by 1–6%, smaller than without adaptation (10–12). Furthermore, a study that considers adaptation of sowing date and cycle duration for six crops predicts a yield increase of 12–16% (14). This diversity of projections led us to develop a more explicit approach based on experiments and process-based modeling and to use a precise definition of adaptation involving biological variables and management practices currently used by farmers.

The duration of crop cycle (*i*) is largely affected by climate change through increase in temperature; (*ii*) has a major effect on crop yield via cumulated canopy photosynthesis; and (*iii*) presents a large genetic variability in most species, in particular via the genetic control of flowering time that involves networks of genes that interact with environmental conditions (15–18). This raises the possibility that farmers can counteract the effects of climate change by making the best use of the genetic variability of flowering time (10, 19), thereby adapting phenology to climate changes as it has been the case over centuries in natural ecosystems (20). This raises the questions of whether (*i*) farmers can access an organized genetic variability of cycle duration to adapt crop cycle to a range of environmental conditions; (*ii*) one can model the decision rules that farmers currently use for adapting cycle duration over environmental gradients, together with sowing dates; and (*iii*) adapting crop cycle duration can counteract the effects of climate change. More specifically, we have questioned whether the decision rules currently used by farmers to adapt crop cycle duration over environmental gradients would reduce the impact of climate change on European maize production.

Addressing these questions required an experimental approach for the first question, a model of farmer's decision rules together with a comparison of model outputs with European statistics for the second question, and a crop simulation model that explicitly accounts for the genetic variability of flowering time and of crop responses to environmental conditions for the third question. We combined multilocation field experiments

Significance

The consequences of climate change on European maize yields may become positive if farmers in 2050 use the decision rules they currently follow for adapting plant cycle duration and sowing dates to the diversity of environmental conditions. Experiments and simulations show that the current genetic variability of flowering time allows identifying a cycle duration that maximizes yield at every maize field in Europe. The assumption that farmers use this optimal cycle length in each site was supported by comparison with historical data. Simulated European production for 2050 was stable under the hypotheses of unchanged practices but was increased if farmers continued adopting the decision rules they currently use for adjusting sowing date and crop cycle duration to local environment.

Author contributions: B.P. and F.T. designed research; B.P., M.L., S.L., M.A.S., C.W., and F.T. performed research; B.P., M.L., S.L., M.A.S., C.W., P.M., and F.T. analyzed data; and B.P., M.A.S., P.M., and F.T. wrote the paper.

The authors declare no conflict of interest.

This article is a PNAS Direct Submission.

[1]Present address: UMR Agronomie, INRA, AgroParisTech, Université Paris-Saclay, 78850 Thiverval-Grignon, France.

[2]To whom correspondence should be addressed. Email: francois.tardieu@inra.fr.

This article contains supporting information online at www.pnas.org/lookup/suppl/doi:10.1073/pnas.1720716115/-/DCSupplemental.

Published online October 1, 2018.

that analyzed the consequences of the genetic variability of crop duration, historical yields, crop management and phenology information, and projections of midterm climate change impacts. These were performed for European maize, whose flowering time is a constitutive trait, depending on temperature but independent of photoperiod sensitivity or cold requirement.

Results

The Existing Genetic Variability of Cycle Duration Allows Optimizing Yield in a Wide Range of Current Environmental Scenarios. We first tested whether the current genetic variability of cycle duration allowed identification of an optimum cycle duration that maximizes grain yield in each site. This was based on six experiments, extended to the variability of climate over Europe via modeling. A panel of 121 maize accessions with a large range of flowering time, due to allelic variations in the VGT1 (18), VGT2 (15), and other loci (16), was analyzed in six experiments with different climatic scenarios and water regimes (Fig. 1*A* and *SI Appendix*, Figs. S1–S3). Because the main source of variation of maize cycle duration is the length of the vegetative phase via the allelic effects of genes involved in flowering time (17, 21), we focus hereafter on the sowing-to-flowering period. For each accession, the duration of this period was common to all sites if expressed in time corrected for temperature (*SI Appendix*, Fig. S1) and closely correlated to leaf number, which itself depends on the time to floral transition (22) (*SI Appendix*, Fig. S2). Accessions with sowing-to-flowering durations that optimize yield were identified in each experiment (Fig. 1*A* and *SI Appendix*, Fig. S3). Yield increased with vegetative duration below this optimum (Fig. 1*A*), because of increased light interception (*SI Appendix*, Fig. S4), and decreased beyond it, due to flowering and/or grain filling occurring in adverse conditions such as low light or terminal drought (23). As expected, different optimum durations were observed among sites and water regimes, depending on local environmental conditions (*SI Appendix*, Fig. S3).

We extended this analysis to 59 European sites representative of the European maize growing area (*SI Appendix*, Table S1) (24). Simulations were performed over 36 y (1975–2010) with a modified version of the crop simulation model Agricultural Production Systems Simulator (APSIM) maize (25), in which vapor pressure deficit (VPD) and, indirectly, high temperature have direct effects on leaf expansion rate and grain set, with calculations run with a 3-h time step. This model also accounts for the genetic variability of phenology by considering the maximum leaf number as a genotypic input for the simulations of cycle duration, individual leaf expansion, and grain abortion (26, 27). Simulations were run for each individual year in either rainfed or irrigated conditions. The mean value of yield over the 36-y period was related to the sowing-to-flowering duration with bell shapes similar to those observed experimentally (Fig. 1*B* and *SI Appendix*, Fig. S5 *A*, *C*, and *E*). In irrigated conditions, optimum durations differed among sites and correlated with latitude (*SI Appendix*, Figs. S2*A* and S6*A*). Simulated optimum crop cycle durations were lower in rainfed than in irrigated conditions, especially in most southern locations in which short crop cycles allowed escaping water deficit during flowering time (Fig. 2*B* and *SI Appendix*, Fig. S6*B*).

Overall, both experiments and simulations showed that optimum cycle durations that maximize yield can be identified based on the genetic variation of flowering time in a wide diversity of environmental scenarios throughout Europe.

A Model of Cycle Duration and Sowing Date Closely Matched with the Management Practices That Farmers Currently Use in the Diversity of Environmental Scenarios. The above paragraphs suggest that, by trial and error, farmers and extension services might identify a cycle duration that maximizes yield in the most frequent climatic scenario corresponding to each site ("autonomous adaptation,"

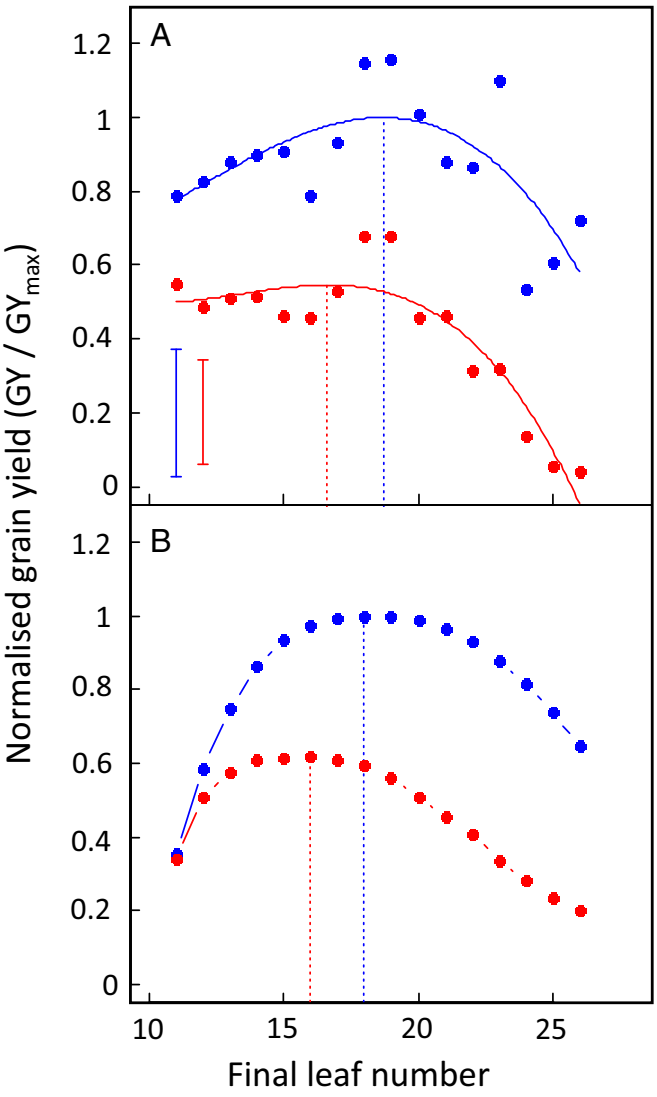

Fig. 1. Observed and simulated optimum durations of the vegetative period (sowing–flowering time), expressed in final plant leaf number. (*A*) Experimental relationships between final plant leaf number and yield in irrigated (blue dots and lines) or rainfed conditions (red dots and line) in a field with 121 maize accessions (two additional field experiments are presented in *SI Appendix*, Fig. S3). For better intuition, the duration of the vegetative period is expressed as final leaf number, closely related to it. Yield is normalized by its maximum value in fully irrigated conditions. Dots are mean values for accessions presenting a common leaf number. Error bars, confidence intervals (P = 0.95). Plain lines, third-order polynomial regressions. Vertical dashed lines, optimum leaf number. (*B*) Simulated relationship between plant leaf number and yield at Achenheim, France (*SI Appendix*, Table S1, two additional sites are presented in *SI Appendix*, Fig. S5). Each dot, mean of 36 y (1975–2010). Error bars, confidence intervals (P = 0.95).

ref. 28). This has allowed us to model their decision rules about cycle duration, but also sowing date, and to compare simulation outputs to farmers' practices reported in European databases (29, 30). The simulation of cycle duration used by farmers at each site was based on the calculated optimum sowing-to-flowering duration presented above. Simulated sowing dates occurred on the first day of early spring for which the risk of frost for 10 d after sowing was lower than 5% over 36 y, thereby combining a minimum risk of plant damage with highest potentials of cumulated photosynthesis and yield. They ranged from March 20 to April 30, with later dates at northern latitudes.

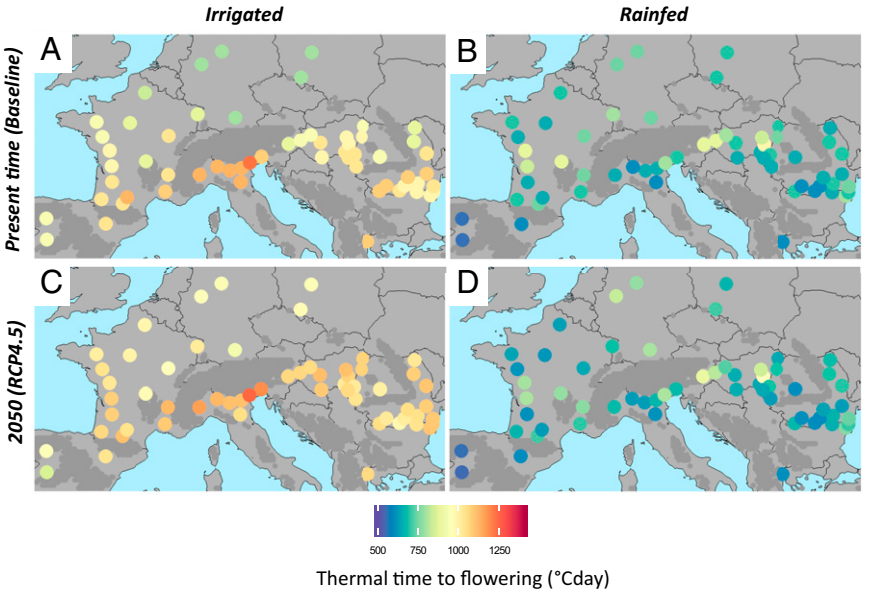

Fig. 2. Maps of optimum cycle duration in current (*A* and *B*) and future conditions (*C* and *D*), under irrigated (*A* and *C*) or rainfed (*B* and *D*). Colors depict the optimum thermal time between sowing and flowering time in each site for maximizing yield for present time (over the 1975–2010 period) or 2050 (30 y, RCP4.5, average duration for six GCMs, calculated under the hypothesis of an increase in transpiration efficiency with CO_2 concentration).

The spatial distribution of sowing dates and flowering times simulated in this way closely matched with those reported in the European AgroPheno database (29) (*SI Appendix*, Fig. S7*A*). Cycle duration decreased with latitude: later sowing dates in northern sites such as Germany or Poland were compensated for by shorter vegetative durations (Fig. 2*A* and *SI Appendix*, Fig. S6*A*), resulting in simulated flowering dates that were nearly independent of latitude in both simulations and historical data (29) (*SI Appendix*, Fig. S7*A*).

Hence, the decision rules simulated as above allowed correct prediction of farmer practices throughout Europe. In addition, simulated yields at country level calculated by using local practices of irrigation, density, and fertilization closely correlated with historical yields for the period 2000–2010 (30) (*SI Appendix*, Fig. S7*B*). To compare environmental effects independently of sowing density and fertilization, simulations were then run by considering a common sowing density over Europe (eight plants m^{-2}) and no nitrogen limitation. In irrigated conditions, simulated yields (9.2–13.6 t ha^{-1}, Fig. 3*A* and *SI Appendix*, Fig. S8) were negatively related to latitude with highest yield in southern sites (Fig. 3*A*); this relationship disappeared in rainfed conditions due to the higher risk of water deficit in southern Europe, so maximum yields were observed at intermediate latitudes 44–47° N (Fig. 3*D* and *SI Appendix*, Fig. S8).

Adapting Crop Cycle Duration Based on Current Farmer's Decision Rules Improved the Simulated Impacts of Climate Change Compared with Invariant Practices. We projected yields for 2050 by considering that the farmer's decision rules presented above, based on the assumption of optimal practices, will apply in the future. We then compared the yields simulated with either adapted or invariant cycle durations and sowing dates. Daily local-scale climate scenarios for 2050 were generated by the Long Ashton Research Station Weather Generator (LARS-WG) (31) for the representative concentration pathways (RCPs) 4.5 and 8.5 (487 and 541 ppm CO_2 in 2050, respectively). For each RCP, we used six global climate models (GCMs) that cover the range and present similar mean values for changes in temperature, VPD, and precipitations compared with 18 GCMs from the Coupled Model Intercomparison Project Phase 5 (CMIP5) model ensemble for the studied area (32) (*SI Appendix*, Fig. S9). Thirty years of daily weather data were generated for each site–RCP–GCM combination. The direct impact of increase in atmospheric CO_2 concentration in 2050 was taken into account in the crop model by increasing transpiration efficiency (TE) by 0.1% per additional parts per million CO_2 in RCP4.5 and RCP8.5, i.e., the mean TE increase reviewed in ref. 33. We have also considered the possibility of unchanged TE with CO_2 concentration in view of the debate on the long-term effect of CO_2 on TE (34). Radiation use efficiency, a proxy for photosynthetic

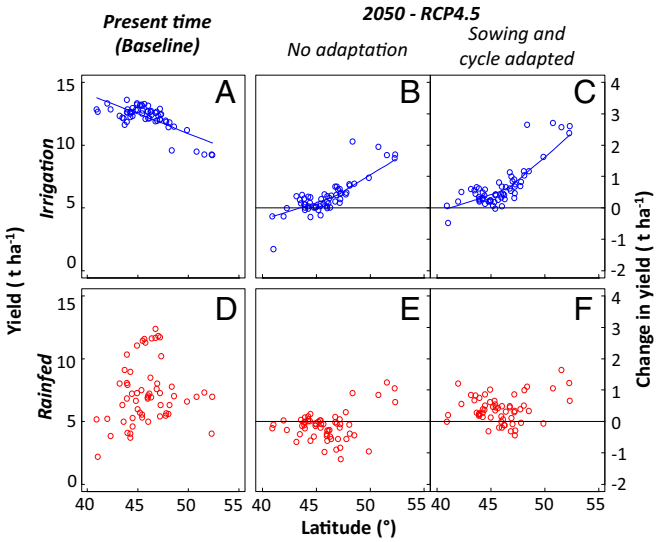

Fig. 3. Change in yield depending on farmer adaptation to climate change. (*A–D*) Current yield in irrigated and rainfed conditions. (*B*, *C*, *E*, and *F*) Change in yield between the 1975–2010 period and 2050 (RCP4.5), either without adaptation (*B* and *E*) or with adaptation of sowing date and duration of growth cycle (*C* and *F*) under irrigated (*B* and *C*) or rainfed conditions (*E* and *F*). Each point, one site, mean value for six GCMs and 30 y, calculated under the hypothesis of an increase in transpiration efficiency with CO_2 concentration.

capacity, was kept constant despite higher atmospheric CO_2 concentration because maize is a C4 species (34, 35). Simulations were run over 30 y for each combination of site, RCP, GCM, watering regime, crop cycle duration, and CO_2 effect on TE (2.6 million simulations). Climate change was represented in *SI Appendix*, Fig. S10 as sensed by plants during the optimum flowering time calculated individually for each combination of site, scenario, GCM, watering regime, and option for TE.

This resulted in increased maximum temperature, VPD, and incident light at flowering time between baseline and 2050 (*SI Appendix*, Fig. S10 *A*, *B*, and *E*), with values that were similar for RCP8.5 and RCP4.5 because flowering time was earlier in the season for RCP8.5, thereby compensating for the limited difference in temperature between RCPs at a common date. For the same reason, water deficit during flowering time was similar in 2050 compared with the baseline period 1975–2010 if TE was considered as unchanged because the earlier flowering time compensated for the negative effect of VPD increase (*SI Appendix*, Fig. S10*D*). It tended to become milder in 2050 if TE increased with atmospheric CO_2 concentration (33) because the increase in TE with CO_2 concentration reduced water use (*SI Appendix*, Fig. S10*C*).

As in previous climate impact studies, a decrease in yield was simulated in rainfed fields between the baseline period and 2050 under the hypothesis of unchanged varieties and sowing dates (RCP4.5), with a negative effect in 70% of rainfed fields (Fig. 3*D*). This negative effect was maximum at latitudes 43–47° N that represent the major growing area for maize. Conversely, simulated yields tended to increase in well-watered fields at latitudes higher than 47° N due to increased light intensity around flowering time (*SI Appendix*, Fig. S10*F*). Overall, upscaling these results for Europe as a whole across latitudes resulted in a small effect on overall production in rainfed fields (−2% and +0.6% for RCP4.5 and RCP8.5, respectively) (Fig. 4), with high negative effects in two GCMs out of six (*SI Appendix*, Fig. S11). Irrigated fields had a yield slightly increased or decreased depending on GCMs (mean, +1.8% and +1.0% for RCP4.5 and RCP8.5, respectively). Yields, weighted for the proportion of irrigated/rainfed maize in the Eurostat 25 × 25 km grid cell (*SI Appendix*, Table S1), were nearly unaffected in 2050 compared with baseline (mean, −0.8% and +0.8% for RCP4.5 and RCP8.5, respectively) if TE was considered as changing with CO_2 concentration. They were more affected if TE was considered constant in our simulations, due to more frequent water deficit, or if restrictions of water availability reduced the current portion of land area under irrigation (36).

The projected impact of climate change became positive if one assumed that farmers will adapt cycle duration and sowing date by using the decision rules they currently follow (Fig. 4). Optimal sowing dates were earlier by 10–39 d depending on sites in 2050 under RCP4.5 compared with the baseline period (*SI Appendix*, Fig. S12*A*). The cycle duration of adapted varieties increased by 207 °Cd (degree days) for RCP4.5 in irrigated fields at high latitudes (>49°), corresponding to an increase in leaf number by 3.4 (Fig. 2 and *SI Appendix*, Figs. S6 and S12). This increase disappeared in irrigated southern fields and in rainfed conditions because optimum durations were limited by the probability of negative effects of drought or heat stresses with later flowering time. If farmers followed these decision rules in 2050, the simulated impact of climate change would be positive in irrigated fields in RCP4.5 and RCP8.5, (Fig. 4*A*), regardless of hypotheses on TE and GCMs (*SI Appendix*, Figs. S11 and S13), with an effect that increased with latitude (Fig. 3*C*) and was largely accounted for by the increase in intercepted light during the crop cycle (*SI Appendix*, Fig. S14). Adapting the crop cycle duration also had a positive effect in rainfed fields (Figs. 4*B* and 3*H* and *SI Appendix*, Fig. S11 and S13), but this effect was only observed if TE was considered as increasing with CO_2 concentration and was GCM dependent. Overall, if the effect of climate change was

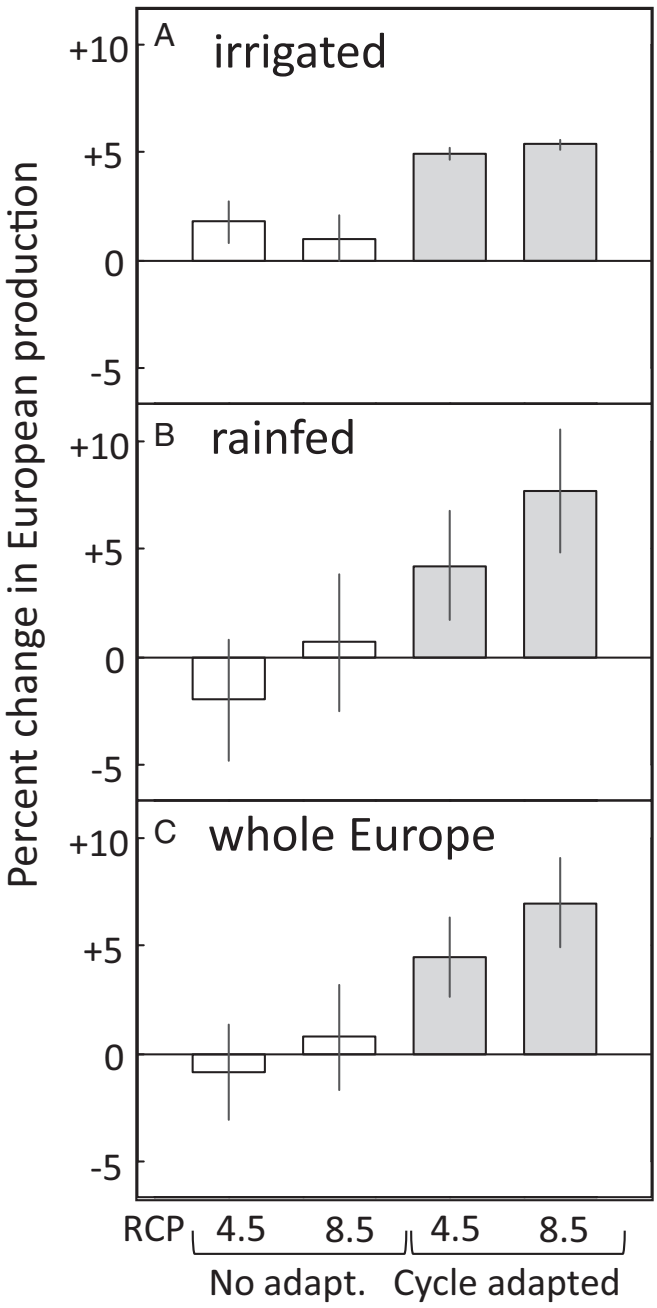

Fig. 4. Impact of climate change on European maize production depending on farmer adaptation to climate change in well-watered conditions (*A*), rainfed conditions (*B*), or Europe as a whole (*C*). The latter calculation considered the proportion of irrigated vs. rainfed maize fields in the Eurostat 25 × 25 km grid cells. Simulations consider that the maize area and access to water will be the same in 2050 compared with the 1975–2010 period, and the hypothesis of an increase in TE with CO_2 concentration. White, no adaptation; gray, adaptation of sowing date and cycle duration. Simulations for individual GCMs, with or without change in TE, are in *SI Appendix*, Fig. S11. Error bars, SE calculated over the six considered GCMs.

synthesized by weighing irrigated and rainfed fields over Europe, the total maize production increased by 4.5% and 7.0% for RCP 4.5 and 8.5, respectively, if the crop cycle was adapted, in the likely hypothesis of a moderate increase in TE.

The combined effects of climate change and of adaptation of crop cycle duration were much larger in northern than in southern locations (Fig. 3 *C*–*F*). The gradient of yield, of 0.31 t ha^{-1} per

AGRICULTURAL SCIENCES

degree of latitude for the baseline period (Fig. 3*A*) decreased to 0.09 t ha^{-1} per degree in 2050 (RCP4.5). The current north–south difference in yield in the absence of stress was therefore largely decreased by the combined effects of climate change and adaptation practices (Fig. 3 *C*–*F*).

Discussion

The approach used here to predict the impact of climate change on yield differs from those previously published, which led to contrasting results ranging from steep decrease to appreciable gains of yield (1–6, 10–12, 14). Here, we have considered adaptation via one biological process, the use of the observed genetic variability of flowering time, and explicit management practices, sowing date, and irrigation, considered with rules that mimic those currently used by farmers. This was in the line of Lobell (8) who considered it essential to precisely identify the actions (adaptation) that affect the impact of climate change and of Rezaei et al. (37) who proposed that climate change impacts should not rely on a single-cultivar concept. Furthermore, we have based our approach on experimental evidences for evaluating the effect on yield of the genetic variability of flowering time and on comparisons with historical data for testing the farmer's decision rules used in crop simulations. This has also required an improved crop simulation model that can predict the effect of the genetic variability of phenology and of responses to environmental conditions on leaf growth, grain set, and transpiration (26, 27), together with advanced phenotyping techniques for establishing the model (38). We believe that this represents progress, compared with studies that use current trends of temperature effect together with nonexplicit hypotheses on adaptation possibilities (10–12, 39).

Are farmers likely to use the genetic variability of flowering time and to adapt sowing dates by 2050? We can consider this hypothesis as reasonable because (*i*) genetic resources and alleles for adapting crop cycle duration have been identified and are increasingly available (16); and (*ii*) farmers have already adapted maize varieties in recent years, as they have done for wheat in the United States for over a century (40). For example, varieties of the group midearliness dent lines were mostly grown in France at latitudes of 44.8–45.9° in 1996 while they have shifted to 46.5–47.5° in 2009 (41). The same tendency for farmers to increasingly use late-maturing cultivars has also been observed in other species such as winter rapeseed and rye, thereby partly or fully compensating for the decrease in cycle duration linked to the increase in temperature (42).

Hence, the effect of climate change on yield might be more positive than previously reported (3–6). This particularly concerns northern areas where yield increases are maximum. However, resulting increases presented here will not be sufficient to meet the increasing demands for food and industrial usages (43). Further improvements of plant performance based on increased photosynthesis, adapted reproductive development, or resistance to pests and diseases will be necessary. Southern fields will have less of a competitive advantage in both irrigated and rain-fed conditions (Fig. 3 *D*–*H*), whereas farmers in northern areas will have the option of growing maize with high yields. This may change the maize growing area, in such a way that the positive impact of climate change on European maize production might be higher than predicted here.

Material and Methods

Field Experiments. We tested a panel of 121 maize accessions representative of main components of the maize genetic diversity (36) in three experimental fields with two watering regimes each. Sites included a Mediterranean field, Mauguio [43°36′37″N; 3°58′39″E; 23 m above sea level (asl)], and oceanic sites in Sainte Pexine (46°33′43″N; 1°08′17″W; 45 m asl) and Le Magneraud (46°24′16″N; 00°04′45″E; 26 m asl). In each site, two water regimes were imposed, with either irrigation over the crop cycle or restricted irrigation with soil water deficit at flowering time. A rainout shelter was used in Le Magneraud to ensure water deficit so the number of accessions was 57 because of the limited available space. Irrigation was withdrawn at the eight-visible-leaf stage, until flowering time plus 10 d but was still applied when plants showed leaf rolling in early morning for 2 consecutive days. The experimental design was an alpha lattice with two replicates in the irrigated treatments and three replicates in rain-fed treatments. Plots were 6 m long, with 0.8 m between rows and a plant density of 8 m^{-2}. Light, air temperature, relative humidity, and wind speed were measured every hour in each experiment at 2-m height over a reference grass canopy. Soil water potential was measured every day at 30-, 60-, and 90-cm depths in watered and rain-fed plots with three and two replicates, respectively. Mean soil water potential was −0.3 MPa on average during water deficit in Sainte Pexine and Le Magneraud, and was −0.6 MPa in Mauguio. Thermal time was calculated from sowing time as in APSIM maize (25) at a 3-h time step.

Emergence, flowering time, yield, and yield components were assessed at plot level. The length and width of every second leaf and leaf number were measured in 10 plants per plot. The leaf appearance rate of each accession was calculated by dividing the mean thermal time at flowering time by the final number of leaves of the studied accession. The duration of the vegetative period was expressed as final leaf number in Fig. 1 and *SI Appendix*, Figs. S2 and S3. We then averaged data for accessions with common final leaf number. Leaf area and light interception were calculated every day from sowing to harvest for all accessions. For that, profiles of final leaf length and width for each variety with final leaf number from 11 to 25 were obtained from measured data. The time of appearance of each leaf was calculated from the phyllochron. Leaf expansion was considered linear during 10 d from leaf appearance (27). Light interception was then calculated by using measured incident light and the proportion of intercepted light calculated from leaf area as in APSIM maize (25).

Model Parameterization and Evaluation.

Crop parameters and varieties. We used the model APSIM maize (25) modified for expansion of individual leaves (26) and calibrated (in particular for responses to water deficit and VPD) with data of the reference hybrid B73xUH007 in replicated field experiments in Mauguio, France (24) and in the phenotyping platforms PhenoArch and Phenodyn (https://www6.montpellier.inra.fr/lepse/M3P). Temperature at 3-h time step was calculated from daily minimum and maximum temperatures with the third order polynomial function used in APSIM maize (25). VPD was calculated for each 3-h time step based on current temperature and daily minimum temperature, an estimate for dew-point temperature. Leaf expansion rate was calculated every third hour, based on values VPD and soil water status with parameters as in ref. 27. The parameter representing TE before correction by the effect of VPD (parameter transp_eff_cf in APSIM maize) was set at 0.0075 g kPa g^{-1} for the baseline period and increased by 0.1% per additional μmol CO_2 mol^{-1} resulting in +11% and 17% in 2050 for RCP4.5 and RCP8.5, respectively (33).

A set of virtual hybrids with contrasted crop cycle durations was derived from the reference hybrid, in which crop cycle duration depended on the duration of the vegetative stage. The duration of the vegetative period was driven by the final leaf number (ref. 22 and *SI Appendix*, Fig. S2). We parameterized hybrids with contrasted cycle duration by (*i*) changing leaf number from 11 to 30, with a constant leaf appearance of 0.0193 °Cd $leaf^{-1}$ for all accessions (*SI Appendix*, Fig. S2) and (*ii*) a constant thermal time from flowering to maturity corresponding to the reference hybrid. The durations of each phenological stage of the vegetative period were affected proportionally to changes in time from emergence to flowering. All other parameters were those of the reference hybrid (24). Hence, the 16-leaf hybrid was the reference hybrid and hybrids with leaf number ranging from 11 to 30 were similar to the reference hybrid but with different final leaf number.

Sites. We used 59 locations representative of the European maize growing area and of typical soil types of these regions. Fifty-five sites were those described previously (24), representing the 10 European countries with the highest maize growing areas in the 2004–2009 period (30) and the main maize growing regions within these countries (24). Four sites were added to improve the spatial distribution of locations. Soil data were obtained from the Joint Research Centre (JRC) European Soil Commission database and from the Crop Growth Monitoring System (24). Because soil depth can highly vary within each region and because the aim of this study was a sensitivity analysis on other variables, we considered a soil depth of 1.5 m in all sites. Meteorological data used for the baseline period were 36 y of daily weather (1975–2010) obtained from (*i*) the AGRI4CAST database of the JRC for the 55 sites (24) and (*ii*) the INRA CLIMATIK database for the four added sites. The atmospheric CO_2 concentration was 380 ppm. For comparing predicted and observed current European yields, plant density and nitrogen supply were adjusted for each site based on the JRC database* and local knowledge. Because there is no reason to hypothesize that these values will stay the

*JRC (2013) JRC database crop knowledge. ed JRC (Joint Research Centre, Ispra, Italy).

same in 2050, common sowing density of eight plants m^{-2} and no nitrogen limitation were used in the final set of simulations to compare the baseline period and future climate scenarios.

Modeling sowing and harvesting dates. Sowing dates were simulated in each field as the first day from January to May in which the frequency of frost was <5% in the following 10 d (calculated over 36 y in each site). The same rule was used for the 2050 climate scenarios. Harvest date was simulated as occurring after physiological maturity, on the first day when soil water content of the 0- to 30-cm top layer was below 90% saturation. The latter rule simulated the impossibility for harvester machines to enter into the considered field because of an insufficient load-bearing capacity. The model simulated a total yield loss if harvest could not happen before November 1, due to the high risk of ear fall and diseases, combined with the necessity for farmers to sow the next winter crop at that time.

Two watering regimes were simulated in each site, either rainfed or with systematic watering until field capacity over the entire soil profile every 3rd day. The optimums for each of these cultivation practices were calculated for each combination of site, year, scenario, GCM, watering regime, and option for TE. In simulations, we considered one single optimum for all studied years, simulating the fact that farmers can estimate frequencies at each site but cannot forecast climatic conditions for adjusting decisions to individual years.

Simulations and upscaling. The climate scenarios in 2050 were simulated at each site by using the stochastic weather generator LARS-WG (32) and were based on climate projections from the CMIP5 ensemble with RCPs 4.5 and 8.5 (487 and 541 ppm CO_2 in 2050, respectively) and six GCMs, namely GFDL-CM3, HadGEM2-ES, MIROC5, MPI-ESM-MR, CMCC-CM, and MIROC-ESM. The respective positions of these GCMs are compared in *SI Appendix*, Fig. S9 to 18 GCMs from the CMIP5 ensemble in terms of changes in precipitation, VPD, relative humidity, and in mean temperature calculated over land in Northern and Southern Europe. In Southern Europe, GFDL-CM3 is the hottest and nearly the driest GCM from the CMIP5 ensemble. One-hundred years of daily weather data were generated for each combination of site, RCP, and GCM.

A total of 2,897,136 crop simulations were run (for the baseline period: 2 managements × 2 irrigations scenarios × 31 accessions × 59 sites × 36 y; for climate scenarios: 2 scenarios × 6 GCMs × 2 irrigations scenarios × 31 accessions × 59 sites × 30 y × 2 options for TE). To upscale results from sites to each country, simulated data under full-irrigation and rainfed scenarios were weighted for each site by the proportion of irrigated maize fields in the area from the JRC database, data originally from Siebert et al. (36) (*SI Appendix*, Table S1). Results were then averaged at country level. To upscale to European level, results at country levels were multiplied by the area of maize cultivation in each site, based on the 25 × 25 km grid cell of the Eurostat database on year 2010.

ACKNOWLEDGMENTS. We thank Josiane Lorgeou (Arvalis) and Brigitte Gouesnard (INRA) for their contributions to the experiments. This work was supported by the European project FP7-244374 (DROPS), and the Agence Nationale de la Recherche projects ANR-10-BTBR-01 (Amaizing) and ANR-11-INBS-0012 (Phenome). Rothamsted Research receives strategic funding from the Biotechnology and Biological Sciences Research Council.

1. Asseng S, et al. (2015) Rising temperatures reduce global wheat production. *Nat Clim Chang* 5:143–147.
2. Cammarano D, et al. (2016) Using historical climate observations to understand future climate change crop yield impacts in the Southeastern US. *Clim Change* 134:311–326.
3. Xu H, Twine TE, Girvetz E (2016) Climate change and maize yield in Iowa. *PLoS One* 11:e0156083.
4. Yang CY, Fraga H, Van Ieperen W, Santos JA (2017) Assessment of irrigated maize yield response to climate change scenarios in Portugal. *Agric Water Manage* 184:178–190.
5. Zhang Y, Zhao YX, Chen SN, Guo JP, Wang EL (2015) Prediction of maize yield response to climate change with climate and crop model uncertainties. *J Appl Meteorol Climatol* 54:785–794.
6. Urban DW, Sheffield J, Lobell DB (2015) The impacts of future climate and carbon dioxide changes on the average and variability of US maize yields under two emission scenarios. *Environ Res Lett* 10:045003.
7. Fischer EM, Knutti R (2012) Robust projections of combined humidity and temperature extremes. *Nat Clim Chang* 3:126–130.
8. Lobell DB (2014) Climate change adaptation in crop production: Beware of illusions. *Global Food Secur* 3:72–76.
9. Moore FC, Lobell DB (2015) The fingerprint of climate trends on European crop yields. *Proc Natl Acad Sci USA* 112:2670–2675.
10. Butler EE, Huybers P (2013) Adaptation of US maize to temperature variations. *Nat Clim Chang* 3:68–72.
11. Challinor AJ, et al. (2014) A meta-analysis of crop yield under climate change and adaptation. *Nat Clim Chang* 4:287–291.
12. Moore FC, Lobell DB (2014) Adaptation potential of European agriculture in response to climate change. *Nat Clim Chang* 4:610–614.
13. White JW, Hoogenboom G, Kimball BA, Wall GW (2011) Methodologies for simulating impacts of climate change on crop production. *Field Crops Res* 124:357–368.
14. Zimmermann A, et al. (2017) Climate change impacts on crop yields, land use and environment in response to crop sowing dates and thermal time requirements. *Agric Syst* 157:81–92.
15. Bouchet S, et al. (2013) Adaptation of maize to temperate climates: Mid-density genome-wide association genetics and diversity patterns reveal key genomic regions, with a major contribution of the Vgt2 (ZCN8) locus. *PLoS One* 8:e71377.
16. Buckler ES, et al. (2009) The genetic architecture of maize flowering time. *Science* 325:714–718.
17. Romero Navarro JA, et al. (2017) A study of allelic diversity underlying flowering-time adaptation in maize landraces. *Nat Genet* 49:476–480.
18. Salvi S, et al. (2007) Conserved noncoding genomic sequences associated with a flowering-time quantitative trait locus in maize. *Proc Natl Acad Sci USA* 104:11376–11381.
19. Zheng B, Chenu K, Fernanda Dreccer M, Chapman SC (2012) Breeding for the future: What are the potential impacts of future frost and heat events on sowing and flowering time requirements for Australian bread wheat (Triticum aestivum) varieties? *Glob Chang Biol* 18:2899–2914.
20. Debieu M, et al. (2013) Co-variation between seed dormancy, growth rate and flowering time changes with latitude in Arabidopsis thaliana. *PLoS One* 8:e61075.
21. Li YX, et al. (2016) Identification of genetic variants associated with maize flowering time using an extremely large multi-genetic background population. *Plant J* 86:391–402.
22. Li D, et al. (2016) The genetic architecture of leaf number and its genetic relationship to flowering time in maize. *New Phytol* 210:256–268.
23. Tardieu F (2012) Any trait or trait-related allele can confer drought tolerance: Just design the right drought scenario. *J Exp Bot* 63:25–31.
24. Harrison MT, Tardieu F, Dong Z, Messina CD, Hammer GL (2014) Characterizing drought stress and trait influence on maize yield under current and future conditions. *Glob Chang Biol* 20:867–878.
25. Hammer GL, et al. (2010) Adapting APSIM to model the physiology and genetics of complex adaptive traits in field crops. *J Exp Bot* 61:2185–2202.
26. Chenu K, et al. (2008) Short-term responses of leaf growth rate to water deficit scale up to whole-plant and crop levels: An integrated modelling approach in maize. *Plant Cell Environ* 31:378–391.
27. Lacube S, et al. (2017) Distinct controls of leaf widening and elongation by light and evaporative demand in maize. *Plant Cell Environ* 40:2017–2028.
28. IPCC (2007) Autonomous adaptions. *Climate Change 2007: Impacts, Adaptation, and Vulnerability*. Contribution of Working Group II to the Fourth Assessment Report of the Intergovernmental Panel on Climate Change, eds Parry M, Canziani O, Palutikof J, van der Linden P, Hanson C (Cambridge Univ Press, New York).
29. JRC, IES, MARS (2015) JRC Database Agri4cast 2015-1.0. ed JRC (Joint Research Centre, Ispra, Italy). Available at agri4cast.jrc.ec.europa.eu/DataPortal/Index.aspx. Accessed November, 2016.
30. JRC (2016) European commission. Eurostat database. Available at ec.europa.eu/eurostat/web/agriculture/data/database. Accessed November, 2016.
31. Semenov MA, Stratonovitch P (2010) Use of multi-model ensembles from global climate models for assessment of climate change impacts. *Clim Res* 41:1–14.
32. Semenov MA, Stratonovitch P (2015) Adapting wheat ideotypes for climate change: Accounting for uncertainties in CMIP5 climate projections. *Clim Res* 65:123–139.
33. Lobell DB, et al. (2015) The shifting influence of drought and heat stress for crops in northeast Australia. *Glob Chang Biol* 21:4115–4127.
34. Kimball BA (2016) Crop responses to elevated CO2 and interactions with H2O, N, and temperature. *Curr Opin Plant Biol* 31:36–43.
35. Kim SH, et al. (2006) Canopy photosynthesis, evapotranspiration, leaf nitrogen, and transcription profiles of maize in response to CO2 enrichment. *Glob Chang Biol* 12:588–600.
36. Siebert S, et al. (2005) Development and validation of the global map of irrigation areas. *Hydrol Earth Syst Sci* 9:535–547.
37. Rezaei EE, Siebert S, Hüging H, Ewert F (2018) Climate change effect on wheat phenology depends on cultivar change. *Sci Rep* 8:4891.
38. Tardieu F, Cabrera-Bosquet L, Pridmore T, Bennett M (2017) Plant phenomics, from sensors to knowledge. *Curr Biol* 27:R770–R783.
39. Challinor AJ, Koehler AK, Ramirez-Villegas J, Whitfield S, Das B (2016) Current warming will reduce yields unless maize breeding and seed systems adapt immediately. *Nat Clim Chang* 6:954–958.
40. Olmstead AL, Rhode PW (2011) Adapting North American wheat production to climatic challenges, 1839-2009. *Proc Natl Acad Sci USA* 108:480–485.
41. Arvalis (2016) Choisir et Decider. Préconisations régionales 2016. Available at https://www.arvalis-infos.fr/file/galleryelement/pj/1c/49/26/b7/choisirmais2016_aquitaine_midipyrenees3339212978836866791.pdf. Accessed November, 2017.
42. Rezaei EE, Siebert S, Ewert F (2017) Climate and management interaction cause diverse crop phenology trends. *Agric For Meteorol* 233:55–70.
43. IPCC (2014) Summary for policymakers. *Climate Change 2014: Impacts, Adaptation, and Vulnerability. Part A: Global and Sectoral Aspects*. Contribution of Working Group II to the Fifth Assessment Report of the Intergovernmental Panel on Climate Change, eds Field CB, etc. (Cambridge Univ Press, New York), pp 1–32.

New Phytologist

Temperature responses of developmental processes have not been affected by breeding in different ecological areas for 17 crop species

Boris Parent[1] and François Tardieu[2]

[1]Australian Centre for Plant Functional Genomics, PMB1, Glen Osmond, SA 5064, Australia; [2]INRA, UMR759 Laboratoire d'Ecophysiologie des Plantes sous Stress Environnementaux. Place Viala, F-34060 Montpellier, France

Author for correspondence:
François Tardieu
Tel: +33 04 99 61 26 32
Email: francois.tardieu@supagro.inra.fr

Received: *30 November 2011*
Accepted: *19 January 2012*

New Phytologist (2012) **194**: 760–774
doi: 10.1111/j.1469-8137.2012.04086.x

Key words: development, growth, genetic variability, maize (*Zea mays*), response, rice (*Oryza* spp.), temperature, wheat (*Triticum aestivum*).

Summary

- Rates of tissue expansion, cell division and progression in the plant cycle are driven by temperature, following common Arrhenius-type response curves.
- We analysed the genetic variability of this response in the range 6–37°C in seven to nine lines of maize (*Zea mays*), rice (*Oryza* spp.) and wheat (*Triticum aestivum*) and in 18 species (17 crop species, different genotypes) via the meta-analysis of 72 literature references.
- Lines with tropical or north-temperate origins had common response curves over the whole range of temperature. Conversely, appreciable differences in response curves, including optimum temperatures, were observed between species growing in temperate and tropical areas.
- Therefore, centuries of crop breeding have not impacted on the response of development to short-term changes in temperature, whereas evolution over millions of years has. This slow evolution may be a result of the need for a synchronous shift in the temperature response of all developmental processes, otherwise plants will not be viable. Other possibilities are discussed. This result has important consequences for the breeding and modelling of temperature effects associated with global changes.

Introduction

Lines and species of crop plants have evolved and been selected in different latitudes and altitudes, thereby generating differences in temperature adaptation via a large range of mechanisms (Atkin *et al.*, 2006). Indeed, gradients of latitude are accompanied by gradients of traits, such as the duration of the plant cycle, specific leaf area and survival from heat or cold stresses (Kratsch & Wise, 2000; Atkin *et al.*, 2006; Barnabas *et al.*, 2008; Penfield, 2008). The analysis of the genetic variability of the response of crop plants to temperature is therefore essential in a context in which climate changes increase the risk of yield loss because of high temperatures, without necessarily reducing the risk of exposure to low temperatures (Battisti & Naylor, 2009; Lobell *et al.*, 2011).

The analysis of short-term response curves differs from the study of the irreversible effects at high or low temperature, which require several weeks to become evident (Wise *et al.*, 1983; Bukovnik *et al.*, 2009; Gorsuch *et al.*, 2010). It involves the quantitative analysis of the short-term effects of changes in temperature over a large range, not limited to its low or high ends, in which effects are reproducible for a given line and a given range of conditions, are reversible and not dependent on the temperature history of the plant, and are independent of the intrinsic value of the studied variable measured at a standard temperature. When these conditions are fulfilled, meta-analyses of a series of experiments result in response curves to temperature or other environmental variables that allow the comparison of life kingdoms (Gillooly *et al.*, 2001; Dell *et al.*, 2011) or fitness between species in ecological studies (Poorter *et al.*, 2010). They also allow the study of quantitative genetics based on response parameters (Reymond *et al.*, 2003; Yin *et al.*, 2004) or analysis of the coordination between different mechanisms under fluctuating conditions (Parent *et al.*, 2010b; Tardieu *et al.*, 2011).

Following pioneering studies that compared the temperature responses of phyllochron and leaf elongation rate (LER) (Ong, 1983a,b; Warrington & Kanemasu, 1983a,b), we have shown recently that the germination rate, cell division rate, leaf initiation rate, LER and the reciprocal of the duration of phenological phases follow a common response to temperature after normalization by their absolute rates at 20°C (Parent *et al.*, 2010b). This implies that these processes have similar temperature responses. Conversely, the responses of *in vitro* enzyme activities and of net photosynthesis differ from those mentioned above (Parent *et al.*, 2010b). It is therefore relevant to analyse jointly the temperature responses of rates involved in the progression of plant development or in expansive growth (called 'developmental rates' hereafter), independent of those involved in plant metabolism and biomass production.

The response to temperature of enzyme activities has been described by the equation of Johnson *et al.* (1942), adequately extended to processes as diverse as the growth of bacteria (Johnson & Lewin, 1946), parameters of photosynthesis (Farquhar *et al.*, 1980), insect development (Sharpe & Demichele, 1977), plant development (Feng *et al.*, 1990; Parent *et al.*, 2010b) and 1072 physiological and ecological traits in microbes, animals and plants (Dell *et al.*, 2011).

$$F(T) = \frac{A\,T e^{\left(\frac{-\Delta H_A^{\ddagger}}{RT}\right)}}{1 + e^{\left[\frac{\Delta S_D}{R} - \frac{\Delta H_D}{RT}\right]}} \qquad \text{Eqn 1}$$

(Johnson *et al.*, 1942) ($F(T)$ is the considered rate, T is the temperature (K), $\Delta H_A^{\ddagger}$ (J mol^{-1}) is the enthalpy of activation of the reaction and determines the curvature at low temperature (Supporting Information Fig. S1a), ΔH_D (J mol^{-1}) and ΔS_D (J mol^{-1} K^{-1}) are the enthalpy and entropy of enzyme inactivation at high temperature and A is the trait scaling coefficient). When describing integrated variables instead of enzyme activities, the parameters lose their biochemical nature, and so a more intuitive modified version was preferred:

$$F(T) = \frac{A\,T e^{\left(\frac{-\Delta H_A^{\ddagger}}{RT}\right)}}{1 + \left[e^{\left(\frac{-\Delta H_A^{\ddagger}}{RT}\right)}\right]^{\alpha\left(1 - \frac{T}{T_0}\right)}} \qquad \text{Eqn 2}$$

where α (dimensionless) is the ratio $\Delta H_D/\Delta H_A^{\ddagger}$ in Eqn 1 and determines how sharp is the decrease in rate at high temperature (Fig. S1c). T_0 (K) equals the ratio $\Delta H_D/\Delta S_D$ in Eqn 1. It is the temperature at which half of the system is in an inactive state (Fig. S1b) and determines the temperature at which the rate is at a maximum (T_{opt}, Methods S1). After normalization by the rate at 20°C (to scale different processes and species and to compare them independently of their absolute values; Parent *et al.*, 2010b), parameter A is not free and depends on $\Delta H_A^{\ddagger}$, T_0 and α.

The analysis of the genetic variability of the temperature response of the developmental rates will provide essential elements to understand the thermal adaptation of contrasting genotypes grown in common ranges of temperature. A very low or nonexistent genetic variability between species or lines originating from cold or warm areas may suggest that this relationship is based on an immutable law (Eqn 2) with parameters based on physical constraints. The existence of genetic variability would indicate that mutations on key genes can substantially alter the regulatory pathways that govern the temperature response of developmental rates (McClung & Davis, 2010). Although large-scale comparisons between the temperature responses of different species and life kingdoms have been studied for enzyme activities (Campbell *et al.*, 2007) and metabolic rates (Gillooly *et al.*, 2001), such comparisons are not available for developmental processes. In this study, we performed the following investigations:

- We tested the working hypotheses for the analysis of temperature responses, that is, that these responses are reproducible and reversible without after-effects of previous temperature, and that different developmental processes have similar temperature responses after normalization by their absolute rate at a standard temperature.
- We tested whether lines originating from cold or warm areas have different temperature responses; this was performed for lines of maize (*Zea mays*), wheat (*Triticum aestivum*) and rice (*Oryza*) with diverse breeding histories and ecological origins, from temperate to tropical, by testing whether the parameters of Eqn 2 were common or differed between the lines of one species.
- We extended our analysis to the diversity of responses in 18 species (17 major crop species comprising the 14 most cultivated species in the world (http://faostat.fao.org; Table 1) and *Arabidopsis thaliana*) by compiling literature data. We tested the commonality of response curves by asking whether one or more parameter(s) of Eqn 2 could be considered as common to several species and, within each species, to different genotypes.

Description

Genetic material

Eight maize (*Zea mays* L.) lines were used in the experiments, originating from the Caribbean zone (latitudes 10–20°), tropical areas (lines CML69 and CML444; http://apps.cimmyt.org/english/wps/obtain_seed/cimmytCMLS.htm) or tropical highlands (line F331); the US corn belt (latitudes 30–40°; dent lines B73, A188 and Io); and Canada, grown since then in Europe in latitudes 40–50° (flint lines UH007 and F2). These lines are genetically very distant (Camus-Kulandaivelu *et al.*, 2006; A. Charcosset, pers. comm.) and were bred in different thermal environments (average temperature of 19°C in temperate environments, for example, north USA, or 24°C in tropical environments; Lobell *et al.*, 2011). The hybrid Io × *F2* (Dea) was considered in the same analysis.

The seven studied rice lines belonged to two species, *Oryza glaberrima* Steud. (CG14) and *Oryza sativa* L. (other cultivars), and three subfamilies of *Oryza sativa*: temperate *japonica* (Nipponbare), tropical *japonica* (Azucena, Moroberekan) and *indica* (Apo, Vandana and IR64). They originated from temperate (Nipponbare; Koumura, 1972) or tropical (others) regions. They therefore experienced different thermal environments during their breeding history, from nearly constant high temperatures in tropical areas (23–31°C in the Philippines; Peng *et al.*, 2004) to large temperature amplitudes (5–30°C in Japan; http://www.knowledgebank.irri.org). These lines also differ in their year of release, from traditional cultivars (Azucena), cultivars developed during the green revolution (IR64) in the 1980s (Moroberekan) and recently released cultivars (Vandana, Apo).

Seven wheat (*Triticum aestivum* L.) lines were analysed (Drysdale, Gladius, Kukri, Excalibur, RAC875, Chinese Spring and Bob White). Chinese Spring is a Chinese landrace, selected in a cool climate (average temperature *c.* 10°C; Lobell *et al.*, 2011), whereas South Australian lines were selected under high thermal

Table 1 Origin of the data for the different processes in 18 species

Species	Origin of data	Process
Maize	New data	Leaf elongation
	Database	Leaf elongation
	Parent *et al.* (2010b)	Germination
	Barlow & Boersma (1972)	Seedling elongation
	Ben-Haj-Salah & Tardieu (1995)	Cell division
	Blacklow (1972)	Shoot initiation
		Shoot elongation
		Radicle elongation
		Radicle initiation
	Hesketh & Warrington (1989)	Development (primordium–tip)
		Development (tip–ligule)
		Growth duration^{-1}
		Leaf elongation
		Leaf appearance
	Lehenbauer (1914)	Seedling elongation
	Tollenaar *et al.* (1979)	Leaf appearance
	Warrington & Kanemasu (1983a)	Development (sowing–anthesis)
		Development (sowing–tassel initiation)
		Emergence
	Warrington & Kanemasu (1983b)	Leaf appearance
		Leaf initiation
	Weaich *et al.* (1996)	Coleoptyl elongation
		Internode elongation
Rice	New data	Leaf elongation
	Database	Leaf elongation
	Parent *et al.* (2010b)	Germination
	Summerfield *et al.* (1992)	Development (sowing–flowering)
	Yin & Kropff (1996)	Leaf appearance (f5–f6)
	Yin *et al.* (1996)	Development (sowing–flowering)
Wheat	New data	Emergence
		Seedling elongation
		Germination
	Addae & Pearson (1992)	Emergence
		Germination
	Cutforth *et al.* (1992)	Emergence
	Dejong & Best (1979)	Emergence
		Coleoptyl elongation
		Internode elongation
	Gallagher *et al.* (1979)a	Leaf elongation
	Kemp & Blacklow (1982)	Leaf elongation
	Lafond & Baker (1986)	Germination
	Lafond & Fowler (1989)	Germination
	Lindstrom *et al.* (1976)	Emergence
Arabidopsis thaliana	Parent *et al.* (2010b)	Germination
	Granier *et al.* (2002)	Growth duration^{-1}
		Leaf expansion
		Leaf initiation
	Orbovic & Poff (2007)	Seedling elongation
Soybean	Covell *et al.* (1986)	Germination
	Hesketh *et al.* (1973)	Development (3rd trifoliate–flower)
		Development (planting–trifoliate)
		Development (unifoliate–trifoliate)
		Trifoliate production
	Lawn & Hume (1985)	Node production
		Pod production
Sorghum	Lafarge *et al.* (1998)	Leaf elongation
	Lawlor *et al.* (1990)	Germination
	Wade *et al.* (1993)	Germination
Millet	Garciahuidobro *et al.* (1982)	Germination
	Mohamed *et al.* (1988a)	Germination
	Mohamed *et al.* (1988b)	Leaf elongation
	Ong & Monteith (1985)	Root elongation
	Ong (1983a)	Leaf appearance
	Ong (1983b)	Leaf elongation
	Pearson (1975)	Leaf appearance
Cotton	Arndt (1945)	Cotyledon emergence
		Hypocotyl elongation
		Primary root elongation
	Hesketh *et al.* (1972)	Development (flower–boll)
		Development (square–flower)
		Relative leaf growth
		Plastochrons (flower, square, leaf)
	Mutsaers (1983)	Relative growth
	Reddy *et al.* (1997)	Relative internode expansion
		Relative leaf expansion
		Leaf unfolding
Canola	Marshall & Squire (1996)	Germination
	Morrison *et al.* (1989)	Development (sowing–maturity)
	Singh *et al.* (2008)	Pollen tube elongation
		Pollen germination
	Vigil *et al.* (1997)	Emergence
Sunflower	Chimenti *et al.* (2001)	Embryo growth
	Gay *et al.* (1991)	Hypocotyl elongation
		Root growth
		Germination
	Villablobos & Ritchie (1992)	Leaf appearance
Peanut	Kakani *et al.* (2002)	Pollen tube elongation
	Mohamed *et al.* (1988a)	Germination
	Prasad *et al.* (2006)	Development (sowing–V2 stage)
		Emergence
Sugar cane	Campbell *et al.* (1998)	Node production
	Inmanbamber (1994)	Plant expansion
	Mongelar & Mimura (1972)	Spindel elongation
Cassava	Akparobi *et al.* (2000)	Growth duration^{-1}
		Leaf initiation
		Leaf opening
	Keating & Evenson (1979)	Emergence
Potato	Benoit *et al.* (1986)	Stem elongation
	Fleisher & Timlin (2006)	Cell expansion and division
		Growth
	Fleisher *et al.* (2006)	Leaf appearance
	Kirk & Marshall (1992)	Leaf elongation
		Leaf appearance
Cowpea	Covell *et al.* (1986)	Germination
	Craufurd *et al.* (1996a)	Emergence
		Germination
	Craufurd *et al.* (1996b)	Development (sowing–flowering)
	Craufurd *et al.* (1996c)	Development (sowing–flowering)
	Craufurd *et al.* (1997)	Leaf appearance
	Hadley *et al.* (1983)	Development (sowing–flowering)

Table 1 (Continued)

Species	Origin of data	Process	Species	Origin of data	Process
Barley	New data	Emergence			Development (sowing–ripe pods)
		Seedling elongation			Development (sowing–visible bud)
		Germination	Common bean	Moss & Mullett (1982)	Seedling elongation
	Ellis *et al.* (1987)	Germination		Scully & Waines (1987)	Germination
	Gallagher & Biscoe (1979)	Leaf elongation		White & Montes (1993)	Germination
			Cauliflower	Olesen & Grevsen (1997)	Leaf area expansion
				Wurr *et al.* (1990)	Curd growth

Information on exact processes, materials and methods, and genotypes is available in the original papers.

amplitude (RAC875, Excalibur, Gladius, temperature from 3 to 40°C, average temperature *c.* 16°C, records from ACPFG weather stations). Excalibur and RAC875 are considered as heat tolerant and Kukri as heat sensitive (Izanloo *et al.*, 2008; Bukovnik *et al.*, 2009). Lines differ in their year of selection, from the old cultivars Chinese Spring (1940) and Bob White (1970) to recent varieties Drysdale (2002) and Gladius (2008). A barley line (Golden Promise) was added to this series to analyse the behaviour of another species from the Triticeae tribe.

LER in maize and rice subjected to short-term temperature changes

All measurements of LER were performed during the night, under well-watered conditions with wet air (air vapour pressure deficit maintained under 0.8 kPa) to avoid confusion between the effects of temperature and of evaporative demand (Ben-Haj-Salah & Tardieu, 1997). Data presented in this study are the result of a meta-analysis of several independent experiments with similar protocols.

Maize and rice plants were grown in polyvinylchloride (PVC) columns in a glasshouse with temperature fluctuating in the range 18–32°C, light in the range 10–20 mol d^{-1} m^{-2} and air vapour pressure deficit in the range 1–2.5 kPa. Soil was maintained at a water potential above − 0.05 MPa via irrigation with a 1/10 Hoagland-type nutrient solution controlled by individual pot weight (http://bioweb.supagro.inra.fr/phenodyn/). Temperatures taken into account in this article are the meristem temperatures, measured with thermocouples inserted near the meristem of at least five plants (http://bioweb.supagro.inra.fr/phenodyn). Meristem temperatures were averaged every 15 min and stored in the database PhenodynDB (http://bioweb.supagro.inra.fr/phenodyn), together with air temperature, irradiance, air vapour pressure deficit and soil water content. At the six-leaf stage, plants were transferred to the growth chamber under different temperature conditions. Environmental conditions were measured using the same methods as in the glasshouse. Typical temperature scenarios are presented in Fig. 1(c). They were intentionally varied between days and plants to avoid any confounding effect of sequences of temperature (e.g. the step at 16°C that would systematically follow a step at 28°C). In 10 plants of lines B73, CML444, A188, F-2 and UH007, LER was measured at 20°C after periods of 4 h at 6 or 35°C in order to test the possible after-effect of low or high temperature.

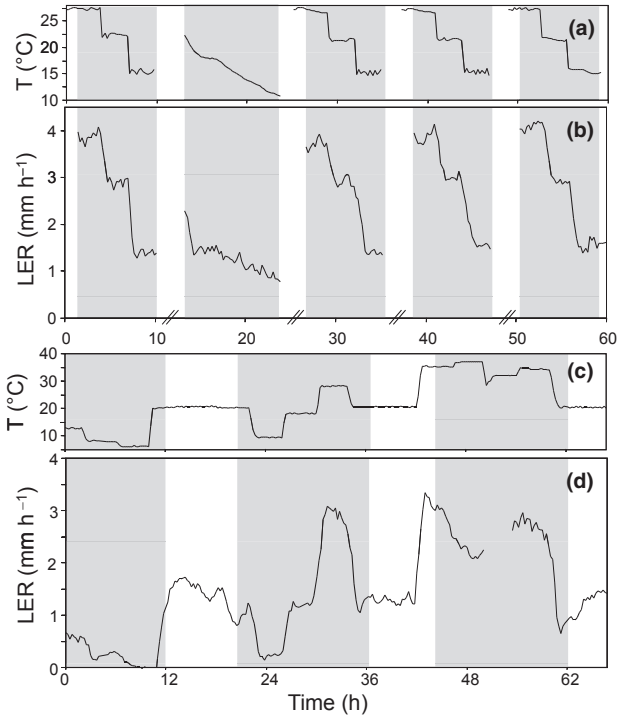

Fig. 1 Time courses of meristem temperature (*T*) and leaf elongation rate (LER) of the maize (*Zea mays*) line CML444. Grey panels indicate night periods. (a,b) Plants were placed in the growth chamber under a controlled environment, transferred to the glasshouse for a cold night (second night) and then transferred back to the growth chamber (third night) under a similar temperature scenario. (c,d) Plants were placed in the growth chamber under a wide range of temperatures from 6 to 37°C. It should be noted that temperature scenarios changed every day.

The temperature control of the growth chamber was based on the meristem temperature. Relative humidity, light intensity and air temperature were measured as in Parent *et al.* (2010b). The night temperature varied in steps of 3–4 h (Fig. 1c). LER was measured in leaf 6 with rotating displacement transducers (http://bioweb.supagro.inra.fr/phenodyn/) during the period with linear elongation (i.e. 2 d after leaf appearance in rice, Parent *et al.*, 2009; 5–6 d in maize, Sadok *et al.*, 2007), and after stabilization of temperature and LER (usually the last 2 h of each temperature step). A cloud of points of LER vs temperature, corresponding to one line in one experiment, can be seen in Fig. S2(a).

In addition, glasshouse experiments with maize or rice were included in the dataset, in particular that presented in Fig. 1(a) in maize. During the latter experiment, plants were transferred between the growth chamber and the glasshouse in order to test the after-effect of a cold night with continuously decreasing temperature. Each data point for regression is a coupled value of the meristem temperature and LER for 3 h. A cloud of points corresponding to one line in several experiments can be seen in Fig. S2b. A total of 2630 coupled values of LER and temperature were collected for maize and 598 for rice in growth chamber and glasshouse experiments. Finally, a dataset was added, for hybrid Dea only, comprising measurements of the cell division rate in leaves (Ben-Haj-Salah & Tardieu, 1995).

Germination rate at constant temperature in wheat, barley, maize and rice

The germination rate was measured under constant temperature in the seven above-mentioned wheat lines, one barley line (Golden Promise), one maize hybrid (Dea) and two rice lines (Azucena and IR64). Seeds were sown in Petri dishes (100 seeds per Petri dish) lined with saturated Whatman filter paper and placed under different temperatures (4, 9, 15.5, 20, 24.5, 28 and 35°C). Germination was scored every 8 h (6 h in rice and maize) for 2 d, every 12 h for the next 3 d, and every 1 d after that. The appearance of a radicle was scored as a germinated seed. The time for 50% cumulative germination was determined by regression on the progression curves. Data points were not taken into account when fewer than 50% of seeds germinated.

Emergence rate and seedling elongation rate at constant temperature in wheat and barley

Seedling elongation rate was measured in the wheat and barley lines presented above. Twelve seeds per line and per tested temperature were sown at a depth of 1 cm in pots filled with coco peat. Pots were placed in trays with 1 cm of free water and kept in the dark, with saturated soil and air. The appearance of coleoptiles at the soil surface was scored, and the length of the emerged coleoptiles was measured every 12 h during 5 d, and every 1 d thereafter. The time for 50% cumulative emergence was determined by regression on the progression curves. Data points were not taken into account when fewer than 50% of the initial number of seeds emerged. The coleoptile elongation rate was calculated by linear regression between 10 and 100 mm length for wheat (common linear phase in all lines) and between 10 and 60 mm length for barley.

Meta-analysis of lines originating from our database

Normalization and pooling of data Each process rate (e.g. LER, germination rate, etc.) was normalized by its mean value at 20°C (Parent *et al.*, 2010b), thereby allowing joint analysis for different processes, regardless of dimensions, units or absolute values. The normalization at 20°C was chosen because data at 20°C are available in most publications, species and processes. The rate at 20°C was determined via a linear regression performed in the vicinity of 20°C (e.g. from 18 to 22°C). Because information criteria for model comparison are sensitive to the number of data points, analyses were performed after pooling data points in 15–16 groups (example in Fig. S2c).

Test of differences in model parameters The model presented in Eqn 2 has three parameters (because A depends on $\Delta H_A^{\ddagger}$, T_0 and α, Methods S2). In order to determine which parameters are common/differ between lines, the model with three parameters (called M.3 hereafter) was compared with seven models in which one, two or three parameters were common to the studied lines (Table 2). Three models had two free parameters (M.2a, M.2b and M.2c) and one parameter common to the studied lines. Three models (M.1a, M.1b and M.1c) had one free parameter and two parameters common to the studied lines. Finally, one model (M.0) had no free parameter, thereby resulting in a common temperature response for all lines.

Calculation of model parameters Parameters of individual response curves were calculated using the nonlinear regression function *nls* of the R language (R Development Core Team, 2005). Depending on the number of free/fixed parameters, different procedures were used to ensure convergence in the fitting procedure (Fig. S3).

Model comparison We used several indicators to compare nonlinear models, including the root-mean-square error (RMSE) and the coefficient of variation of the RMSE (CV_{RMSE}). We also used indicators that add a penalty to the number of estimated parameters, thereby avoiding overfitting, namely the Akaike information criterion (AIC; Akaike, 1974; function *AIC*() in R software) and the Bayesian information criterion (BIC; Schwarz, 1978; function *BIC*()). The best model according to these indicators is that with the lowest values of BIC and AIC. The Akaike weights (Akaike, 1978) indicate the probability for one model to be the best model given the dataset. Here, we calculated these weights for BIC values (w_{BIC}).

Table 2 Number of free/fixed parameters in each of the eight studied models

Model	No. of free parameters	$\Delta H_A^{\ddagger}$	T_0	α
M.3 (Eqn 2)	3	Free	Free	Free
M.2a	2	Fixed	Free	Free
M.2b	2	Free	Free	Fixed
M.2c	2	Free	Fixed	Free
M.1a	1	Fixed	Free	Fixed
M.1b	1	Fixed	Fixed	Free
M.1c	1	Free	Fixed	Fixed
M.0	0	Fixed	Fixed	Fixed

The three parameters are those of Eqn 2. In each model, a free parameter is calculated individually for each genotype or species. A fixed parameter is common to all considered genotypes or species.

For an easier interpretation of these criteria, we compared model indicators with that of model M.3. ΔCV is the difference between CV_{RMSE} of one model and that of model M.3, and is interpreted as the additional error when fixing parameters. With regard to experimental errors and the difference targeted between lines, an additional error of 5% was accepted for models with fewer parameters. ΔAIC and ΔBIC are the differences in values between the considered model and model M.3. ΔAIC and ΔBIC of < 5 were accepted for models with fewer parameters compared with model M.3.

Sensitivity analysis on model comparison The sensitivity of statistical indicators to changes in the temperature response was tested using the procedure described in Fig. S4. New datasets were created by modifying that of maize. To test a shift in the whole response curve, including T_{opt}, all temperatures in the original dataset were shifted by a step of 1°C between − 2 to + 2°C in relation to the original values (for example, the temperature was lowered by −1°C for each coupled value of rate/temperature; Fig. S4c,d). To test a difference in the sensitivity of rates to high temperature, rates above the optimum temperature were lowered or increased by a step of 5% from − 20% to + 20% in relation to the original values (e.g. for + 10%, all data points above 30.8°C were multiplied by 1.1; Fig. S4a,b). Each new dataset was compared with the original by calculating ΔBIC and ΔCV between model M.3 and model M.0.

Comparison of four species from our database Normalized data corresponding to different lines were pooled within each of the four tested species (maize, rice, wheat and *Arabidopsis thaliana*). We used a similar procedure to that explained above to compare lines, taking into account 13–20 groups of data per species. Parameter calculation and model comparison were carried out as described above for lines. To confirm the results of model comparison obtained with the Bayesian approach, a cascade of *F*-tests was carried out on the nested models (R function anova.nls()). The simplest model was accepted unless the test was significant ($P < 0.05$).

Comparison of 18 species from our database or from the literature

All other data were collected from the literature (Table 1), from tables or figures of the original papers. The positions of data points were recorded in figures by image analysis (software ImageJ (http://rsbweb.nih.gov/ij/)). In Covell *et al.* (1986) and Ellis *et al.* (1987), only the 50% germination rates were retained in the analysis. For the germination rates taken from Scully & Waines (1987), only the crop species were analysed. In Hadley *et al.* (1983), only the photoperiod insensitive lines were analysed. In Weaich *et al.* (1996), the coleoptile elongation rate was calculated as the reciprocal of the duration to reach a length of 15 mm. The internode elongation rate was calculated as the reciprocal of the duration to reach a length of 25 mm. In Summerfield *et al.* (1992), Yin & Kropff (1996) and Yin *et al.* (1996), only data obtained under constant temperature were used in the analysis.

Each dataset was normalized by the corresponding value at 20°C using the procedure described above. A pooling of the data resulted in 13–20 groups per species. For each model, the fixed parameter values were those of the four species analysed. Parameter values and model criteria were calculated as in the line analysis.

The optimum temperature T_{opt}, at which the rate is at a maximum, was calculated from model parameters (Methods S1):

$$\frac{1}{T_{opt}} = \frac{1}{T_0} + \frac{R}{\alpha \Delta H_A^{\ddagger}} \log\left(\frac{(\alpha - 1)\Delta H_A^{\ddagger} - R * 303}{\Delta H_A^{\ddagger} + R * 303}\right) \qquad \text{Eqn 3}$$

Confidence intervals of model parameters and T_{opt} were calculated by bootstrapping (1000 replicates).

Results

The working hypotheses for the analysis of temperature responses were fulfilled

The first condition mentioned in the Introduction is that a trait has a unique response to temperature over a large range of conditions for a given line of the studied species. This was the case when either similar or different temperature scenarios were applied on several days (Fig. 1a,b, days 1, 3, 4, 5, and Fig. S2a). Similar results were found in rice (Parent *et al.*, 2010b).

Second, the establishment of response curves requires that the temperature effect is reversible, that is, the rate at a given temperature is independent of previous temperatures during the experiment. This was the case for durations of exposure ranging from hours to days. Exposures to 6 or 34°C for 4 h (the duration of a typical peak of temperature in natural conditions) had no significant effect on LER at 20°C ($P = 0.6$; Figs 1c,d, S5a,b). In the same way, LER was unaffected by a previous long night at low temperature (Fig. 1a,b, night 2). This resulted in a unique response curve per line, regardless of plant, experiment and thermal history, even though absolute rates at a given temperature differed between lines (Fig. S2). Lines of rice showed a similar behaviour in this respect (data not shown).

The domain of validity of the response covered a large range of developmental processes. After normalization by the rate at 20°C, which allows one to scale different processes that have different units, the response to temperature in one line was common between several developmental processes in maize (hybrid Dea; Fig. 2a), rice (line Azucena; Fig. 2r) and wheat (variety Drysdale; Fig. 2j). A meta-analysis of 21 sources of information (Table 1) extended this conclusion to traits referring to leaves, roots or seedlings, growth rates, cell division rate, germination rate or reciprocal of duration of phenological phases. This led to a common response curve for all of these processes, exemplified in Fig. 3(b) for maize. It is noteworthy that processes associated with response times of a few days (e.g. phyllochron) showed similar response curves to those having a response time of minutes (e.g. elongation rates; Figs 2a, 3b), indicating that the responses of the processes studied here were essentially time independent in the range 6–37°C.

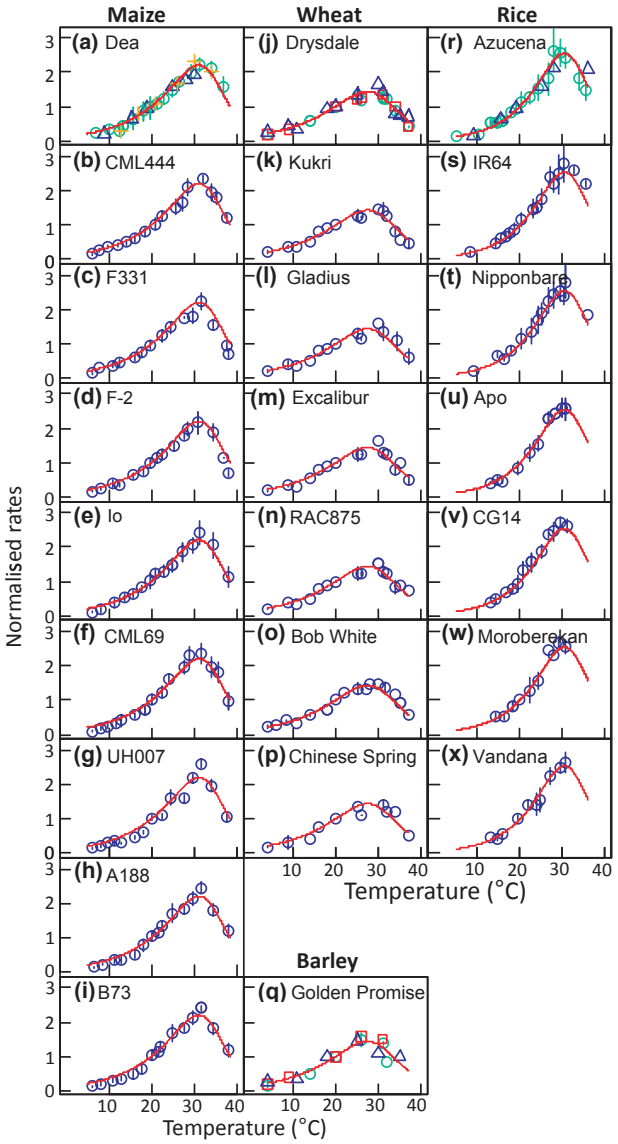

Fig. 2 Response curves to temperature of several rates involved in plant development in lines of maize (a–i), wheat (j–p), barley (q) and rice (r–x). Rates are normalized by their mean value at 20°C, set to unity. For each species, the red line corresponds to a common model for all genotypes (model M.0, Table 2). A common model applies to barley (q) and wheat (j–p). (a,j,r,q) The normalized responses to temperature of several developmental processes presented on the same graph. Green circles, leaf (a,r) or seedling (j,q) elongation rate; red squares, reciprocal of the duration from sowing to emergence; blue triangles, germination rate; orange circles, cell division rate. In all panels, blue circles represent the average of all studied processes. Other panels present the response of leaf elongation rate (maize and rice) or germination and seedling elongation (wheat). Error bars indicate standard deviation (SD).

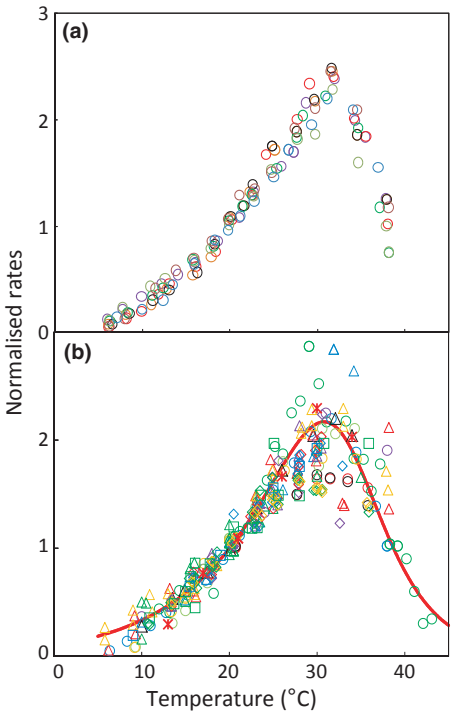

Fig. 3 Response curve to temperature of leaf elongation rate for nine maize (*Zea mays*) lines (a) and of several processes in a meta-analysis of literature data (b). Each process is normalized by its corresponding value at 20°C. The red line represents a common model for all processes and genotypes (M.0, Table 2). Regression parameters are summarized in Table 3. (a) Leaf elongation rate for genotypes: CML444, purple; CML69, red; B73, orange; A188, black; F2, cyan; F331, green; Io, brown; Dea, deep blue. (b) Temperature dependence of several developmental processes. Circles represent expansion processes: leaf elongation, new data (blue); coleoptile elongation from Weaich *et al.* (1996) (red); seedling elongation from Lehenbauer (1914) (cyan) and Barlow & Boersma (1972) (purple); internode elongation from Weaich *et al.* (1996) (black); shoot elongation from Blacklow (1972) (green); radicle elongation from Blacklow (1972) (yellow). Triangles represent organ initiation and appearance: radicle initiation from Blacklow (1972) (black); shoot initiation from Blacklow (1972) (blue); leaf initiation from Warrington & Kanemasu (1983b) (red); leaf appearance from Hesketh & Warrington (1989) (purple); leaf appearance from Warrington & Kanemasu (1983b) (yellow); leaf appearance from Tollenaar *et al.* (1979) (cyan). Diamonds represent development rate between two events: leaf primordium to leaf tip appearance from Hesketh & Warrington (1989) (purple); leaf tip appearance to ligulation from Hesketh & Warrington (1989) (red); growth duration from Hesketh & Warrington (1989) (blue); sowing to tassel initiation from Warrington & Kanemasu (1983a) (cyan); sowing to anthesis from Warrington & Kanemasu (1983a) (yellow). Squares represent germination and emergence: germination from Parent *et al.* (2010b) (blue); emergence from Warrington & Kanemasu (1983a) (turquoise). Stars represent cell division from Ben-Haj-Salah & Tardieu (1995).

Hence, response curves were established hereafter by considering data points originating from different thermal scenarios, different developmental processes and from our own experiments or from the literature. In the experiments presented below, most comparisons between lines were performed on the temperature response of LER.

The genetic variability was very low between lines originating from tropical or temperate regions, from different breeding generations and with different heat tolerances

In maize, the nine studied lines originating from various regions and climates (Caribbean zone, tropical highlands, US corn belt and temperate regions of Canada and Europe) were associated

with similar response curves (Fig. 2), almost indistinguishable over the whole range of temperature when plotted together (Fig. 3a). To identify putative differences between these curves, we tested whether one or more parameters of Eqn 2 could be considered as common to all lines. A model with three free parameters (model M.3, three parameters differing between lines) was compared with seven models with zero, one or two free parameters (Table 2). Statistical criteria indicated that the best model was model M.0, which considers that all three parameters are common to the nine studied lines (Fig. 4a,b and Table S1). Furthermore, CVs of errors increased by 2% only in model M.0 compared with the others, far from the 5% error that was considered as the limit in view of experimental errors (Fig. 4b). A sensitivity analysis showed that this procedure was able to detect a 1°C shift in the whole response curve towards higher or lower temperature (Fig. 4c,d). It also showed that we could detect a difference in rate of ± 10% in the range above T_{opt}, where precision was lower than in the range below T_{opt} (Fig. 4a,b). It can therefore be concluded that a unique response curve applied to maize lines with very different origins, to hybrid as well as to inbred lines. This conclusion can be extended to 23 lines described in the literature, with different origins and dates of release, including one line released in 1914 (Table 1, Fig. 3b). All lines had a response curve with common parameters to those calculated with our data (Fig. 3b).

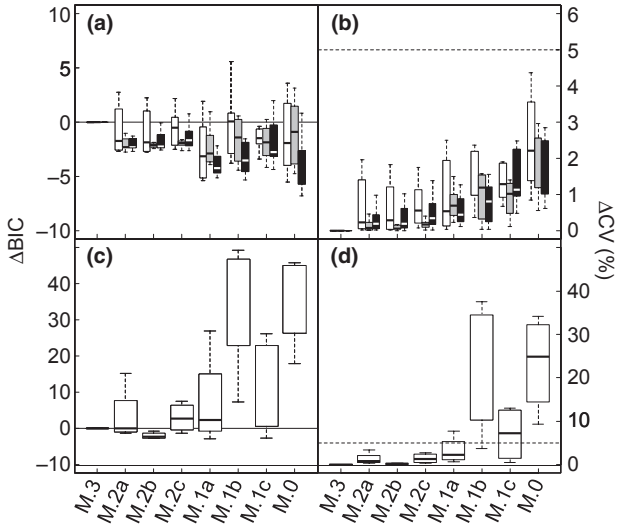

Fig. 4 Comparison of models presented in Table 2. (a,b) Comparison of models assuming that zero to three parameters differ between genotypes of each species. (a) Box-plot of the differences in the Bayesian information criterion (ΔBIC) between model M.3 and the seven other models for genotypes of maize (white), rice (grey) and wheat (black). The lowest values of ΔBIC indicate the best models. (b) Difference in coefficient of variation of the error (ΔCV, in % of CV of model M3) between model M.3 and the seven other models for genotypes of the three species. Lowest values of ΔCV indicate the best models. The horizontal line represents the threshold of tolerance of 5% of additional error compared with model M.3. (c,d) Comparison of models assuming that zero to three parameters differ between four species (maize, wheat, rice and *Arabidopsis thaliana*). (c) Box-plot of ΔBIC between model M.3 and the seven other models for the four species. (d) ΔCV between model M.3 and the seven other models for the four species. Line in (d) as in (b). Other model selection criteria are presented in Supporting Information Table S1.

In rice, the seven studied lines belonged to different species and subspecies (*O. glaberrima*, *O. sativa* ssp. *indica* and *japonica)* from tropical or temperate regions of Asia or Africa. As in maize, the comparison of the different statistical criteria led to the conclusion that the model with common parameters for all lines was acceptable (Fig. 4a and Table S1), with an added error lower than the 5% threshold compared with models specific to each line (2.0% on average; Fig. 4b and Table S1). This indicated that differences between rice lines with regard to the response curve and T_{opt} corresponded, if they existed, to a shift lower than 1°C (Fig S4). Lines originating from different ecological areas and from different species or subspecies therefore had a common temperature–rate relationship. There was no trend for an effect of breeding between lines that were traditional (Azucena, Moroberekan), developed during the green revolution (IR64) or recently released (Vandana, Apo).

In wheat, we compared several lines selected in cool or warm climates, tolerant or sensitive to heat stress and released from the 1940s until recently. As above, a common model applied to the whole dataset (Fig. 2), with no significant differences between lines, as shown by the statistical criteria comparing models (Fig. 4a), as well as by the low additional error obtained when considering that the three parameters were common to all lines (ΔCV = 1.4% on average; Fig. 4b and Table S1). It can be concluded that any difference between lines would involve a shift of < 1°C (Fig S4c,d). The response was also common for a barley line (*Hordeum vulgare* cv. Golden Promise), which, like wheat, belongs to the Triticeae tribe (Fig. 2q), with an increase in error of < 2% when considering a unique model compared with separate models for each species (not shown).

The responses of developmental processes differed in 18 species with a trend between cool-/warm-adapted species

The variability of the temperature response was explored in 18 species (17 crop species comprising the 14 most cultivated species worldwide and *Arabidopsis thaliana*). Results were collected from either our own database or the literature, with 42 variables, 73 references and 122 experiments (Table 1). The variables analysed in this study involved different genotypes for each species and developmental processes as different as the expansion rates of several organs (pollen tube, roots, leaves and embryo), the reciprocal of durations of phases, the cell division rate and germination rate.

In order to select the model that best suited the comparison between species, the analysis was first restricted to four species in which we had access to well-controlled datasets obtained by our groups (dataset of Fig. 2 in maize, rice and wheat, and the *Arabidopsis thaliana* dataset presented in Parent *et al.*, 2010b). When comparing the eight models of Table 2, statistical indicators showed that the response curves differed between species, because a unique model for different species (M.0) was not acceptable (ΔBIC = + 40 and ΔCV = 25%, far from the thresholds of + 5 and + 5%, respectively; Fig. 4c,d and Table S1). An *F*-test procedure resulted in a similar conclusion (Fig. S6). The model M.2b, with a common α for all species, was the best model (ΔBIC = − 2.2; Fig. 4c, Table S1, Fig. S4), with 0.1% of

additional error compared with the model with three parameters. The other models, in particular those assuming that T_0 was common between species, were rejected. We therefore compared the 18 species using model M.2b, in which species differ by two parameters of Eqn 2, namely the characteristic temperature T_0 and activation enthalpy $\Delta H_A^{\ddagger}$.

Response curves corresponding to the 18 studied species followed similar patterns with different parameters (Fig. 5). The model M.2b applied to all species, with r^2 ranging from 0.92 to 0.98 (Table 3). Its two parameters, $\Delta H_A^{\ddagger}$ and T_0, are presented for each species in Table 3 and in spreadsheet format in Table S2. They were independent (Fig. S7a), confirming the two degrees of freedom of this model. In the following paragraph, we have transformed them into two more intuitive characteristics of response curves for each species, namely the optimum temperature T_{opt}, for which rates are at a maximum (related to T_0; Eqn 3; Figs S1b, S7b), and the range of temperature in which the considered rate is higher than 50% of the maximum rate ($range_{50\%}$), related to $\Delta H_A^{\ddagger}$ (Figs 5, 6 and Table 3).

Species originating from cool areas, such as canola (*Brassica napus* L.) and cauliflower (*Brassica oleracea*), showed the lowest values for T_{opt} (23.1 ± 0.7 and 21.6 ± 1.2°C; Table 3 and Fig. 6). Species adapted to warm climates, such as pearl millet (*Pennisetum glaucum*), peanut (*Arachis hypogaea*), cotton (*Gossypium*), sorghum (*Sorghum bicolor*) and cowpea (*Vigna unguiculata*), showed high values of T_{opt} (from 32.4 ± 0.5 to 34.1 ± 1.5°C). This climatic effect applied within families of species, for instance in Poaceae species, in which T_{opt} ranged from relatively low to high values in wheat and sorghum (27.7 ± 0.2 and 34.1 ± 1.5°C, respectively).

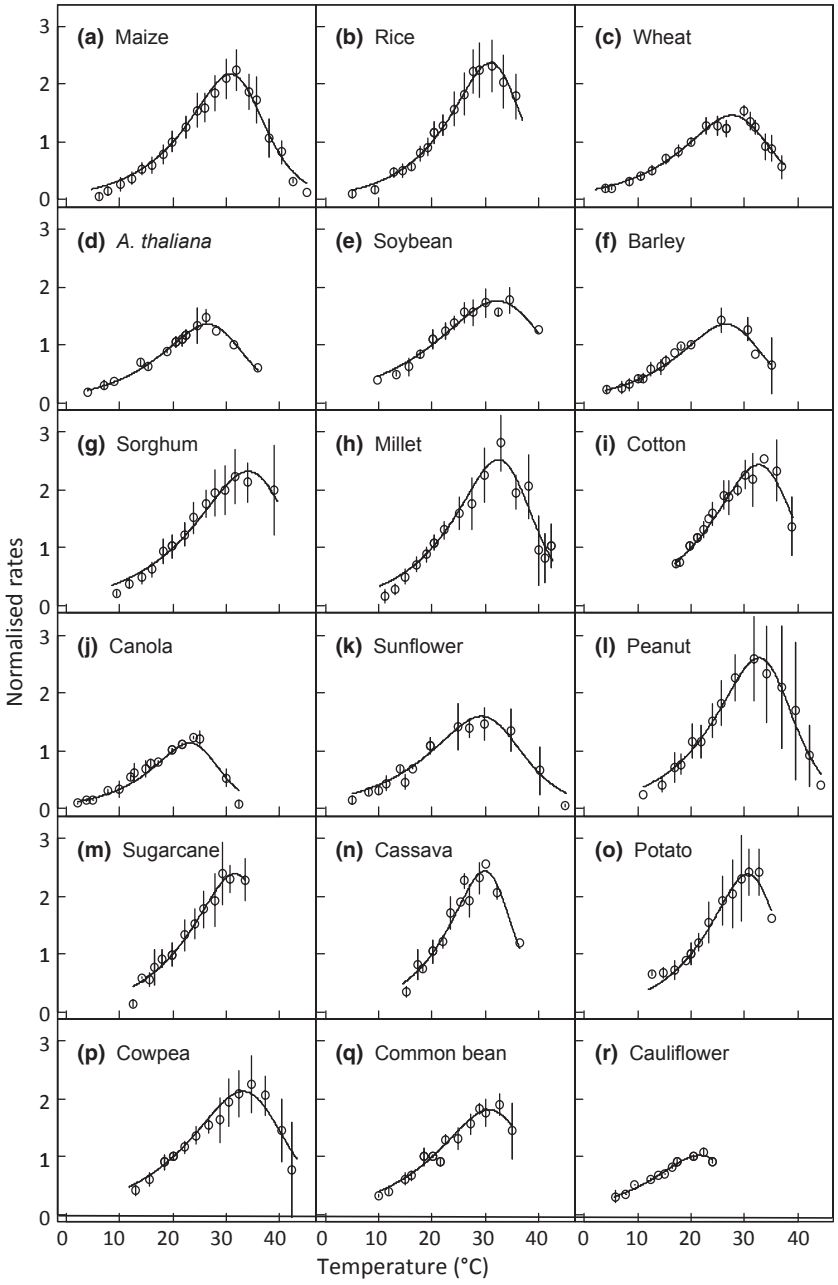

Fig. 5 Response curve to temperature of developmental processes in 18 species. Each variable is normalized by its corresponding value at 20°C. Lines represent models for the considered species (model 2b). The origin of the data is given in Table 1. Model parameters are shown in Table 3 and Supporting Information Table S2.

Table 3 Parameter values and quality of regression for the 18 studied species (model M.2b)

	Model M.2b					
Species	R^2	$\Delta H_A^{\ddagger}$ (kJ mol^{-1})	T_0 (°C)	T_{opt} (°C)	$Range_{50\%}$ (°C)	$Rate_{max}$
Arabidopsis thaliana	0.98	65.1 ± 3.5	29.3 ± 0.4	26.5 ± 0.5	15.6–34.7	1.35
Barley	0.95	65.1 ± 3.5	29.4 ± 0.9	26.5 ± 0.9	15.6–34.7	1.36
Canola	0.94	80 ± 6	25.4 ± 0.8	23.1 ± 0.7	15.0–29.6	1.13
Cassava	0.95	89.6 ± 5.5	32 ± 0.6	29.9 ± 0.6	21.6–35.9	2.43
Cauliflower	0.98	63.6 ± 4.3	24.4 ± 1.2	21.6 ± 1.2	15.0–29.7	1.02
Common bean	0.96	61.7 ± 3.8	33.8 ± 1.2	30.7 ± 1	18.9–39.6	1.81
Cotton	0.95	70.3 ± 3.7	35.4 ± 0.9	32.6 ± 0.7	22.1–40.5	2.44
Cowpea	0.93	60 ± 3.5	36.3 ± 1.1	33.1 ± 0.9	20.8–42.4	2.13
Maize	0.98	73.9 ± 2.1	33.4 ± 0.2	30.8 ± 0.2	20.8–38.2	2.17
Millet	0.92	73.6 ± 4.3	35.1 ± 0.5	32.4 ± 0.5	22.3–39.9	2.53
Peanut	0.97	73.9 ± 2.9	35.3 ± 0.4	32.7 ± 0.3	22.6–40.2	2.61
Potato	0.97	81.7 ± 4	33 ± 1.4	30.6 ± 0.9	21.6–37.3	2.38
Rice	0.99	78.9 ± 3.1	33.4 ± 0.5	30.9 ± 0.5	21.6–37.8	2.36
Sorghum	0.98	60.6 ± 6	37.3 ± 1.7	34.1 ± 1.5	21.8–43.3	2.32
Soybean	0.97	52.3 ± 4.7	35.8 ± 1.2	32.2 ± 1	18.3–42.9	1.76
Sugarcane	0.98	75.2 ± 6	34.2 ± 1.2	31.6 ± 1.3	21.7–38.9	2.39
Sunflower	0.94	60.4 ± 5.8	32.4 ± 1.1	29.3 ± 0.9	17.3–38.3	1.60
Wheat	0.97	63.3 ± 3.6	30.6 ± 0.3	27.7 ± 0.2	16.4–36.2	1.46

R^2, coefficient of determination of the regression between fitted and observed values; $\Delta H_A^{\ddagger}$, T_0 and α are the three parameters of Eqn 2. In model M.2b, α was common to all species (α = 3.5). T_{opt} (optimum temperature) is the temperature at which the development rate is at a maximum. $Range_{50\%}$ is the temperature range within which the development rate reaches 50% of its maximum value. $Rate_{max}$ is the maximum rate in proportion to the value at 20°C. Parameter values are given ± SE calculated by bootstrapping.

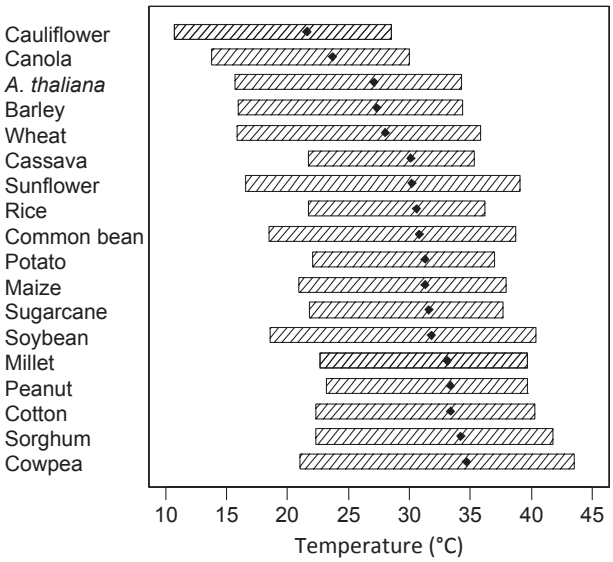

Fig. 6 Temperature at which rates are at a maximum (T_{opt}, black dots) and range of temperature for which the rate of development is at least 50% of its maximum (horizontal bars) in 18 species. Species are ranked by values of T_{opt}, also representing a gradient from temperate to tropical species.

Discussion

Coordination between developmental processes and absence of acclimation of temperature responses

The results presented here confirm and extend to a larger range of processes and species those observations recorded earlier on the coordination of developmental processes via a common response curve to temperature (Ong, 1983a,b; Warrington & Kanemasu, 1983a,b; Parent *et al.*, 2010b). By contrast, photosynthesis and enzyme activities have response curves that differ markedly from those presented here (Campbell *et al.*, 2007; Sage *et al.*, 2008; Parent *et al.*, 2010b). Furthermore, they have nonunique temperature responses because they acclimate to changes in temperature within a few days (Sage & Kubien, 2007).

The absence of acclimation of the temperature response of developmental processes is not in contradiction with plant adaptation to low or high temperatures. Marked differences in the duration of the plant cycle (e.g. number of days after sowing at a given temperature) are observed following selection over several generations in plants, but without modification of the temperature response of this duration (Craufurd *et al.*, 1999). We show here that the response to temperature of these durations was common to all lines within a cultivated species. Morphological or anatomical adaptations to low or high temperature occur over periods of weeks (Gorsuch *et al.*, 2010). For example, changes in anatomy are still small after 6 d at 5°C, are noticeable after 30 d and become dramatic in new leaves developing under cold temperatures (Gorsuch *et al.*, 2010). The same conclusion applies to trees grown in different environments (Rehfeldt *et al.*, 2002).

Morphological changes linked to temperature may be an emerging property generated by the difference in behaviour between metabolic processes, with changes in response to temperature after acclimation, and developmental processes which do not acclimate. This would cause changes in carbon accumulation and specific leaf area (Tardieu *et al.*, 1999), observed experimentally by several groups (Loveys *et al.*, 2002; Shahba & Bauerle, 2009; Atkinson *et al.*, 2010; Fajardo & Piper, 2011).

A similar view has been proposed recently for the response to water deficit (Tardieu *et al.*, 2011).

An absence of genetic variability of responses within the most common species

A different choice of lines within each species is unlikely to have yielded a different conclusion with regard to the genetic variability within species. In maize, the set of studied lines included tropical lines at very large genetic distances from the temperate lines (Camus-Kulandaivelu *et al.*, 2006). Data originating from the literature confirm this conclusion (Fig. 3b). Furthermore, no quantitative trait loci were detected for the temperature response of LER over a shorter range of temperature in three mapping populations (Reymond *et al.*, 2003; Sadok *et al.*, 2007; Welcker *et al.*, 2007), confirming the absence of a structured genetic variability. In the same way, the diversity tested in rice was large, with different species or subspecies, origins and generations of selection. The same result applied to wheat lines with different stress tolerances, suggesting that differences in heat tolerance involve the lowest and highest temperatures for which response curves can be established, but not the response curves themselves. It is noteworthy that, in the panels of lines tested here or in mapping populations derived from them, other traits showed a large genetic variability and clear quantitative trait loci (Reymond *et al.*, 2003; Chardon *et al.*, 2004; Izanloo *et al.*, 2008; Parent *et al.*, 2010a; Welcker *et al.*, 2011). Hence, the lack of genetic variability on the temperature response observed here was not a consequence of a poor choice of lines. It was probably not the result of a low power of statistical tests either, because our sensitivity analysis showed that we could identify a shift of < 1°C when comparing response curves of lines or species. Finally, the conclusion with regard to the absence of genetic variability can be extended to the other crop species presented in Table 1, which were analysed on at least three genotypes each (except barley, two genotypes).

A shift in temperature response probably requires millennia under very contrasting climates

The above paragraph shows that breeding in climates involving either high or low temperature has not affected the response of developmental processes to temperature, in particular T_{opt}. Centuries of mutations and selection are therefore not sufficient to affect this response within each species, contrary to most other traits that have responded to breeding. We therefore propose that a shift in temperature response requires two conditions. First, it requires millennia, i.e. at least the period during which most species have been bred. The second proposed condition is a marked contrast of climate. *Triticum* and *Hordeum* genera that genetically diverged more than 10 million yr (My) ago (Feuillet *et al.*, 2008) still have response curves with common parameters, probably because they grew under similar climatic conditions. This may apply to rice species and subspecies that have diverged for a longer period than that of agriculture (*c.* 11 000 years). No significant difference was observed between the subspecies *indica* and *japonica*, which diverged 0.4 My ago, or between the species *O. sativa* and *O. glaberrima*, which diverged 0.6 My ago (Ma & Bennetzen, 2004). This is probably also the case for sorghum and sugarcane, which diverged 5 My ago (Ming *et al.*, 1998), and sorghum and maize, which diverged 10 My ago (Ramakrishna *et al.*, 2002). Differences were only observed in the case of very ancient divergence and very different climates, as in the contrast between Triticeae species and tropical grasses, such as sorghum, maize, millet or sugarcane, which diverged 50 My ago (Gale & Devos, 1998) and grew for a long period in different climates.

Hypotheses for very slow evolution

A first hypothesis is that the evolution of temperature responses has been slowed down by the necessity for a synchronous shift in the responses of several processes. What would happen if a mutation changed the temperature response of one developmental process but not of the others? Simple computer simulations (not shown) suggest that a plant which loses the coordination between developmental processes because of a mutation would have highly disturbed performances, with, for example, a reproductive development occurring too early in comparison with vegetative development, or a disturbed aspect because of the lack of coordination between processes involved in the control of growth. We can therefore hypothesize that natural and breeder's selection has eliminated mutations that affect temperature responses of one process only, thereby requiring a very long time to obtain the response of all processes to shift simultaneously.

A second hypothesis is based on the fact that even the diversity found in the 18 tested species is low when compared with the six-fold differences in activation enthalpy found in different traits and life kingdoms (Dell *et al.*, 2011). The theory of 'thermodynamic constraint' (or 'warmer is better'), developed in animal studies (Huey & Kingsolver, 1989; Frazier *et al.*, 2006), argues that low temperatures slow down all biochemical reactions and that adaptation cannot change this rule. Because maximum rates occur at low temperature in cold-adapted plant species, such species would have lower maximum rates and performances than warm-adapted species, for which maximum rates occur at higher temperature, with higher rates of all biochemical reactions. By focusing mainly on plant performance, breeding may have selected lines and species with high optimum temperatures regardless of the ecological area. In our results, T_{opt} was generally higher than the mean temperature during the crop cycle. Eleven of the 17 studied crop species had optimum temperatures above 30°C, higher than those commonly observed in their growing regions. In these species, the temperature response may have reached a final equilibrium between a broad adaptation to a range of climate and maximum growth.

Consequences for breeding and modelling

Our study suggests that there is little chance that breeding can substantially affect the temperature responses of the developmental rates analysed here, because of a nonexistent source of genetic

variability in crop species. This does not rule out several possibilities related to genetic adaptations of other traits related to temperature responses. First, the duration of the plant cycle has a considerable genetic variability, in particular between tropical and temperate materials. We therefore argue here that, although durations or rates have a large genetic variability, the change with temperature in these durations or rates does not vary between tropical and temperate lines. One way to avoid a decrease in yield with increasing temperature is to use lines with a longer crop cycle (Lobell *et al.*, 2008). Manipulating the respective durations of crop phases would also improve the yield potential in cereals (Borràs *et al.*, 2010). Second, a genetic gain has been obtained by breeding for the range of temperatures in which plant metabolism is not damaged under prolonged high or low temperature. For instance, the wheat line Excalibur used here tolerates high temperatures that cannot be tolerated by Kukri (Bukovnik *et al.*, 2009). This implies that the responses observed here, which apply to nonstressed ranges, are largely independent of tolerance to cold or heat stress. Third, high temperatures usually occur together with high evaporative demand, which has a considerable effect on gas exchange and growth, with a large genetic variability of this effect (Sadok *et al.*, 2007; Welcker *et al.*, 2007).

Our results also simplify the modelling of the effects of global changes, because lines grown in 50 or 100 yr will probably have a response to temperature similar to that of current lines. Existing crop models (Brisson *et al.*, 2003; Hammer *et al.*, 2010) already implicitly assume a common response of developmental processes, which is confirmed here. The response to temperature of a large range of species can be characterized by two traits that are relatively easy to measure, namely T_{opt} and the ratio between the rate at T_{opt} and that at 20°C. The parameters of Eqn 2 can be derived from these two traits (Eqn 3). Furthermore, because of the similar values of species in a given ecological area or not too distant genetically, modelling can be performed using the values of related species.

Acknowledgements

This work has been funded in part by the project DROPS (DROught tolerant yielding PlantS; http://www.drops-project.eu), which received funding from the European Community's Seventh Framework Programme under the grant agreement no FP7-244374.

References

Addae PC, Pearson CJ. 1992. Thermal requirements for germination and seedling growth of wheat. *Australian Journal of Agricultural Research* **43**: 585–594.

Akaike H. 1974. New look at statistical-model identification. *Ieee Transactions on Automatic Control* **AC19**: 716–723.

Akaike H. 1978. Likelihood of a time-series model. *Statistician* **27**: 217–235.

Akparobi SO, Togun AO, Ekanayake IJ. 2000. Temperature effects on leaf growth of cassava (*Manihot esculenta* Crantz) in controlled environments. *African Journal of Root and Tuber Crops* **4**: 1–4.

Arndt CH. 1945. Temperature–growth relations of the roots and hypocotyls of cotton seedlings. *Plant Physiology* **20**: 200–220.

Atkin OK, Loveys BR, Atkinson LJ, Pons TL. 2006. Phenotypic plasticity and growth temperature: understanding interspecific variability. *Journal of Experimental Botany* **57**: 267–281.

Atkinson LJ, Campbell D, Zaragoza-Castells J, Hurry V, Atkin OK. 2010. Impact of growth temperature on scaling relationships linking photosynthetic metabolism to leaf functional traits. *Functional Ecology* **2010**: 1181–1191.

Barlow EWR, Boersma L. 1972. Growth response of corn to changes in root temperature and soil-water suction measured with an LVDT. *Crop Science* **12**: 251.

Barnabas B, Jager K, Feher A. 2008. The effect of drought and heat stress on reproductive processes in cereals. *Plant, Cell & Environment* **31**: 11–38.

Battisti DS, Naylor RL. 2009. Historical warnings of future food insecurity with unprecedented seasonal heat. *Science* **323**: 240–244.

Ben-Haj-Salah H, Tardieu F. 1995. Temperature affects expansion rate of maize leaves without change in spatial distribution of cell length: analysis of the coordination between cell division and cell expansion. *Plant Physiology* **109**: 870.

Ben-Haj-Salah H, Tardieu F. 1997. Control of leaf expansion rate of droughted maize plants under fluctuating evaporative demand: a superposition of hydraulic and chemical messages? *Plant Physiology* **114**: 893–900.

Benoit GR, Grant WJ, Devine OJ. 1986. Potato top growth as influenced by day–night temperature differences. *Agronomy Journal* **78**: 264–269.

Blacklow WM. 1972. Influence of temperature on germination and elongation of radicle and shoot of corn (*Zea mays* L.). *Crop Science* **12**: 647.

Borràs G, Slafer GA, Casas AM, van Eeuwijk F, Romagosa I. 2010. Genetic control of pre-heading phases and other traits related to development in a double haploid barley (*Hordeum vulgare* L.) population. *Field Crops Research* **119**: 36–47.

Brisson N, Gary C, Justes E, Roche R, Mary B, Ripoche D, Zimmer D, Sierra J, Bertuzzi P, Burger P *et al.* 2003. An overview of the crop model STICS. *European Journal of Agronomy* **18**: 309–332.

Bukovnik U, Fu JM, Bennett M, Prasad PVV, Ristic Z. 2009. Heat tolerance and expression of protein synthesis elongation factors, EF-Tu and EF-1 alpha, in spring wheat. *Functional Plant Biology* **36**: 234–241.

Campbell C, Atkinson L, Zaragoza-Castells J, Lundmark M, Atkin O, Hurry V. 2007. Acclimation of photosynthesis and respiration is asynchronous in response to changes in temperature regardless of plant functional group. *New Phytologist* **176**: 375–389.

Campbell JA, Robertson MJ, Grof CPL. 1998. Temperature effects on node appearance in sugarcane. *Australian Journal of Plant Physiology* **25**: 815–818.

Camus-Kulandaivelu L, Veyrieras JB, Madur D, Combes V, Fourmann M, Barraud S, Dubreuil P, Gouesnard B, Manicacci D, Charcosset A. 2006. Maize adaptation to temperate climate: relationship between population structure and polymorphism in the *Dwarf8* gene. *Genetics* **172**: 2449–2463.

Chardon F, Virlon B, Moreau L, Falque M, Joets J, Decousset L, Murigneux A, Charcosset A. 2004. Genetic architecture of flowering time in maize as inferred from quantitative trait loci meta-analysis and synteny conservation with the rice genome. *Genetics* **168**: 2169–2185.

Chimenti CA, Hall AJ, Lopez MS. 2001. Embryo-growth rate and duration in sunflower as affected by temperature. *Field Crops Research* **69**: 81–88.

Covell S, Ellis RH, Roberts EH, Summerfield RJ. 1986. The influence of temperature on seed-germination rate in grain legumes. 1. A comparison of chickpea, lentil, soybean and cowpea at constant temperatures. *Journal of Experimental Botany* **37**: 705–715.

Craufurd PQ, Ellis RH, Summerfield RJ, Menin L. 1996a. Development in cowpea (*Vigna unguiculata*). 1. The influence of temperature on seed germination and seedling emergence. *Experimental Agriculture* **32**: 1–12.

Craufurd PQ, Mahalakshmi V, Bidinger FR, Mukuru SZ, Chantereau J, Omanga PA, Qi A, Roberts EH, Ellis RH, Summerfield RJ *et al.* 1999. Adaptation of sorghum: characterisation of genotypic flowering responses to temperature and photoperiod. *Theoretical and Applied Genetics* **99**: 900–911.

Craufurd PQ, Qi A, Ellis RH, Summerfield RJ, Roberts EH. 1996b. Development in cowpea (*Vigna unguiculata*). 2. Effect of temperature and saturation deficit on time to flowering in photoperiod-insensitive genotypes. *Experimental Agriculture* **32**: 13–28.

Craufurd PQ, Qi A, Summerfield RJ, Ellis RH, Roberts EH. 1996c. Development in cowpea (*Vigna unguiculata*). 3. Effects of temperature and

photoperiod on time to flowering in photoperiod-sensitive genotypes and screening for photothermal responses. *Experimental Agriculture* **32**: 29–40.

Craufurd PQ, Subedi M, Summerfield RJ. 1997. Leaf appearance in cowpea: effects of temperature and photoperiod. *Crop Science* **37**: 167–172.

Cutforth HW, Jame YW, Jefferson PG. 1992. Effect of temperature, vernalisation, and water-stress on phyllochron and final main-stem leaf number of HY320 and Neepawa spring wheats. *Canadian Journal of Plant Science* **72**: 1141–1151.

Dejong R, Best KF. 1979. Effects of soil water potential, temperature and seeding depth on seedlings emergence of wheat. *Canadian Journal of Soil Science* **59**: 259–264.

Dell AI, Pawar S, Savage VM. 2011. Systematic variation in the temperature dependence of physiological and ecological traits. *Proceedings of the National Academy of Sciences, USA* **108**: 10591–10596.

Ellis RH, Hong TD, Roberts EH. 1987. Comparison of cumulative germination and rate of germination of dormant and aged barley seed lots at different constant temperatures. *Seed Science and Technology* **15**: 717–727.

Fajardo A, Piper FI. 2011. Intraspecific trait variation and covariation in a widespread tree species (*Nothofagus pumilio*) in southern Chile. *New Phytologist* **189**: 259–271.

Farquhar GD, Caemmerer Sv, Berry JA. 1980. A biochemical model of photosynthetic CO_2 assimilation in leaves of C3 species. *Planta* **149**: 78–90.

Feng YS, Li XM, Boersma L. 1990. The Arrhenius equation as a model for explaining plant-responses to temperature and water stresses. *Annals of Botany* **66**: 237–244.

Feuillet C, Langridge P, Waugh R. 2008. Cereal breeding takes a walk on the wild side. *Trends in Genetics* **24**: 24–32.

Fleisher DH, Shillito RM, Timlin DJ, Kim SH, Reddy VR. 2006. Approaches to modeling potato leaf appearance rate. *Agronomy Journal* **98**: 522–528.

Fleisher DH, Timlin D. 2006. Modeling expansion of individual leaves in the potato canopy. *Agricultural and Forest Meteorology* **139**: 84–93.

Frazier MR, Huey RB, Berrigan D. 2006. Thermodynamics constrains the evolution of insect population growth rates: "warmer is better". *The American Naturalist* **168**: 512–520.

Gale MD, Devos KM. 1998. Comparative genetics in the grasses. *Proceedings of the National Academy of Sciences, USA* **95**: 1971–1974.

Gallagher JN, Biscoe PV. 1979. Field studies of cereal leaf growth. 3. Barley leaf extension in relation to temperature, irradiance and water potential. *Journal of Experimental Botany* **30**: 645–655.

Gallagher JN, Biscoe PV, Wallace JS. 1979. Field studies of cereal leaf growth. 4. Winter-wheat leaf extension in relation to temperature and leaf water status. *Journal of Experimental Botany* **30**: 657–668.

Garciahuidobro J, Monteith JL, Squire GR. 1982. Time, temperature and germination of pearl-millet (*Pennisetum-typhoides* S.and H.). 1. Constant temperature. *Journal of Experimental Botany* **33**: 288–296.

Gay C, Corbineau F, Come D. 1991. Effects of temperature and oxygen on seed-germination and seedling growth in sunflower (*Helianthus-annuus* L.). *Environmental and Experimental Botany* **31**: 193–200.

Gillooly JF, Brown JH, West GB, Savage VM, Charnov EL. 2001. Effects of size and temperature on metabolic rate. *Science* **293**: 2248–2251.

Gorsuch PA, Pandey S, Atkin OK. 2010. Temporal heterogeneity of cold acclimation phenotypes in *Arabidopsis* leaves. *Plant, Cell & Environment* **33**: 244–258.

Granier C, Massonnet C, Turc O, Muller B, Chenu K, Tardieu F. 2002. Individual leaf development in *Arabidopsis thaliana*: a stable thermal-time-based programme. *Annals of Botany* **89**: 595–604.

Hadley P, Roberts EH, Summerfield RJ, Minchin FR. 1983. A quantitative model of reproductive development in cowpea (*Vigna-unguiculata* (L) Walp.) in relation to photoperiod and temperature, and implications for screening germplasm. *Annals of Botany* **51**: 531–543.

Hammer GL, van Oosterom E, McLean G, Chapman SC, Broad I, Harland P, Muchow RC. 2010. Adapting APSIM to model the physiology and genetics of complex adaptive traits in field crops. *Journal of Experimental Botany* **61**: 2185–2202.

Hesketh JD, Duncan WG, Baker DN. 1972. Simulation of growth and yield in cotton. 2. Environmental conditions of morphogenesis. *Crop Science* **12**: 436–439.

Hesketh JD, Myhre DL, Willey CR. 1973. Temperature control of time intervals between vegetative and reproductive events in soybeans. *Crop Science* **13**: 250–254.

Hesketh JD, Warrington IJ. 1989. Corn growth-response to temperature: rate and duration of leaf emergence. *Agronomy Journal* **81**: 696–701.

Huey RB, Kingsolver JG. 1989. Evolution of thermal sensitivity of exotherm performance. *Trends in Ecology and Evolution* **4**: 131–135.

Inmanbamber NG. 1994. Temperature and seasonal effects on canopy development and light interception of sugarcane. *Field Crops Research* **36**: 41–51.

Izanloo A, Condon AG, Langridge P, Tester M, Schnurbusch T. 2008. Different mechanisms of adaptation to cyclic water stress in two South Australian bread wheat cultivars. *Journal of Experimental Botany* **59**: 3327–3346.

Johnson FH, Eyring H, Williams RW. 1942. The nature of enzyme inhibitions in bacterial luminescence: sulfanilamide, urethane, temperature and pressure. *Journal of Cellular and Comparative Physiology* **20**: 247–268.

Johnson FH, Lewin I. 1946. The growth rate of *E. coli* in relation to temperature, quinine, and coenzyme. *Journal of Cellular and Comparative Physiology* **28**: 47–75.

Kakani VG, Prasad PVV, Craufurd PQ, Wheeler TR. 2002. Response of in vitro pollen germination and pollen tube growth of groundnut (*Arachis hypogaea* L.) genotypes to temperature. *Plant, Cell & Environment* **25**: 1651–1661.

Keating BA, Evenson JP. 1979. Effect of soil-temperature on sprouting and sprout elongation of stem cuttings of cassava (*Manihot esculenta* Crantz.). *Field Crops Research* **2**: 241–251.

Kemp DR, Blacklow WM. 1982. The responsiveness to temperature of the extension rates of leaves of wheat growing in the field under different levels of nitrogen fertiliser. *Journal of Experimental Botany* **33**: 29–36.

Kirk WW, Marshall B. 1992. The influence of temperature on leaf development and growth in potatoes in controlled environments. *Annals of Applied Biology* **120**: 511–525.

Koumura T. 1972. Breeding of new rice variety 'Nipponbare'. *Agricultural Technology* **27**: 112–116.

Kratsch HA, Wise RR. 2000. The ultrastructure of chilling stress. *Plant, Cell & Environment* **23**: 337–350.

Lafarge T, de Raissac M, Tardieu F. 1998. Elongation rate of sorghum leaves has a common response to meristem temperature in diverse African and European environmental conditions. *Field Crops Research* **58**: 69–79.

Lafond GP, Baker RJ. 1986. Effects of temperature, moisture stress, and seed size on germination of 9 spring wheat cultivars. *Crop Science* **26**: 563–567.

Lafond GP, Fowler DB. 1989. Soil-temperature and moisture stress effects on kernel water-uptake and germination of winter-wheat. *Agronomy Journal* **81**: 447–450.

Lawlor DJ, Kanemasu ET, Albrecht WC, Johnson DE. 1990. Seed production environment influence on the base temperature for growth of sorghum genotypes. *Agronomy Journal* **82**: 643–647.

Lawn RJ, Hume DJ. 1985. Response of tropical and temperate soybean genotypes to temperature during early reproductive growth. *Crop Science* **25**: 137–142.

Lehenbauer PA. 1914. Growth of maize seedlings in relation to temperature. *Physiological Researches* **1**: 247.

Lindstrom MJ, Papendick RI, Koehler FE. 1976. Model to predict winter-wheat emergence as affected by soil temperature, water potential and depth of planting. *Agronomy Journal* **68**: 137–141.

Lobell DB, Burke MB, Tebaldi C, Mastrandrea MD, Falcon WP, Naylor RL. 2008. Prioritizing climate change adaptation needs for food security in 2030. *Science* **319**: 607–610.

Lobell DB, Schlenker W, Costa-Roberts J. 2011. Climate trends and global crop production since 1980. *Science* **333**: 616–620.

Loveys BR, Sceurwater T, Pons TL, Fitter AH, Atkin OK. 2002. Growth temperature influences the underlying components of relative growth rate: an investigation using inherently fast- and slow-growing plant species. *Plant, Cell & Environment* **25**: 975–987.

Ma JX, Bennetzen JL. 2004. Rapid recent growth and divergence of rice nuclear genomes. *Proceedings of the National Academy of Sciences, USA* **101**: 12404–12410.

Marshall B, Squire GR. 1996. Non-linearity in rate–temperature relations of germination in oilseed rape. *Journal of Experimental Botany* **47**: 1369–1375.

McClung CR, Davis SJ. 2010. Ambient thermometers in plants: from physiological outputs towards mechanisms of thermal sensing. *Current Biology* **20**: 1086–1092.

Ming R, Liu SC, Lin YR, da Silva J, Wilson W, Braga D, van Deynze A, Wenslaff TF, Wu KK, Moore PH *et al.* 1998. Detailed alignment of *Saccharum* and *Sorghum* chromosomes: comparative organization of closely related diploid and polyploid genomes. *Genetics* **150**: 1663–1682.

Mohamed HA, Clark JA, Ong CK. 1988a. Genotypic differences in the temperature responses of tropical crops. 1. Germination characteristics of groundnut (*Arachis hypogaea* L.) and pearl-millet (*Pennisetum typhoides* S. & H.). *Journal of Experimental Botany* **39**: 1121–1128.

Mohamed HA, Clark JA, Ong CK. 1988b. Genotypic differences in the temperature responses of tropical crops. 2. Seedling emergence and leaf growth of groundnut (*Arachis hypogaea* L.) and pearl-millet (*Pennisetum typhoides* S. & H.). *Journal of Experimental Botany* **39**: 1129–1135.

Mongelar JC, Mimura L. 1972. Growth studies of sugarcane plant. 2. Some effects of root temperature and gibberellic-acid and their interactions on growth. *Crop Science* **12**: 52.

Morrison MJ, McVetty PBE, Shaykewich CF. 1989. The determination and verification of a baseline temperature for the growth of Westar summer rape. *Canadian Journal of Plant Science* **69**: 455–464.

Moss GI, Mullett JH. 1982. Potassium release and seed vigor in germinating bean (*Phaseolus vulgaris* L.) seed as influenced by temperature over the previous 5 generations. *Journal of Experimental Botany* **33**: 1147–1160.

Mutsaers HJW. 1983. Leaf growth in cotton (*Gossypium hirsutum* L.). 2. The influence of temperature, light, water-stress and root restriction on the growth and initiation of leaves. *Annals of Botany* **51**: 521–529.

Olesen JE, Grevsen K. 1997. Effects of temperature and irradiance on vegetative growth of cauliflower (*Brassica oleracea* L. *botrytis*) and broccoli (*Brassica oleracea* L. *italica*). *Journal of Experimental Botany* **48**: 1591–1598.

Ong CK. 1983a. Responses to temperature in a stand of pearl-millet (*Pennisetum typhoides* S. & H.). 1. Vegetative development. *Journal of Experimental Botany* **34**: 322–336.

Ong CK. 1983b. Responses to temperature in a stand of pearl-millet (*Pennisetum typhoides* S. & H.). 1. Extension of individual leaves. *Journal of Experimental Botany* **34**: 1731–1739.

Ong CK, Monteith JL. 1985. Response of pearl-millet to light and temperature. *Field Crops Research* **11**: 141–160.

Orbovic V, Poff K. 2007. Effect of temperature on growth and phototropism of *Arabidopsis thaliana* seedlings. *Journal of Plant Growth Regulation* **26**: 222–228.

Parent B, Conejero G, Tardieu F. 2009. Spatial and temporal analysis of non-steady elongation of rice leaves. *Plant, Cell & Environment* **32**: 1561–1572.

Parent B, Suard B, Serraj R, Tardieu F. 2010a. Rice leaf growth and water potential are resilient to evaporative demand and soil water deficit once the effects of root system are neutralized. *Plant, Cell & Environment* **33**: 1256–1267.

Parent B, Turc O, Gibon Y, Stitt M, Tardieu F. 2010b. Modelling temperature-compensated physiological rates, based on the co-ordination of responses to temperature of developmental processes. *Journal of Experimental Botany* **61**: 2057–2069.

Pearson CJ. 1975. Thermal adaptation of *Pennisetum*: seedling development. *Australian Journal of Plant Physiology* **2**: 413–424.

Penfield S. 2008. Temperature perception and signal transduction in plants. *New Phytologist* **179**: 615–628.

Peng S, Jianliang H, John ES, Rebecca CL, Romeo MV, Xuhua Z, Grace SC, Gurdev SK, Kenneth GC. 2004. Rice yields decline with higher night temperature from global warming. *Proceedings of the National Academy of Sciences, USA* **101**: 9971–9975.

Poorter H, Niinemets U, Walter A, Fiorani F, Schurr U. 2010. A method to construct dose–response curves for a wide range of environmental factors and plant traits by means of a meta-analysis of phenotypic data. *Journal of Experimental Botany* **61**: 2043–2055.

Prasad PVV, Boote KJ, Thomas JMG, Allen LH, Gorbet DW. 2006. Influence of soil temperature on seedling emergence and early growth of peanut cultivars in field conditions. *Journal of Agronomy and Crop Science* **192**: 168–177.

R Development Core Team 2005. *R: a language and environment for statistical computing*. Vienna, Austria: R Foundation for Statistical Computing. ISBN 3-900051-07-0, http://www.R-project.org.

Ramakrishna W, Dubcovsky J, Park YJ, Busso C, Emberton J, SanMiguel P, Bennetzen JL. 2002. Different types and rates of genome evolution detected by comparative sequence analysis of orthologous segments from four cereal genomes. *Genetics* **162**: 1389–1400.

Reddy KR, Hodges HF, McKinion JM. 1997. Modeling temperature effects on cotton internode and leaf growth. *Crop Science* **37**: 503–509.

Rehfeldt GE, Tchebakova JM, Parfenova YI, Wykoff WR, Kuzmina NA, Milyiutin LI. 2002. Intraspecific response to climate in *Pinus sylvestris*. *Global Change Biology* **8**: 1–18.

Reymond M, Muller B, Leonardi A, Charcosset A, Tardieu F. 2003. Combining quantitative trait loci analysis and an ecophysiological model to analyze the genetic variability of the responses of maize leaf growth to temperature and water deficit. *Plant Physiology* **131**: 664–675.

Sadok W, Naudin P, Boussuge B, Muller B, Welcker C, Tardieu F. 2007. Leaf growth rate per unit thermal time follows QTL-dependent daily patterns in hundreds of maize lines under naturally fluctuating conditions. *Plant, Cell & Environment* **30**: 135–146.

Sage RF, Kubien DS. 2007. The temperature response of C3 and C4 photosynthesis. *Plant, Cell & Environment* **30**: 1086–1106.

Sage RF, Way DA, Kubien DS. 2008. Rubisco, Rubisco activase, and global climate change. *Journal of Experimental Botany* **59**: 1581–1595.

Schwarz G. 1978. Estimating the dimension of a model. *Annals of Statistics* **6**: 461–464.

Scully B, Waines JG. 1987. Germination and emergence response of common and tepary beans to controlled temperature. *Agronomy Journal* **79**: 287–291.

Shahba MA, Bauerle WL. 2009. Growth temperature modulates the spatial variability of leaf morphology and chemical elements within crowns of climatically divergent *Acer rubrum* genotypes. *Tree Physiology* **29**: 869–877.

Sharpe PJH, Demichele DW. 1977. Reaction-kinetics of poikilotherm development. *Journal of Theoretical Biology* **64**: 649–670.

Singh SK, Kakani VG, Brand D, Baldwin B, Reddy KR. 2008. Assessment of cold and heat tolerance of winter-grown canola (*Brassica napus* L.) cultivars by pollen-based parameters. *Journal of Agronomy and Crop Science* **194**: 225–236.

Summerfield RJ, Collinson ST, Ellis RH, Roberts EH, Devries F. 1992. Photothermal responses of flowering in rice (*Oryza sativa*). *Annals of Botany* **69**: 101–112.

Tardieu F, Granier C, Muller B. 1999. Modelling leaf expansion in a fluctuating environment: are changes in specific leaf area a consequence of changes in expansion rate? *New Phytologist* **143**: 33–43.

Tardieu F, Granier C, Muller B. 2011. Water deficit and growth. Co-ordinating processes without an orchestrator? *Current Opinion in Plant Biology* **14**: 283–289.

Tollenaar M, Daynard TB, Hunter RB. 1979. Effect of temperature on rate of leaf appearance and flowering date in maize. *Crop Science* **19**: 363–366.

Vigil MF, Anderson RL, Beard WE. 1997. Base temperature and growing-degree-hour requirements for the emergence of canola. *Crop Science* **37**: 844–849.

Villablobos FJ, Ritchie JT. 1992. The effect of temperature on leaf emergence rates of sunflower genotypes. *Field Crops Research* **29**: 37–46.

Wade LJ, Hammer GL, Davey MA. 1993. Response of germination to temperature amongst diverse sorghum hybrids. *Field Crops Research* **31**: 295–308.

Warrington IJ, Kanemasu ET. 1983a. Corn growth response to temperature and photoperiod. 1. Seedling emergence, tassel initiation, and anthesis. *Agronomy Journal* **75**: 749–754.

Warrington IJ, Kanemasu ET. 1983b. Corn growth response to temperature and photoperiod. 2. Leaf-initiation and leaf-appearance rates. *Agronomy Journal* **75**: 755–761.

Weaich K, Bristow KL, Cass A. 1996. Modeling preemergent maize shoot growth. 1. Physiological temperature conditions. *Agronomy Journal* **88**: 391–397.

Welcker C, Boussuge B, Bencivenni C, Ribaut JM, Tardieu F. 2007. Are source and sink strengths genetically linked in maize plants subjected to water deficit? A QTL study of the responses of leaf growth and of anthesis–silking interval to water deficit. *Journal of Experimental Botany* **58**: 339–349.

Welcker C, Sadok W, Dignat G, Renault M, Salvi S, Charcosset A, Tardieu F. 2011. A common genetic determinism for sensitivities to soil water deficit and evaporative demand: meta-analysis of quantitative trait loci and introgression lines of maize. *Plant Physiology* **157**: 718–729.

White JW, Montes C. 1993. The influence of temperature on seed-germination in cultivars of common bean. *Journal of Experimental Botany* **44**: 1795–1800.

Wise RR, McWilliam JR, Naylor AW. 1983. A comparative study of low-temperature-induced ultrastructural alteration of 3 species with different chilling sensitivities. *Plant, Cell & Environment* **6**: 525–535.

Wurr DCE, Fellows JR, Sutherland RA, Elphinstone ED. 1990. A model of cauliflower curd growth to predict when curds reach a specified size. *Journal of Horticultural Science* **65**: 555–564.

Yin XY, Kropff MJ. 1996. The effect of temperature on leaf appearance in rice. *Annals of Botany* **77**: 215–221.

Yin XY, Kropff MJ, Goudriaan J. 1996. Differential effects of day and night temperature on development to flowering in rice. *Annals of Botany* **77**: 203–213.

Yin XY, Struik PC, Kropff MJ. 2004. Role of crop physiology in predicting gene-to-phenotype relationships. *Trends in Plant Science* **9**: 426–432.

Supporting Information

Additional supporting information may be found in the online version of this article.

Fig. S1 Sensitivity analysis of the model M.3.

Fig. S2 Data handling, example of genotype CML444.

Fig. S3 Calculation of parameter values for models M.3, M.2b and M.0 in the maize hybrid 'Dea'.

Fig. S4 Analysis of the sensitivity of the information criterion (ΔBIC, a,c) and supplemental error (ΔCV, b,d) to changes in the temperature response. BIC, Bayesian information criterion; CV, coefficient of variation.

Fig. S5 Effect of previous high or low temperature on leaf elongation rate at 20°C.

Fig. S6 *F*-test between the different nested models in four species.

Fig. S7 Correlation between model parameters and the optimum temperature in 18 species.

Table S1 Goodness-of-fit evaluation of the different models considering one species (maize, rice or wheat) or four species

Table S2 Spreadsheet with parameters and temperature response functions for the 17 crop species and *Arabidopsis thaliana*

Methods S1 Calculation of optimum temperature from parameters of Eqn 2.

Methods S2 Fitting version of Eqn 2 after normalization at 20°C.

Please note: Wiley-Blackwell are not responsible for the content or functionality of any supporting information supplied by the authors. Any queries (other than missing material) should be directed to the *New Phytologist* Central Office.

Journal of Experimental Botany
doi:10.1093/jxb/eru223

Journal of Experimental Botany
www.jxb.oxfordjournals.org

REVIEW PAPER

Can current crop models be used in the phenotyping era for predicting the genetic variability of yield of plants subjected to drought or high temperature?

Boris Parent* and François Tardieu

INRA, UMR759 Laboratoire d'Ecophysiologie des Plantes sous Stress Environnementaux, Place Viala, F-34060 Montpellier, France

* To whom correspondence should be addressed. E-mail: boris.parent@supagro.inra.fr

Received 29 January 2014; Revised 18 April 2014; Accepted 28 April 2014

Abstract

A crop model with genetic inputs can potentially simulate yield for a large range of genotypes, sites, and years, thereby indicating where and when a given combination of alleles confers a positive effect. We discuss to what extent current crop models, developed for predicting the effects of climate or cultivation techniques on a reference genotype, are adequate for ranking yields of a large number of genotypes in climatic scenarios with water deficit or high temperatures. We compare here the algorithms involved in 19 crop models. Marked differences exist in the representation of the combined effects of temperature and water deficit on plant development, and in the coordination of these effects with biomass production. The current literature suggests that these differences have a small impact on the yield prediction of a reference genotype because errors on the effects of different traits compensate each other. We propose that they have a larger impact if the crop model is used in a genetic context, because the model has to account for the genetic variability of studied traits. Models with explicit genetic inputs will be increasingly feasible because model parameters corresponding to each genotype can now be measured in phenotyping platforms for large plant collections. This will in turn allow prediction of parameter values from the allelic composition of genotypes. It is therefore timely to adapt crop models to this new context to simulate the allelic effects in present or future climatic scenarios with water or heat stresses.

Key words: Crop model, drought, temperature, tolerance, genetic variability, yield, phenotyping.

Introduction

Genetic progress is based on the pyramiding of alleles that confer advantages in plant production. Semi-empiric breeding has been extremely efficient in achieving this, with a genetic progress of about 1% per year in several species (Cooper *et al.*, 2009; Brisson *et al.*, 2010), even under water deficit (Cooper *et al.*, 2009). However, yields have tended to reach a plateau for the last ten years, largely linked to increasingly adverse environmental conditions, in particular water and heat stresses (Brisson *et al.*, 2010; Lobell *et al.*, 2011, 2012). Furthermore, such adverse conditions tend to increase the genotype by environment interaction (G×E) (Cooper *et al.*, 2001), thereby contributing to the slowing down of genetic progress. Indeed, quantitative trait loci (QTLs) have non-stable effects on yield of plants subjected to drought, with negative, positive, or no effect of a given QTL in different locations and years (Maccaferri *et al.*, 2008; Bonneau *et al.*, 2013). A breeding programme based on phenotypic values may therefore result in the oscillation between years of allele frequencies in the breeding population, following year-to-year climatic variations (Chapman *et al.*, 2003; Hammer *et al.*, 2005, 2006). A widely accepted idea is that G×E increases with the degree of integration and complexity, so underlying traits contributing to yield have a lower G×E than yield does (Fukai *et al.*, 1999; Price and Courtois, 1999; Hammer *et al.*, 2005). Selecting for traits has been successful in several cases (Richards, 2006; Edmeades *et al.*, 1999).

Nevertheless, a given trait itself confers positive or negative effects on crop production depending on the environmental scenario (Tardieu, 2012).

To solve the difficulties linked to high G×E, it has been proposed to simulate the yield of virtual plants characterized by their allelic values at QTLs in a large set of environmental scenarios (Chapman *et al.*, 2002; Tardieu, 2003; Yin *et al.*, 2000; Hammer *et al.*, 2006). A crop model with genetic inputs potentially indicates where and when a given combination of alleles confers a positive or negative effect on plant performance (Tardieu and Tuberosa 2010; Messina *et al.*, 2011). This use of modelling differs from that of the first crop models (de Wit *et al.*, 1970, 1978; Duncan *et al.*, 1967), which simulate the consequences of crop management and climatic conditions on yield (i.e. sowing dates, Acosta Gallegos *et al.*, 1996; row spacing, Egli and Bruening, 1992; Whish *et al.*, 2005; irrigation, Chauhan *et al.*, 2013; or diverse climatic conditions, Kumar *et al.*, 2009; Kim *et al.*, 2010). Recently, crop models have also been used for predicting the trends of yield as affected by climate change in different regions (Brisson *et al.*, 2010; Asseng *et al.*, 2013; Harrison *et al.*, 2014; Rosenzweig *et al.*, 2013; Potgieter *et al.*, 2013), or for environment characterization (Chenu *et al.*, 2011).

The use of crop models in a genetic context became possible when model parameters began to be estimated at high throughput in phenotyping platforms (Yin *et al.*, 2000; Reymond *et al.*, 2003; Tardieu 2003; Hammer *et al.* 2006). A conceptual framework has been proposed for this by Tardieu and Tuberosa (2010). (i) The first step aims at dissecting raw traits obtained in phenotyping platforms, which rapidly vary with the plant environment, into a set of model-based "hidden traits" that characterize each genotype as independently as possible from environmental conditions (phenotypic profile, Module 1 in Figure 1). Specific 'dissection' models are used for this (not reviewed in this paper). (ii) This allows the identification of QTLs of model parameters such as the sensitivities of flowering time to photoperiod and temperature (Nakagawa *et al.*, 2005), of leaf growth to water deficit (Reymond *et al.*, 2003; Welcker *et al.*, 2011) or of fruit quality to carbon availability (Quilot *et al.*, 2005). The allelic profile of any genotype can in this way be connected to a phenotypic profile via a matrix of additive QTL effects (Module 2 in Figure 1). (iii) Climatic series, or models of climate change, feed the crop model with environmental scenarios (Module 3 in Figure 1). (iv) Finally, the crop model predicts the performance of genotypes characterized by a given combination of alleles at QTLs of model parameters, under a range of climatic scenarios (Chapman *et al.*, 2002; Chenu *et al.*, 2009, Module 4 in Fig. 1).

The purpose of this paper is to discuss to what extent current crop models are adequate to simulate the performances of a large number of genotypes under a variety of environmental scenarios (Module 4 Fig. 1), in particular those scenarios involving water or heat stresses. The paper first reviews the ways in which 19 crop models (Table 1) take into account the effects of temperature and water deficit, with a special focus on seven widely used models presenting marked differences in principles. It then discusses the consequences of these differences for predicting the effect of the genetic variability.

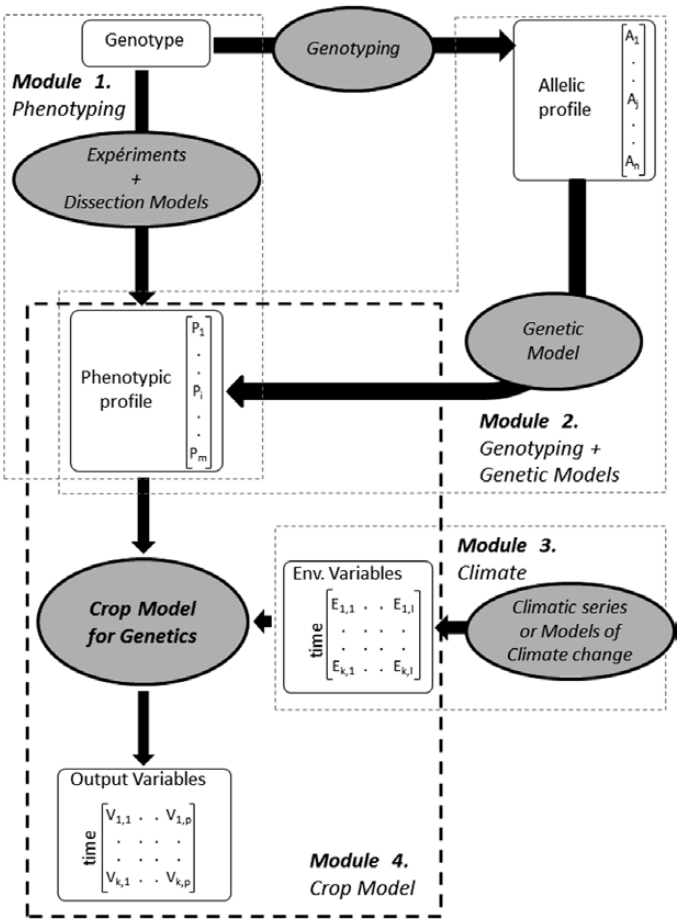

Fig. 1. Conceptual framework for estimating the effects of the genetic diversity on crop performance. Each module involves a different category of models, but only models in Module 4 are reviewed in this paper. Module 1 (Phenotyping) dissects plastic physiological traits measured in phenotyping platforms into a set of environment-independent physiological traits characterizing each genotype (the phenotypic profile). See Tardieu and Tuberosa (2010) for detail. Module 2 (Genetics) links the allelic profile to a vector of parameters specific of a genotype through a genetic model (for example, a matrix of additive QTLs). See Yin *et al.* (2000) or Reymond *et al.* (2003) for detail. Module 3 (climate) generates environmental variables from climatic series or models of climate change. See Harrison *et al.* (2014) or Chenu *et al.* (2011) for detail. Module 4 (Crop model) calculates yield in a large range of environmental conditions from the matrix of environmental variables, the genotype-dependent vector of parameters and the phenotypic profile (reviewed here).

We are aware that the models reviewed here represent a small fraction of available models in the literature and that several versions of each model have been developed, with sometimes appreciable differences between versions. The aim is here to show that different principles coexist for modelling the same effects and to discuss the consequences of this fact.

Response to temperature in current crop models

A consensus among crop modellers is that the growth rates of different organs and the rate of progression of plant cycle from germination to maturity are driven by time corrected for the effect of temperature (thermal time, Bonhomme, 2000; Boote *et al.*, 2013). Several methods have been proposed

Table 1. *List of the crop models reviewed in this paper. Models are often derived from common 'ancestors'. They have been grouped here into independent groups as independent as possible. The seven highlighted models are models for cereals, still currently used, with different modelling options for the responses to temperature and drought.*

Group	Model name	Reference
1	APSIM- maize	Hammer *et al.*, 2010
2	ARCWHEAT1	Weir *et al.*, 1984
	AFRCWHEAT2	Porter, 1993
	Sirius	Jamieson *et al.*, 1998b
3	CERES-wheat	Ritchie & Otter, 1985
	CERES-maize	Lizaso *et al.*, 2003
	CERES-PR	Lizaso *et al.*, 2005
	CSM-IXIM	Lizaso *et al.*, 2011
4	CropSyst	Stöckle *et al.*, 2003
5	STICS	Brisson *et al.*, 2008
6	SUCROS1	Goodriaan & van Laar, 1994
	SUCROS 2	van Laar *et al.*, 1997
	GECROS	Yin and van Laar, 2005
7	SOYGRO	Wilkerson *et al.*, 1983
	PNUTGRO	Boote *et al.*, 1989
	BEANGRO	Hoogenboom *et al.*, 1994
	CROPGRO	Boote *et al.*, 1998
8	CropSim	Hunt and Pararajasingham, 1995
9	SUNFLO	Casadebaig *et al.*, 2011

for calculating thermal time. They differ in the formalism describing the response to temperature of different developmental processes and in the coordination between processes.

Formalism of responses

The responses to temperature are common to developmental processes such as the expansion or division rates of several organs, or the rate of progression of organ development or plant cycle, as shown in Fig. 2a that presents response curves normalized by the value of each process at 20 °C (Parent *et al.*, 2010b). The diversity of temperature response in 18 species is described by a thermodynamic-based equation with two species-dependent parameters, in addition to the scaling parameter (Parent and Tardieu 2012, Fig. 2b). Most current models have adopted simplifications with different principles (Fig. 3).

Several models assume a linear relation between temperature and developmental rates or leaf expansion (Fig 3 Development, Leaf expansion, e.g. Sirius, CERES-Wheat, CSM-IXIM, SUNFLO), thereby limiting the domain of validity of the model to the range of temperature in which the response is approximately linear. This results in the expression of thermal time in degree days because integration of this linear equation results in cumulating temperatures above a threshold. This formalism has been widely used in crop models for 30 years (Hammer *et al.*, 1993; Sinclair, 1994). It involves one parameter, the x-intercept of the linear relationship, plus the scaling factor that results in the slope of the relationship.

Other models use bilinear (e.g. STICS, CropSyst) or trilinear equations (e.g. APSIM- maize, CropSIM) to approximate

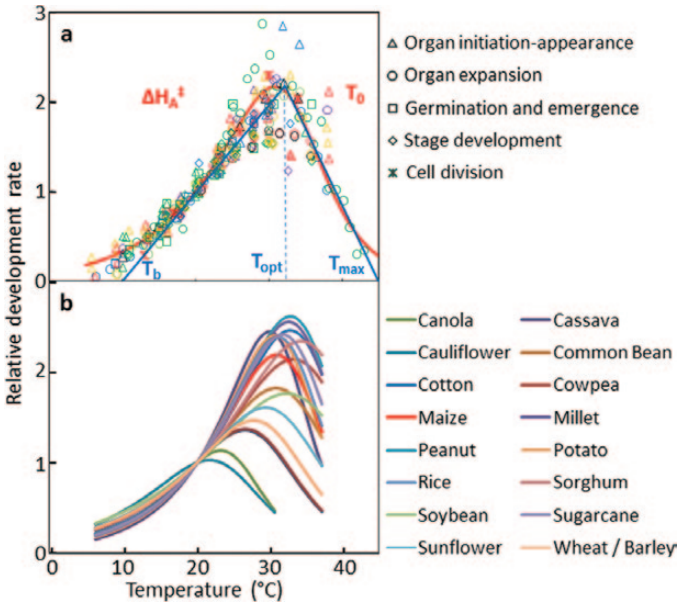

Fig. 2. Temperature responses of development processes in 17 crop species. (a) Responses of development processes in different maize genotypes in a meta-analysis of literature data (Parent and Tardieu, 2012). Each process (symbol) coming from one study (colour) is normalized by its corresponding value at 20 °C. Red line, equation 1, Johnson *et al.*, 1942, modified in Parent and Tardieu, 2012. This equation has two parameters, $\Delta H_A^{\ddagger}$, controlling the curvature at low temperature, and T_0, controlling the decrease in rate at higher temperature. The blue line is the bilinear model used in several crop models with three parameters: T_b, T_{opt}, and T_{max}: base, optimal, and maximal temperatures, respectively. (b) Temperature response of plant development in 17 crop species using the species-dependent parameters of Eq. 1 ($\Delta H_A^{\ddagger}$ and T_0) available in Parent and Tardieu (2012).

$$F(T) = \frac{ATe^{\left(\frac{-\Delta H_A^{\ddagger}}{RT}\right)}}{1+\left[e^{\left(\frac{-\Delta H_A^{\ddagger}}{RT}\right)}\right]^{\alpha\left(1-\frac{T}{T_0}\right)}} \quad \text{(Eq. 1)}$$

where *F(T)* is the considered rate, *T* the temperature (K), R is the gas constant, α is a fixed coefficient for all species, and A is the trait scaling coefficient.

the non-linear shape of the responses (Fig. 3 Development, Leaf expansion). This also results in expression of thermal time in degree days, which accumulate differently in the two or three domains of temperature considered by the model. These formalisms involve three to five parameters, respectively, in bilinear and trilinear equations, plus the scaling factor.

Finally, a few models consider the response as intrinsically curvilinear via either (i) a beta function with four parameters that results in the expression of thermal time in modified degree days (GECROS), (ii) or specific equations as the one used by CSM-IXIM for leaf expansion rate or in CROPGRO for reproductive development (Hoogenboom *et al.*, 1992; Boote *et al.*, 1998; Hartkamp *et al.*, 2002) (iii) or the equation presented in Fig. 2 (Parent *et al.*, 2010b). The last two options result in virtual days whose duration is normalized by temperature ('physiological

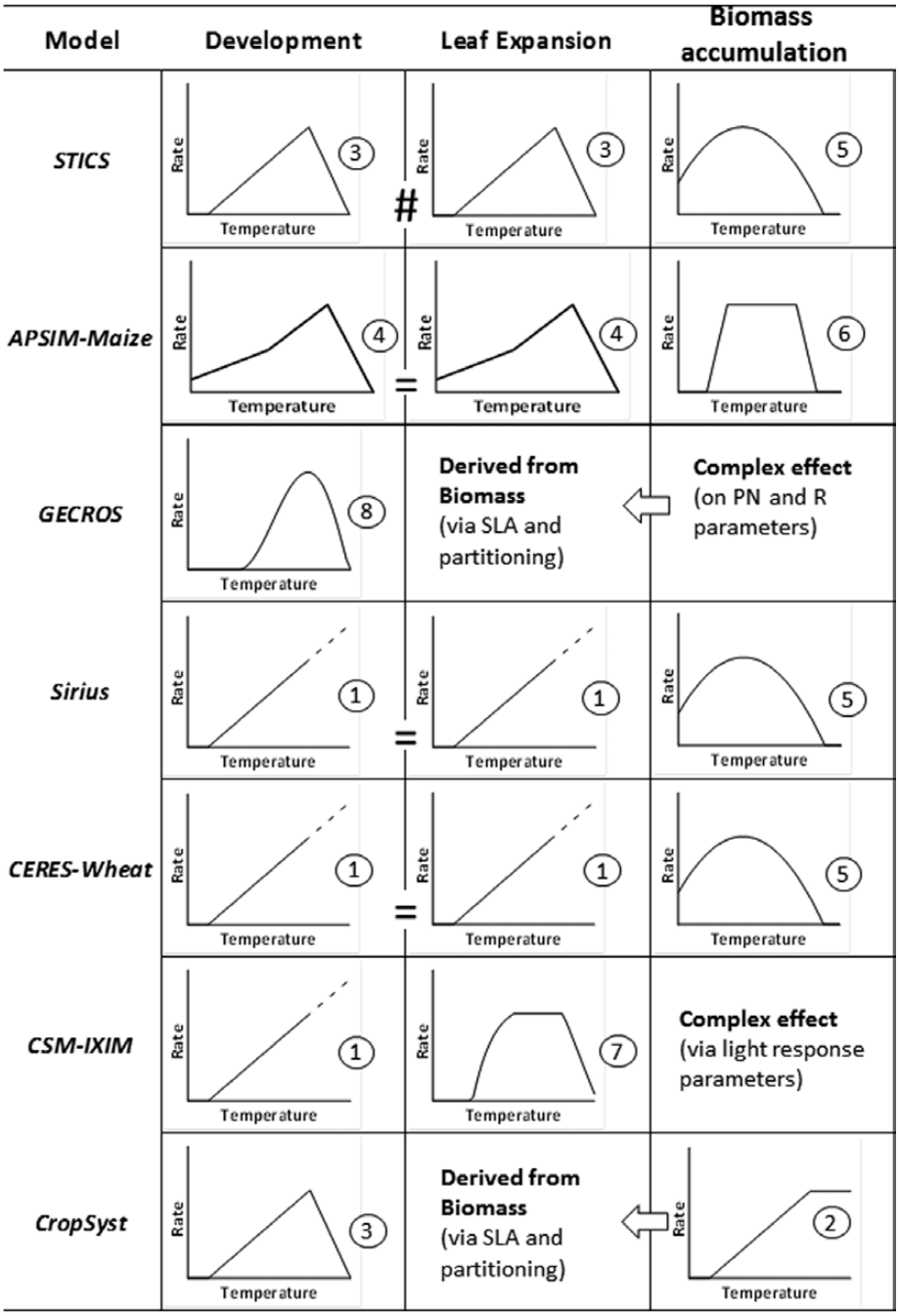

Fig. 3. Formalisms of temperature effects on crop development, leaf expansion, and biomass accumulation in the crop models presented in Table 1. Three components of the different models are presented: responses of the progression in the crop cycle (development); responses of leaf expansion rate; and response of biomass accumulation. The response is replaced by a text when relevant. (1) Linear, with one parameter (T_b). (2) Linear + plateau, with two parameters (T_b, T_{opt}). (3) Bi-Linear with three parameters (T_b, T_{opt}, T_{max}). (4) Tri-linear with 5 parameters (T_b, T_{int}, F_{int}, T_{opt}, T_{max}). (5) Hyperbola with two parameters (b, T_{opt}, see Eq. 2). (6) Trapezoid with four parameters (T_b, T_{opt1}, T_{opt2}, T_{max}). (7) Lizaso *et al.* (2011) equation with 5 parameters (a, b, T_b, T_{opt}, T_{max}), see Eq. 3. (8) Beta function with four parameters (α, β, T_b, T_c). μ is the scaling coefficient, see Eq 4. SLA, specific leaf area.

$$F(t) = 1 - b(T - T_b)^2 \quad \text{(Eq. 2)}$$

$$\begin{cases} F(t) = a\left(1 - exp\left(-b(T - T_b)\right)\right) & \text{if } T < T_{opt} \\ F(t) = \dfrac{(T - T_{max})}{(T_{opt} - T_{max})} & \text{if } T_{opt} \geq T < T_{max} \end{cases} \quad \text{(Eq. 3)}$$

$$F(t) = exp(\mu)(T - T_b)^{\alpha}(T_c - T)^{\beta} \quad \text{(Eq. 4)}$$

days' in CROPGRO; 'biological days' in CropSim; 'equivalent days at 20 °C' in Parent *et al.*, 2010b).

Depending on the chosen formalism, one will detect (or not) the presence of a variability in temperature response between genotypes or between organs. For instance, with the equation presented in Fig. 2, Parent and Tardieu (2012) found no significant genetic differences between lines of different origins (tropical, temperate, or highlands) in maize, wheat, and rice. Because the range of temperatures in which a linear temperature response is fitted usually differs between genotypes, the fitting of a linear equation on an essentially curvilinear response can provide different x-intercepts for each genotype, with higher x-intercepts for genotypes analysed in warmer temperature ranges. The same applies to linear equations fitted to the growths of different organs. Organs growing later in the season are generally subject to warmer conditions, resulting in higher x-intercepts. This results in different intercepts depending on plant stage as in ARCWHEAT or in CropSim-wheat.

Finally, the respective effects of temperature and other variables (in particular light or vapour pressure deficit, VPD) have different weights depending on the formalism of temperature response. The usual procedure for calculating the effects of light or vapour pressure deficit (VPD) is to first take into account the temperature effect, and then to consider the effects of other environmental cues as deviations from the tendency (Ben Haj Salah and Tardieu, 1996; Sadok *et al.*, 2007; Parent *et al.*, 2010a). Hence, the parameterization of VPD or light effects, which have an appreciable genetic variability in maize and rice (Welcker *et al.*, 2011, Parent *et al.*, 2010a), depends on the model formalism for temperature responses.

Coordination between the temperature responses of growth, development, and biomass accumulation

Models also diverge in the way in which the temperature responses of different processes are coordinated. Experimental

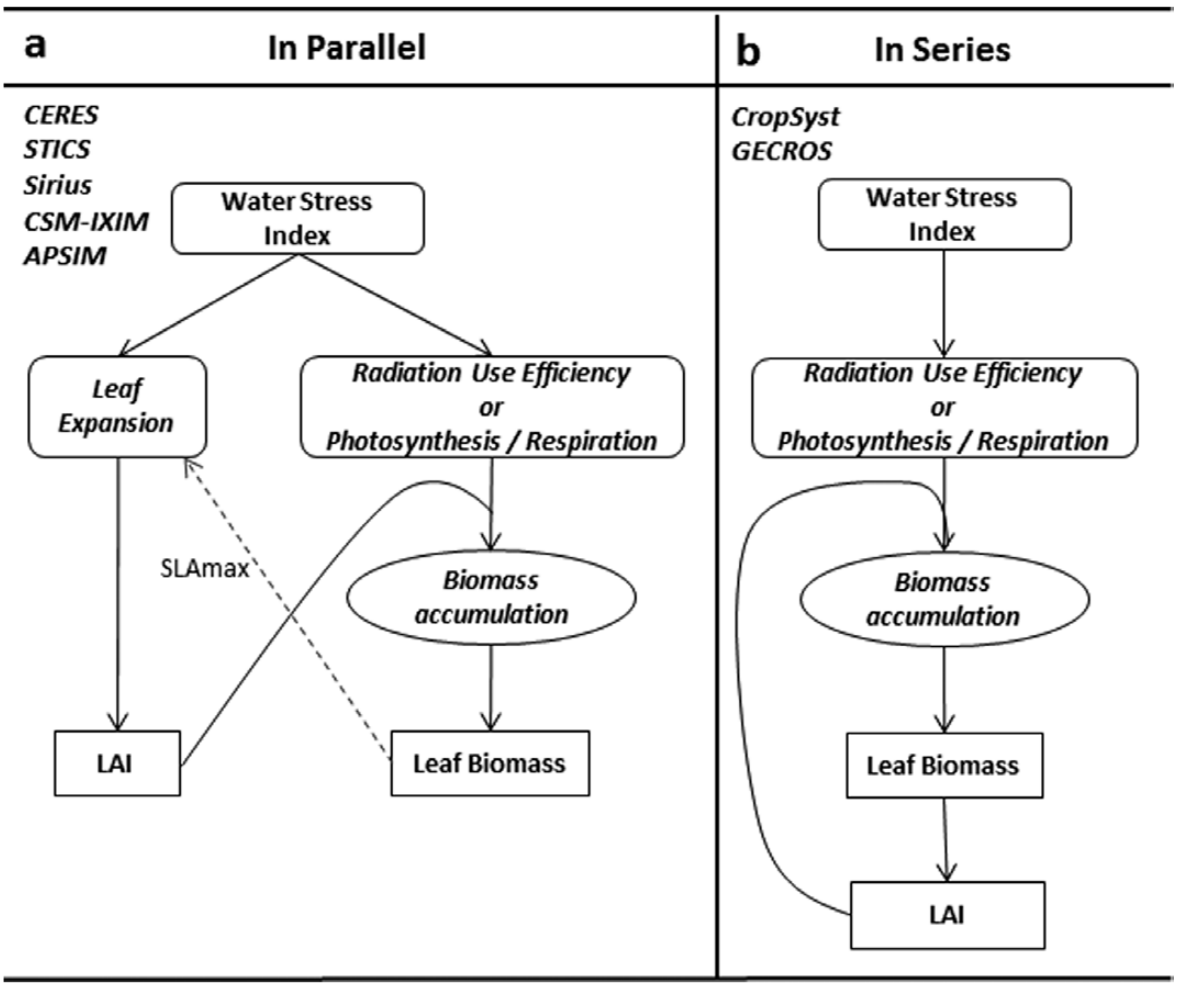

Fig. 4. Flowcharts of water deficit effects on leaf area and biomass in two classes of crop models. (a) Models 'in parallel' in which leaf expansion and biomass production are essentially independent. (b) Models 'in series' in which leaf area index (LAI) depends directly on biomass accumulation, partitioned to leaves and calculated from the specific leaf area (SLA). In both groups, the main feedback is the effect of leaf area index (LAI) on light interception and conversion to biomass. In "in parallel" models, expansion can be limited by biomass accumulation through the maximum specific leaf area, SLA_{max}, in STICS and APSIM, or the effect of water deficit on partitioning to leaves as in CSM-IXIM, CropSyst or GECROS. In CropSyst and APSIM, biomass accumulation is calculated as the minimum of biomass accumulation when calculated from radiation use efficiency (RUE) or transpiration efficiency (TE). Water stress index differs between models: available water content in STICS and Sirius, and ratio of actual/potential transpiration in CERES Wheat, CropSyst, CSM-IXIM, GECROS, and APSIM.

evidences suggest common temperature responses for expansion rate and the reciprocal of durations of cycle phases, phyllochron, or duration of the vegetative phase (Warrington and Kanemasu, 1983a, b; Parent *et al.*, 2010b). This is not the case for the temperature response of photosynthesis or respiration, and more generally for carbon metabolism (Parent *et al.*, 2010b).

The coordination of the temperature responses of biomass accumulation (Fig. 3, Biomass accumulation) and leaf expansion (Fig. 3, Leaf expansion) differs between models. In GECROS and CropSyst, leaf expansion is driven by biomass allocation to leaves (Fig. 4b) and therefore directly depends on the temperature response of photosynthetic activity. Hence, no specific temperature response is implemented for leaf expansion rate. All other models consider different responses for leaf expansion and biomass accumulation, the latter with quite different formalisms between models.

The coordination of development and leaf expansion also differs between models (Fig. 3, Development, Leaf expansion). In APSIM-Maize, Sirius, and CERES-Wheat, the temperature response of leaf expansion rate is common to that of the rate of progression in the cycle (Fig. 2). Conversely, STICS and CSM-IXIM consider different responses, either sharing a similar equation with different parameters (STICS), or using a different equation (CSM-IXIM).

Emergent properties that can affect traits and performances of genotypes result from the modes of coordination chosen by models. Experimentally, expansion is more affected than biomass accumulation by low temperatures (Parent *et al.*, 2010b), resulting in an increase in mass per unit leaf area (Atkin *et al.*, 2006). In the same way, high temperatures result in a reduction in carbon accumulation during the crop cycle (Peng *et al.*, 2004) because cycle duration is more shortened than photosynthesis is increased. These experimentally observed emergent properties can be predicted if shoot biomass on one hand and developmental processes on the other hand have independent temperature responses (as in APSIM, CSM-IXIM, or STICS), but not if leaf expansion and biomass accumulation have common temperature responses, as in CropSyst or GECROS.

Responses to water deficit in current crop models

Transpiration and biomass accumulation

Transpiration flux is simulated in similar ways in most models. Transpiration demand is simulated either via a Penman-Monteith-like equation (Penman, 1948; Allen *et al.*, 1998; Priestley and Taylor, 1972) in STICS, GECROS, CROPGRO, CropSyst, and CERES, or by the product of biomass accumulation by transpiration efficiency and air vapour pressure deficit in APSIM-maize. Plant water status and transpiration are simulated based on indices such as a supply/demand ratio in APSIM-maize, the ratio of actual vs potential transpirations in CERES, CSM-IXIM, SUCROS1&2, GECROS, and CropSyst, or directly via available water content in the root zone in STICS. These simplifications avoid complex equations of water transfer in the soil and in the plant, which include complex determinisms of the water transfer in the plant (Tardieu and Davies, 1993, Caldeira et al 2014) and in the soil (Janott *et al.*, 2011).

Biomass accumulation and its dependence on water deficit are modelled in different ways through either (i) the widely used concept of radiation use efficiency (RUE), which relates biomass to intercepted light in CERES, STICS, APSIM, and CropSyst, or (ii) the simulation of photosynthesis and respiration at leaf level in CERES-PR and CSM-IXIM, or (iii) a more mechanistic approach with the integration of a model of leaf photosynthesis (Farquhar, 1980) in GECROS. An effect of water deficit on RUE or on its components is simulated either by reduction factors depending on a drought index, or indirectly as in APSIM-maize where biomass accumulation is calculated as the minimum of "the light-limited biomass accumulation" and "the water-limited biomass accumulation", which involves transpiration efficiency and available water (Hammer *et al.*, 2010).

Expansive growth

Growth under water deficit is simulated with different principles. Water deficit affects stomatal conductance, photosynthesis, leaf expansion, and the progression in the plant cycle among other traits. A key issue for crop modelling is how these responses are coordinated in the whole plant. Responses can be coordinated in several ways (Tardieu *et al.*, 2011), either (i) via "hubs" that control simultaneously all processes (e.g. due to cascades of transcription factors or common hormonal determinisms), so all of them react in a coordinated way, (ii) in series, with one process governing the others via a cascade of events, or (iii) in parallel, with all processes being affected independently but with feedbacks that coordinate them. It has been argued that the last option better accounts for experimental results than the other two (Tardieu *et al.*, 2011). These options are considered in crop models (Fig. 4, a simplification of the described models that often include more feedbacks than those presented here to ensure model stability).

A coordination 'in series' is hypothesized by CropSyst and GECROS (Fig. 4b). In these models, leaf area expansion is directly derived from biomass accumulation in leaves. Water deficit affects biomass accumulation via reductions in either photosynthesis in GECROS or RUE in CropSyst. Simulated changes in photosynthate availability affect biomass accumulation in leaves, transformed into the increase in leaf area via the specific leaf area (SLA). In this case, SLA is considered as a genotypic parameter used to calculate leaf expansion from leaf dry weight increase.

A coordination 'in parallel' is assumed by CERES-wheat, STICS, SIRIUS, and APSIMmaize (Fig. 4a), in which leaf area expansion and biomass accumulation are essentially independent processes with different response to water deficit. CSM-IXIM works in a similar way, but considering photosynthesis and respiration instead of RUE. In these models, SLA is an emerging property resulting from the balance of leaf expansion and biomass accumulation in leaves,

consistent with experimental results (Bertin and Gary, 1998; Tardieu *et al.*, 1999; Tardieu *et al.*, 2011). However the range of SLA is voluntarily limited in these models, in such a way that biomass accumulation becomes the limiting factor for leaf expansion rate if carbon resources are considered as insufficient to build leaves with an acceptable biomass per unit leaf area.

Depending on the model structure, a given trait and the effect of the QTLs that determine it either has a crucial importance in the overall plant response to water deficit, or is one trait among others. 'In series' structure results in the fact that crucial traits/parameters are the responses of photosynthesis (or RUE) to water deficit, SLA, and the proportion of biomass allocated to each organ. As a consequence, a QTL affecting RUE under water deficit would have a key effect. 'In parallel' structures result in a large effect of water stress indices, largely independently of biomass allocation, resulting in a major effect of QTLs controlling developmental responses to water deficit. Furthermore, the independence of biomass accumulation and leaf expansion results in an increase in carbon availability under water deficit which affects more expansion than photosynthesis, consistent with experimental data (Muller *et al.*, 2011).

An observed genetic variability on a given trait is difficult to simulate if not explicitly present in the model. For instance, it is straightforward to simulate consequences of QTLs affecting leaf expansion (Reymond *et al.*, 2003, Welcker *et al.*, 2011) in an 'in parallel' model as in Chenu *et al.* (2009), whereas inserting them in a 'in series' model would require contrived hypotheses. Even so, simulating the effects on yield of QTLs of leaf expansion still required adjustment of the model (Chenu *et al.*, 2008) and new hypotheses, for instance assuming that QTLs involved in leaf expansion affected both leaves, silk growth, and Anthesis-Silking Interval, consistent with experimental evidences provided by Welcker *et al.* (2007) and Dignat *et al.* (2013).

Simulating the yield of a reference genotype versus simulating the ranking of yield in a panel of genotypes

In a genetic context, a crop model primarily aims at predicting in which environments a given combination of alleles offers a comparative advantage to plants. This potentially allows one to estimate the agronomic value of a combination of QTLs over a long series of climatic data in a mesh of sites covering the considered region (Messina *et al.*, 2011; Harrison *et al.*, 2014). The most essential output of a crop model is in this case the ranking of genotypes in typical environmental scenarios, whereas the absolute value of the mean yield in each environment is probably less essential. Hence, current models simulating the behaviour of a reference genotype in a range of environments have been designed and tested for a purpose that appreciably differs from its purpose in a genetic context.

Are sensitivity analyses based on current crop models suited for designing genotypes in a range of environments? A crucial consequence of the above paragraphs is the large risk associated with sensitivity analyses of traits by using a crop model, in a "you get what you brought" way. Figure 4 strongly suggests that with "parallel" architectures the response of leaf expansion to water deficit is an important trait for improving yield under drought. Because this trait is not explicitly present in 'series' architectures, it cannot be identified as a key trait, whereas RUE and carbon partitioning will. Sensitivity analyses therefore may well predict that most important traits are those that have been placed in the model as a central position in the network. A striking example is found in the work of Jamieson *et al.* (1998a), who showed that a set of crop models provide accurate yield predictions based on the premise that the reduction in biomass accumulation with water deficit is mainly due to changes in photosynthetic efficiency. However, experimental data of the same dataset showed that the decrease in biomass was primarily due to changes in leaf area index. The consistency of observed versus predicted data was based on parameter estimation through model inversion that identifies the parameter value providing the best predictions in a set of experiments. Hence, the studied models provided accurate simulations but a wrong analysis of sensitivity because models would predict better performances for genotypes maintaining a high photosynthetic efficiency at the expense of genotypes maintaining leaf area expansion. In the same way, 27 crop models provide consistent yield predictions (Asseng *et al.* 2013), although these models are based on markedly different principles, equations, and input variables, as reviewed above. These authors propose that the combination of different models (i.e. the median value of all model outputs in a given site) provides the best yield estimate of a reference genotype in a range of environmental conditions.

Overall, crop models used for genetics need to provide accurate estimates of biological processes. As discussed above, accurate yield prediction from inaccurate algorithms (or combination of different algorithms) is probably a more serious problem if one aims at ranking the performance of genotypes that differ in one or another of the mechanisms implemented in the crop models.

Phenotyping, a key for modelling the responses to water deficit and temperature

The use of a crop model for predicting performance of genotypes in water deficit or high temperature scenarios requires that its parameters are measured for each genotype and not optimized. Genotype-dependent parameters were not measured in the past or at too low throughput for hundreds of genotypes. They can be now directly measured in phenotyping platforms (Sadok *et al.*, 2007; Granier *et al.*, 2006; Berger *et al.*, 2010; Fiorani and Schurr, 2013). First attempts of using measured parameters (or QTL-derived parameters originating from measurements) have until now involved *ad hoc* models specifically developed for one function such as flowering time (Yin *et al.*, 2005), leaf elongation rate (Reymond *et al.*, 2003), or peach quality (Quilot *et al.*, 2005). To our knowledge, its use in crop models has until now been limited to "proof of concepts" (Yin *et al.*, 2000; Chenu *et al.*, 2009).

Phenotyping methods may influence the structure of crop models aimed at evaluating genotypes, through the choice of algorithms that involve parameters that can be phenotyped. A striking example is the choice of either a simplified model based on light interception and RUE, or a model predicting photosynthesis and respiration of the canopy. The latter better simulates the effects of environmental conditions, because respiration and photosynthesis have different response to environmental conditions (Oberhuber and Edwards, 1993), potentially resulting in apparently erratic variations of RUE (Loomis and Amthor, 1999). However, such models have a parameter estimation that requires the establishment of the response of photosynthesis to internal CO_2 for each studied genotype, a task currently impossible to carry out on hundreds of genotypes. By contrast, radiation use efficiency (RUE) can be evaluated in a phenotyping platform (Ll. Cabrera, personal communication) and its relation with environmental conditions can be modelled (Loomis and Amthor, 1999). Depending on the phenotyping abilities, one can therefore choose either a process-based model (e.g. with submodels of photosynthesis and respiration) if phenotyping allow its parameterization, or a more empiric model (e.g. involving light interception and RUE) whose parameter can be estimated at high throughput in a phenotyping platform.

Recent years have seen the development of functional-structural plant models (FSPM), linking plant architecture to external physiological function (Prusinkiewicz and Rolland-Lagan, 2006; Barczi *et al.*, 2008). These 3D models allow better estimation of light interception (Fourcaud *et al.*, 2008), currently calculated with a coefficient of extinction and the leaf area index (e.g. APSIM and STICS), or through more complex algorithms but still based on a 2D approach (CERES-PR, CSM-IXIM). In the future, it could be conceivable to include such submodels in crop models for genetics if the large number of parameters were phenotyped in imaging platforms.

Progress in the phenotyping of water flux or water content in organs may lead to future changes in the modelling of water flux and water status *in planta*. Modelling fluxes requires fine time resolutions, a large number of parameters, with differential equation governing flows between reservoirs. This has been considered until now as incompatible with a crop model, resulting in the drought indices reviewed above in "responses to water deficit in current crop models". However, it has become increasingly possible to measure or estimate hydraulic parameters in the plant (Liu *et al.*, 2009; Ehlert *et al.*, 2009) and hydraulic conductivity as a response to several environmental cues (Maurel *et al.*, 2008; Cochard *et al.*, 2007) so they may shortly be evaluated for each genotype. It is therefore tempting to develop a model with hydraulically explicit equations, so QTLs or genes affecting plant hydraulic properties could be accounted for by the model.

Hence, it is proposed here that the level of simplification of any biological process should be based on one's ability to phenotype and get parameters characterizing this process for hundreds of genotypes.

Conclusion

The above paragraphs show that even if current crop models can be used for different objectives, their characteristics may diverge in the future depending on objectives, either simulating the effects of climate change or crop management on the performance of a reference genotype, or simulating the genetic variability of yield responses to climate changes. For engineering or climate change studies, prediction accuracy is the major criteria of decision, and adequate simplifications of the biological complexity can provide good estimation of yield. Conversely, using a model in a genetic context require flexibility, for adapting it to specific questions, traits, and QTLs. Parallel progress of modelling and phenotyping is required to insert independent and relevant biological parameters with genetic diversity into crop models. This is feasible in the short-term for crop models, but more complex models, including genes and metabolic networks (Keurentjes *et al.*, 2011) or functional structural plant models describing 3D architecture of plants, will remain difficult to parameterize and calibrate for a long period.

Overall, we propose that an adequate estimation of QTL impacts requires crop models with algorithms that are closer to actual plant mechanisms, but in such a way that most parameters would be measurable in phenotyping facilities. A solution will probably rise after tries and errors from the community of biologists/modellers. We hope that thoughts as those presented in this paper would result in the building of integrated modelling views developed together by the biologist community.

Acknowledgements

This work was supported by the European project FP7-244374 (DROPS) and the Agence Nationale de la Recherche - Investissement d'Avenir project Amaizing (ANR-10-BTBR-01). The authors are grateful to G. Hammer and P. Martre for useful discussions.

References

Acosta Gallegos JA, VargasVazquez P, White JW. 1996. Effect of sowing date on the growth and seed yield of common bean (*Phaseolus vulgaris* L) in highland environments. *Field Crops Research* **49,** 1–10.

Allen RG, Pereira LS, Raes D, Smith M. 1998. *Crop evapotranspiration: guidelines for computing crop water requirements*. Rome (Italy): Food and Agriculture Organization of the United Nations.

Asseng S, Ewert F, Rosenzweig C *et al*. 2013. Uncertainty in simulating wheat yields under climate change. *Nature Climate Change* **3,** 827–832.

Atkin OK, Loveys BR, Atkinson LJ, Pons TL. 2006. Phenotypic plasticity and growth temperature: understanding interspecific variability. *Journal of Experimental Botany* **57,** 267–281.

Barczi JF, Rey H, Caraglio Y, De Reffye P, Barthelemy D, Dong QX, Fourcaud T. 2008. AmapSim: A structural whole-plant simulator based on botanical knowledge and designed to host external functional models. *Annals of Botany* **101,** 1125–1138.

Ben Haj Salah H, Tardieu F. 1996. Quantitative analysis of the combined effects of temperature, evaporative demand and light on leaf elongation rate in well-watered field and laboratory-grown maize plants. *Journal of Experimental Botany* **47,** 1689 –1698.

Berger B, Parent B, Tester M. 2010. High-throughput shoot imaging to study drought responses. *Journal of Experimental Botany* **61,** 3519–3528.

Bertin N, Gary C. 1998. Short and long term fluctuations of the leaf mass per area of tomato plants—Implications for growth models. *Annals of Botany* **82,** 71–81.

Bonhomme R. 2000. Bases and limits to using 'degree.day' units. *European Journal of Agronomy* **13,** 1–10.

Bonneau J, Taylor J, Parent B, Bennett D, Reynolds M, Feuillet C, Langridge P, Mather D. 2013. Multi-environment analysis and improved mapping of a yield-related QTL on chromosome 3B of wheat. *Theoretical and Applied Genetics* **126,** 747–761.

Boote KJ, Jones JW, Hoogenboom G. 1998. *Simulation of crop growth: CROPGRO model*. New York: Marcel Dekker Inc.

Boote KJ, Jones JW, Hoogenboom G, Wilkerson GG, Jagtap SS. 1989. *PNUTGRO V1.02. Peanut crop growth simulation model user's guide. Florida Agricultural Experiment Station Journal No. 8420*. Gainesville: University of Florida.

Boote KJ, Jones JW, White JW, Asseng S, Lizaso JI. 2013. Putting mechanisms into crop production models. *Plant, Cell and Environment* **36,** 1658–1672.

Brisson N, Gate P, Gouache D, Charmet G, Oury F, Huard F. 2010. Why are wheat yields stagnating in Europe? A comprehensive data analysis for France. *Field Crops Research* **119,** 201–212.

Brisson N, Launay M, Mary B, Beaudoin N. 2008. *Conceptual basis, formalisations and parameterization of the STICS crop model*. Versailles: Editions Quae.

Caldeira CF, Bosio M, Parent B, Jeanguenin L, Chaumont F, Tardieu F. 2014. A hydraulic model is compatible with rapid changes in leaf elongation under fluctuating evaporative demand and soil water status. *Plant Physiology* **164,** 1718–1730.

Casadebaig P, Guilioni L, Lecoeur J, Christophe A, Champolivier L, Debaeke P. 2011. SUNFLO, a model to simulate genotype-specific performance of the sunflower crop in contrasting environments. *Agricultural and Forest Meteorology* **151,** 163–178.

Chapman S, Cooper M, Podlich D, Hammer G. 2003. Evaluating plant breeding strategies by simulating gene action and dryland environment effects. *Agronomy Journal* **95,** 99–113.

Chapman SC, Cooper M, Hammer GL. 2002. Using crop simulation to generate genotype by environment interaction effects for sorghum in water-limited environments. *Australian Journal of Agricultural Research* **53,** 379–389.

Chauhan YS, Wright GC, Holzworth D, Rachaputi RCN, Payero JO. 2013. AQUAMAN: a web-based decision support system for irrigation scheduling in peanuts. *Irrigation Science* **31,** 271–283.

Chenu K, Chapman SC, Hammer GL, McLean G, Salah HBH, Tardieu F. 2008. Short-term responses of leaf growth rate to water deficit scale up to whole-plant and crop levels: an integrated modelling approach in maize. *Plant, Cell and Environment* **31,** 378–391.

Chenu K, Chapman SC, Tardieu F, McLean G, Welcker C, Hammer GL. 2009. Simulating the yield impacts of organ-level quantitative trait loci associated with drought response in maize—a 'gene-to-phenotype' modeling approach. *Genetics* **183,** 1507–1523.

Chenu K, Cooper M, Hammer GL, Mathews KL, Dreccer MF, Chapman SC. 2011. Environment characterization as an aid to wheat improvement: interpreting genotype–environment interactions by modelling water-deficit patterns in North-Eastern Australia. *Journal of Experimental Botany* **62,** 1743–1755.

Cochard H, Venisse J-S, Barigah TS, Brunel N, Herbette S, Guilliot A, Tyree MT, Sakr S. 2007. Putative role of aquaporins in variable hydraulic conductance of leaves in response to light. *Plant Physiology* **143,** 122–133.

Cooper M, van Eeuwijk FA, Hammer GL, Podlich DW, Messina C. 2009. Modeling QTL for complex traits: detection and context for plant breeding. *Current Opinion in Plant Biology* **12,** 231–240.

Cooper M, Woodruff DR, Philips IG, Basford KE, Gilmour AR. 2001. Genotype-by-management interactions for grain yield and grain protein concentration of wheat. *Field Crops Research* **70,** 87–88.

de Wit CT, Brouwer R, Penning de Vries FWT. 1970. The simulation of photosynthetic systems. In: Setlik I, ed. *Prediction and Measurements of Photosynthetic Productivity. Proceedings of the IBP/PP Technical Meeting, Trebon*. Wageningen: Pudoc 47–50.

de Wit CT, Goudriaan J, VanLaar HH, Penning de Vries FWT, Rabbinge R, VanKeulen H, Louwerse W, Sibma L, DeJonge C. 1978. *Simulation of assimilation, respiration and transpiration of crops. Simulation monographs*. Wageningen: Pudoc.

Dignat G, Welcker C, Sawkins M, Ribaut JM, Tardieu F. 2013. The growths of leaves, shoots, roots and reproductive organs partly share their genetic control in maize plants. *Plant, Cell and Environment* **36,** 1105–1119.

Duncan WG, R.S. L, W.A. W, R. H. 1967. A model for simulating photosynthesis in plant communities. *Hilgardia* **38,** 181–205.

Edmeades GO, Bolanos J, Chapman SC, Lafitte HR, Banziger M. 1999. Selection improves drought tolerance in tropical maize populations: I. Gains in biomass, grain yield, and harvest index. *Crop Science* **39,** 1306–1315.

Egli DB, Bruening W. 1992. Planting date and soybean yield. Evaluation of environmental effects with a crop simulation model. Soygro. *Agricultural and Forest Meteorology* **62,** 19–29.

Ehlert C, Maurel C, Tardieu F, Simonneau T. 2009. Aquaporin-mediated reduction in maize root hydraulic conductivity impacts cell turgor and leaf elongation even without changing transpiration. *Plant Physiology* **150,** 1093–1104.

Farquhar GD, Caemmerer SV, Berry JA. 1980. A biochemical model of phtosynthetic CO_2 assimilation in leaves of C-3 species. *Planta* **149,** 78–90.

Fiorani F, Schurr U. 2013. Future scenarios for plant phenotyping. *Annual Review of Plant Biology* **64,** 267–291.

Fourcaud F, Zhang X, Stokes A, Lambers H, Korner C. 2008. Plant growth modelling and applications: The increasing importance of plant architecture in growth models. *Annals of Botany* **101,** 1053–1063.

Fukai S, Inthapanya P, Blamey FPC, Khunthasuvon S. 1999. Genotypic variation in rice grown in low fertile soils and drought-prone, rainfed lowland environments. *Field Crops Research* **64,** 121–130.

Goodriaan J, van Laar HH. 1994. *Modelling potential crop growth processes*. Dordrecht: Kluwer Academic Publishers.

Granier C, Aguirrezabal L, Chenu K *et al*. 2006. PHENOPSIS, an automated platform for reproducible phenotyping of plant responses to soil water deficit in *Arabidopsis thaliana* permitted the identification of an accession with low sensitivity to soil water deficit. *New Phytologist* **169,** 623–635.

Hammer G, Cooper M, Tardieu F, Welch S, Walsh B, van Eeuwijk F, Chapman S, Podlich D. 2006. Models for navigating biological complexity in breeding improved crop plants. *Trends in Plant Science* **11,** 587–593.

Hammer GL, Carberry PS, Muchow RC. 1993. Modelling genotypic and environmental control of leaf area dynamics in grain sorghum. I. Whole plant level. *Field Crops Research* **33,** 293–310.

Hammer GL, Chapman S, van Oosterom E, Podlich DW. 2005. Trait physiology and crop modelling as a framework to link phenotypic complexity to underlying genetic systems. *Australian Journal of Agricultural Research* **56,** 947–960.

Hammer GL, van Oosterom E, McLean G, Chapman SC, Broad I, Harland P, Muchow RC. 2010. Adapting APSIM to model the physiology and genetics of complex adaptive traits in field crops. *Journal of Experimental Botany* **61,** 2185–2202.

Harrison MT, Tardieu F, Dong Z, Messina CD, Hammer GL. 2014. Characterizing drought stress and trait influence on maize yield under current and future conditions. *Global Change Biology* **20,** 867–878.

Hartkamp AD, Hoogenboom G, White JW. 2002. Adaptation of the CROPGRO growth model to velvet bean (*Mucuna pruriens*) I. Model development. *Field Crops Research* **78,** 9–25.

Hoogenboom G, Jones JW, Boote KJ. 1992. Modelling growth, development, and yield of grain legumes using SOYGRO, PNUTGRO, and BEANGRO. A review. *Transactions of the Asae* **35,** 2043–2056.

Hoogenboom G, White JW, Jones JW, Boote KJ. 1994. BEANGRO. A process-oriented dry bean model with a versatile user-interface. *Agronomy Journal* **86,** 182–190.

Hunt LA, Pararajasingham S. 1995. CROPSIM-WHEAT. a model describing the growth and development of wheat. *Canadian Journal of Plant Science* **75,** 619–632.

Jamieson PD, Porter JR, Goudriaan J, Ritchie JT, van Keulen H, Stol W. 1998*a*. A comparison of the models AFRCWHEAT2, CERES-wheat, Sirius, SUCROS2 and SWHEAT with measurements from wheat grown under drought. *Field Crops Research* **55,** 23–44.

Jamieson PD, Semenov MA, Brooking IR, Francis GS. 1998*b*. Sirius: a mechanistic model of wheat response to environmental variation. *European Journal of Agronomy* **8,** 161–179.

Janott M, Gayler S, Gessler A, Javaux M, Klier C, Priesack E. 2011. A one-dimensional model of water flow in soil-plant systems based on plant architecture. *Plant and Soil* **341,** 233–256.

Keurentjes JJB, Angenent GC, Dicke M, Dos Santos VAPM, Molenaar J, Thomma BPHJ. 2011. Redefining plant systems biology: from cell to ecosystem. *Trends in Plant Science* **16,** 183–190.

Kim HK, van Oosterom E, Dingkuhn M, Luquet D, Hammer G. 2010. Regulation of tillering in sorghum: environmental effects. *Annals of Botany* **106,** 57–67.

Kumar SR, Hammer GL, Broad I, Harland P, McLean G. 2009. Modelling environmental effects on phenology and canopy development of diverse sorghum genotypes. *Field Crops Research* **111,** 157–165.

Liu B-B, Steudle E, Deng X-P, Zhang S-Q. 2009. Root pressure probe can be used to measure the hydraulic properties of whole root systems of corn (*Zea mays* L.). *Botanical Studies* **50,** 303–310.

Lizaso JI, Batchelor WD, Boote KJ, Westgate ME. 2005. Development of a leaf-level canopy assimilation model for CERES-Malize. *Agronomy Journal* **97,** 722–733.

Lizaso JI, Batchelor WD, Westgate ME, Echarte L. 2003. Enhancing the ability of CERES-Maize to compute light capture. *Agricultural Systems* **76,** 293–311.

Lizaso JI, Boote KJ, Jones JW, Porter CH, Echarte L, Westgate ME, Sonohat G. 2011. CSM-IXIM: A new maize simulation model for dssat version 4.5. *Agronomy Journal* **103,** 766–779.

Lobell DB, Gourdji SM. 2012. The influence of climate change on global crop productivity. *Plant Physiology* **160,** 1686–1697.

Lobell DB, Schlenker W, Costa-Roberts J. 2011. Climate trends and global crop production since 1980. *Science* **333,** 616–620.

Loomis RS, Amthor JS. 1999. Yield potential, plant assimilatory capacity, and metabolic efficiencies. *Crop Science* **39,** 1584–1596.

Maccaferri M, Sanguineti MC, Corneti S *et al*. 2008. Quantitative trait loci for grain yield and adaptation of durum wheat (*Triticum durum* Desf.) across a wide range of water availability. *Genetics* **178,** 489–511.

Maurel C, Verdoucq L, Luu D-T, Santoni V. 2008. Plant aquaporins: Membrane channels with multiple integrated functions. *Annual Review of Plant Biology* **59,** 595–624.

Messina CD, Podlich D, Dong Z, Samples M, Cooper M. 2011. Yield-trait performance landscapes: from theory to application in breeding maize for drought tolerance. *Journal of Experimental Botany* **62,** 855–868.

Muller B, Pantin F, Genard M, Turc O, Freixes S, Piques M, Gibon Y. 2011. Water deficits uncouple growth from photosynthesis, increase C content, and modify the relationships between C and growth in sink organs. *Journal of Experimental Botany* **62,** 1715–1729.

Nakagawa H, Yamagishi J, Miyamoto N, Motoyama M, Yano M, Nemoto K. 2005. Flowering response of rice to photoperiod and temperature: a QTL analysis using a phenological model. *Theoretical and Applied Genetics* **110,** 778–786.

Oberhuber W, Edwards GE. 1993. Temperature dependence of the linkage of quantum yield of photosystem II to CO_2 fixation in C4 and C3 plants. *Plant Physiology* **101,** 507–512.

Parent B, Suard B, Serraj R, Tardieu F. 2010*a*. Rice leaf growth and water potential are resilient to evaporative demand and soil water deficit once the effects of root system are neutralized. *Plant, Cell and Environment* **33,** 1256–1267.

Parent B, Tardieu F. 2012. Temperature responses of developmental processes have not been affected by breeding in different ecological areas for 17 crop species. *New Phytologist* **194,** 760–774.

Parent B, Turc O, Gibon Y, Stitt M, Tardieu F. 2010*b*. Modelling temperature-compensated physiological rates, based on the coordination of responses to temperature of developmental processes. *Journal of Experimental Botany* **61,** 2057–2069.

Peng SB, Huang JL, Sheehy JE, Laza RC, Visperas RM, Zhong XH, Centeno GS, Khush GS, Cassman KG. 2004. Rice yields decline with higher night temperature from global warming. *Proceedings of the National Academy of Sciences, USA* **101,** 9971–9975.

Penman HL. 1948. Natural evaporation from open water, hare soil and grass. *Proceedings of the Royal Society of London. Series A, Mathematical and physical sciences* **193,** 120–145.

Porter JR. 1993. AFRCWHEAT2: a model of the growth and development of wheat incorporating responses to water and nitrogen. *European Journal of Agronomy* **2,** 69–82.

Potgieter A, Meinke H, Doherty A, Sadras VO, Hammer G, Crimp S, Rodriguez D. 2013. Spatial impact of projected changes in rainfall and temperature on wheat yields in Australia. *Climatic Change* **117,** 163–179.

Price A, Courtois B. 1999. Mapping QTLs associated with drought resistance in rice: Progress, problems and prospects. *Plant Growth Regulation* **29,** 123–133.

Priestley CHB, Taylor RJ. 1972. On the assessment of surface heat flux and evaporation using large-scale parameters. *Monthly Weather Review* **100,** 81–82.

Prusinkiewicz P, Rolland-Lagan AG. 2006. Modelling plant morphogenesis. *Current Opinion in Plant Biology* **9,** 83–88.

Quilot B, Kervella J, Genard M, Lescourret F. 2005. Analysing the genetic control of peach fruit quality through an ecophysiological model combined with a QTL approach. *Journal of Experimental Botany* **56,** 3083–3092.

Reymond M, Muller B, Leonardi A, Charcosset A, Tardieu F. 2003. Combining quantitative trait loci analysis and an ecophysiological model to analyze the genetic variability of the responses of maize leaf growth to temperature and water deficit. *Plant Physiology* **131,** 664–675.

Richards RA. 2006. Physiological traits used in the breeding of new cultivars for water-scarce environments. *Agricultural Water Management* **80,** 197–211.

Ritchie JT, Otter S. 1985. Description and performance of CERES-Wheat: a user-oriented wheat yield model. In: Willis WO, ed. *ARS wheat yield project*. Washington: Agricultural Research Service, US Department of Agriculture, 159–175.

Rosenzweig C, Jones JW, Hatfield JL *et al*. 2013. The agricultural model intercomparison and improvement project (AgMIP): Protocols and pilot studies. *Agricultural and Forest Meteorology* **170,** 166–182.

Sadok W, Naudin P, Boussuge B, Muller B, Welcker C, Tardieu F. 2007. Leaf growth rate per unit thermal time follows QTL-dependent daily patterns in hundreds of maize lines under naturally fluctuating conditions. *Plant, Cell and Environment* **30,** 135–146.

Sinclair T. 1994. Limits to crop yield. In: Boote KJ, Bennet JM, Sinclair TR, Paulsen GM, eds. *Physiology and Determination of crop yield*. Madison: American Society of Agronomy, 509–532.

Stöckle CO, Donatelli M, Nelson R. 2003. CropSyst, a cropping systems simulation model. *European Journal of Agronomy* **18,** 289–307.

Tardieu F. 2003. Virtual plants: modelling as a tool for the genomics of tolerance to water deficit. *Trends in Plant Science* **8,** 9–14.

Tardieu F. 2012. Any trait or trait-related allele can confer drought tolerance: just design the right drought scenario. *Journal of Experimental Botany* **63,** 25–31.

Tardieu F, Davies WJ. 1993. Integration of hydraulic and chemical signaling in the control of stomatal conductance and water status of droughted plants. *Plant, Cell and Environment* **16,** 341–349.

Tardieu F, Granier C, Muller B. 1999. Modelling leaf expansion in a fluctuating environment: are changes in specific leaf area a consequence of changes in expansion rate? *New Phytologist* **143,** 33–44.

Tardieu F, Granier C, Muller B. 2011. Water deficit and growth. Coordinating processes without an orchestrator? *Current Opinion in Plant Biology* **14,** 283–289.

Tardieu F, Tuberosa R. 2010. Dissection and modelling of abiotic stress tolerance in plants. *Current Opinion in Plant Biology* **13,** 206–212.

van Laar HH, Goudriaan J, van Keulen H. 1997. *SUCROS97: Simulation of crop growth for potential and water-limited production situations. As applied to spring wheat*. Wageningen: Haren & PE.

Warrington IJ, Kanemasu ET. 1983*a*. Corn growth response to temperature and photoperiod. I. Seedling emergence, tassel initiation, and anthesis. *Agronomy Journal* **75,** 749–754.

Warrington IJ, Kanemasu ET. 1983*b*. Corn growth response to temperature and photoperiod. II. Leaf-initiation and leaf-appearance rates. *Agronomy Journal* **75,** 755 – 761.

Weir AH, Bragg PL, Porter JR, Rayner JH. 1984. A winter-wheat crop simulation model without water or nutrient limitations. *Journal of Agricultural Science* **102,** 371–382.

Welcker C, Boussuge B, Bencivenni C, Ribaut JM, Tardieu F. 2007. Are source and sink strengths genetically linked in maize plants subjected to water deficit? A QTL study of the responses of leaf growth and of Anthesis-Silking Interval to water deficit. *Journal of Experimental Botany* **58,** 339–349.

Welcker C, Sadok W, Dignat G, Renault M, Salvi S, Charcosset A, Tardieu F. 2011. A common genetic determinism for sensitivities to soil water deficit and evaporative demand: meta-analysis of quantitative trait loci and introgression lines of maize. *Plant Physiology* **157,** 718–729.

Whish J, Butler G, Castor M, Cawthray S, Broad I, Carberry P, Hammer G, McLean G, Routley R, Yeates S. 2005. Modelling the effects of row configuration on sorghum yield reliability in north-eastern Australia. *Australian Journal of Agricultural Research* **56,** 11–23.

Wilkerson GG, Jones JW, Boote KJ, Ingram KT, Mishoe JW. 1983. Modelling soybean growth for crop management. *Transactions of the ASABE* **26,** 63–73.

Yin XY, Chasalow SD, Dourleijn CJ, Stam P, Kropff MJ. 2000. Coupling estimated effects of QTLs for physiological traits to a crop growth model: predicting yield variation among recombinant inbred lines in barley. *Heredity* **85,** 539–549.

Yin XY, van Laar HH. 2005. *Crop Systems Dynamics. An ecophysiological simulation model of genotype-by-environment interactions*. Wageningen: Wageningen Academic Publishers.

Drought and Abscisic Acid Effects on Aquaporin Content Translate into Changes in Hydraulic Conductivity and Leaf Growth Rate: A Trans-Scale Approach[1][W][OA]

Boris Parent, Charles Hachez, Elise Redondo, Thierry Simonneau, François Chaumont, and François Tardieu*

INRA, UMR 759 Laboratoire d'Ecophysiologie des Plantes sous Stress Environnementaux, F–34060 Montpellier, France (B.P., T.S., F.T.); Institut des Sciences de la Vie, Université catholique de Louvain, B–1348 Louvain-la-Neuve, Belgium (C.H., F.C.); and Biogemma Auvergne, ZI du Brézet, F–63028, Clermont-Ferrand, France (E.R.)

The effects of abscisic acid (ABA) on aquaporin content, root hydraulic conductivity (Lp_r), whole plant hydraulic conductance, and leaf growth are controversial. We addressed these effects via a combination of experiments at different scales of plant organization and tested their consistency via a model. We analyzed under moderate water deficit a series of transformed maize (*Zea mays*) lines, one sense and three antisense, affected in *NCED* (for 9-cis-epoxycarotenoid dioxygenase) gene expression and that differed in the concentration of ABA in the xylem sap. In roots, the mRNA expression of most aquaporin *PIP* (for plasma membrane intrinsic protein) genes was increased in sense plants and decreased in antisense plants. The same pattern was observed for the protein contents of four PIPs. This resulted in more than 6-fold differences between lines in Lp_r under both hydrostatic and osmotic gradients of water potential. This effect was probably due to differences in aquaporin activity, because it was nearly abolished by a hydrogen peroxide treatment, which blocks the water channel activity of aquaporins. The hydraulic conductance of intact whole plants was affected in the same way when measured either in steady-state conditions or via the rate of recovery of leaf water potential after rewatering. The recoveries of leaf water potential and elongation upon rehydration differed between lines and were accounted for by the experimentally measured Lp_r in a model of water transfer. Overall, these results suggest that ABA has long-lasting effects on plant hydraulic properties via aquaporin activity, which contributes to the maintenance of a favorable plant water status.

During water deficit, abscisic acid (ABA) is involved in three strategies used by plants to avoid deleterious leaf dehydration. First, plants close stomata and decrease transpiration rate, with a consensus on the effect of ABA (Zhang and Davies, 1990a; Borel et al., 2001) but differences regarding its origin in the plant (Christmann et al., 2007; Endo et al., 2008). Second, plants decrease shoot growth in order to limit transpiration. The contribution of ABA to this reduction differs between studies, with either positive effects of ABA (Sharp, 2002; Sansberro et al., 2004; Thompson et al., 2007a) or negative effects (Zhang and Davies, 1990b; Ben Haj Salah and Tardieu, 1997; Bacon et al., 1998). Third, plants tend to control root water uptake and/or plant water status via root growth (Sharp, 2002) and root hydraulic conductivity (Lp_r; Kaldenhoff et al., 2008; Maurel et al., 2008).

The effects of soil water deficit and of ABA on Lp_r are controversial. Water deficit tends to decrease Lp_r (Lo Gullo et al., 1998; Zhang and Tyerman, 1999; North et al., 2004; Vandeleur et al., 2009), while ABA has the opposite effect in most studies (Morillon and Chrispeels, 2001; Thompson et al., 2007a). In a few studies, exogenous ABA had no effect or a negative effect on hydraulic conductivity (Wan and Zwiazek, 1999; Aroca et al., 2003), while in others a positive effect has been observed at both the cell level (Hose et al., 2000; Wan et al., 2004; Lee et al., 2005) and the whole root level (Quintero et al., 1999; Sauter et al., 2002; Schraut et al., 2005). However, these responses were transient (Hose et al., 2000) and were positive or negative depending on the ABA concentration (Beaudette et al., 2007).

Change in aquaporin mRNA and protein contents in response to water deficit and ABA is also a matter of debate (Kaldenhoff et al., 2008). ABA induces transcription factors that regulate the expression of PIP (for plasma membrane intrinsic protein) aquaporins (Kaldenhoff et al., 1996; Shinozaki et al., 1998). However, exogenous ABA affects a larger number of PIP isoforms than water deficit (Jang et al., 2004), suggesting some degree of independence between ABA and drought signal transduction pathways (Mariaux et al., 1998). In addition, increase in *PIP* mRNA expression is

[1] This work was supported by the Agence Nationale de la Recherche Genoplante project Waterless, the Generation Challenge Programme Generation, the Belgian National Fund for Scientific Research, the Inter-University Attraction Pole Programme-Belgian Science Policy, and the Communauté Française de Belgique-Actions de Recherches Concertées.

* Corresponding author; e-mail tardieu@supagro.inra.fr.

The author responsible for distribution of materials integral to the findings presented in this article in accordance with the policy described in the Instructions for Authors (www.plantphysiol.org) is: François Tardieu (tardieu@supagro.inra.fr).

[W] The online version of this article contains Web-only data.

[OA] Open Access articles can be viewed online without a subscription.

www.plantphysiol.org/cgi/doi/10.1104/pp.108.130682

often transient and dependent on ABA concentration (Zhu et al., 2005; Beaudette et al., 2007) and does not necessarily result in an increase in PIP protein content (Morillon and Chrispeels, 2001; Aroca et al., 2006).

Aquaporins play a key role in radial water transport in roots and leaves under both hydrostatic and osmotic gradients (Steudle, 2000; Tyerman et al., 2002; Maurel et al., 2008). The contribution of aquaporin-mediated water transport has been evaluated with inhibitors, namely mercuric salt (Martre et al., 2001), acid load (Tournaire-Roux et al., 2003), and hydrogen peroxide (H_2O_2; Ye and Steudle, 2006; Boursiac et al., 2008). These studies indicate that water transport by aquaporins accounts for 20% to 85% of the overall water transport depending on the species (Wan and Zwiazek, 1999; Barrowclough et al., 2000). Whereas the importance of aquaporins in Lp_r has been demonstrated (Maurel et al., 2008), the resulting effect on overall plant conductance, leaf water potential, and leaf elongation rate is still poorly studied. Experiments using plants with modified aquaporin expression report differences in leaf water potential during the day (Lian et al., 2004) or during rewetting (Martre et al., 2002).

The purpose of this work was to test whether drought and ABA have consistent effects on plant hydraulic properties at different scales of plant organization, namely the abundance of aquaporin transcripts and proteins, the Lp_r under both osmotic and hydrostatic gradients, the whole plant hydraulic conductance evaluated in steadily transpiring plants or upon rehydration, and the recovery of leaf elongation rate upon rehydration. Hence, we performed independent experiments at each scale of organization and then linked these scales with a model that allows the weighing of relative contributions of Lp_r and other possible causes on the whole plant hydraulic behavior.

To this aim, we have used maize (*Zea mays*) lines affected in the expression of the *NCED/VP14* gene encoding the 9-cis-epoxycarotenoid dioxygenase enzyme, previously identified from the *vp14* mutation (Tan et al., 1997). NCED/VP14 catalyzes the first specific step in ABA biosynthesis and affects ABA production when overexpressed (Thompson et al., 2000, 2007b) or underexpressed (Voisin et al., 2006). *NCED/VP14* expression as well as NCED/VP14 protein content are indeed strongly correlated with ABA levels (Qin and Zeevaart, 1999). These lines were subjected to changes in soil water content, evaporative demand, or pressure on the root system, thereby affecting independently water deficit and the concentration of ABA in the xylem sap.

RESULTS

A Set of Maize Lines Transformed on the *NCED/VP14* Gene Differed in $[ABA]_{xyl}$, Stomatal Conductance, and Transpiration Rate in Greenhouse Experiments

The genetic transformation was targeted to one NCED gene with sense and antisense constructs. It resulted in three antisense lines (AS1, AS2, and AS5) and one sense line (S). The concentrations of ABA in the xylem sap ($[ABA]_{xyl}$) differed significantly between AS, null transformants, and S plants in well-watered conditions as well as in moderate water deficit (Fig. 1A), consistent with the lower and higher transcript amounts of *NCED/VP14* in AS and S plants, respectively (Supplemental Fig. S1). Null transformants resulting from each transformation event had insignificant differences in $[ABA]_{xyl}$. Therefore, they were pooled in all figures and are referred to as WT hereafter. Plants of the three AS lines had a low but still appreciable $[ABA]_{xyl}$ in both well-watered and dry

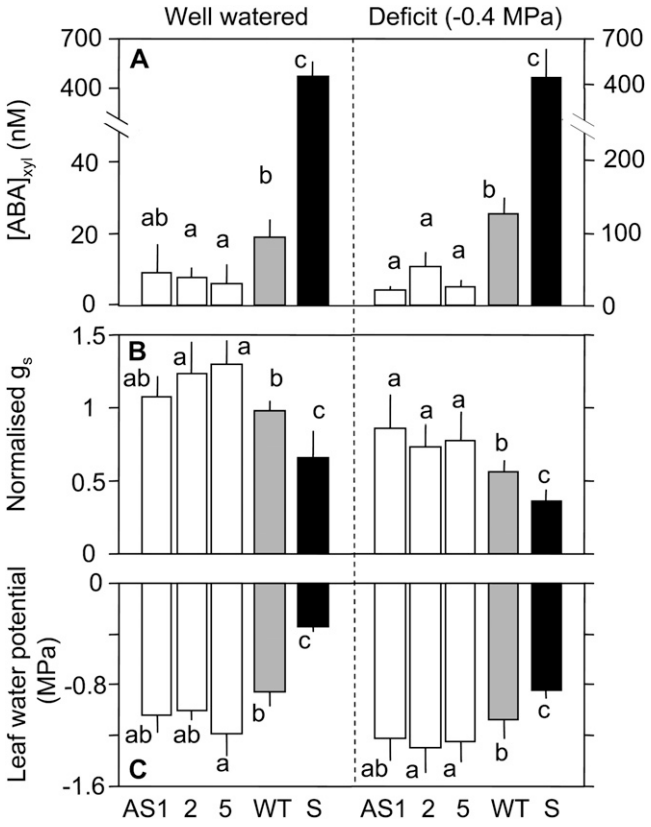

Figure 1. ABA concentration in the xylem sap (A), midday stomatal conductance (B; g_s), and leaf water potential (C) in three greenhouse experiments with high evaporative demand (experiments 1–3 in Table II; only days with noontime VPDs from 2 to 2.8 kPa were kept in the analysis). Two contrasting water regimes were compared, well watered and a mild water deficit with a soil water potential of −0.4 MPa, for three AS lines, one S line, and their null transformants (pooled and named WT). A, Xylem sap was collected at the end of the night. B, Stomatal conductance was measured at noon. Because g_s of WT plants differed between experiments, from 120 to 180 mmol m^{-2} s^{-1}, it was normalized by the mean value in WT. C, Leaf water potential was measured at noon in nonexpanding leaves. Data were averaged from the three experiments ($n > 10$ in each condition and line). Error bars indicate confidence intervals at the 0.95 risk level. Bars associated with the same letter indicate nonsignificant differences ($P > 0.05$) in a Benjamini and Hochberg *t* test (Benjamini and Hochberg, 1995).

conditions (Fig. 1A; insignificant differences between AS lines), so their stomata closed under water deficit (Fig. 1B). The transpiration flow measured at midday in moderately droughted plants grown in the greenhouse was significantly higher in the three AS plants than in WT plants (Fig. 2A). Sense plants had the opposite behavior, with a high $[ABA]_{xyl}$ (>400 nM), a low stomatal conductance in both well-watered and droughted plants (Fig. 1, A and B), and a transpiration rate per unit leaf area 2-fold lower than that of WT plants (Fig. 2A). AS plants had comparable phenotypes to WT plants, except that they germinated more quickly and wilted slightly earlier upon water shortage. Because the three AS lines had similar behaviors, most studies were carried out in the AS5 line. S plants had a smaller leaf area than AS and WT plants, due to differences in leaf growth rate in well-watered conditions before the experiment.

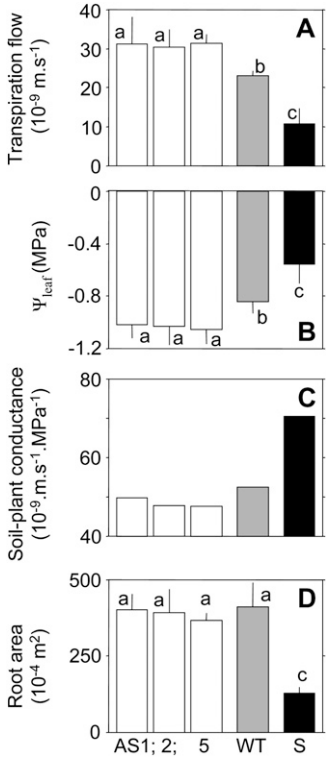

Figure 2. Transpiration flow (A), leaf water potential (B; Ψ_{leaf}), calculated conductance of water transfer from soil to leaves (C), and root area (D) in a greenhouse experiment with moderate evaporative demand (experiment 3 in Table II; only days with noontime VPD from 1.3 to 1.8 kPa were kept in the analysis) and water deficit (soil water potential of −0.4 MPa). Three AS lines (AS1, AS2, and AS5) and one S line were compared with null transformants (WT). A and B, Transpiration flow and leaf water potential were measured at noontime (n = 4–10). C, Soil-leaf resistance was calculated as the ratio of the difference of potential between soil and leaves to the transpiration flow. D, Root area of three plants of each line at the six-leaf stage. Bars represent mean values (n = 3–8). Error bars indicate confidence intervals at the 0.95 risk level. Bars associated with the same letter indicate nonsignificant differences ($P > 0.05$) in a Benjamini and Hochberg t test (Benjamini and Hochberg, 1995).

PIP Expression in Roots Was Highly Dependent on ABA Biosynthesis

We compared by quantitative reverse transcription (RT)-PCR the expression levels of *ZmPIP* genes in roots of S, WT, and AS plants (Fig. 3). Plants were grown hydroponically and sampled in the early morning at the same phenological stage and root water potential (72-h polyethylene glycol [PEG] stress, −0.4 MPa) as in the water deficit treatments presented in Figures 1 and 2. Expression levels of the five *PIP* genes belonging to the PIP1 subgroup were significantly higher in S plants and lower in AS plants. The strongest effect was observed for *ZmPIP1;2*, *ZmPIP1;3*, and *ZmPIP1;4*, with a 9- to 10-fold difference in expression between AS and S plants ($P < 10^{-5}$). In the *PIP2* subgroup, the expression levels of two *PIP* genes were increased in S plants (*ZmPIP2;1* and *ZmPIP2;2*) and those of four *PIP* genes were decreased in AS plants (*ZmPIP2;1*, *ZmPIP2;2*, *ZmPIP2;3*, and *ZmPIP2;6*). Overall, for most *PIP* isoforms, the expression levels were affected by changes in ABA biosynthesis in a long-lasting way, with higher expression levels in S plants and lower levels in AS plants.

Increased and Decreased ABA Biosynthesis Largely Affected the Protein Contents of Three PIPs in Roots and of Two PIPs in Leaves

PIPs belonging to either PIP1 or PIP2 subgroups were chosen for further investigation using specific antibodies raised against each PIP (Fig. 4A). These were ZmPIP1;2, whose gene expression was the most increased in S plants and four proteins of the PIP2 subgroup; and ZmPIP2;1/2;2, ZmPIP2;5, and ZmPIP2;6, whose gene expression was the highest in maize roots in this study and in the study of Hachez et al. (2006). All ZmPIP immunoblot analyses revealed two major bands at about 28 and 55 kD, corresponding to monomeric and dimeric forms (Fig. 4A). Primary roots coming from AS lines showed strongly decreased amounts of the isoforms ZmPIP1;2 (−75%), ZmPIP2;1/2;2 (−43%), and ZmPIP2;5 (−49%; Fig. 4). Opposite effects on the amounts of the same proteins were observed in the S line, especially in ZmPIP1;2 (12-fold increase; Fig. 4). The intermediate band (around 40 kD) detected with ZmPIP2;6 antibodies corresponds to a cross-reacting unrelated protein (data not shown).

Leaves also showed differences in PIP protein amounts, although to a lesser extent than roots (Fig. 4B). S plants had higher amounts of ZmPIP1;2 and ZmPIP2;1/2;2 than WT plants (1.9- and 1.3-fold increases, respectively), with an opposite effect for AS plants (0.75 and 0.9). In contrast, no signals were

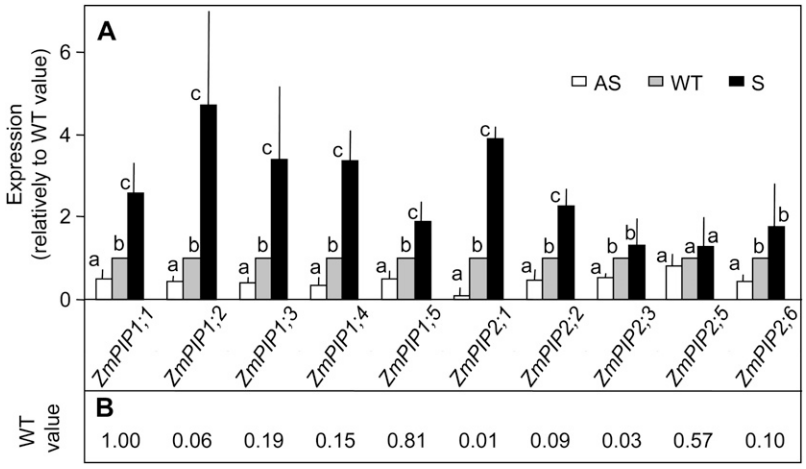

Figure 3. Expression levels (measured by quantitative RT-PCR) of 10 *ZmPIP* genes in roots. Plants were grown hydroponically (experiment 7 in Table II) and sampled at the same phenological stage as in Figures 1 and 2. The geometric mean of the expression levels of two control genes (tubulin and actin) was used to normalize data. Expression levels of *ZmPIP1;6* and *ZmPIP2;4* were very low (<10- to 4-fold the *ZmPIP1;1* level) and are not shown. A, Expression levels in AS (AS5) and S plants relative to expression in WT plants. Bars represent mean values ($n = 6$). Error bars indicate confidence intervals at the 0.95 risk level. Bars associated with the same letter indicate nonsignificant differences ($P > 0.05$) in a t test comparing each normalized value with unity. B, Expression level in WT plants, with PIP1;1 as a reference.

detected for ZmPIP2;5 and ZmPIP2;6, which were shown to be much less expressed in leaves compared with roots (Hachez et al., 2008).

Increased and Decreased ABA Biosyntheses Affected the Lp_r in Hydroponics, But This Effect Was Abolished by H_2O_2 Treatment

Root systems were placed during the morning in a hydroponic solution, with a hydrostatic tension of −0.02 MPa applied to the hypocotyls of detopped plants. WT plants released a stable water flux for 40 min, which was multiplied by 3 and 0.5 in S and AS plants, respectively (Fig. 5A). H_2O_2 was then brought to the nutrient solution in order to decrease the hydraulic conductivity of the transcellular pathway (Ye and Steudle, 2006; Boursiac et al., 2008). This caused a steep decrease in water flux in both S and WT plants but had nearly no effect in AS plants. The water fluxes, therefore, were insignificantly different in the three treatments after the H_2O_2 treatment.

Differences in water flux were analyzed by measuring root hydraulic conductivities under hydrostatic (Lp_h) and osmotic (Lp_{os}) gradients of water potential. Lp_h was calculated as the slope of the relationship between the applied suction and the flux released by

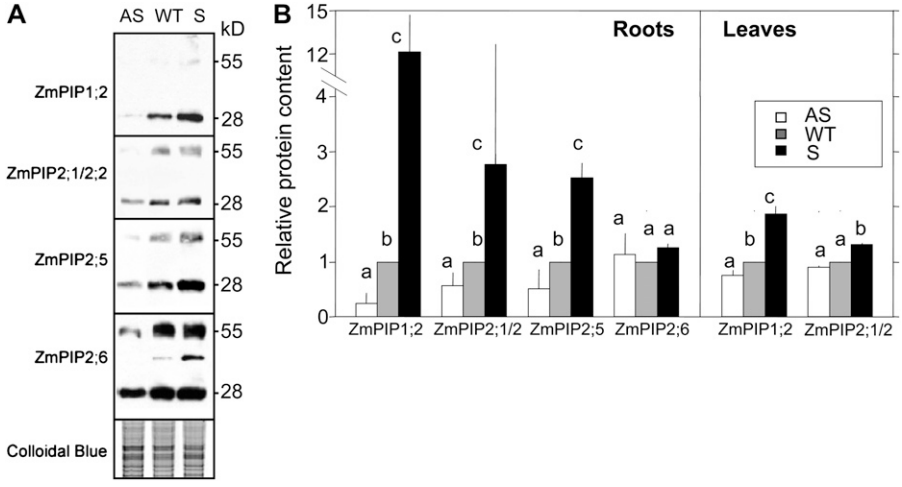

Figure 4. Immunoblots of ZmPIPs and protein quantification in AS (AS5), WT, and S plants. Plants were grown and sampled in the same conditions as in Figure 3 (experiment 5 in Table II). A, Western blot on root protein extract. Microsomal membranes were extracted from the first 5 cm of primary roots of plants grown hydroponically until the six-leaf stage and then subjected to 3 d at −0.4 MPa obtained with the addition of PEG to the solution. The proteins (15 μg) were subjected to western blotting using antibodies against plasma membrane ATPase (H^+-ATPases), ZmPIP1;2, ZmPIP2;1/2;2, ZmPIP2;5, and ZmPIP2;6. Colloidal blue gel staining was used as a gel-loading control. B, Quantification of PIP protein spots in roots and mature leaves coming from two independent experiments (three WT, two AS, and one S plant in each experiment). Three blot exposure times were used for the quantification. Each data point is a mean value of three experiments relative to the intensity in WT plants. Error bars indicate confidence intervals at the 0.95 risk level. Bars associated with the same letter indicate nonsignificant differences ($P > 0.05$) in a Benjamini and Hochberg t test (Benjamini and Hochberg, 1995).

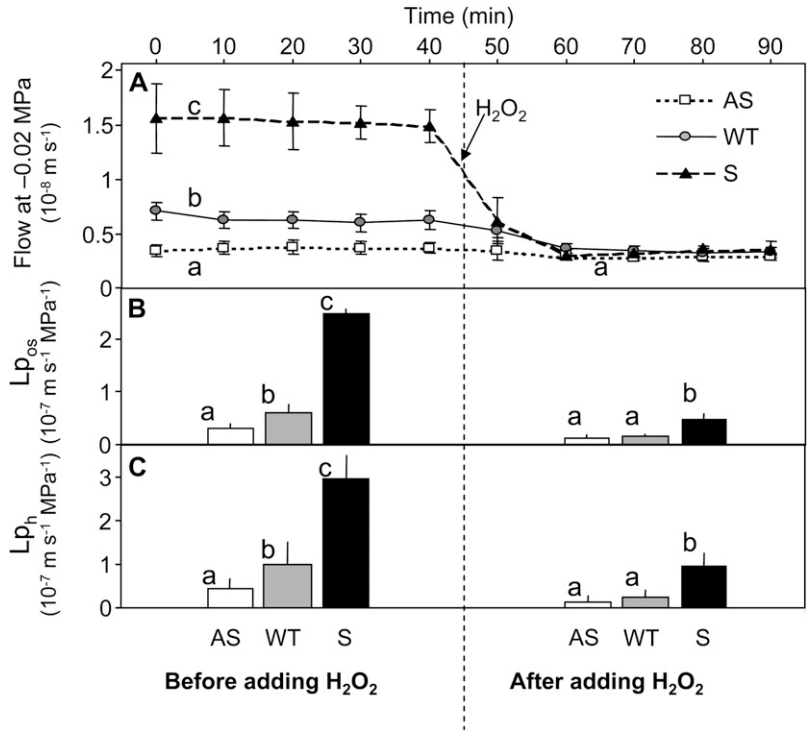

Figure 5. Water flow (A) through excised root systems placed in a nutrient solution and subjected to a tension of −0.02 MPa, and Lp_r under osmotic (B; Lp_{os}) and hydrostatic (C; Lp_h) gradients, before and after the addition of H_2O_2 in the nutrient solution, in AS (AS5), null transformants (WT), and S plants. Plants were grown in the same conditions as in Figures 3 and 4 (experiments 6 and 7 in Table II). A, Mean values of water flow (n = 3–10). The nutrient solution was changed to 2 mM H_2O_2 at 40 min. B, Lp_{os} was calculated from free exudation flow and osmotic gradient between the solution and the xylem sap (n = 4–9). C, Lp_h was calculated as the slope of water flow under a hydrostatic gradient (0, −0.02, −0.04, and −0.06 MPa; n = 4–9). Error bars indicate confidence intervals at the 0.95 risk level. Bars or lines associated with the same letter indicate nonsignificant differences ($P > 0.05$) in a Benjamini and Hochberg t test (Benjamini and Hochberg, 1995).

the root system at −0.02, −0.04, and −0.06 MPa. Lp_{os} was calculated as the ratio between the free exudation flux and the gradient of osmotic potential between the nutrient solution and the sap released by the root system. Both Lp_h and Lp_{os} were highly affected by the manipulation of ABA synthesis before the H_2O_2 treatment (Fig. 5, B and C). AS plants had a lower Lp_h and Lp_{os} (−45% and −52%, respectively) than WT plants, while the S plants had higher Lp_h and Lp_{os} (3- and 4-fold, respectively). Differences in Lp_h and Lp_{os} between AS and WT plants were abolished after the H_2O_2 treatment, and those between S and WT plants were strongly reduced. The fact that flows were similar between WT and S plants after H_2O_2 treatment despite differences of Lp_r was due to a lower gradient of osmotic potential between the solution and the xylem sap in S plants.

Overall, these results show that the manipulation of ABA synthesis strongly affected the water flux through the root system via changes in the hydraulic conductivities under both hydraulic and osmotic gradients. This effect was strongly reduced or disappeared with the H_2O_2 treatment, with a drop in Lp_r that can be interpreted as the contribution of aquaporins to the water flux.

The Total Hydraulic Conductance between Soil and Leaves Increased with ABA Biosynthesis

The total hydraulic conductance between soil and leaves was estimated in a greenhouse experiment by dividing the water flux by the gradient of water potential between soil and leaves (Fig. 2C). Leaf water potential of AS plants was lower than that of WT plants in well-watered conditions as well as in water deficit (Fig. 2B; see also Fig. 1C), while transpiration rate was higher in AS than in WT plants (Fig. 2A). Sense plants had a significantly higher leaf water potential in all conditions, consistent with a lower transpiration rate. The three AS lines had lower hydraulic conductances, and the S line had a higher conductance than the WT plants (Fig. 2C). The differences in soil-plant conductance were not due to changes in root system architecture, because root length and area were very close in WT and AS plants and were lower in S plants than in WT plants (Fig. 2D). Hence, the higher hydraulic conductance observed in S plants in spite of a lower root area suggests a high Lp_r.

S and AS Lines Exhibited Marked Differences in Leaf Rehydration Half-Times and Recovery of Leaf Elongation Rate

We have evaluated the consequences of observed differences in Lp_r on the time courses of the recoveries of leaf water status and leaf elongation rate upon rehydration in a growth chamber experiment with soil-grown plants. Plants initially subjected to a soil water potential of −0.4 MPa and a vapor pressure deficit (VPD) of 2.5 kPa were rewatered and subjected to dark conditions at a VPD of 0.8 kPa that virtually stopped transpiration (time 0; Fig. 6). Before rewatering, leaf water potential differed between lines, consistent with experiments in

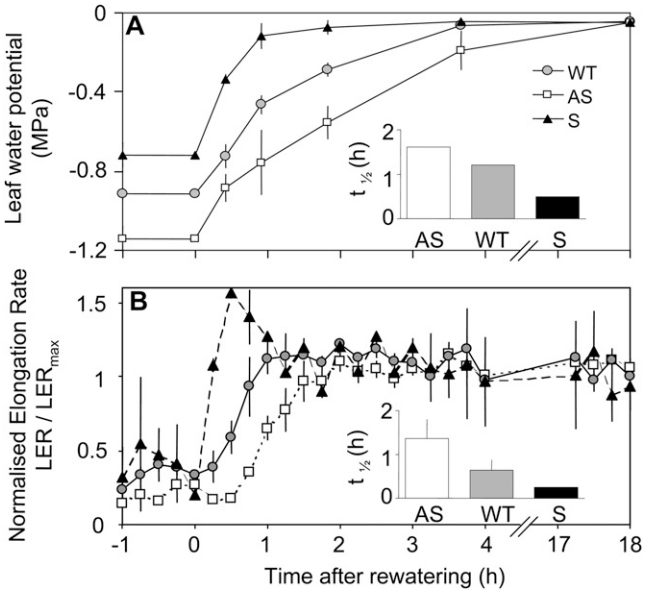

Figure 6. Time courses of recoveries of leaf water potential (A) and of leaf elongation rate (LER; B) upon rewatering in AS (AS5), WT, and S plants in a growth chamber experiment (experiment 3 in Table II; n = 3–10). Normalized leaf elongation rates were calculated as the absolute leaf elongation rate divided by the mean rate observed in the same line during the night in well-watered plants. Plants were transpiring under high evaporative demand (VPD = 2.5 kPa) and subjected to water deficit (soil water potential, −0.4 MPa) until time 0 h. At that time, plants were rewatered and lights were turned off. Insets show half-times ($t_{1/2}$) of recovery. Error bars indicate confidence intervals at the 0.95 risk level.

the greenhouse (Figs. 1 and 2), with higher and lower values in S and AS plants, respectively, than in WT plants. Leaf elongation rates normalized by their maximum values under well-watered conditions for each line also differed before rewatering, with highest and lowest values for S and AS plants, respectively.

Leaf water potential recovered more rapidly in S plants and more slowly in AS plants compared with WT plants, with half-times of 0.5, 1.2, and 1.6 h, respectively (Fig. 6B, inset). Full recovery of leaf water potential occurred in 3, 5, and 7 h, respectively, and all lines reached a common water potential after 18 h. The recovery of leaf elongation rate also largely differed between the three lines, with the same trend as that of leaf water potential. It was more rapid than the recovery of leaf water potential, with half-times and times for full recovery of about 50% of those corresponding to leaf water potential. This difference in time course of recovery was consistently observed in three experiments in the growth chamber (data not shown).

The Differences in Time Course of Rehydration between Lines Are Accounted for by a Model Taking into Account the Measured Hydraulic Parameters

We have evaluated the relative contributions of Lp_r and other possible causes of the differences in time courses presented in Figure 6, with the sensitivity analysis of a model. The model of stomatal control, biosynthesis of ABA, and water transfer is that of Tardieu and Davies (1993), widely tested since then and used by other groups (Dewar, 2002; Gutschick and Simonneau, 2002). It was combined with a model that calculates the water potential at leaf evaporating sites and with a module of capacitance, which allows the calculation of recovery rates (see ''Materials and Methods''). The parameters used in the model are presented in Table I, and the outputs are presented in Figure 7 for S, WT, and AS plants.

In transpiring plants (before time 0), leaf and xylem water potentials of simulated plants were lower in AS plants than in WT and S plants, because of a higher stomatal conductance that caused a higher water flux,

Table I. *Plant characteristics in the three treatments and parameters of the model of water transfer*

All parameters are as described by Tardieu and Davies (1993) with values for maize, except those in this table. ABA synthesis, ABA = $\alpha + \beta\,\psi_{root}$, where α is the ABA synthesis at a water potential of 0 and β is the increase in ABA synthesis with root water potential (ψ_{root}). Hydraulic conductivities and conductances are as in the text. The parameters of the pressure-volume curves are as described in ''Materials and Methods.''

Characteristic	Unit	AS	WT	S	Origin
ABA synthesis, constitutive, α	μmol m^{-3}	0	0	400	Fitted from Figure 1 and data at other water potentials
ABA synthesis, response to root water potential, β	μmol m^{-3} MPa^{-1}	−600	−600	−50	Fitted from Figure 1 and data at other water potentials
Root hydraulic conductivity, Lp_r	m s^{-1} MPa^{-1} 10^{-7}	0.421	0.971	2.92	Measured (Fig. 5)
Conductance from xylem to evaporating sites, g_{x-s} (Eq. 3)	mg MPa^{-1} s^{-1} plant^{-1}	7	7	7	Measured
Conductance from xylem to leaf cells, g_{x-l} (Eq. 4)	mg MPa^{-1} s^{-1} plant^{-1}	0.40	0.40	0.40	Fitted on rehydration data
Pressure-volume parameter, n (Eq. 7)		1.6	1.6	1.6	Parameters of measured pressure-volume curve (Fig. 8)
Pressure-volume parameter, α (Eq. 7)		0.075	0.075	0.075	Parameters of measured pressure-volume curve (Fig. 8)
Root area	cm^2	350	350	150	Measured (Fig. 2)
Leaf area	cm^2	110	110	55	Measured
Plant volume	mm^3	9,000	9,000	4,500	Estimated from leaf area

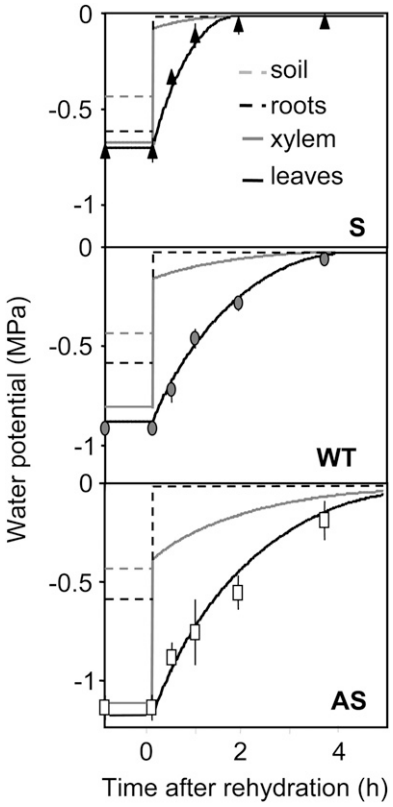

Figure 7. Simulated time course of recovery of water potential in the soil, roots, xylem, and leaves in AS, WT, and S plants. Symbols represent experimental measurements of leaf water potential.

consistent with experimental data. Both this steady state and the recovery of leaf water potential after rehydration could be adequately simulated by the model without the necessity of additional parameters. In particular, a single value for the hydraulic conductance of leaf tissues ($g_{x\text{-}l}$) could be assumed for the WT, AS, and S lines. The model was then used to determine the contributions of several possible causes for the differences in time courses of leaf rehydration. (1) The elastic modulus had here a minor role because all studied lines had similar pressure-volume curves (Fig. 8). (2) The hydraulic conductance of the path between the xylem and leaf cells ($g_{x\text{-}l}$) could potentially have an important effect on the recovery of water potential according to the model. However, simulations with measured values of Lp_r accounted for the whole differences between AS, WT, and S lines, leaving a marginal role or no role for differences in $g_{x\text{-}l}$. This is consistent with the low differences in PIP amounts in leaves. Simulations were only slightly improved if a small difference in $g_{x\text{-}l}$ was assumed between lines, but the effect was too small to justify different fitted values of $g_{x\text{-}l}$ between lines (Table I). (3) The volume of water in the leaf tissues potentially has a large effect on the time courses of leaf water potential upon rehydration. It did not contribute to the difference between AS and WT plants, which had similar leaf areas and weights, but accounted for a large part of the difference between WT and S plants. When simulations were run with a common leaf water volume, the time course of rehydration still differed between WT and S plants, but with a half-time in S plants that increased to 1 h versus 0.5 h in experimental data (Fig. 9).

Overall, this sensitivity analysis suggests that the Lp_r measured in detached root systems accounted for a large part of the differences between lines in whole plant conductance, both in steady-state transpiration and during rehydration. In AS plants, which presented no difference in leaf volume, the increase in half-time of rehydration could be entirely attributed to differences in Lp_r. Part of the difference between S and WT plants was due to a difference in leaf volume, but Lp_r still accounted for 23% of the difference in half-time of rehydration.

DISCUSSION

Consistent effects were observed across different scales of plant organization, suggesting a simpler picture for the role of ABA on plant hydraulic properties than that presented in the introduction. This was probably because differences in ABA supply to the shoot were stable over a long period, thereby avoiding the complexity of transient effects of exogenous ABA application (Hose et al., 2000; Zhu et al., 2005), and because the effects of ABA and drought were not confused.

Effects of Overproduction or Underproduction of ABA on Aquaporin Gene Expression and Protein Content

ABA increased gene expression and protein content of most PIP isoforms and never decreased them. This is consistent with the results of Jang et al. (2004) obtained in roots of Arabidopsis (*Arabidopsis thaliana*), in which exogenous ABA increased the expression of 12 *PIPs*, although one isoform was decreased by the same treatment. However, this is the first time, to our knowledge, that a long-lasting effect was observed, with a stable increase in expression levels for most *PIPs*, in opposition to the results of Zhu et al. (2005) in maize roots, in which an application of exogenous

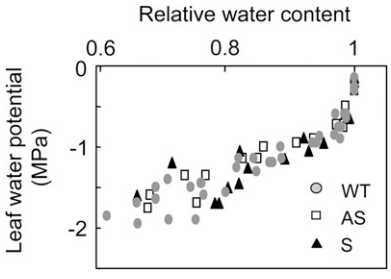

Figure 8. Relationship between leaf relative water content and leaf water potential in AS (AS5), WT, and S plants (experiment 4 in Table II). Each point shows one coupled value of relative water content and water potential corresponding to one leaf.

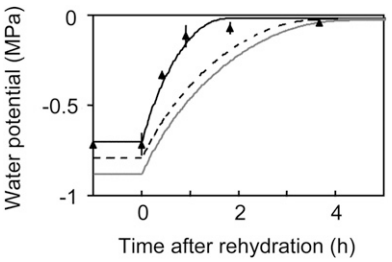

Figure 9. Sensitivity analysis of several possible causes of the difference in time courses between WT and S lines. Simulations were carried out taking into account differences in root hydraulic conductance only (dashed black line) or both hydraulic conductance and leaf volume (black line). The gray line represents WT plants.

ABA caused an increase in expression of only one PIP (*ZmPIP1;2*) after 24 h. This difference is probably due to the fact that changes in ABA concentration were obtained through a transgenic approach in this study instead of the application of exogenous ABA.

The ABA effects on PIP expression resulted in differences between lines in PIP protein contents, in opposition to the data obtained by Morillon and Chrispeels (2001) in Arabidopsis leaves. However, we observed some discrepancies between mRNA and protein levels. ZmPIP2;6 did not show any significant variation at the protein level, although its mRNA expression profile was strongly correlated with endogenous ABA concentration. On the contrary, ZmPIP2;5 was found to have a fairly similar mRNA expression level in the different lines, whereas its protein level showed a clear correlation with ABA content. These observations suggest the existence of posttranscriptional mechanisms to regulate the amount of PIP proteins.

PIP1 gene expression was more affected than that of *PIP2* in our study, especially that of *ZmPIP1;2*, resulting in protein content more affected in ZmPIP1;2 than in PIP2s. This is important in view of the regulating role of this PIP (Zelazny et al., 2007). Gene expression of the PIP2 subfamily was lower than that observed by Hachez et al. (2006) without osmotic or water stress. This could be due to genotypic differences but also to an ABA-independent negative effect of drought on *PIP2* expression, due to mild water stress (Jang et al., 2004).

ABA Effect on Hydraulic Conductivity via Aquaporin Activity Modulation

The variation in the amount of ZmPIP isoforms in AS, WT, and S lines was correlated with the measured differences in Lp_r, indicating that PIP aquaporins play a crucial role in controlling Lp_r. ZmPIP2;1/2;2 and ZmPIP2;5 proteins were reported to be highly expressed in the exodermis and the endodermis, suggesting that they are involved in root radial water movement (Hachez et al., 2006). In addition, the detection of a polar localization of ZmPIP2;5 to the external periclinal side of epidermal cells indicates an important role in water transfer from the soil into the roots (Hachez et al., 2006). The increase in ZmPIP1;2 amount could also induce an increase in the water permeability of root cells. Although PIP1 proteins expressed alone in maize protoplasts were retained in the endoplasmic reticulum, their coexpression with PIP2s resulted in a relocalization to the plasma membrane due to physical interaction (Zelazny et al., 2007). When coexpressed in oocytes, this interaction enhanced the water membrane permeability (Chaumont et al., 2000; Fetter et al., 2004).

The fact that differences in Lp_r disappeared or were largely decreased after H_2O_2 treatment suggests that they were due to differences in aquaporin activity. Boursiac et al. (2008) showed that millimolar concentrations of H_2O_2, as applied in this work, enhance the accumulation of PIPs in intracellular structures, resulting in 60% inhibition of Lp_r. This difference in activity between lines was probably due, at least in part, to the difference in the amount of PIP isoforms in both AS and S plants. We do not rule out the possibility that ABA also had an effect on aquaporin gating, which is the most likely mechanism in short-term experiments with artificial ABA (Hose et al., 2000). However, the latter effect disappeared after 3 h in that study (Hose et al., 2000), suggesting that the effect of ABA on Lp_r, initially due to aquaporin gating, is linked to other mechanisms, including change in PIP content over

Table II. *Summary of experiments carried out in this study*

T_{min} and T_{max}, Minimum and maximum daily temperature during the experiment; VPD_{max}, maximum vapor pressure deficit.

Experiment	Lines	Place	Medium	T_{min}/T_{max}	VPD_{max}	PPFD	Measured Variable
				°C	kPa	$\mu mol\ m^{-2}\ s^{-1}$	
1	AS1, AS2, AS5, WT	Greenhouse	Soil	19/26	2.5	500	g_s, [ABA], ψ
2	AS1, AS2, AS5, WT	Greenhouse	Soil	19/30	3	700	g_s, [ABA], ψ
3	AS1, AS2, AS5, WT, S	Greenhouse	Soil	21/29	2.8	660	g_s, [ABA], ψ, transpiration, root and leaf area
3	AS1, AS2, AS5, WT, S	Growth chamber	Soil	28/28	2.8	400	ψ and leaf elongation rate during rehydration
4–8	AS5, WT, S	Growth chamber	Hydroponics	20/24	0.8	400	Aquaporin expression and protein content, pressure-volume, Lp_r

longer time scales. Therefore, the difference between the clear effect of ABA on Lp_r observed here and the transient (Hose et al., 2000) or nonexisting (Wan and Zwiazek, 2001; Aroca et al., 2003) effects observed by other authors may be due to the difference in mechanisms between endogenous ABA and artificially fed ABA or to a rapid degradation of exogenously applied ABA.

Differences in Lp_r Translate into Changes in Whole Plant Hydraulic Conductance

Two independent ways of evaluating whole plant hydraulic conductance, each of which has its drawbacks, gave consistent results. (1) The conductance calculated from the water flux and the gradient of water potential in the soil-leaves continuum differed between lines. It represents the overall water transport in plants and in the soil and can be affected by any difference in soil water potential (which has a large effect on soil hydraulic conductivity) or in root system architecture (which affects the distance that water has to cross from the soil to the nearest root). This was probably not the case here, because the soil water content did not differ between pots carrying plants of each line and because measured root areas were similar in AS and WT plants and lower in S plants. (2) The difference in the time course of leaf water potential upon rehydration also indicates a difference in overall plant conductance, although other differences between genotypes could also account for this effect. The model showed that the differences in Lp_r measured in detached root systems were sufficient to account for the longer half-time of recovery of leaf water potential in AS plants. The shorter half-time of recovery observed in S plants was only partly due to measured differences in Lp_r, with a contribution of the leaf volume to the behavior of S plants.

Leaf Elongation Rate followed the Changes in Hydraulic Properties upon Rehydration

The effect of ABA on leaf growth via changes in aquaporin activity and Lp_r is usually obscured by the superposition of several effects of ABA at different time scales. In particular, leaf elongation rate during the night was faster and slower, respectively, in AS and S plants than in WT plants in both well-watered and water deficit treatments. This suggests an intrinsic negative effect of ABA on leaf elongation rate consistent with earlier results (Zhang and Davies, 1990b; Ben Haj Salah and Tardieu, 1997; Bacon et al., 1998) and caused a smaller plant size of S plants. During the day, a lower stomatal conductance and higher hydraulic conductivity in S plants compared with WT and AS plants translated into a higher leaf water potential and a higher leaf elongation rate normalized by its value in well-watered plants, as shown in Figure 6.

The complex situation described above led us to concentrate this study on the changes in leaf elongation rate during rehydration. The first surprising result was that growth recovery after rehydration had half-times of around 1 h. The recovery of leaf elongation rate was even faster than that of leaf water potential and responded to ABA production with half-times lower for the S line and higher for the AS line than for WT plants. The beneficial effect of ABA on Lp_r, therefore, had consequences on leaf water status and then on leaf elongation rate upon rewatering.

MATERIALS AND METHODS

Genetic Material

A series of transformed maize (*Zea mays*) lines were analyzed, one S line (S) and three AS lines (AS1, AS2, and AS5; already presented in the study of Voisin et al. [2006] with the names FCN-001a, FCN-002a, and FCN-005b, respectively). AS lines were engineered by transformation of the line A188 with *Agrobacterium tumefaciens* carrying the pRec518 superbinary vector (Ishida et al., 1996). The pRec518 vector was obtained after recombination between *A. tumefaciens* pSB1 superbinary vector and pBIOS518, which contains a 1.8-kb coding sequence of NCED/VP14 under the constitutive viral promoter *Cassava vein mosaic virus* (CsVMV) and the upstream Nos terminator. pBIOS518 carries the BAR marker gene driven by the actin constitutive promoter and its first intron and is stopped by the Nos terminator. The sense transgenic line, FVC-002b (S), was engineered by biolistic and was obtained by cotransformation of the pCsVMVNCEDsens plasmid, which carries the NCED/VP14 sequence in the sense orientation under the CsVMV constitutive promoter and upstream Nos terminator, and the pDM302 vector, which contains the following cassette: actin promoter and its first intron, marker gene BAR, and the Nos terminator (Gordon-Kamm et al., 1990). Primary transformants were grown in vitro, acclimated in the greenhouse (16-h day, 24°C, 80% relative humidity and 8-h night, 20°C, 100% relative humidity). They were then crossed with the line A188, and the resulting material (T1) was used in this study. It was checked by Southern blotting that transformed plants containing one or two copies of the transgene. To identify T1 plants carrying the insertion (50% of the plants), a PCR test (Taq Hot Start master mix; Qiagen) was performed in each studied plant on a 50-mg fresh weight leaf sample at the third leaf stage. Primers were designed for the *NCED/VP14* gene (forward, 5′-AGTTGTTGTCACCCAGTCCAG-3′; reverse, 5′-CACGCACCGATAGCCACA-3′). In all cases, nontransformed plants, sisters from transformed plants, were used as controls.

Plant Growth Conditions in Hydroponics

Maize seeds were placed in tubes with a wet sponge and germinated at 24°C in the dark and saturated air. After 3 to 5 d, the germinated seeds were placed in the growth chamber with their roots bathing in a continuously aerated solution with the following composition: 0.25 mM $CaSO_4$, 0.8 mM KNO_3, 0.6 mM KH_2PO_4, 0.2 mM $MgSO_4(7H_2O)$, 0.4 mM NH_4NO_3, 2×10^{-3} mM $MnSO_4$, 0.4×10^{-3} mM $ZnSO_4$, 0.4×10^{-3} mM $CuSO_4$, 0.2×10^{-3} mM Na_2MoO_4 $(2H_2O)$, 1.6×10^{-2} mM H_3Bo_3, 0.04 mM Fe-EDDHA, and 2.5 mM MES, pH 5.5 to 5.8. The hydroponic solution was renewed every third to fourth day. Air temperature and relative humidity were measured at plant level every 30 s with two sensors (HMP35A; Vaisala Oy). The temperature of the meristematic zone was measured with fine copper-constantan thermocouples (0.2 mm diameter), inserted between the sheaths of leaves 2 and 3 of four to six plants per experiment. Photosynthetic photon flux density (PPFD) was measured every 30 s using two sensors (LI-190SB from Li-Cor and SOLEMS 01/012/012). All climatic data were averaged and stored every 15 min in a data logger (Campbell Scientific, LTD-CR10X Wiring Panel). Environmental conditions are summarized in Table II.

Plant Growth Conditions in the Greenhouse

Plants were grown in PVC columns (0.23 m diameter and 0.4 m height) containing a 40:60 (v/v) mixture of filtered loamy soil (particle diameter ranging from 0.1 to 4 mm) and organic compost. Columns were filled with 10.5 kg of soil and sampled for measurement of water content at filling time. Seeds were sown at 2.5 cm depth and watered with water until the two-leaf stage

and with a modified one-tenth-strength Hoagland solution after that. Environmental data were measured as above and are presented in Table II (experiments 1–3).

Soil water content was determined by weighing columns automatically every 15 min. Differences in weight were attributed to changes in soil water content, after correction for the increase in mean plant biomass as a function of phenological stage and for the effect of displacement transducers. A water-release curve of the soil was obtained by measuring the soil water potential of soil samples with different water contents, in the range 0.4 to 0.2 g g^{-1} (WP4-T Dewpoint Meters; Decagon Devices), thereby allowing calculation of the mean soil water potential in each soil column every 15 min.

Plant Growth Conditions in the Growth Chamber, Rewetting Experiment, and Measurement of Leaf Elongation Rate

Plants with mild water deficit (soil water potential of −0.4 MPa) and growing in the greenhouse under high evaporative demand were transferred at noontime to a growth chamber with a moderate evaporative demand (Table II, experiment 3; VPD = 2.5 kPa, 28°C, PPFD = 400 μmol m^{-2} s^{-1}). They were left to transpire under these conditions for 3 h, during which leaf water potential was measured with a pressure chamber (Soil Moisture Equipment) and leaf elongation rate of the sixth leaf was monitored every 15 min with rotational displacement transducers (601-1045 Full 360° Smart Position Sensor; Spectrol Electronics), following the protocol of Sadok et al. (2007). At time 0, plants were rewatered until retention capacity and placed in dark conditions at a VPD of 0.8 kPa, which virtually stopped transpiration. Measurements of leaf elongation rate and leaf water potential were carried out in the following 18 h.

Plant Measurements in Greenhouse Experiments

All measurements were carried out in plants at the six- or seven-leaf stage. Leaf water potential of nonexpanding leaves was measured at midday with a pressure chamber (experiments 1–3, days without clouds between 11 AM and 1 PM). Stomatal conductance was measured with a diffusion porometer (AP4; Delta-T Devices) calibrated every 30 min (same experiments and conditions as for leaf water potential measurements). Only nonexpanding leaves receiving full light were measured. Because values differed slightly between experiments (from 120 to 180 mmol m^{-2} s^{-1}), each value was normalized by the mean value of the well-watered WT plants of the corresponding day.

Plant transpiration was estimated from the weight loss of each column every 15 min (Table II, experiment 3). Direct evaporation from the soil was estimated by measuring the weight loss of soil columns without plants watered at the same time as other columns. Plant transpiration was divided by leaf area, measured nondestructively every third day by measuring the length and width of each leaf (Chenu et al., 2008).

Root area was measured in one experiment (Table II, experiment 3) at the six-leaf stage. Roots were first cleaned with water, and then primary and secondary roots were separated. Three samples (5–10 cm length) of each root type of each plant were scanned and area was determined with an image analyzer. All samples plus the whole root systems were dried at 85°C for 3 d and weighed. The ratio of area to weight was determined for each root type and each genotype, so the area of each root system was calculated from the biomass of each root type and the ratio of area to weight of the corresponding sample.

Pressure-Volume Curves and ABA Measurements

Water-release curves of plants at the six-leaf stage were obtained in three to five plants per line (experiment 4). Leaves of well-watered plants, grown in the dark for 12 h, were cut, weighed (fresh weight), and placed into a pressure chamber. The pressure was increased in five steps of 0.5 MPa for 15 min each, during which the sap exudate was collected in a tube. When the sap flow stopped, the water potential was determined and the accumulated sap flow was estimated by weighing the tube. It was determined that sap evaporation did not exceed 10% of the total sap collected in each leaf. At the end of the measurements, the leaf was dried at 85°C for 3 d and weighed. The relative water content was calculated as the difference between weight and dry weight divided by the difference between fresh weight and dry weight.

The concentration of ABA was measured in sap samples obtained by pressurizing leaves in the pressure chamber in the early morning (experiments 1–3). Sap samples were then stored at −80°C until analysis. ABA concentration was then measured in crude samples of xylem sap by radioimmunoassay (Quarrie et al., 1988) as described previously (Barrieu and Simonneau, 2000).

RNA Extraction and Quantitative RT-PCR (Experiment 8)

RNA extraction was carried out as described by Hachez et al. (2006). Briefly, total RNA was extracted from thoroughly ground frozen root sections using an RNeasy Plant Extraction Minikit (Qiagen). DNase I digestion was performed on a column during RNA extraction according to the manufacturer's recommendations. cDNA synthesis and real-time PCR were then performed as described by Hachez et al. (2006). Results were normalized using two maize internal control genes, *α-tubulin* (gi: 450292; Hachez et al., 2006) and *actin* (gi:168403; forward primer, 5′-TTGGGTCAGAAAGGTTCAGG-3′; reverse primer, 5′-GCACTTCATGTGGACAATGC-3′). ZmPIP primers were those used by Hachez et al. (2006) targeting a 100-bp-long sequence from the 3′ untranslated region. NCED mRNA levels were assessed using 20-bp-long specific primers (forward primer, 5′-ATCAAGAGGCCGTACCTCAA-3′; reverse primer, 5′-GCATCTCCTGGAGCTTGAAC-3′). PCR efficiency of the NCED primers was checked and found to be appropriate.

Protein Extraction and Analysis

Measurements were carried out on plants grown hydroponically until the six-leaf stage (experiment 5) and subjected to a 72-h water stress obtained with PEG (−0.4 MPa; PEG8000, 150 g L^{-1}). Root tips (4 cm) and the leaf elongation zone (6 cm) were collected during early morning, immediately placed in a tube immersed in liquid nitrogen, and stored at −80°C. To prepare the microsomal fraction, 1 g of tissue was ground in 1.5 mL of solution (250 mM sorbitol, 50 mM Tris-HCl [pH 8], and 2 mM EDTA) containing 0.6% polyvinylpyrrolidone, 0.5 mM dithiothreitol, and protease inhibitors (1 μg mL^{-1} each of leupeptin, aprotinin, antipain, chymostatin, and pepstatin [Sigma]). All subsequent steps were performed at 4°C as described (Hachez et al., 2006). Fifteen micrograms of crude microsomal membranes was solubilized for 15 min at 60°C in a buffer (80 mM Tris-HCl, 2% SDS, 10% glycerol, 0.005% bromphenol blue, and 1% dithiothreitol), and the proteins were separated by SDS-PAGE on a 12% polyacrylamide gel. After electrophoresis, the gel was incubated for 5 min in semidry buffer (48 mM Tris, 39 mM Gly, 20% methanol, and 0.0375% SDS) before semidry transfer to a polyvinylidene difluoride (Millipore) membrane for 40 min at 23 V. Western-blot analysis was performed on the polyvinylidene difluoride membrane using antiserum raised against the N-terminal peptides of ZmPIP1;2, ZmPIP2;1, ZmPIP2;5, and ZmPIP2;6 (Chaumont et al., 2001). The antiserum raised against ZmPIP2;1 also recognized ZmPIP2;2 (Hachez et al., 2006). The dilutions used were 1:1,000 for the ZmPIP1;2, ZmPIP2;5, and ZmPIP2;6 antiserum and 1:3,500 for the ZmPIP2;1/2;2 antiserum. Detection and protein quantification were carried out using a Kodak 4000R image station and the associated software. Three different exposure times were used per experiment for accurate protein quantification.

Measurement of Lp_r in Nutrient Solution

Measurements were carried out from 10 AM to 1 PM, while Lp_r was maximum (experiments 6 and 7). The free exudation rate of the excised seminal root system was measured by collecting exuded sap with a micropipette and weighing it in microtubes. The osmotic potentials of the sap and of the nutrient solution were measured with a vapor pressure osmometer (Vapro 5520; Wescor).

A hydrostatically driven xylem sap flow was triggered in excised root systems by applying a vacuum-induced tension (Freundl et al., 1998). The seminal root system was excised by sectioning the mesocotyl and then fixed tightly to a silicon tube using low-viscosity dental paste (President Light; Coltene Whaledent). The silicon tube was connected to a vacuum port equipped with a tension gauge. A two-valve system driven by the data logger allowed automatic control of the tension applied to the seminal roots. After 30 min, needed to stabilize the exudation rate, the water flux was

measured every 10 min. The suction force applied to the root system was varied every 10 min in a standardized way (0, −0.02, −0.04, −0.06, −0.06, −0.04, −0.02, and 0 MPa). The water flow across the root system was measured with a water trap made of a 2-mL tube filled with dry cotton and inserted onto the tubing between the roots and the vacuum port. Water flow was measured by weighing the sap absorbed by the cotton that was renewed every 10 min. H_2O_2 treatment (2 mM) was applied to the root system after 40 min, and the depressurization protocol was then applied in the same way. At the end of each experiment, the root system was scanned and root area (A) was determined with an image analyzer.

The Lp_r under an osmotic gradient (Lp_{os}) was calculated as follows:

$$Lp_{os} = J(\pi_{sap} - \pi_{sol})^{-1} \times A^{-1} \quad (1)$$

where J is the water flux through the root system without depressurization, π_{sap} and π_{sol} are the osmotic potentials of the sampled sap and of the nutrient solution, respectively, and A is the area of the root system. Lp_r under a hydrostatic gradient (Lp_h) was calculated from the slope of the regression between water flow and the suction applied to the root system (dJ/dP):

$$Lp_h = (dJ/dP) \times A^{-1} \quad (2)$$

Model of Water Transfer

The model of stomatal control, biosynthesis of ABA, and water transfer is that of Tardieu and Davies (1993). This model calculates stomatal conductance, $[ABA]_{xyl}$, water flux, root and the water potentials in transpiration sites from soil water potential, light intensity, and air VPD. The parameters used in calculations were those of the original paper, except for (1) the parameter that relates ABA biosynthesis to root water potential, which was calibrated for WT, AS, and S lines according to the measured $[ABA]_{xyl}$, and (2) the root hydraulic conductance, which was calculated from the hydraulic conductivities presented in Figure 5 and the measured root area presented in Figure 2 (Table I).

Changes in the model were added to allow simulation of the water potential of leaf cells. The water potential at leaf evaporating sites (Ψ_{evap}) was calculated from the xylem water potential (Ψ_{xyl}), the water flux (J), and the conductance to the flux from xylem to leaves ($g_{x\text{-}s}$):

$$\Psi_{evap} = \Psi_{xyl} - J/g_{x\text{-}s} \quad (3)$$

This conductance was estimated by measuring leaf and xylem water potentials of maize plants at the same stage (Table I).

Leaves presented a capacitance that was calculated from the pressure-volume curve presented in Figure 8 and the estimate of the leaf volume. They were a sink for water when their potential was lower than that of the evaporating sites and a source otherwise. The water flux corresponding to leaf growth during the considered 6 h of the simulation was negligible. Therefore, we solved the differential equation for calculating the cell water potential (Ψ_{cel}) and the water flux from the xylem to the leaf cells (J_{xc}):

$$J_{xc} = dV_{cell}/dt = g_{x\text{-}l}(\Psi_{xyl} - \Psi_{cel}) \quad (4)$$

where $g_{x\text{-}l}$ is the conductance of the pathway from xylem to leaf cells. At each time i, the flux through roots and xylem was the sum of the transpiration flux (J) and of the water flux from the xylem to the leaf cells (J_{xc}), so

$$\Psi_{cel} = \Psi_{soil}(i) - R_{sp}(i \times (J + J_{xc})) - R_r \times (J + J_{xc}) - (J + J_{xc})/g_{x\text{-}l} \quad (5)$$

where R_{sp} is the resistance to water flow in the soil, calculated as by Tardieu and Davies (1993), R_r is the resistance to water flux in the root system, calculated from Lp_r measured experimentally and root area (Table I), and $g_{x\text{-}l}$ is as in Equation 4 (Table I).

A first calculation of J_{xc} was derived from Equations 4 and 5:

$$J_{xc} = (g_{x\text{-}l} \times (-\Psi_{cel} + \Psi_{soil} - R_{sp} \times J - R_r \times J - J/g_{x\text{-}l}))/ (1 + L_p \times R_{sp} + L_p \times R_r + L_p/g_{x\text{-}l}) \quad (6)$$

A second expression of J_{xc} was obtained from the relationship between V_{cell} and Ψ_{cel}:

$$V_{cell} = V_{res} + (V_{sat} - V_{res}) \times (1/(1 + (\alpha \times (-\Psi_{cel}))^n))^{(1 - 1/n)} \quad (7)$$

where V_{sat} is the leaf volume at saturation (early morning), V_{res} is the residual volume at the water potential at the end of the experiment, and α and n are the parameters of a Van Genuchten equation fitted on the pressure volume curve. J_{xc} was calculated as the difference in V_{cell} between two different times for the optimization process of resolution of the differential equation. L_p was the only fitted parameter of the model. The elastic modulus of leaves was common to the three lines because the curves relating turgor to volume were indistinguishable in AS, S, and WT lines (Fig. 8).

Supplemental Data

The following materials are available in the online version of this article.

Supplemental Figure S1. Expression levels of the *NCED/VP14* gene in roots in AS (AS5) and S plants relatively to their value in WT plants.

ACKNOWLEDGMENTS

We thank P. Hamard for the development of the technique for measuring Lp_r and Gaelle Rolland for measurements of ABA concentration.

Received October 1, 2008; accepted February 6, 2009; published February 11, 2009.

LITERATURE CITED

Aroca R, Ferrante A, Vernieri P, Chrispeels MJ (2006) Drought, abscisic acid and transpiration rate effects on the regulation of PIP aquaporin gene expression and abundance in *Phaseolus vulgaris* plants. Ann Bot (Lond) **98:** 1301–1310

Aroca R, Vernieri P, Irigoyen JJ, Sànchez-Diaz M, Tognoni F, Pardossi A (2003) Involvement of abscisic acid in leaf and root of maize (*Zea mays* L.) in avoiding chilling-induced water stress. Plant Sci **165:** 671–679

Bacon MA, Wilkinson S, Davies WJ (1998) pH-regulated leaf cell expansion in droughted plants is abscisic acid dependent. Plant Physiol **118:** 1507–1515

Barrieu P, Simonneau T (2000) The monoclonal antibody MAC252 does not react with the (−) enantiomer of abscisic acid. J Exp Bot **51:** 305–307

Barrowclough DE, Peterson CA, Steudle E (2000) Radial hydraulic conductivity along developing onion roots. J Exp Bot **51:** 547–557

Beaudette PC, Chlup M, Yee J, Emery RJN (2007) Relationships of root conductivity and aquaporin gene expression in *Pisum sativum*: diurnal patterns and the response to $HgCl_2$ and ABA. J Exp Bot **58:** 1291–1300

Ben Haj Salah H, Tardieu F (1997) Control of leaf expansion rate of droughted maize plants under fluctuating evaporative demand: a superposition of hydraulic and chemical messages? Plant Physiol **114:** 893–900

Benjamini Y, Hochberg Y (1995) Controlling the false discovery rate: a practical and powerful approach to multiple testing. J R Stat Soc Ser B Stat Methodol **57:** 289–300

Borel C, Frey A, Marion-Poll A, Tardieu F, Simonneau T (2001) Does engineering abscisic acid biosynthesis in *Nicotiana plumbaginifolia* modify stomatal response to drought? Plant Cell Environ **24:** 477–489

Boursiac Y, Boudet J, Postaire O, Luu DT, Tournaire-Roux C, Maurel C (2008) Stimulus-induced downregulation of root water transport involves reactive oxygen species-activated cell signalling and plasma membrane intrinsic protein internalization. Plant J **56:** 207–218

Chaumont F, Barrieu F, Jung R, Chrispeels MJ (2000) Plasma membrane intrinsic proteins from maize cluster in two sequence subgroups with differential aquaporin activity. Plant Physiol **122:** 1025–1034

Chaumont F, Barrieu F, Wojcik E, Chrispeels MJ, Jung R (2001) Aquaporins constitute a large and highly divergent protein family in maize. Plant Physiol **125:** 1206–1215

Chenu K, Chapman SC, Hammer GL, McLean G, Ben Haj Salah H, Tardieu F (2008) Short-term responses of leaf growth rate to water deficit scale up to whole-plant and crop levels: an integrated modelling approach in maize. Plant Cell Environ **31:** 378–391

Christmann A, Weiler EW, Steudle E, Grill E (2007) A hydraulic signal in root-to-shoot signalling of water shortage. Plant J **52:** 167–174

Dewar RC (2002) The Ball-Berry-Leuning and Tardieu-Davies stomatal

models: synthesis and extension within a spatially aggregated picture of guard cell function. Plant Cell Environ **25:** 1383–1398

Endo A, Sawada Y, Takahashi H, Okamoto M, Ikegami K, Koiwai H, Seo M, Toyomasu T, Mitsuhashi W, Shinozaki K, et al (2008) Drought induction of Arabidopsis 9-cis-epoxycarotenoid dioxygenase occurs in vascular parenchyma cells. Plant Physiol **147:** 1984–1993

Fetter K, Van Wilder V, Moshelion M, Chaumont F (2004) Interactions between plasma membrane aquaporins modulate their water channel activity. Plant Cell **16:** 215–228

Freundl E, Steudle E, Hartung W (1998) Water uptake by roots of maize and sunflower affects the radial transport of abscisic acid and its concentration in the xylem. Planta **207:** 8–19

Gordon-Kamm WJ, Spencer TM, Mangano ML, Adams TR, Daines RJ, Start WG, O'Brien JV, Chambers SA, Adams WR Jr, Willetts NG, et al (1990) Transformation of maize cells and regeneration of fertile transgenic plants. Plant Cell **2:** 603–618

Gutschick VP, Simonneau T (2002) Modelling stomatal conductance of field-grown sunflower under varying soil water content and leaf environment: comparison of three models of stomatal response to leaf environment and coupling with an abscisic acid-based model of stomatal response to soil drying. Plant Cell Environ **25:** 1423–1434

Hachez C, Heinen RB, Draye X, Chaumont F (2008) The expression pattern of plasma membrane aquaporins in maize leaf highlights their role in hydraulic regulation. Plant Mol Biol **68:** 337–353

Hachez C, Moshelion M, Zelazny E, Cavez D, Chaumont F (2006) Localization and quantification of plasma membrane aquaporin expression in maize primary root: a clue to understanding their role as cellular plumbers. Plant Mol Biol **62:** 305–323

Hose E, Steudle E, Hartung W (2000) Abscisic acid and hydraulic conductivity of maize roots: a study using cell- and root-pressure probes. Planta **211:** 874–882

Ishida Y, Saito H, Ohta S, Hiei Y, Komari T, Kumashiro T (1996) High efficiency transformation of maize (*Zea mays* L.) mediated by *Agrobacterium tumefaciens*. Nat Biotechnol **14:** 745–750

Jang JY, Kim DG, Kim YO, Kim JS, Kang H (2004) An expression analysis of a gene family encoding plasma membrane aquaporins in response to abiotic stresses in *Arabidopsis thaliana*. Plant Mol Biol **54:** 713–725

Kaldenhoff R, Kölling A, Richter G (1996) Regulation of the *Arabidopsis thaliana* aquaporin gene AthH2 (*PIP1b*). J Photochem Photobiol B **36:** 351–354

Kaldenhoff R, Ribas-Carbo M, Flexas J, Lovisolo C, Heckwolf M, Uehlein U (2008) Aquaporins and plant water balance. Plant Cell Environ **31:** 658–666

Lee SH, Chung GC, Steudle E (2005) Low temperature and mechanical stresses differently gate aquaporins of root cortical cells of chilling-sensitive cucumber and -resistant figleaf gourd. Plant Cell Environ **28:** 1191–1202

Lian HL, Yu X, Ye Q, Ding XS, Kitagawa Y, Kwak SS, Su WA, Tang ZC (2004) The role of aquaporin RWC3 in drought avoidance in rice. Plant Cell Physiol **45:** 481–489

Lo Gullo MA, Nardini A, Salleo S, Tyree MT (1998) Changes in root hydraulic conductance (KR) of *Olea oleaster* seedlings following drought stress and irrigation. New Phytol **140:** 25–31

Mariaux JB, Bockel C, Salamini F, Bartels D (1998) Desiccation- and abscisic acid-responsive genes encoding major intrinsic proteins (MIPs) from the resurrection plant *Craterostigma plantagineum*. Plant Mol Biol **38:** 1089–1099

Martre P, Morillon R, Barrieu F, North GB, Nobel PS, Chrispeels MJ (2002) Plasma membrane aquaporins play a significant role during recovery from water deficit. Plant Physiol **130:** 2101–2110

Martre P, North GB, Nobel PS (2001) Hydraulic conductance and mercury-sensitive water transport for roots of *Opuntia acanthocarpa* in relation to soil drying and rewetting. Plant Physiol **126:** 352–362

Maurel C, Verdoucq L, Luu DT, Santoni V (2008) Plant aquaporins: membrane channels with multiple integrated functions. Annu Rev Plant Biol **59:** 595–624

Morillon R, Chrispeels MJ (2001) The role of ABA and the transpiration stream in the regulation of the osmotic water permeability of leaf cells. Proc Natl Acad Sci USA **98:** 14138–14143

North GB, Martre P, Nobel PS (2004) Aquaporins account for variations in hydraulic conductance for metabolically active root regions of *Agave deserti* in wet, dry, and rewetted soil. Plant Cell Environ **27:** 219–228

Qin X, Zeevaart JAD (1999) The 9-cis-epoxycarotenoid cleavage reaction is the key regulatory step of abscisic acid biosynthesis in water-stressed bean. Proc Natl Acad Sci USA **96:** 15354–15361

Quarrie S, Whitford P, Appleford N, Wang T, Cook S, Henson I, Loveys B (1988) A monoclonal antibody to (S)- abscisic acid: its characterization and use in a radioimmunoassay for measuring abscisic acid in crude extracts of cereal and lupin leaves. Planta **173:** 330–339

Quintero J, Fournier J, Benlloch M (1999) Water transport in sunflower root systems: effects of ABA, Ca^{2+} status and $HgCl_2$. J Exp Bot **50:** 1607–1612

Sadok W, Naudin P, Boussuge B, Muller B, Welcker C, Tardieu F (2007) Leaf growth rate per unit thermal time follows QTL-dependent daily patterns in hundreds of maize lines under naturally fluctuating conditions. Plant Cell Environ **30:** 135–146

Sansberro PA, Mroginski LA, Bottini R (2004) Foliar sprays with ABA promote growth of *Ilex paraguariensis* by alleviating diurnal water stress. Plant Growth Regul **42:** 105–111

Sauter A, Abrams S, Hartung W (2002) Structural requirements of abscisic acid (ABA) and its impact on water flow during radial transport of ABA analogues through maize roots. J Plant Growth Regul **21:** 50–59

Schraut D, Heilmeier H, Hartung W (2005) Radial transport of water and abscisic acid (ABA) in roots of *Zea mays* under conditions of nutrient deficiency. J Exp Bot **56:** 879–886

Sharp RE (2002) Interaction with ethylene: changing views on the role of abscisic acid in root and shoot growth responses to water stress. Plant Cell Environ **25:** 211–222

Shinozaki K, Yamaguchi-Shinozaki K, Mizoguchi T, Urao T, Katagiri T, Nakashima K, Abe H, Ichimura K, Liu Q, Nanjyo T, et al (1998) Molecular responses to water stress in *Arabidopsis thaliana*. J Plant Res **111:** 345–351

Steudle E (2000) Water uptake by plant roots: an integration of views. Plant Soil **226:** 45–56

Tan BC, Schwartz SH, Zeevaart JAD, McCarty DR (1997) Genetic control of abscisic acid biosynthesis in maize. Proc Natl Acad Sci USA **94:** 12235–12240

Tardieu F, Davies WJ (1993) Integration of hydraulic and chemical signalling in the control of stomatal conductance and water status of droughted plants. Plant Cell Environ **16:** 341–349

Thompson AJ, Andrews J, Mulholland BJ, McKee JMT, Hilton HW, Horridge JS, Farquhar GD, Smeeton RC, Smillie IRA, Black CR, et al (2007a) Overproduction of abscisic acid in tomato increases transpiration efficiency and root hydraulic conductivity and influences leaf expansion. Plant Physiol **143:** 1905–1917

Thompson AJ, Jackson AC, Symonds RC, Mulholland BJ, Dadswell AR, Blake PS, Burbidge A, Taylor IB (2000) Ectopic expression of a tomato 9-cis-epoxycarotenoid dioxygenase gene causes over-production of abscisic acid. Plant J **23:** 363–374

Thompson AJ, Mulholland BJ, Jackson AC, McKee JMT, Hilton HW, Symonds RC, Sonneveld T, Burbidge A, Stevenson P, Taylor IB (2007b) Regulation and manipulation of ABA biosynthesis in roots. Plant Cell Environ **30:** 67–78

Tournaire-Roux C, Sutka M, Javot H, Gout E, Gerbeau P, Luu DT, Bligny R, Maurel C (2003) Cytosolic pH regulates root water transport during anoxic stress through gating of aquaporins. Nature **425:** 393–397

Tyerman SD, Niemietz CM, Bramley H (2002) Plant aquaporins: multifunctional water and solute channels with expanding roles. Plant Cell Environ **25:** 173–194

Vandeleur RK, Mayo G, Shelden MC, Gilliham M, Kaiser BN, Tyerman SD (2009) The role of plasma membrane intrinsic protein aquaporins in water transport through roots: diurnal and drought stress responses reveal different strategies between isohydric and anisohydric cultivars of grapevine. Plant Physiol **149:** 445–460

Voisin AS, Reidy B, Parent B, Rolland G, Redondo E, Gerentes D, Tardieu F, Muller B (2006) Are ABA, ethylene or their interaction involved in the response of leaf growth to soil water deficit? An analysis using naturally occurring variation or genetic transformation of ABA production in maize. Plant Cell Environ **29:** 1829–1840

Wan X, Steudle E, Hartung W (2004) Gating of water channels (aquaporins) in cortical cells of young corn roots by mechanical stimuli (pressure pulses): effects of ABA and of $HgCl_2$. J Exp Bot **55:** 411–422

Wan X, Zwiazek JJ (1999) Mercuric chloride effects on root water transport in aspen seedlings. Plant Physiol **121:** 939–946

Wan X, Zwiazek JJ (2001) Root water flow and leaf stomatal conductance in

aspen (*Populus tremuloides*) seedlings treated with abscisic acid. Planta **213:** 741–747

Ye Q, Steudle E (2006) Oxidative gating of water channels (aquaporins) in corn roots. Plant Cell Environ **29:** 459–470

Zelazny E, Borst JW, Muylaert M, Batoko H, Hemminga MA, Chaumont F (2007) FRET imaging in living maize cells reveals that plasma membrane aquaporins interact to regulate their subcellular localization. Proc Natl Acad Sci USA **104:** 12359–12364

Zhang J, Davies WJ (1990a) Changes in the concentration of ABA in xylem sap as a function of changing soil water status can account for changes in leaf conductance. Plant Cell Environ **13:** 277–285

Zhang J, Davies WJ (1990b) Does ABA in the xylem control the rate of leaf growth in soil-dried maize and sunflower plants? J Exp Bot **41:** 1125–1132

Zhang WH, Tyerman SD (1999) Inhibition of water channels by $HgCl_2$ in intact wheat root cells. Plant Physiol **120:** 849–858

Zhu C, Schraut D, Hartung W, Schaffner AR (2005) Differential responses of maize MIP genes to salt stress and ABA. J Exp Bot **56:** 2971–2981